frontiers | Research Topics

Engineering plant-microbiomes to improve the health of economic crops

Edited by
Manoj Kumar Solanki, Ajay Kumar, Rachana Singh, Zhen Wang and Lucas Carvalho Basilio Azevedo

Published in
Frontiers in Plant Science

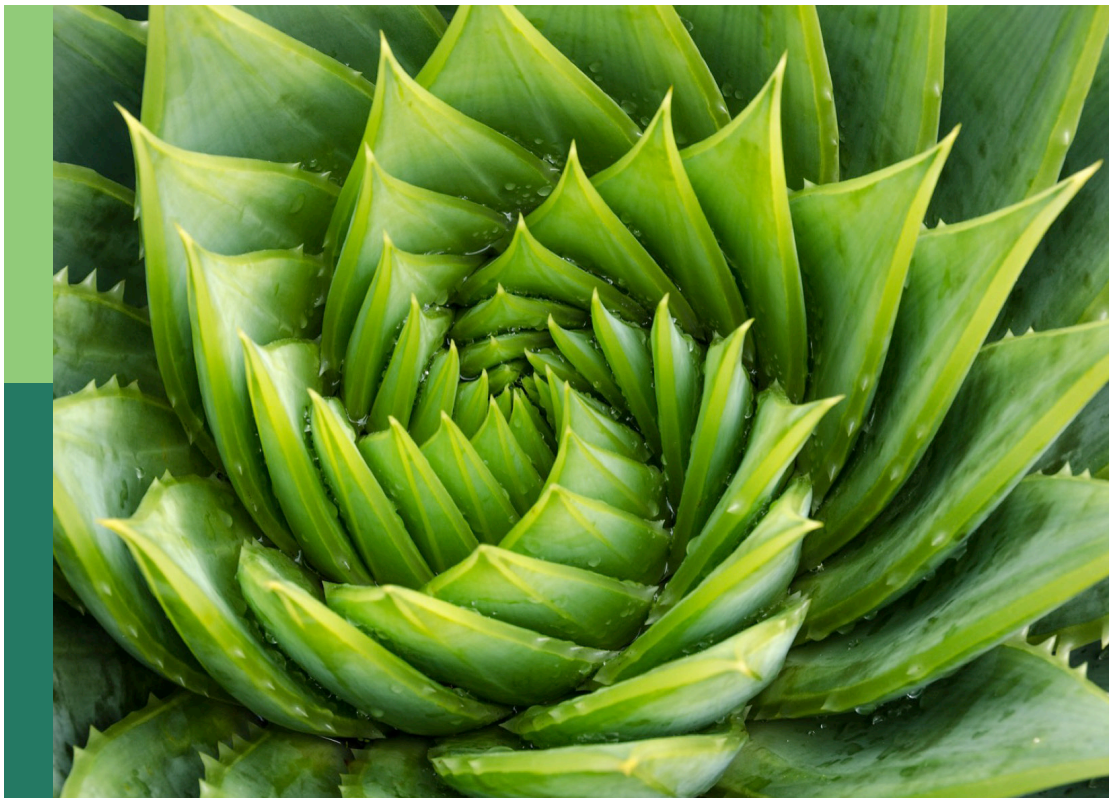

ISSN 1664-8714
ISBN 978-2-8325-7497-3
DOI 10.3389/978-2-8325-7497-3

Generative AI statement
Any alternative text (Alt text) provided alongside figures in the articles in this ebook has been generated by Frontiers with the support of artificial intelligence and reasonable efforts have been made to ensure accuracy, including review by the authors wherever possible. If you identify any issues, please contact us.

About Frontiers

Frontiers is more than just an open access publisher of scholarly articles: it is a pioneering approach to the world of academia, radically improving the way scholarly research is managed. The grand vision of Frontiers is a world where all people have an equal opportunity to seek, share and generate knowledge. Frontiers provides immediate and permanent online open access to all its publications, but this alone is not enough to realize our grand goals.

Frontiers journal series

The Frontiers journal series is a multi-tier and interdisciplinary set of open-access, online journals, promising a paradigm shift from the current review, selection and dissemination processes in academic publishing. All Frontiers journals are driven by researchers for researchers; therefore, they constitute a service to the scholarly community. At the same time, the *Frontiers journal series* operates on a revolutionary invention, the tiered publishing system, initially addressing specific communities of scholars, and gradually climbing up to broader public understanding, thus serving the interests of the lay society, too.

Dedication to quality

Each Frontiers article is a landmark of the highest quality, thanks to genuinely collaborative interactions between authors and review editors, who include some of the world's best academicians. Research must be certified by peers before entering a stream of knowledge that may eventually reach the public - and shape society; therefore, Frontiers only applies the most rigorous and unbiased reviews. Frontiers revolutionizes research publishing by freely delivering the most outstanding research, evaluated with no bias from both the academic and social point of view. By applying the most advanced information technologies, Frontiers is catapulting scholarly publishing into a new generation.

What are Frontiers Research Topics?

Frontiers Research Topics are very popular trademarks of the *Frontiers journals series*: they are collections of at least ten articles, all centered on a particular subject. With their unique mix of varied contributions from Original Research to Review Articles, Frontiers Research Topics unify the most influential researchers, the latest key findings and historical advances in a hot research area.

Find out more on how to host your own Frontiers Research Topic or contribute to one as an author by contacting the Frontiers editorial office: frontiersin.org/about/contact

Engineering plant-microbiomes to improve the health of economic crops

Topic editors

Manoj Kumar Solanki — University of Silesia in Katowice, Poland
Ajay Kumar — Amity University, India
Rachana Singh — Amity University, India
Zhen Wang — Yunnan Agricultural University, China
Lucas Carvalho Basilio Azevedo — Federal University of Uberlandia, Brazil

Citation

Solanki, M. K., Kumar, A., Singh, R., Wang, Z., Azevedo, L. C. B., eds. (2026). *Engineering plant-microbiomes to improve the health of economic crops*. Lausanne: Frontiers Media SA. doi: 10.3389/978-2-8325-7497-3

Table of contents

04 Editorial: Engineering plant-microbiomes to improve the health of economic crops
Zhen Wang, Ajay Kumar, Rachana Singh, Lucas Carvalho Basilio Azevedo and Manoj Kumar Solanki

08 Mechanistic understanding of metabolic cross-talk between *Aloe vera* and native soil bacteria for growth promotion and secondary metabolites accumulation
Neha Singh Chandel, H. B. Singh and Anukool Vaishnav

20 Structure and composition of arbuscular mycorrhizal fungal community associated with mango
Cuifeng Yang, Zheng Teng, Zhibo Jin, Qiufei Ouyang, Lingling Lv, Xianbin Hou, Muzammil Hussain and Zhengjie Zhu

32 Better than one: a synthetic community of Gram-positive bacteria protects pepper plants from aphid infestation through *de novo* volatile production
Sang-Moo Lee, Hyeonu Yang, Hyun Gi Kong, Myoungjoo Riu and Choong-Min Ryu

43 Comprehensive analysis of the physiological and molecular responses of phosphate-solubilizing bacterium *Burkholderia gladioli* DJB4–8 in promoting maize growth
Dao-Jun Guo, Guo-Rong Yang, Pratiksha Singh, Juan-Juan Wang, Xue-Mei Lan, Rajesh Kumar Singh, Jing Guo, Yu-Die Dong, Dong-Ping Li and Bin Yang

63 Soybean green manure intercropping improves citrus quality by improving soil quality and altering microbial communities
Sufeng Deng, Binbin Huang, Bin Zeng, Sheng Cao, Biya Gong, Wei Liao, Wen Zhang, Sainan Luo and Shuizhi Yang

78 *Aureobasidium pullulans*: a microbiome-based perspective from global biomes to edible plant tissues
Nina Bziuk, Birgit Wassermann, Samuel Bickel, Reza Omidvar, Andrea Manica and Gabriele Berg

85 Comparative analysis of rhizosphere microbial communities and secondary metabolites in cultivated *Rheum officinale* from different regions of China
Yan Wang, Feng Yan, Yujie Liang, Xiaochen Hu, Jing Gao, Mingying Zhang, Yonggang Yan, Gang Zhang and Yimin Li

99 Functional genome analysis reveals that serine carboxypeptidase *Bd-SCP10* mediates vegetative growth, pathogenicity, and stress tolerance in *Botryosphaeria dothidea*
Muhammad Umer, Naureen Anwar, Mustansar Mubeen, Yun Li, Khalid M. Alsyaad, Ahmed Ezzat Ahmed and Pingwu Liu

112 Nature's pre-installed helpers: diverse seed endophytes enhance rice nitrogen use efficiency
Ruimin Lao, Shaoxing Fang, Wenjun Fang, Zhiwei Zhao, Haiyan Li and Tao Li

frontiers | Frontiers in Plant Science

TYPE Editorial
PUBLISHED 27 January 2026
DOI 10.3389/fpls.2026.1782531

OPEN ACCESS

EDITED AND REVIEWED BY
Andrea Genre,
University of Turin, Italy

*CORRESPONDENCE
Zhen Wang
wang798110510@163.com
Manoj Kumar Solanki
mkswings321@gmail.com

RECEIVED 07 January 2026
ACCEPTED 19 January 2026
PUBLISHED 27 January 2026

CITATION
Wang Z, Kumar A, Singh R, Azevedo LCB and Solanki MK (2026) Editorial: Engineering plant-microbiomes to improve the health of economic crops. *Front. Plant Sci.* 17:1782531. doi: 10.3389/fpls.2026.1782531

Editorial: Engineering plant-microbiomes to improve the health of economic crops

Zhen Wang[1]*, Ajay Kumar[2], Rachana Singh[2], Lucas Carvalho Basilio Azevedo[3] and Manoj Kumar Solanki[4]*

[1]Sugarcane Research Institute, College of Agronomy and Biotechnology, Yunnan Agricultural University, Kunming,, China, [2]Amity Institute of Biotechnology, Amity University, Noida,, India, [3]Institute of Agricultural Sciences, Federal University of Uberlândia, Santa Monica,, Brazil, [4]Department of Life Sciences and Biological Sciences, IES University, Bhopal, Madhya Pradesh,, India

KEYWORDS

economic crops, growth regulation, microbiome, plant health, stress adaptation

Editorial on the Research Topic
Engineering plant-microbiomes to improve the health of economic crops

Economic crops are agricultural crops with specific economic uses and provide raw materials for industry. Together with food crops, they constitute the backbone of agricultural production, meeting daily dietary needs, supporting industrial systems, driving economic development, and optimizing agricultural structure, thereby forming a diversified, high-value sector of the global economy (Priyadarshan and Jain, 2022). Economic crops occupy a central position in global agricultural output value. In China, their output value accounts for approximately two-thirds of the total output value of the planting industry, significantly outweighing the contribution of food crops to increases in farmers' income. Economic crops play an indispensable role in the global agricultural landscape by driving economic growth, ensuring food security, shaping trade patterns, and promoting technological innovation. The role of microbiome in plant health and growth is multidimensional and systematic, encompassing nutrient absorption, disease resistance, stress adaptation, and growth regulation (Noman et al., 2024). Through close symbiosis with plants, microbiomes become core partners in maintaining plant health. With continued advances in research, the precise application of microbial resources—such as synthetic microbial communities, microbial fertilizers, and biopesticides—is expected to become a key direction for sustainable agricultural development, providing strong support for achieving green development goals related to improving crop quality and yield (Wang et al., 2023). Building a healthy and stable plant microbiome is a core strategy for enhancing stress resistance and productivity in economic crops. Microbiomes play a key role in promoting nutrient uptake and maintaining plant health and therefore have substantial scientific and agronomic value for crop growth and yield.

This Research Topic focuses on advancing understanding of recent studies on interactions between economic crops and microbiomes. A total of 15 manuscripts were submitted, of which 9 articles were published, including 8 original research articles and 1 mini-review. These studies involve 7 crops—rice, *Rheum officinale*, citrus, maize, pepper, mango, and Aloe vera—and specifically describe the roles of *Botryosphaeria dothidea*,

Aureobasidium pullulans, and *Burkholderia gladioli* in economic crops. The articles cover various biological and abiotic stress-related topics, such as plant nitrogen use efficiency, phosphorus solubilization and growth promotion, crop quality improvement, aphid infestation, and pathogen pathogenicity.

Bziuk et al. systematically explored the global distribution, ecological functions, and application potential of *Aureobasidium pullulans* within the frameworks of sustainable agriculture and the "One Health" concept, adopting a fungus with significant application value, from a novel microbiome-based perspective. Using the publicly available GlobalFungi database, the authors generated a macroscale global distribution map of *A. pullulans*. The analysis revealed a truly global distribution, with significantly higher detection rates in environments closely associated with human activities compared to natural ecosystems, highlighting a strong link to anthropogenic influence. These findings not only confirm the established value of *A. pullulans* as an effective biocontrol agent but also identity it as a natural core member of the plant microbiome. The results indicate that *A. pullulans* is not a transient colonizer but a resident symbiotic fungus with significant ecological influence. As a common component of the edible microbiome, *A. pullulans* may enter the human body through the food chain. Its potentially effects on the gut microbiome and human health was preliminarily explored, elevating its ecological significance to a "One Health" level that integrates plant, environmental, and human health. These findings provide a theoretical foundation for future in-depth development and application of *A. pullulans* in sustainable agriculture and health-related fields.

To explore how soybean green manure with different intercropping durations affects citrus fruit quality by altering soil physicochemical properties and microbial communities in acidified citrus orchards, Deng et al. established field experimental groups with varying intercropping durations. They systematically measured citrus fruit quality indicators and soil physicochemical properties and analyzed the community structures of soil bacteria and fungi using high-throughput sequencing. Through correlation network analysis, they revealed complex associations among intercropping duration, soil parameters, key microbial groups, and fruit quality. Soybean green manure significantly enhanced fruit quality, improved the soil environment, and reshaped the soil microbial community. Intercropping soybean green manure in citrus orchards is an effective ecological agricultural practice. Its core mechanism is the synergistic improvement of fruit quality through dual pathways: enhancement of soil physicochemical properties and regulation of soil microbial communities. This study provides a solid theoretical and practical basis for applying green manure intercropping in acidified orchard soils to support sustainable ecological restoration and improve agricultural production efficiency.

Lee et al. constructed a synthetic microbial community (SynCom) based on previous analyses of the tomato rhizosphere microbiome. They applied SynCom to pepper plants and compared its effects with those of individual strain inoculation, the chemical inducer benzothiadiazole (BTH), and a sterile water control. By analyzing volatile organic compounds (VOCs), and combining aphid infestation data, fruit yield measurements, and defense gene expression analyses, they comprehensively evaluated the effects of SynCom. SynCom significantly reduced aphid damage and increased crop yield. The microorganisms cooperatively produced the key volatile compound 1-nonanol, which could not be effectively produced by individual strains or partial combinations. Through exogenous addition experiments, treatment with 1 mM 1-nonanol reduced aphid numbers by 26–48% and activated expression of the pepper salicylic acid signaling pathway marker gene *CaPR1*, indicating a role in systemic resistance induction. This study demonstrates that microbial community cooperation can generate functional metabolites that cannot be synthesized by single strains. As a key signaling molecule, 1-nonanol indirectly surpasses pests by activating plant immunity. SynCom also maintained stability in complex field environments, providing a promising alternative to chemical pesticides and a theoretical foundation for designing efficient microbial fertilizers and biopesticides.

Wang et al. systematically examined the relationships among rhizosphere microbial community structure, soil physicochemical properties, and secondary metabolite accumulation in the cultivated medicinal plant *Rheum officinale* from three major production areas in China (ZB in Shaanxi, HB in Hubei, and CQ in Chongqing). *Rheum officinale* from the ZB region exhibited the highest content of rhein and catechin, whereas the CQ region was enriched in physcion. Microbial diversity followed the pattern ZB > HB > CQ, with bacteria dominated by Proteobacteria and fungi predominantly represented by Ascomycota. Soil properties, such as pH, moisture content, and zinc and copper ion concentrations, were closely correlated with microbial community structure. Increased pH and nutrient availability significantly promoted enrichment of beneficial bacterial groups such as Actinobacteria. Bacteria belonging to the order Rokubacteriales showed a significant positive correlation with anthraquinone accumulation, indicating that specific microbial groups may directly participate in regulating secondary metabolism through pathways such as nitrogen and phosphorus metabolism. This study elucidates the ecological mechanisms underlying geographical quality differentiation in rhubarb. Soil physicochemical properties indirectly regulate medicinal compound synthesis by shaping the rhizosphere microbiome, providing microbiome-level insights into the ecological cultivation of geographically indicated medicinal plants.

Guo et al. systematically investigated how *Burkholderia gladioli* DJB4-8, a highly efficient phosphate-solubilizing bacterium isolated from corn rhizosphere soil, promotes corn growth. By integrating multi-omics technologies with microbiology and plant physiology approaches, the study revealed the complete pathway by which the strain enhances crop growth through root colonization, regulation of endogenous plant hormones, and reprogramming of host metabolic pathways. Inoculation with DJB4–8 significantly promoted corn growth. After 40 days, plant height, root, stem,

and leaf biomass, as well as photosynthetic rate, were significantly increased, and auxin content in the roots was elevated. At the molecular level, transcriptome analysis identified 303 differentially expressed genes, significantly enriched in pathways such as glutathione metabolism, plant hormone signal transduction, and phenylpropanoid biosynthesis. Metabolomic analysis further detected hundreds of differentially accumulated metabolites. Joint multi-omics analysis demonstrated that DJB4–8 synergistically regulates corn growth and development by activating core physiological processes such as plant hormone signaling, enhancing phenylpropane metabolism, and antioxidation in maize. This study elucidates the mechanism by which the phosphate-solubilizing bacterium DJB4–8 promotes corn growth via root colonization, physiological regulation, and metabolic reprogramming.

Umer et al. functionally characterized a serine carboxypeptidase gene, *Bd-SCP10*, from *Botryosphaeria dothidea*, a globally distributed pathogenic fungus affecting various fruit trees. The study aimed to uncover the enzyme's role in fungal growth, pathogenicity, and stress tolerance, providing molecular targets for environmentally friendly disease management strategies. Bioinformatics analysis identified *Bd-SCP10* as a member of the S10 family in the *B. dothidea* genome. A gene knockout mutant (*ΔBd-SCP10*) was subsequently constructed, and a complementation strain (*CΔBd-SCP10*) was obtained through gene complementation. Systematic comparison of wild-type, mutant, and complementation strains under various conditions comprehensively evaluated the gene's function. *Bd-SCP10* was confirmed as a pleiotropic gene regulating growth, pathogenicity, and stress response of *B. dothidea*. Its mechanism of action may include supplying nutrients for fungal growth by enzymaticallyhydrolyzing host proteins, modifying or degrading host defense proteins to suppress immune responses, and facilitating fungal colonization by maintaining cell wall integrity and redox balance. This study elucidates the core function of *Bd-SCP10* and establishes it as a promising molecular target.

Chandel et al. investigated the metabolic interactions between the medicinal plant *Aloe vera* and its rhizosphere-associated bacteria. *Aloe vera* selectively recruits beneficial bacteria from its rhizosphere and analyzes the mechanisms by which these bacteria promote plant growth and accumulation of medicinal active compounds. Using *Paenibacillus* sp. GLAU-BT2 and *Arthrobacter* sp. GLAU-BT16, separate and mixed inoculation treatments were established. The effects of these treatments on *Aloe vera* growth, leaf secondary metabolite content, and root exudate composition were evaluated in a pot experiment. Mixed bacterial inoculation significantly promoted plant growth and increased total phenolic, flavonoid, and flavonol content in leaves, as well as antioxidant activity, indicating that PGPR can enhance the medicinal quality of *Aloe vera*. Flavonoids were identified as key signaling molecules in rhizosphere metabolic interactions. *Aloe vera* attracts and shapes beneficial microbial communities by secreting flavonoids and other metabolites into its rhizosphere. These recruited PGPR (such as GLAU-BT2 and GLAU-BT16) colonize the roots and promote nutrient absorption by secreting plant hormones and solubilizing nutrients, thereby stimulating synthesis and accumulation of medicinal secondary metabolites. Some newly synthesized metabolites are then secreted back into the rhizosphere, further maintaining and enriching the beneficial bacterial community, forming a positive feedback loop. This study provides a theoretical basis and practical direction for improving the yield and active ingredient content of medicinal plants and developing sustainable agriculture through microbial regulation strategies.

Yang et al. investigated how different seasons (spring and autumn) and tree ages (10 and 28 years) affect the structure of arbuscular mycorrhizal fungi (AMF) communities in the rhizosphere soil of two mango orchards in Baise, Guangxi, China. They also conducted an in-depth analysis of the key environmental factors driving community changes. The study aimed to elucidate the core mechanisms influencing the assembly of mango AMF communities, providing a theoretical basis for promoting sustainable mango production through microbial approaches. Changes in tree age and season had no significant impact on the diversity or richness of mango rhizosphere AMF communities. Conversely, soil chemical properties—especially the contents of phosphorus (P), potassium (K), and their available forms (AP and AK)—were the dominant factors driving differences in AMF community structure. Compared to biological factors (tree age and season), abiotic factors (soil nutrients) were more crucial in shaping mango rhizosphere AMF communities. This study provides a novel microbial strategy for precision nutrient management and sustainable development in mango orchards.

Lao et al. conducted an in-depth study on the structure and function of endophytic bacterial communities within the seeds of rice varieties with different nitrogen use efficiency (NUE). Rice seeds harbor rich and diverse endophytic bacterial communities, and their structure varies significantly among varieties. Rare taxa are the main drivers of community diversity and differentiation, while core taxa are highly conserved across varieties, primarily composed of high-abundance taxa, and occupy central positions in the co-occurrence network, thereby maintaining community stability. Five representative bacterial strains successfully isolated from seeds exhibited various plant growth-promoting characteristics *in vitro*, including siderophore production, phosphate solubilization, and indole-3-acetic acid synthesis. All strains promoted rice growth, increased nitrogen accumulation, and enhanced NUE. However, their growth-promoting effects were co-regulated by strain identity and nitrogen supply levels. Under low nitrogen conditions, the growth-promoting effects of the strains were pronounced, highlighting their potential for application in nutrient-stressed environments. The endophytic bacterial community within rice seeds co-evolve with the host through strategies of innovation and adaptation driven by rare taxa, and stability and inheritance maintained by core taxa. These natural symbiotic bacterial communities, as microbial allies of the host, enhance host adaptability in low-nitrogen soils through synergistic mechanisms such as nitrogen fixation, regulation of nitrogen metabolism, and production of plant hormones.

Future research will focus on multi-dimensional analyses of plant-microbiome interaction networks. Synthetic biology and genome-editing technologies will facilitate the design of customized microbial communities, such as constructing SynComs with nitrogen fixation, phosphorus solubilization, and disease-resistance functions, enabling precise regulation of multiple effects from a single microbial inoculum. Simultaneously, strategies to enhance environmental adaptability are crucial. By utilizing directed evolution and metabolic engineering to modify microbial metabolic pathways, colonization stability under adverse conditions such as salinity, alkalinity, and drought can be improved. Furthermore, interdisciplinary collaboration will accelerate the exploration and industrialization of microbial resources, developing innovative solutions for agricultural carbon neutrality and food security, including living biopesticides based on endophytes and the construction of rhizosphere microbial seed banks.

Author contributions

ZW: Conceptualization, Funding acquisition, Writing – original draft, Writing – review & editing. AK: Methodology, Writing – review & editing. RS: Investigation, Writing – review & editing. LA: Investigation, Writing – review & editing. MS: Conceptualization, Supervision, Writing – review & editing.

Funding

The author(s) declared that financial support was received for this work and/or its publication. This work was funded by the Guangxi Natural Science Foundation (CN) (2023GXNSFAA026182).

Conflict of interest

The author(s) declared that this work was conducted in the absence of any commercial or financial relationships that could be construed as a potential conflict of interest.

The authors ZW, AK, RS, MS declared that they were an editorial board member of Frontiers, at the time of submission. This had no impact on the peer review process and the final decision.

Generative AI statement

The author(s) declared that generative AI was not used in the creation of this manuscript.

Any alternative text (alt text) provided alongside figures in this article has been generated by Frontiers with the support of artificial intelligence and reasonable efforts have been made to ensure accuracy, including review by the authors wherever possible. If you identify any issues, please contact us.

Publisher's note

References

Noman, M., Ahmed, T., Wang, J., and White, J. C. (2024). Micronutrient–microbiome interplay: a critical regulator of soil–plant health. *Trends Microbiol.* 32, 319–320. doi: 10.1016/j.tim.2024.02.008

Priyadarshan, P. M., and Jain, S. M. (2022). "Cash crops: an introduction," in *Cash Crops*. Eds. P. Priyadarshan and S. M. Jain (Springer, Cham), 1–19.

Wang, Z., Hu, X., Solanki, M. K., and Pang, F. (2023). A synthetic microbial community of plant core microbiome can be a potential biocontrol tool. *J. Agric. Food Chem.* 71, 5030–5041. doi: 10.1021/acs.jafc.2c08017

frontiers | Frontiers in Plant Science

TYPE Original Research
PUBLISHED 27 March 2025
DOI 10.3389/fpls.2025.1577521

OPEN ACCESS

EDITED BY
Manoj Kumar Solanki,
University of Silesia in Katowice, Poland

REVIEWED BY
Prafull Salvi,
National Agri-Food Biotechnology Institute, India
Prassan Choudhary,
Chhattisgarh, India
Dao-Jun Guo,
Hexi University, China

*CORRESPONDENCE
Anukool Vaishnav
anukool.vaishnav@gla.ac.in

RECEIVED 15 February 2025
ACCEPTED 07 March 2025
PUBLISHED 27 March 2025

CITATION
Chandel NS, Singh HB and Vaishnav A (2025) Mechanistic understanding of metabolic cross-talk between *Aloe vera* and native soil bacteria for growth promotion and secondary metabolites accumulation. *Front. Plant Sci.* 16:1577521. doi: 10.3389/fpls.2025.1577521

Mechanistic understanding of metabolic cross-talk between *Aloe vera* and native soil bacteria for growth promotion and secondary metabolites accumulation

Neha Singh Chandel, H. B. Singh and Anukool Vaishnav*

Department of Biotechnology, GLA University, Mathura, Uttar Pradesh, India

Plants release a wealth of metabolites into the rhizosphere that can influence the composition and activity of microbial communities. These communities, in turn, can affect the growth and metabolism of the host plant. The connection between medicinal plant and its associated microbes has been suggested, yet the mechanisms underlying selection of indigenous microbes, and their biological function in medicinal plants are largely unknown. In this study, we investigated how the *Aloe vera* plants select its rhizosphere bacteria and examined their functional roles in relation to plant benefit. We utilized two native plant growth promoting rhizobacterial (PGPR) strains of *Aloe vera*: *Paenibacillus* sp. GLAU-BT2 and *Arthrobacter* sp. GLAU-BT16, as either single or consortium inoculants for plant growth experiment. We analyzed non-targeted root metabolites in the presence of both single and consortium bacterial inoculants and confirmed their exudation in the rhizosphere. The GC-MS analysis of metabolites revealed that the bacterial inoculation in *Aloe vera* plants amplified the abundance of flavonoids, terpenes and glucoside metabolites in the roots, which also exuded into the rhizosphere. Flavonoids were the most common prevalent metabolite group in individual and consortium inoculants, highlighting their role as key metabolites in interactions with rhizosphere microbes. In addition, the bacterial inoculants significantly increased antioxidant activity as well as total phenolic and flavonoid content in the leaves of *Aloe vera*. In conclusion, we propose a model of circular metabolic communication in which rhizosphere bacteria induce the production of flavonoids in plants. In turn, the plant releases some of these flavonoids into the rhizosphere to support the indigenous microbial community for its own benefit.

KEYWORDS

***Aloe vera*, flavonoids, PGPR, plant-soil-microbe interaction, metabolic communication, secondary metabolites**

Introduction

Soil microbes have undeniably established close association with their host plants for ages, ranging from mutualistic to parasitic. In mutualistic interactions, there are dynamic changes in the physiology and metabolism of the symbiotic partners (Singh et al., 2022). This relationship provides various benefits to the host plant, including growth promotion, improved nutrient uptake, enhanced tolerance against biotic and abiotic stresses, and modulation of metabolic pathway to accumulate more bioactive metabolite contents (Kumar and Nautiyal, 2022). In return, plants provide a nutrient-rich environment for the survival of selective microbes in their surroundings. The association of plant roots with numerous soil organisms is an interesting ecological niche known as the rhizosphere, which is beneficial for most plant symbionts (Maitra et al., 2024). Plants use a variety of mechanisms to modulate their microbiome, including the exudation of secondary metabolites and the coordinated action of different defense responses (Afridi et al., 2024). The relationships that exist between plants and rhizosphere microbes are dynamic and can be species-specific or environment-dependent (Berihu et al., 2023). Host plants can actively modulate the assembly of their rhizosphere microbiome in response to stressors and other environmental factors (Luo et al., 2023). Plants communicate with beneficial microorganisms in the rhizosphere through root exudates, creating a regulated microbial community. Changes in root microbiota throughout development influence soil-microbe feedback and rhizosphere chemistry, which are vital for survival in varying conditions (Korenblum et al., 2020). This dynamic response further emphasizes the need to understand the individual interactions between rhizosphere microbes and their hosts or specific crops, and the chemical basis of such interactions, which remains elusive in most cases and is a major reason for the failure of microbial products under field conditions (Bakker et al., 2018; Liu et al., 2019).

Plant growth-promoting rhizobacteria (PGPR) are beneficial bacteria found in the rhizosphere that form symbiotic relationships with plant roots through metabolic communication (Vaishnav et al., 2017; Singh H. et al., 2021; Singh J. et al., 2021). During this interaction, plants release signaling compounds, such as organic acids and phenolic compounds, to attract PGPR in the rhizosphere (Strehmel et al., 2014; Miller et al., 2019). Plants selectively exude these compounds based on their specific needs, which influences the composition of PGPR populations (Mashabela et al., 2022). In return, PGPR produce various traits that promote plant growth, including siderophores, organic acids for nutrient solubilization, and phytohormones (Vaishnav et al., 2014; Jain et al., 2014). These contributions lead to root elongation, improved overall growth, enhanced nutrient uptake, and increased plant defenses (Noumavo et al., 2013; Prasad et al., 2019). Among these beneficial bacteria, *Paenibacillus* spp. is the most abundant operational taxonomic unit (OTU) in the plant microbiome (Langendries and Goormachtig, 2021). It promotes growth through nitrogen fixation, phosphate solubilization, and phytohormone production, while also offering protection against pests and pathogens through antimicrobial compounds (Grady et al., 2016). Inoculating soil with *P. polymyxa* has been shown to improve microbial diversity and crop yields. For instance, in poplar plantations, it increased beneficial bacteria and reduced harmful fungi (Sui et al., 2019). Similarly, *Arthrobacter* spp. also hold significant potential as PGPR and can be found in various extreme environments, such as saline areas, drought-prone regions, and polluted soils. They play a vital role in protecting plants from abiotic stresses and enhancing plant nutrition, health, and yield (Sziderics et al., 2007; Tiwari et al., 2011; Qin et al., 2014). As key PGPR, *Arthrobacter* spp. improve iron acquisition by reducing and dissolving Fe^{3+} in the soil and also promote the growth of both leguminous and monocot plants by producing beneficial volatile compounds (Velázquez-Becerra et al., 2011; del-Carmen-Orozco-Mosqueda et al., 2013; Flores-Cortez et al., 2019).

In recent years, several studies on medicinal plants have enhanced our understanding of how the plant symbionts impact the quality of the host plant by influencing their medicinal metabolite compounds (Sharma et al., 2023). The microbial symbionts associated with medicinal plants have shown the ability to produce new leads of secondary metabolites with industrial and biotechnological implications, as well as stimulate plant growth and development (Wu W. et al., 2021). *Aloe vera* is highly sought after for its medicinal and cosmetic uses globally, attributed to therapeutic properties of its several secondary metabolites found in the leaf gel (Taher et al., 2024). Despite India being the largest producer of *Aloe vera*, it still struggles to meet the increasing demand for it (Lawal et al., 2021). Reproductive challenges and susceptibility to diseases pose threats to the productivity and yield of metabolite contents in *Aloe vera* (Kiran et al., 2017; Berhe et al., 2023). In addition, the excessive or unsustainable use of different cultivars of *Aloe vera* has placed them at a high risk of extinction, categorized in the red list by the International Union for Conservation of Nature (IUCN) (Bachman et al., 2020). Although efforts have been made to increase productivity and yield of metabolite contents in *Aloe vera*, they have limitations in large-scale production due to limited knowledge of the defined metabolic pathway in *Aloe vera*. The existing approaches such as heterologous gene expression, plant cell culture engineering, and breeding methods are insufficient to meet industrial demand (Isah et al., 2018; Wu T. et al., 2021). Reports indicate that the production of bioactive secondary metabolites in medicinal plants is stimulated by their associated microbes (Wu W. et al., 2021; Tripathi et al., 2022). The isolation of these plant associated microbes could be highly beneficial for large-scale production of bioactive secondary metabolites with medicinal value. However, the understanding of the relationship between the accumulation of bioactive components of *Aloe vera* and the root-associated microbiome is still limited and fragmented in the few studies (Chandra et al., 2024).

In this study, we aimed to assess how *Aloe vera* recruits beneficial bacteria in the rhizosphere. To do this, we used two native PGPR strains *Paenibacillus* sp. GLAU-BT2 (GenBank accession number- PV083208) and *Arthrobacter* sp. GLAU-BT16 (GenBank accession number- PV083209), previously isolated from *Aloe vera*'s rhizosphere (Unpublished data). These bacterial strains

were used as a single and consortium inoculant to perform plant growth experiment with *Aloe vera*. We then assessed the effects of these bacterial strains on root metabolites and their secretion in the rhizosphere soil as well. We further investigated the bacterial effects on plant growth and secondary metabolites accumulation in the leaves of *Aloe vera*.

Materials and methods

Biological materials

We utilized pure cultures of two PGPR isolates *Paenibacillus* sp. GLAU-BT2 and *Arthrobacter* sp. GLAU-BT16, previously isolated from *Aloe vera* rhizosphere and stored in slant cultures at 4°C in the Plant biotechnology laboratory, Department of Biotechnology, GLA University, Mathura, India. *Aloe vera*'s root suckers were collected from a field crop growing in Horticulture Garden, GLA University, Mathura, India. All root suckers were surface sterilized before using in pot experiment. For bacterial inoculum preparation, a 24-hour-old bacterial culture was used, and the cell pellet was resuspended in sterile water to achieve a final concentration of 10^8 CFU/mL for inoculation.

Cross-compatibility of bacterial strains and development of the consortium inoculum

The cross-compatibility of both *Paenibacillus* sp. GLAU-BT2 and *Arthrobacter* sp. GLAU-BT16 was tested for growth by spotting them on Luria-Bertani (LB) agar plates and for biofilm formation in microtiter plates under broth medium. Bacterial growth occurring together indicated that the selected strains can work together as a consortium. The consortium was formed by growing the bacterial strains individually in LB broth until reaching the desired population (10^8 CFU). After that, both cultures were mixed in equal ratios and used to inoculate *Aloe vera* rhizomes.

Plant growth experiment with bacterial inoculation

The pot experiment aimed to assess the efficacy of both bacterial strains individually and in a consortium on the growth and metabolite contents of *Aloe vera* plants. This experiment was conducted in 5-liter earthen pots filled with sterilized soil. The bacterial inoculums were applied through dipping pre-sterilized root suckers of *Aloe vera* in the bacterial solutions for 1 hour before planting them in pots. This experiment was consisted of four treatment groups: (T1)- Control (without bacterial inoculation); (T2) GLAU-BT2 inoculation; (T3) GLAU-BT16 inoculation; (T4) Consortium inoculation (GLAU-BT2+GLAU-BT16). Each treatment was conducted with four replicates. The plants were watered weekly with sterile water, and all necessary plant protection measures were followed throughout the experiment. Plants were harvested 90 days after inoculation, and leaf parameters were measured, including number of leaves and their width and fresh weight.

Biochemical estimation of secondary metabolites in the leaves of *Aloe vera*

After harvesting, the plants were taken for testing phytochemical estimations. The plant leaves were dried in the oven at 50 °C for 48 hours, ground into powder, and used to estimate the total phenol, flavonol, flavonoid contents, and DPPH, following the protocol provided by Sharma et al. (2014). Total phenol contents were measured using Folin-Ciocalteu reagent and absorbance was taken at 765 nm. The total phenolic contents were expressed in terms of gallic acid equivalent (mg/g dry weight). Similarly, the total flavonoid contents were measured by aluminum chloride colorimetric method, and absorbance was measured at 415 nm. The total flavonoid contents were expressed in terms of quercetin equivalent (mg/g dry weight). Furthermore, the total flavonol contents were measured at an absorbance of 440 nm and expressed in terms of quercetin equivalent (mg/g dry weight). Additionally, the DPPH was used to measure the free radical scavenging activity of the leaf extract, and absorbance was measured by a spectrophotometer at 517 nm, in which ascorbic acid was used as the standard (Sharma et al., 2014). The antioxidant activity percentage (%) was determined by the following formula, whereas AC = absorbance of DPPH solution without extract and AE = absorbance of the tested extract.

$$\text{Antioxidant activity (\%)} = [(AC - AE)/AC] \times 100$$

Extraction of metabolites from root and rhizosphere soil

To verify the exudation of root metabolites in the rhizosphere, nontargeted metabolites were extracted from both the roots and the adhering soil. For the root extracts, 50 mg of dried root samples were ground, and metabolites were extracted using 1 mL of precooled methanol. The mixture was subjected for sonication on ice bath followed by centrifugation at 14,000 g for 20 minutes at 4°C. The supernatant was collected and concentrated to dryness under vacuum and finally dissolved in 400 µL of cold methanol for gas chromatography-mass spectrometry (GC-MS) analysis (Kang et al., 2019). For rhizosphere soil sampling, soil was collected at 1 cm from the roots by gently scraping the surface. Additionally, soil attached directly to the roots was shaken off and collected. The extraction of exudates from soil samples was done according to method of Eze and Amuji (2024) and was subsequently dissolved in methanol for final analysis. Two different reference controls were used in this experiment to eliminate native soil metabolites and bacterial metabolites without presence of plant. These controls involved setups with no plants grown in the pots: (A) only sterile soil in the pot and (B) soil inoculated with a consortium of microorganisms.

Characterization of metabolite compounds through GC–MS analysis

The purified methanolic extract was subjected to GC-MS analysis in a Perkin Elmer GC-MS Clarus® SQ 8 equipped with DB-5MS (Agilent, USA) capillary standard non-polar column with dimensions 0.25 mm OD x 0.25 µm ID x 30 m length. The instrument was set to an initial temperature of 40°C, and the injection port temperature was ensured at 220°C, interface temperature set 250°C, source kept at 220°C, oven temperature programmed as 75°C for 2 min, 150°C @ 10°C/min, up to 250°C at 10°C per min. The GC conditions were: 1:12 split, helium carrier at 20 psi. The MS conditions were positive ion mode, electron impact spectra at 70 eV. The mass spectral scan range was set at 50 to 600 Da. The MS peaks were determined by their scatter pattern. The linear regression coefficient was used to calculate the concentrations in the samples from peak areas obtained in the chromatographs. The bioactive molecules were identified by comparison of mass spectra with NIST 08 Mass Spectra Library (National Institute of Standards and Technology). The name, molecular weight, and structure were ascertained from NIST, PubChem, and HMDB databases (Leylaie and Zafari, 2018).

Data processing and statistical analysis

Conformity with the assumptions of analysis of variance (ANOVA) were checked for the different data by ShapiroWilk test for normality and Levene's test for homogeneity of variances using the "car" package in R 4.2.2 (R Core Team, 2022). The data were analyzed by one-way ANOVA, followed by *post hoc* Tukey's test to separate treatment means if ANOVA results were significant ($p<0.05$). For comparative analysis of metabolites in different treatments, the GC-MS data from six distinct groups were imported into separate data frames using RStudio. The initial step involved processing the data to generate chord diagrams that illustrate the connections between compounds and their respective properties. To achieve this, we created new data frames for each group, focusing on the "Compound" and "Properties" columns. Properties listed in a single cell and separated by commas were then expanded so that each cell contained only a single property, thereby ensuring the singularity of the "Properties" column. The information about compounds was replicated for the new rows to maintain consistency, reducing redundancy where the same property was previously recorded in multiple cells. Preprocessing included the removal of leading and trailing whitespaces from both columns. We used the circlize package (Gu et al., 2014) to create chord diagrams for each group, which were subsequently combined into a composite collage. For visualization of intersections among the sets of compounds, we utilized the UpSetR package (Conway et al., 2017), opting for this approach over a Venn diagram due to the complexity of having more than five sets, which can obscure intersection details in Venn diagrams. Color schemes were adjusted discretely to clearly differentiate between intersections and other visual representations.

Results

Co-inoculation of bacterial strains promote leaf growth parameters

The impact of both bacterial strains on the growth of *Aloe vera* plants was examined by determining different leaf growth parameters. There was a significant effect of different treatments in the leaf number ($F_{3,12}$= 14.56, $p<0.001$), leaf width ($F_{3,12}$= 5.5, $p<0.05$) and leaf fresh weight ($F_{3,12}$= 1322, $p<0.001$). The highest value of leaf growth parameters were observed in consortium inoculation, while individual inoculation showed similar trend to control plants (Figure 1).

Bacterial inoculation induces production of secondary metabolites in leaves

Different treatments had a significant impact on the total flavonoid content ($F_{3,12}$= 187.7, $p<0.001$), total flavonol content ($F_{3,12}$= 93.6, $p<0.001$) and total phenolic content ($F_{3,12}$= 241.5, $p<0.001$) in the leaves of *Aloe vera* plant. The highest concentrations of all secondary metabolites were observed in consortium inoculated plants. In terms of total phenolic and flavonol content, both individual bacterial inoculations also resulted in significantly higher levels compared to control plants. However, for total flavonoids, the GLAU-BT16 individual inoculum showed a similar content to the control (Figures 2A–C). Additionally, the antioxidant activity measured by the DPPH assay in the leaf extract was significantly influenced by treatment groups ($F_{3,12}$= 660.6, $p<0.001$). The highest DPPH activity was observed in the consortium treatment compared to the other treated plants (Figure 2D).

Bacterial inoculated roots release distinctive metabolites into the rhizosphere

GC-MS profiling of metabolites from both roots and rhizosphere soil was conducted across all treatment groups, resulting in a final list of compounds after excluding their respective control groups. The number of compounds varied among the treatments. The highest number, 39 compounds, was observed in the rhizosphere soil of GLAU-BT16, while the lowest number, 35 compounds, was observed in the rhizosphere soil of GLAU-BT2 and in the roots of consortium inoculated plants. The final list of compounds, along with their properties, is summarized in Supplementary Tables S1-S6. Most compounds were detected within a retention time (RT) range of 3.1 to 31.3 minutes.

A total of 10 compounds were consistently identified in both the roots and rhizosphere soils across all treatment groups, indicating their stable presence. These compounds are "2,5-di-tert-Butylaniline", "7-Tetradecyne", "3-Octadecyne", "trans-2-Decen-1-ol, methyl ether", "1-Methylbicycloctane", "Octadecadienoic acid, methyl ester", "2H-Benzocyclohepten-2-one", "Octadecatrienoic acid", "3,4-Dimethyl-1-dimethyl(trimethylsilylmethyl)" and

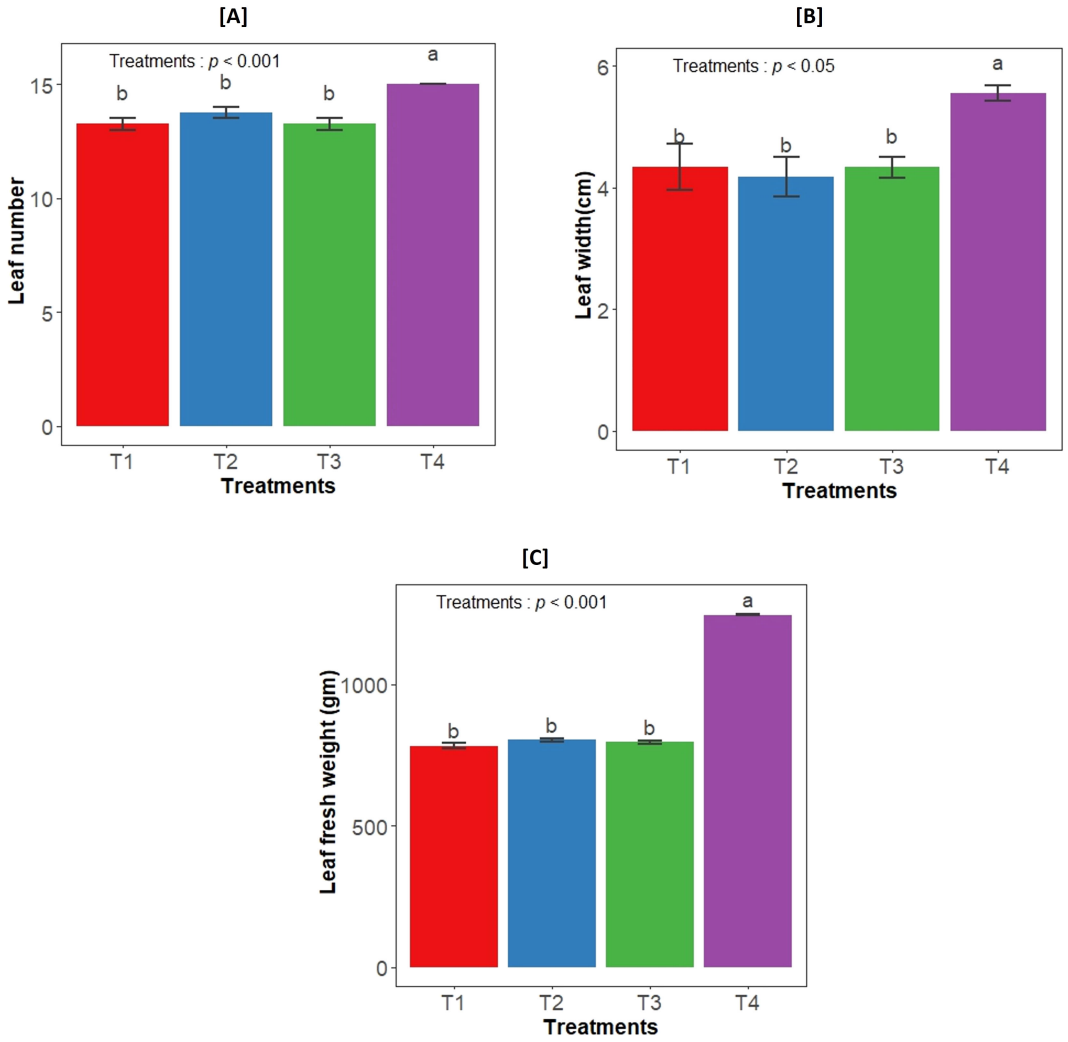

FIGURE 1
Effect of bacterial inoculation on **(A)** Leaf number, **(B)** Leaf width, and **(C)** Leaf fresh weight. T1- uninoculated plant (control); T2- GLAU-BT2 inoculation; T3- GLAU-BT16 inoculation; and T4- Consortium inoculation (GLAU-BT2 + GLAU-BT16). The results are presented as mean values± SE, (n=4). The presence of different letters on each bar indicates a statistically significant difference between the treatment means. The means were separated by Tukey's *post-hoc* test (p<0.05), following a significant one-way ANOVA analysis.

"Cyclooctene, 5,6-diethenyl". Each treatment group also exhibited unique compounds that were not found in other groups. The highest number of unique compounds, 9, was identified in the rhizosphere soil of GLAU-BT16 inoculated treatment, which were absent in all other treatments.

In terms of root metabolite exudation into the rhizosphere, two unique compounds "2-Butenoic acid, 2-methyl" and "Pentanedioic acid, bis-dodecylamide" were exuded from the consortium treated roots into their rhizosphere soil. Additionally, two unique compounds, "1,3-dioxane-5,5-dimethanol, 2-hexyl" and "Cyclohexane, [6-cyclopentyl-3-(3-cyclopentylpropyl)hexyl]", were exuded from the roots inoculated with GLAU-BT16, while one unique compound "Myricitrin" was exuded from the roots of GLAU-BT2 inoculated plants.

All identified compounds were researched in the available literature, and their reported activities are listed in the compiled Supplementary Tables S1-S6. The property "Antimicrobial" emerged as the most prevalent across all treatment groups, followed by "Antioxidant". A collage of chord diagrams was created to visually represent the connections between individual compounds and their properties (Figure 3). An UpSet plot was also generated to understand the intersections of compounds among different treatment groups (Figure 4).

Discussion

Plant-microbe interactions are complex and play a significant role in the metabolism of both plants and microbes. Using a metabolomics approach, researchers can identify low molecular weight metabolites involved in these interactions. Changes in these metabolites can provide insights into how plants and microbes respond to each other during specific physiological periods (Fiehn, 2002; Yang et al., 2017). Research on soil metabolomics has focused

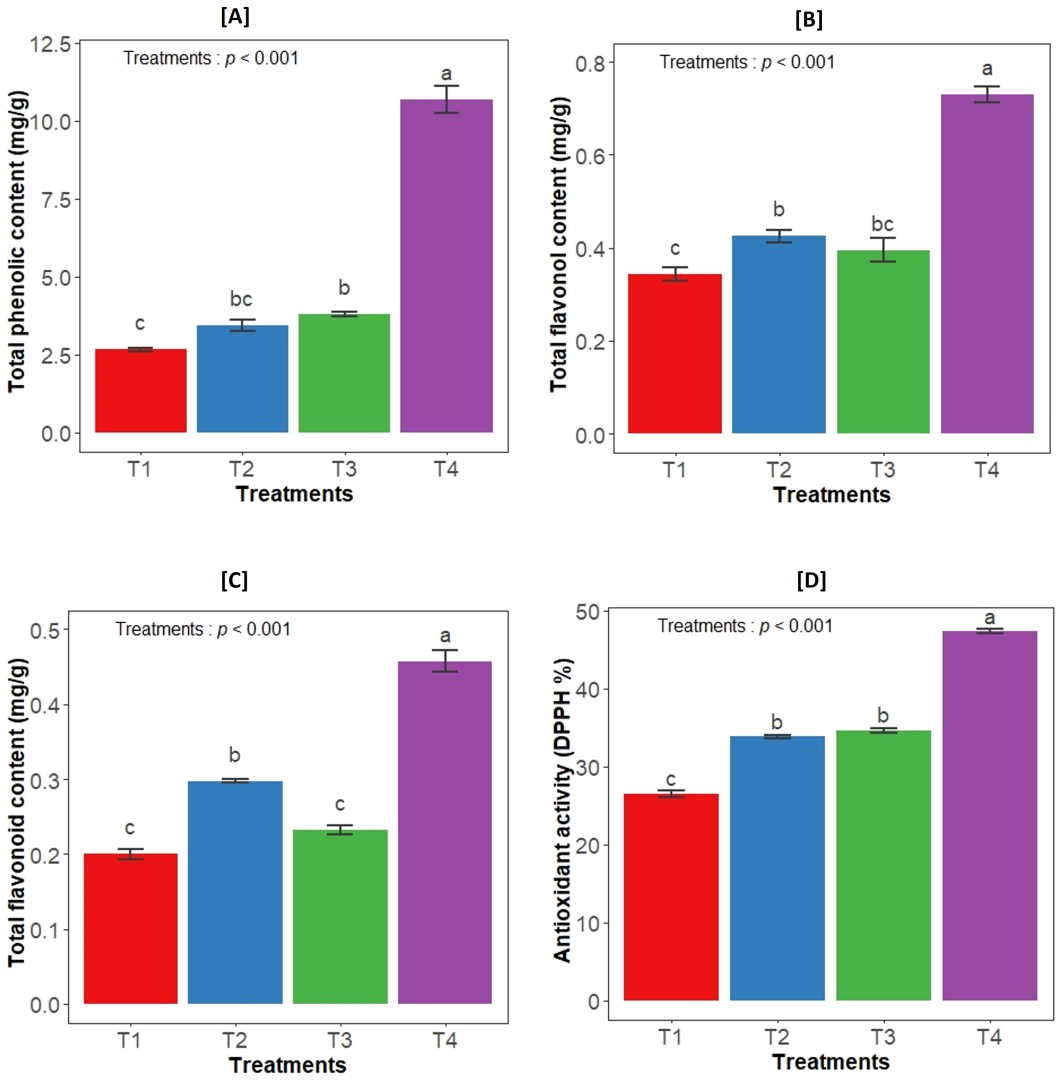

FIGURE 2
Effect of bacterial inoculation on **(A)** total phenolic content, **(B)** total flavonol content, **(C)** total flavonoid content and **(D)** antioxidant activity (DPPH). T1- uninoculated plant (control); T2- GLAU-BT2 inoculation; T3- GLAU-BT16 inoculation; and T4- Consortium inoculation (GLAU-BT2 + GLAU-BT16). The results are presented as mean values± SE, (n=4). The presence of different letters on each bar indicates a statistically significant difference between the treatment means. The means were separated by Tukey's *post-hoc* test (p<0.05), following a significant one-way ANOVA analysis.

on understanding the relationships among plants, soil, and microbes by exploring "community metabolomics", which considers both plant root exudates and microbial products (Jones et al., 2014; Huang et al., 2014). In this study, we examined the root metabolites of *Aloe vera* and their exudation into the rhizosphere while inoculating with two PGPR strains. Although collecting exudates from *Aloe vera* is challenging due to the large size of its roots, we aimed to identify common compounds present in both the roots and rhizosphere soil, even considering potential changes caused by microbial activity.

Our findings indicate that the consortium inoculum of *Paenibacillus* sp. GLAU-BT2 and *Arthrobacter* sp. GLAU-BT16 has a greater positive effect on the growth of *Aloe vera* plant than individual inoculants. Previous studies have demonstrated that using a mixed inoculant, rather than individual, promotes plant growth by increasing the number of surviving cells in their natural environments (Tittabutr et al., 2007; Sharma et al., 2017; Thanni et al., 2024). Our results align with previous studies on *Paenibacillus* sp. and *Arthrobacter* sp., which showed that plants inoculated with these bacterial strains exhibited enhanced growth parameters (Mohd Din et al., 2020; Chhetri et al., 2022; Jia et al., 2022; Özdoğan et al., 2022). Notably, co-inoculating *A. ureafaciens* DnL1-1 and *Trichoderma harzianum* significantly boosts biomass in wheat (Yang et al., 2021). In our results, the higher leaf biomass observed in bacterial-inoculated plants suggest that PGPR strains may increase nutrient uptake in *Aloe vera* plants through their nutrient solubilizing activities, as seen in GLAU-BT2 and GLAU-BT16 strains (Unpublished data). Earlier research also highlights nutrient solubilizing and other plant growth promoting properties in various

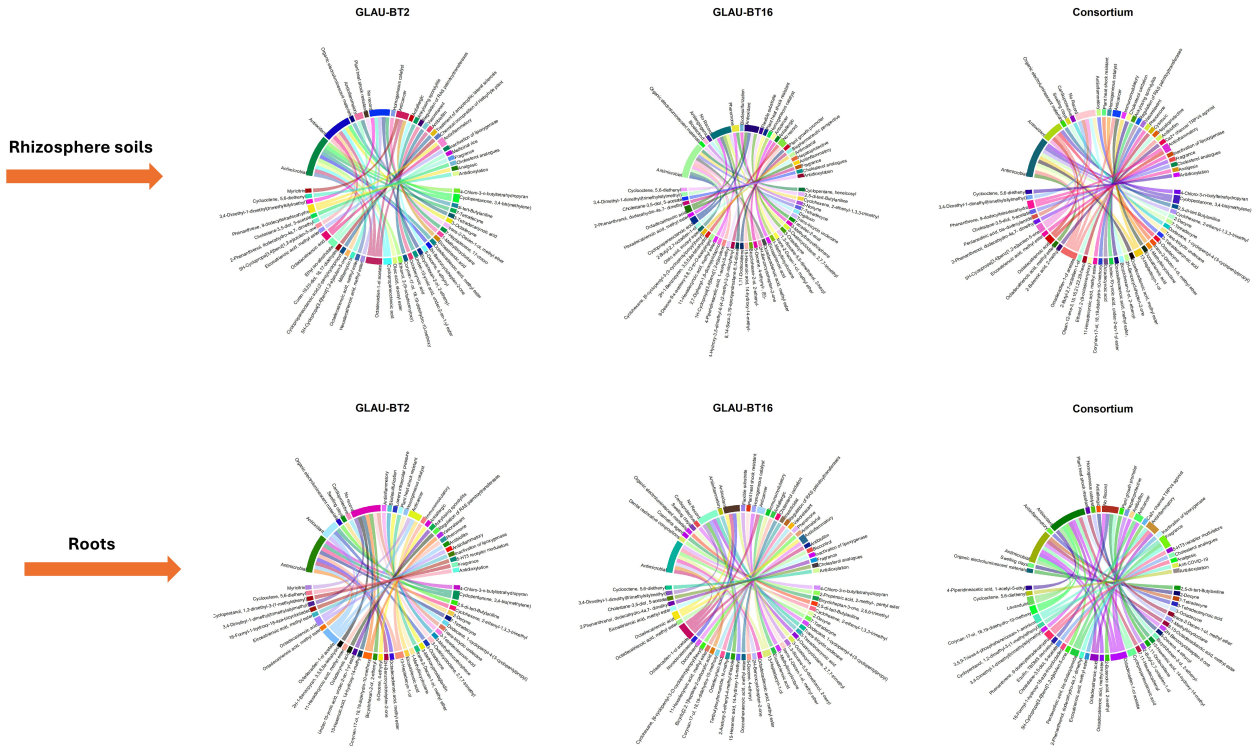

FIGURE 3
Chord diagrams illustrating the associations between compounds and properties across root metabolites and rhizosphere soil metabolites present in all bacterial treatments. The figure is presented as a collage, with each chord diagram representing a separate group. The diagrams are organized into with each plot titled according to its respective group.

strains of *Paenibacillus* and *Arthrobacter* (Banerjee et al., 2010; Grady et al., 2016; Chhetri et al., 2022).

The co-inoculation of GLAU-BT2 and GLAU-BT16 in the host plant *Aloe vera* significantly increased the leaf metabolite contents, including total flavonoids, flavonol, phenolic compounds, and total antioxidant activity. The therapeutic benefits of *Aloe vera* are attributed to the antioxidant properties of its phytochemical components, which can scavenge free radicals and reduce oxidative damage associated with various plant diseases (Mahapatra, 2021; Singh and Vaishnav, 2022; Nwozo et al., 2023). These findings align with previous studies that demonstrated that plants inoculated with different species of *Arthrobacter* induced the accumulation of secondary metabolites, particularly influencing carbohydrate metabolism in the plant leaves (Ramírez-Ordorica et al., 2020; Chhetri et al., 2022). Similarly, a co-inoculation experiment with *Paenibacillus* and *Bacillus subtilis* in wheat cultivars revealed a differential accumulation of compounds across several classes of metabolites, including phenylpropanoids, organic acids, lipids, organoheterocyclic compounds, and benzenoids in leaf tissue (Mashabela et al., 2022). The higher accumulation of flavonoids and phenolic compounds is primarily exuded from the roots to attract beneficial microbes in the rhizosphere (Gu et al., 2020; Sharma et al., 2021; Korenblum et al., 2022). In our findings, we also observed flavonoid compound 'Myricitrin' especially in *Paenibacillus* sp. GLAU-BT2 treated plant roots as well as in rhizosphere soil. It can be suggested that the presence of *Paenibacillus* sp. GLAU-BT2 and *Arthrobacter* sp. GLAU-BT16 in the *Aloe vera* rhizosphere may result from the exudation of flavonoid and phenolic compounds (Reynolds, 1985). Once these microbes colonize the rhizosphere, they stimulate nutrient uptake in the host plant, leading to increased production of flavonoids and phenolic compounds. These compounds are then exuded and recirculated in the rhizosphere, allowing beneficial microbes to enhance their population and colonization within the host plant (Figure 5). This hypothesis is based on the concept of a circular metabolic economy in plant-microbe interactions, where flavonoids, the most studied class of chemical exudates, have diverse effects on soil microorganisms (Korenblum et al., 2022).

The GC-MS analysis identified various categories of compounds in both root and rhizosphere soil. Plant root exudates play a significant role in transforming and modifying the conditions of the rhizosphere. These exudates are often considered the first line of communication between plants and the microorganisms residing in the rhizosphere (Oburger et al., 2009; Sharma et al., 2021). The presence of antimicrobial metabolites in both the root and rhizosphere suggests that these compounds inhibit the growth of pathogenic microbes in the soil and reduce competition for *Paenibacillus* sp. GLAU-BT2 and *Arthrobacter* sp. GLAU-BT16,

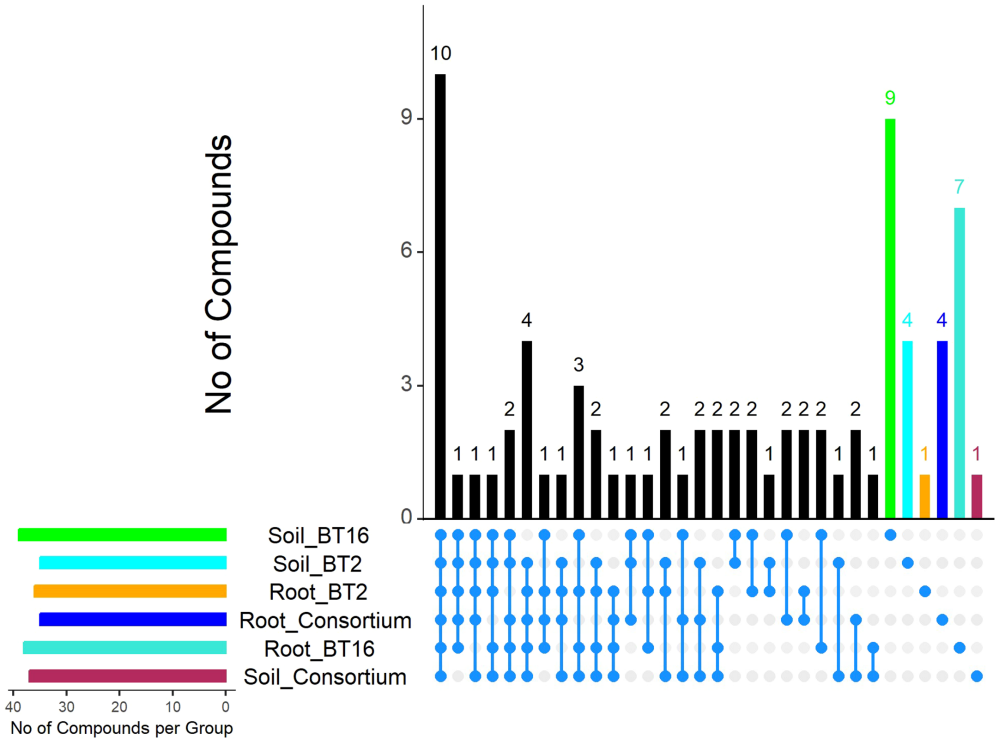

FIGURE 4
UpSet plot depicting the intersection statistics of compounds across root metabolites and rhizosphere soil metabolites present in all bacterial treatments. The bars are arranged in descending order of the number of intersections across the groups. The last six bars represent distinct values specific to each group. The colors of these bars are matched to the colors of the horizontal bars in the lower left corner, which indicate the total number of compounds in each group.

thus facilitating their growth in the rhizosphere. Moreover, *Arthrobacter* spp. have been reported to produce antimicrobial metabolites that exhibit biocontrol activity; for instance, *Arthrobacter agilis* produces dimethylhexadecylamine, which inhibits the growth of phytopathogenic fungi *in vitro* (Velázquez-Becerra et al., 2013). Additionally, interactions between wheat and *A. ureafaciens* DnL1-1, as well as *Trichoderma harzianum*, led to the modulation of soil metabolites, particularly amino acids, organic acids, triterpenoids, coumarins, and flavonoid contents in the rhizosphere soil (Yang et al., 2021).

Benzenoids and their derivatives were the most detected compounds in the metabolites of both root and rhizosphere soil, followed by lipids and organoheterocyclic compounds. These specialized aromatic metabolites, often classified as volatile organic compounds (VOCs), are produced by microorganisms and play crucial roles in plant defense, stress response, and interactions at the plant–microbe interface (Misztal et al., 2015; Vaishnav et al., 2017; Lackus et al., 2021). Their significance in belowground plant-plant and plant-microbe communications has gained increased attention (Schenkel et al., 2018; Singh J. et al., 2021). Furthermore, phenolic compounds serve as substrates or signaling molecules for various soil microbes (Badri et al., 2013). They enhance plant defenses against pathogens and contribute to abiotic stress responses (Irfan et al., 2019).

Other common compounds included organic acids and fatty acids (Butenoic acid, Hexenoic acid, 3-Tetradecynoic acid, Eicosatrienoic acid, Octadecynoic acid, and Piperidineacetic acid) were present in the metabolites of both root and rhizosphere soil from bacterial treatments. Organic acids are common exudates that have gained interest for their diverse roles as metabolites in the rhizosphere, as they can be produced by both plant roots and microorganisms (Tuason and Arocena, 2009). These acids facilitate nutrient solubilization, promote microbial growth, detoxify harmful and influence bacterial chemotaxis (Menezes-Blackburn et al., 2016; Jiang et al., 2017; Macias-Benitez et al., 2020). Additionally, fatty acids serve as energy reserves and are crucial for membrane lipids, acting as markers for microorganisms while also playing a role in plant defense (Kang et al., 2019).

Moreover, terpenes, fatty aldehydes, glucosides, and flavonoids were also detected in the metabolites of both root and rhizosphere soil. Terpenes, the largest group of plant secondary metabolites with vast diversity, have been found to have dual effects on soil microbes. Terpenes are reported to promote the proliferation of bacterial strains belonging to Proteobacteria while inhibiting the growth of Actinobacteria strains (Bai et al., 2021). Similarly, the biosynthesis of glucoside metabolites in plants is crucial for interaction with soil microbes and in shaping the rhizosphere community for their host plants (Hu et al., 2018; Koprivova et al., 2019). These findings

emphasize the importance of understanding the role of root metabolites in the rhizosphere for attracting PGPR strains and enhancing the accumulation of secondary metabolites within plant tissue.

Conclusion

Our observations provided insights into a proposed model of circular metabolic communication within the *Aloe vera* rhizosphere. In this model, *Aloe vera* plants may release flavonoids and phenolic metabolites that shape the rhizosphere bacteria. In turn, these rhizosphere bacteria produce phytohormones and nutrient-solubilizing enzymes in the soil, which enhance nutrient uptake by the plant roots. This process leads to improved plant growth and the accumulation of flavonoids, phenolic compounds, and other secondary metabolites, which then recirculate in the rhizosphere (Figure 5). Thus, this study enriches our understanding of the metabolic interactions between plants and microbes. This knowledge could facilitate the development of metabolome-engineering strategies aimed at enhancing plant growth, priming plants for defense, and promoting sustainable agriculture.

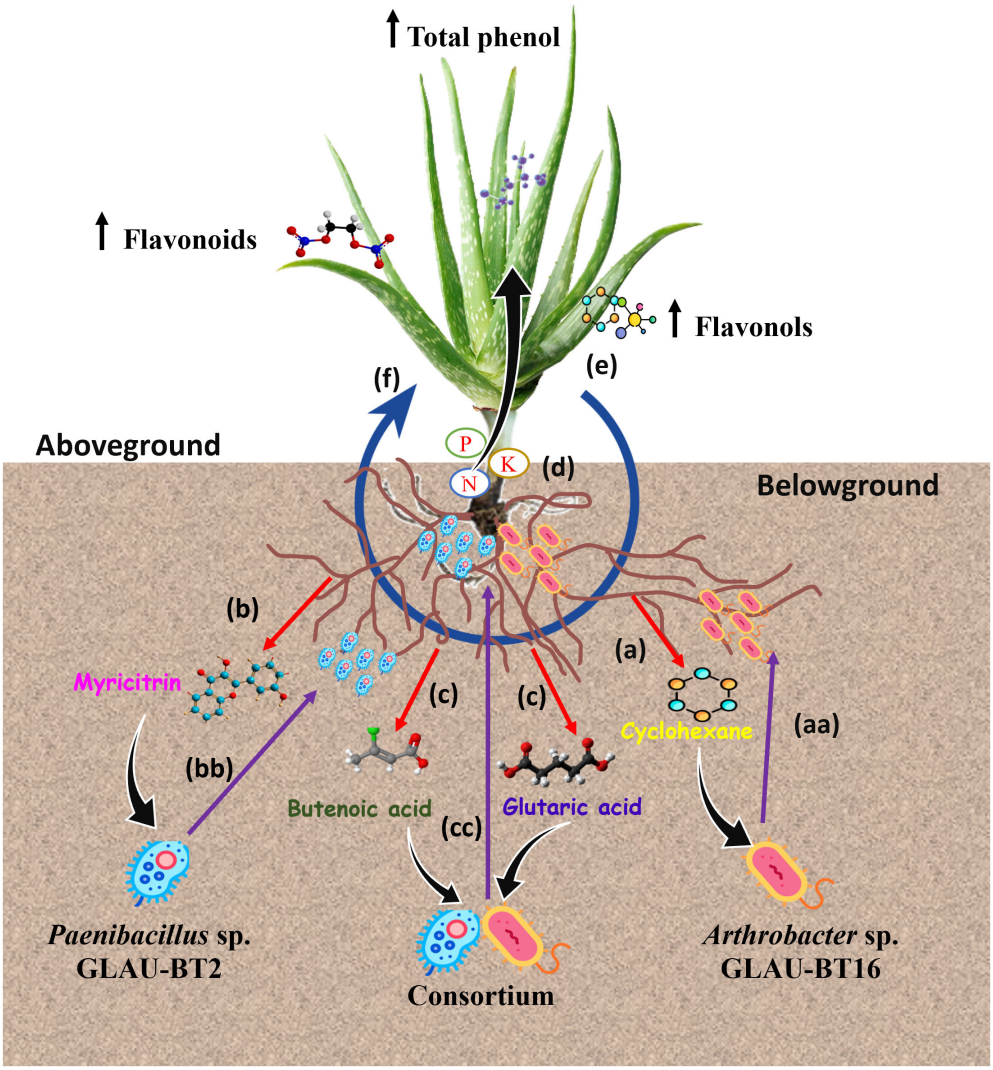

FIGURE 5
A model framework illustrating circular metabolic communication within the Aloe vera rhizosphere. Our findings suggest the following steps in metabolic communication: **(a)** Roots exude 'Cyclohexane' in response to *Arthrobacter* sp. GLAU-BT16. **(aa)** In response to 'Cyclohexane', *Arthrobacter* sp. migrate towards the rhizosphere, increasing their abundance. **(b)** Roots exude 'Myricitrin' in response to *Paenibacillus* sp. GLAU-BT2. **(bb)** In response to 'Myricitrin', *Paenibacillus* sp. move towards the rhizosphere and increase their abundance. **(c)** In response to consortium inoculation of GLAU-BT2 and GLAU-BT16, roots exude 'Butanoic acid' and 'Glutaric acid'. **(cc)** Both *Paenibacillus* sp. GLAU-BT2 and *Arthrobacter* sp. GLAU-BT16 move towards the rhizosphere, increasing their populations in response to 'Butanoic acid' and 'Glutaric acid'. **(d)** In the rhizosphere, these bacteria (GLAU-BT2 and GLAU-BT16) solubilize nutrients, aiding in their uptake by plants. **(e)** The enhanced nutrient uptake leads to an increase in the accumulation of total phenols, flavonoids, and flavonol in the plants. **(f)** Some of the accumulated metabolites are recirculated in the rhizosphere.

Data availability statement

The original contributions presented in the study are included in the article/Supplementary Material. Further inquiries can be directed to the corresponding author.

Author contributions

NC: Formal Analysis, Investigation, Methodology, Writing – original draft. HS: Conceptualization, Project administration, Supervision, Writing – review & editing. AV: Supervision, Writing – review & editing.

Funding

The author(s) declare that no financial support was received for the research and/or publication of this article.

Acknowledgments

The authors would like to express their gratitude to Prof. Shoorvir Singh, Head of the Department of Biotechnology at GLA University, Mathura, for his unwavering support during this experiment. Authors also extend thanks to Prof. Sivakumar Uthandi and Dr. Shobana Narayanasamy at Department of Agricultural Microbiology, Tamil Nadu Agricultural University for their support in GC-MS analysis. Additionally, Authors are thankful to Dr. Jagajjit Sahu for analyzing the GC-MS results.

Conflict of interest

The authors declare that the research was conducted in the absence of any commercial or financial relationships that could be construed as a potential conflict of interest.

Generative AI statement

The author(s) declare that no Generative AI was used in the creation of this manuscript.

Publisher's note

Supplementary material

The Supplementary Material for this article can be found online at: https://www.frontiersin.org/articles/10.3389/fpls.2025.1577521/full#supplementary-material

References

Afridi, M. S., Kumar, A., Javed, M. A., Dubey, A., de Medeiros, F. H. V., and Santoyo, G. (2024). Harnessing root exudates for plant microbiome engineering and stress resistance in plants. *Microbiological Res.* 279, 127564. doi: 10.1016/j.micres.2023.127564

Bachman, S. P., Wilkin, P., Reader, T., Field, R., Weber, O., Nordal, I., et al. (2020). Extinction risk and conservation gaps for Aloe (Asphodelaceae) in the Horn of Africa. *Biodivers. Conserv.* 29, 77–98.

Badri, D. V., Chaparro, J. M., Zhang, R., Shen, Q., and Vivanco, J. M. (2013). Application of natural blends of phytochemicals derived from the root exudates of Arabidopsis to the soil reveal that phenolic-related compounds predominantly modulate the soil microbiome. *J. Biol. Chem.* 288, 4502–4512. doi: 10.1074/jbc.M112.433300

Bai, Y., Fernández-Calvo, P., Ritter, A., Huang, A. C., Morales-Herrera, S., Bicalho, K. U., et al. (2021). Modulation of Arabidopsis root growth by specialized triterpenes. *New Phytol.* 230, 228–243. doi: 10.1111/nph.v230.1

Bakker, P. A., Pieterse, C. M., de Jonge, R., and Berendsen, R. L. (2018). The soil-borne legacy. *Cell* 172, 1178–1180. doi: 10.1016/j.cell.2018.02.024

Banerjee, S., Palit, R., Sengupta, C., and Standing, D. (2010). Stress induced phosphate solubilization by Arthrobacter sp. and *Bacillus* sp. isolated from tomato rhizosphere. *Aust. J. Crop Sci.* 4, 378–383.

Berhe, B. D., Sbhatu, D. B., Munawar, T. M., and Gebreyohannes, G. (2023). Aloe monticola Reynolds: A refugee of the mountains– contributing towards its conservation through *in vitro* propagation. . *Heliyon* 9. doi: 10.1016/j.heliyon.2023.e22955

Berihu, M., Somera, T. S., Malik, A., Medina, S., Piombo, E., Tal, O., et al. (2023). A framework for the targeted recruitment of crop-beneficial soil taxa based on network analysis of metagenomics data. *Microbiome* 11, 8. doi: 10.1186/s40168-022-01438-1

Chandra, H., Yadav, A., Prasad, R., Kalra, S. J. S., Singh, A., Bhardwaj, N., et al. (2024). Fungal endophytes from medicinal plants acting as natural therapeutic reservoir. *Microbe* 100073. doi: 10.1016/j.microb.2024.100073

Chhetri, G., Kim, I., Kang, M., So, Y., Kim, J., and Seo, T. (2022). An isolated Arthrobacter sp. enhances rice (*Oryza sativa* L.) plant growth. *Microorganisms* 10, 1187. doi: 10.3390/microorganisms10061187

Conway, J. R., Lex, A., and Gehlenborg, N. (2017). UpSetR: an R package for the visualization of intersecting sets and their properties. *Bioinformatics* 33, 2938–2940. doi: 10.1093/bioinformatics/btx364

del-Carmen-Orozco-Mosqueda, M., Velázquez-Becerra, C., Macías-Rodríguez, L. I., Santoyo, G., Flores-Cortez, I., Alfaro-Cuevas, R., et al. (2013). *Arthrobacter agilis* UMCV2 induces iron acquisition in *Medicago truncatula* (strategy I plant) *in vitro* via dimethylhexadecylamine emission. *Plant Soil* 362, 51–66. doi: 10.1007/s11104-012-1263-y

Eze, M. O., and Amuji, C. F. (2024). Elucidating the significant roles of root exudates in organic pollutant biotransformation within the rhizosphere. *Sci. Rep.* 14, 2359. doi: 10.1038/s41598-024-53027-x

Fiehn, O. (2002). Metabolomics – the link between genotypes and phenotypes. *Plant Mol. Biol.* 48, 155–171. doi: 10.1023/A:1013713905833

Flores-Cortez, I., Winkler, R., Ramírez-Ordorica, A., Elizarraraz-Anaya, M. I. C., Carrillo-Rayas, M. T., Valencia-Cantero, E., et al. (2019). A mass spectrometry-based study shows that volatiles emitted by *Arthrobacter agilis* UMCV2 increase the content of brassinosteroids in *Medicago truncatula* in response to iron deficiency stress. *Molecules* 24, 3011. doi: 10.3390/molecules24163011

Grady, E. N., MacDonald, J., Liu, L., Richman, A., and Yuan, Z. C. (2016). Current knowledge and perspectives of *Paenibacillus*: a review. *Microbial Cell factories* 15, 1–18. doi: 10.1186/s12934-016-0603-7

Gu, Z., Gu, L., Eils, R., Schlesner, M., and Brors, B. (2014). circlize Implements and enhances circular visualization in R. *Bioinformatics* 30, 2811–2812. doi: 10.1093/bioinformatics/btu393

Gu, Y., Wang, X., Yang, T., Friman, V. P., Geisen, S., Wei, Z., et al. (2020). Chemical structure predicts the effect of plant-derived low-molecular weight compounds on soil

microbiome structure and pathogen suppression. *Funct. Ecol.* 34, 2158–2169. doi: 10.1111/1365-2435.13624

Hu, L., Robert, C. A., Cadot, S., Zhang, X. I., Ye, M., Li, B., et al. (2018). Root exudate metabolites drive plant-soil feedbacks on growth and defense by shaping the rhizosphere microbiota. *Nat. Commun.* 9, 2738. doi: 10.1038/s41467-018-05122-7

Huang, Y., Chen, G., Liu, X., Shao, Y., Gao, P., Xin, C., et al. (2014). Serum metabolomics study and eicosanoid analysis of childhood atopic dermatitis based on liquid chromatography–mass spectrometry. *J. Proteome Res.* 13, 5715–5723. doi: 10.1021/pr5007069

Irfan, M., Dar, M. I., Raghib, F., Ahmad, B., Raina, A., Khan, F. A., et al. (2019). "Role and regulation of plants phenolics in abiotic stress tolerance: an overview." in *Plant signaling molecules*. (Woodhead Publishing), 157–168. doi: 10.1016/B978-0-12-816451-8.00009-5

Isah, T., Umar, S., Mujib, A., Sharma, M. P., Rajasekharan, P. E., Zafar, N., et al. (2018). Secondary metabolism of pharmaceuticals in the plant *in vitro* cultures: strategies, approaches, and limitations to achieving higher yield. *Plant Cell Tissue Organ Culture (PCTOC)* 132, 239–265. doi: 10.1007/s11240-017-1332-2

Jain, S., Vaishnav, A., Kasotia, A., Kumari, S., and Choudhary, D. K. (2014). "Plant growth-promoting bacteria elicited induced systemic resistance and tolerance in plants." in *Emerging technologies and management of crop stress tolerance* (Academic Press), 109–132. doi: 10.1016/B978-0-12-800875-1.00005-3

Jia, Z., Zhao, L., Zhang, J., Jiang, W., Wei, M., Xu, X., et al. (2022). Glucose increases the abundance of phosphate solubilizing bacterial community for better apple seedling growth and phosphate uptake. *Agronomy* 12, 1181. doi: 10.3390/agronomy12051181

Jiang, S., Xie, F., Lu, H., Liu, J., and Yan, C. (2017). Response of low-molecular-weight organic acids in mangrove root exudates to exposure of polycyclic aromatic hydrocarbons. *Environ. Sci. pollut. Res.* 24, 12484–12493. doi: 10.1007/s11356-017-8845-4

Jones, O. A., Sdepanian, S., Lofts, S., Svendsen, C., Spurgeon, D. J., Maguire, M. L., et al. (2014). Metabolomic analysis of soil communities can be used for pollution assessment. *Environ. Toxicol. Chem.* 33, 61–64. doi: 10.1002/etc.2418

Kang, Z., Babar, M. A., Khan, N., Guo, J., Khan, J., Islam, S., et al. (2019). Comparative metabolomic profiling in the roots and leaves in contrasting genotypes reveals complex mechanisms involved in post-anthesis drought tolerance in wheat. *PloS One* 14, e0213502. doi: 10.1371/journal.pone.0213502

Kiran, S., Tirkey, A., Jha, Z., and Porte, S. S. (2017). In–vitro regeneration of aloe vera (*Aloe barbadensis* mill). *Int. J. Curr. Microbiol. Appl. Sci.* 6, 1829–1834. doi: 10.20546/ijcmas.2017.611.218

Koprivova, A., Schuck, S., Jacoby, R. P., Klinkhammer, I., Welter, B., Leson, L., et al. (2019). Root-specific camalexin biosynthesis controls the plant growth-promoting effects of multiple bacterial strains. *Proc. Natl. Acad. Sci.* 116, 15735–15744. doi: 10.1073/pnas.1818604116

Korenblum, E., Dong, Y., Szymanski, J., Panda, S., Jozwiak, A., Massalha, H., et al. (2020). Rhizosphere microbiome mediates systemic root metabolite exudation by root-to-root signaling. *Proc. Natl. Acad. Sci.* 117, 3874–3883. doi: 10.1073/pnas.1912130117

Korenblum, E., Massalha, H., and Aharoni, A. (2022). Plant–microbe interactions in the rhizosphere via a circular metabolic economy. *Plant Cell* 34, 3168–3182. doi: 10.1093/plcell/koac163

Kumar, V., and Nautiyal, C. S. (2022). Plant abiotic and biotic stress alleviation: From an endophytic microbial perspective. *Curr. Microbiol.* 79, 311. doi: 10.1007/s00284-022-03012-2

Lackus, N. D., Schmidt, A., Gershenzon, J., and Köllner, T. G. (2021). A peroxisomal β-oxidative pathway contributes to the formation of C6–C1 aromatic volatiles in poplar. *Plant Physiol.* 186, 891–909. doi: 10.1093/plphys/kiab111

Langendries, S., and Goormachtig, S. (2021). *Paenibacillus polymyxa*, a Jack of all trades. *Environ. Microbiol.* 23, 5659–5669. doi: 10.1111/1462-2920.15450

Lawal, I., Oyediran, I., R., B., Okanlawon, F., Oyeleye, O., Akanni, O., et al. (2021). A Review on the Diverse Uses, Conservation Measures and Agronomic Aspect of Aloe vera (L.) Burm. f. *Eur. J. Medicinal Plants* 32, 39–51. doi: 10.9734/ejmp/2021/v32i930417

Leylaie, S., and Zafari, D. (2018). Antiproliferative and antimicrobial activities of secondary metabolites and phylogenetic study of endophytic Trichoderma species from Vinca plants. *Front. Microbiol.* 9, 1484. doi: 10.3389/fmicb.2018.01484

Liu, F., Hewezi, T., Lebeis, S. L., Pantalone, V., Grewal, P. S., and Staton, M. E. (2019). Soil indigenous microbiome and plant genotypes cooperatively modify soybean rhizosphere microbiome assembly. *BMC Microbiol.* 19, 1–19. doi: 10.1186/s12866-019-1572-x

Luo, M., Li, B., Jander, G., and Zhou, S. (2023). Non-volatile metabolites mediate plant interactions with insect herbivores. *Plant J.* 114, 1164–1177. doi: 10.1111/tpj.v114.5

Macias-Benitez, S., Garcia-Martinez, A. M., Caballero Jimenez, P., Gonzalez, J. M., Tejada Moral, M., and Parrado Rubio, J. (2020). Rhizospheric organic acids as biostimulants: monitoring feedbacks on soil microorganisms and biochemical properties. *Front. Plant Sci.* 11, 633. doi: 10.3389/fpls.2020.00633

Mahapatra, S. S. (2021). Antioxidants as modulators of plant defence against soilborne fungal pathogens upon microbial interaction. *Antioxidants Plant-Microbe Interaction*, 305–314. doi: 10.1007/978-981-16-1350-0_14

Maitra, P., Hrynkiewicz, K., Szuba, A., Jagodziński, A. M., Al-Rashid, J., Mandal, D., et al. (2024). Metabolic niches in the rhizosphere microbiome: dependence on soil horizons, root traits and climate variables in forest ecosystems. *Front. Plant Sci.* 15, 1344205. doi: 10.3389/fpls.2024.1344205

Mashabela, M. D., Tugizimana, F., Steenkamp, P. A., Piater, L. A., Dubery, I. A., and Mhlongo, M. I. (2022). Untargeted metabolite profiling to elucidate rhizosphere and leaf metabolome changes of wheat cultivars (*Triticum aestivum* L.) treated with the plant growth-promoting rhizobacteria *Paenibacillus alvei* (T22) and *Bacillus subtilis*. *Front. Microbiol.* 13, 971836. doi: 10.3389/fmicb.2022.971836

Menezes-Blackburn, D., Paredes, C., Zhang, H., Giles, C. D., Darch, T., Stutter, M., et al. (2016). Organic acids regulation of chemical–microbial phosphorus transformations in soils. *Environ. Sci. Technol.* 50, 11521–11531. doi: 10.1021/acs.est.6b03017

Miller, R. G., Tangney, R., Enright, N. J., Fontaine, J. B., Merritt, D. J., Ooi, M. K., et al. (2019). Mechanisms of fire seasonality effects on plant populations. *Trends Ecol. Evol.* 34, 1104–1117. doi: 10.1016/j.tree.2019.07.009

Misztal, P. K., Hewitt, C. N., Wildt, J., Blande, J. D., Eller, A. S., Fares, S., et al. (2015). Atmospheric benzenoid emissions from plants rival those from fossil fuels. *Sci. Rep.* 5, 12064. doi: 10.1038/srep12064

Mohd Din, A. R. J., Rosli, M. A., Mohamad Azam, Z., Othman, N. Z., and Sarmidi, M. R. (2020). *Paenibacillus polymyxa* role involved in phosphate solubilization and growth promotion of *Zea mays* under abiotic stress condition. *Proc. Natl. Acad. Sciences India Section B: Biol. Sci.* 90, 63–71. doi: 10.1007/s40011-019-01081-1

Noumavo, P. A., Kochoni, E., Didagbé, Y. O., Adjanohoun, A., Allagbé, M., Sikirou, R., et al. (2013). Effect of different plant growth promoting rhizobacteria on maize seed germination and seedling development. *Am. J. Plant Sci.* 4, 1013–1021. doi: 10.4236/ajps.2013.45125

Nwozo, O. S., Effiong, E. M., Aja, P. M., and Awuchi, C. G. (2023). Antioxidant, phytochemical, and therapeutic properties of medicinal plants: A review. *Int. J. Food Properties* 26, 359–388. doi: 10.1080/10942912.2022.2157425

Oburger, E., Kirk, G. J., Wenzel, W. W., Puschenreiter, M., and Jones, D. L. (2009). Interactive effects of organic acids in the rhizosphere. *Soil Biol. Biochem.* 41, 449–457. doi: 10.1016/j.soilbio.2008.10.034

Özdoğan, D. K., Akçelik, N., and Akçelik, M. (2022). Genetic diversity and characterization of plant growth-promoting effects of bacteria isolated from rhizospheric soils. *Curr. Microbiol.* 79, 132. doi: 10.1007/s00284-022-02827-3

Prasad, M., Srinivasan, R., Chaudhary, M., Choudhary, M., and Jat, L. K. (2019). Plant growth promoting rhizobacteria (PGPR) for sustainable agriculture: perspectives and challenges. *PGPR amelioration Sustain. Agric.*, 129–157. doi: 10.1016/B978-0-12-815879-1.00007-0

Qin, S., Zhang, Y. J., Yuan, B., Xu, P. Y., Xing, K., Wang, J., et al. (2014). Isolation of ACC deaminase-producing habitat-adapted symbiotic bacteria associated with halophyte *Limonium sinense* (Girard) Kuntze and evaluating their plant growth-promoting activity under salt stress. *Plant Soil* 374, 753–766. doi: 10.1007/s11104-013-1918-3

Ramírez-Ordorica, A., Valencia-Cantero, E., Flores-Cortez, I., Carrillo-Rayas, M. T., Elizarraraz-Anaya, M. I. C., Montero-Vargas, J., et al. (2020). Metabolomic effects of the colonization of Medicago truncatula by the facultative endophyte Arthrobacter agilis UMCV2 in a foliar inoculation system. *Sci. Rep.* 10, 8426. doi: 10.1038/s41598-020-65314-4

R Development Core Team. (2024). *R: a language and environment for statistical computing, v.4.4.2*. (Vienna, Austria: R foundation for Statistical Computing). Available online at: http://www.r-project.org (Accessed October 31, 2024).

Reynolds, T. (1985). The compounds in Aloe leaf exudates: a review. *Botanical J. Linn. Soc.* 90, 157–177. doi: 10.1111/j.1095-8339.1985.tb00377.x

Schenkel, D., Maciá-Vicente, J. G., Bissell, A., and Splivallo, R. (2018). Fungi indirectly affect plant root architecture by modulating soil volatile organic compounds. *Front. Microbiol.* 9, 1847. doi: 10.3389/fmicb.2018.01847

Sharma, K., Chaturvedi, U., Sharma, S., Vaishnav, A., and Singh, S. V. (2021). Fenugreek-rhizobium symbiosis and flavonoids under stress condition. *Antioxidants Plant-Microbe Interaction*, 449–459. doi: 10.1007/978-981-16-1350-0_21

Sharma, P., Kharkwal, A. C., Abdin, M. Z., and Varma, A. (2014). *Piriformospora indica* improves micropropagation, growth and phytochemical content of Aloe vera L. plants. *Symbiosis* 64, 11–23. doi: 10.1007/s13199-014-0298-7

Sharma, R., Paliwal, J. S., Chopra, P., Dogra, D., Pooniya, V., Bisaria, V. S., et al. (2017). Survival, efficacy and rhizospheric effects of bacterial inoculants on Cajanus cajan. *Agriculture, Ecosystems & Environment. 240*, 244–252. doi: 10.1016/j.agee.2017.02.018

Sharma, A., Vaishnav, A., Jamali, H., Keswani, C., Srivastava, A. K., Kaushik, R., et al. (2023). Unraveling the plant growth-promoting mechanisms of Stenotrophomonas sp. CV83 for drought stress tolerance and growth enhancement in chickpea. *J. Plant Growth Regul.* 42, 6760–6775. doi: 10.1007/s00344-023-11010-2

Singh, A., Hidangmayum, A., Yashu, B. R., Kumar, V., Singh, B. N., and Dwivedi, P. (2022). "Underlying forces of plant microbiome and their effect on plant development," in *New and future developments in microbial biotechnology and bioengineering*. (Elsevier), 159–180. doi: 10.1016/B978-0-323-85577-8.00008-1

Singh, H. B., Vaishnav, A., and Sayyed, R. Z. (Eds.). (2021). *Antioxidants in plant–microbe interaction* (Springer Singapore), 3–20. doi: 10.1007/978-981-16-1350-0

Singh, J., Singh, P., Vaishnav, A., Ray, S., Rajput, R. S., Singh, S. M., et al. (2021). Belowground fungal volatiles perception in okra (Abelmoschus esculentus) facilitates plant growth under biotic stress. *Microbiological Res.* 246, 126721. doi: 10.1016/j.micres.2021.126721

Singh, H. B., and Vaishnav, A. (Eds.). (2022). *New and future developments in microbial biotechnology and bioengineering: sustainable agriculture: advances in microbe-based biostimulants*. (Elsevier). doi: 10.1016/C2020-0-02089-X

Strehmel, N., Böttcher, C., Schmidt, S., and Scheel, D. (2014). Profiling of secondary metabolites in root exudates of *Arabidopsis thaliana*. *Phytochemistry* 108, 35–46. doi: 10.1016/j.phytochem.2014.10.003

Sui, J., Ji, C., Wang, X., Liu, Z., Sa, R., Hu, Y., et al. (2019). A plant growth-promoting bacterium alters the microbial community of continuous cropping poplar trees' rhizosphere. *J. Appl. Microbiol.* 126, 1209–1220. doi: 10.1111/jam.14194

Sziderics, A. H., Rasche, F., Trognitz, F., Sessitsch, A., and Wilhelm, E. (2007). Bacterial endophytes contribute to abiotic stress adaptation in pepper plants (Capsicum annuum L.). *Can. J. Microbiol.* 53, 1195–1202. doi: 10.1139/W07-082

Taher, M. A., Rashid, S. A., Yenn, T. W., Ring, L. C., Hway, T. S., and Tan, W.-N. (2024). The myriad therapeutic benefits of Aloe vera and its endophytes–A review. *AIP Conf. Proc.* 2923. doi: 10.1063/5.0195499

Thanni, B., Merckx, R., Hauser, S., Soretire, A., and Honnay, O. (2024). Multiple taxa inoculants of arbuscular mycorrhizal fungi enhanced colonization frequency, biomass production, and water use efficiency of cassava (Manihot esculenta). *Int. Microbiol.* 27, 1219–1230. doi: 10.1007/s10123-023-00466-7

Tittabutr, P., Payakapong, W., Teaumroong, N., Singleton, P. W., and Boonkerd, N. (2007). Growth, survival and field performance of bradyrhizobial liquid inoculant formulations with polymeric additives. *Sci. Asia* 33, 69–77. doi: 10.2306/scienceasia1513-1874.2007.33.069

Tiwari, S., Singh, P., Tiwari, R., Meena, K. K., Yandigeri, M., Singh, D. P., et al. (2011). Salt-tolerant rhizobacteria-mediated induced tolerance in wheat (Triticum aestivum) and chemical diversity in rhizosphere enhance plant growth. *Biol. Fertility soils* 47, 907–916. doi: 10.1007/s00374-011-0598-5

Tripathi, A., Pandey, P., Tripathi, S. N., and Kalra, A. (2022). Perspectives and potential applications of endophytic microorganisms in cultivation of medicinal and aromatic plants. *Front. Plant Sci.* 13985429. doi: 10.3389/fpls.2022.985429

Tuason, M. M. S., and Arocena, J. M. (2009). Root organic acid exudates and properties of rhizosphere soils of white spruce (Picea glauca) and subalpine fir (*Abies lasiocarpa*). *Can. J. Soil Sci.* 89, 287–300. doi: 10.4141/CJSS08021

Vaishnav, A., Jain, S., Kasotia, A., Kumari, S., Gaur, R. K., and Choudhary, D. K. (2014). Molecular mechanism of benign microbe-elicited alleviation of biotic and abiotic stresses for plants. *Approaches to Plant Stress their Manage.*, 281–295. doi: 10.1007/978-81-322-1620-9_16

Vaishnav, A., Varma, A., Tuteja, N., and Choudhary, D. K. (2017). Characterization of bacterial volatiles and their impact on plant health under abiotic stress. *Volatiles Food security: role volatiles agro-ecosystems*, 15–24. doi: 10.1007/978-981-10-5553-9_2

Velázquez-Becerra, C., Macías-Rodríguez, L. I., López-Bucio, J., Altamirano-Hernández, J., Flores-Cortez, I., and Valencia-Cantero, E. (2011). A volatile organic compound analysis from *Arthrobacter agilis* identifies dimethylhexadecylamine, an amino-containing lipid modulating bacterial growth and *Medicago sativa* morphogenesis in *vitro*. *Plant Soil* 339, 329–340. doi: 10.1007/s11104-010-0583-z

Velázquez-Becerra, C., Macías-Rodríguez, L. I., López-Bucio, J., Flores-Cortez, I., Santoyo, G., Hernández-Soberano, C., et al. (2013). The rhizobacterium *Arthrobacter agilis* produces dimethylhexadecylamine, a compound that inhibits growth of phytopathogenic fungi in *vitro*. *Protoplasma* 250, 1251–1262. doi: 10.1007/s00709-013-0506-y

Wu, W., Chen, W., Liu, S., Wu, J., Zhu, Y., Qin, L., et al. (2021). Beneficial relationships between endophytic bacteria and medicinal plants. *Front. Plant Sci.* 12, 646146. doi: 10.3389/fpls.2021.646146

Wu, T., Kerbler, S. M., Fernie, A. R., and Zhang, Y. (2021). Plant cell cultures as heterologous bio-factories for secondary metabolite production. *Plant Commun.* 2. doi: 10.1016/j.xplc.2021.100235

Yang, K., Li, H., Li, L., Hu, J., Wei, Y., Yang, H., et al. (2021). Soil metabolomics reveal complex interactions between *Arthrobacter ureafaciens* and *Trichoderma harzianum* when co-inoculated on wheat. *Pedobiologia* 85, 150723. doi: 10.1016/j.pedobi.2021.150723

Yang, D. S., Zhang, J., Li, M. X., and Shi, L. X. (2017). Metabolomics analysis reveals the salt-tolerant mechanism in *Glycine soja*. *J. Plant Growth Regul.* 36, 460–471. doi: 10.1007/s00344-016-9654-6

frontiers | Frontiers in Plant Science

TYPE Original Research
PUBLISHED 08 May 2025
DOI 10.3389/fpls.2025.1578936

OPEN ACCESS

EDITED BY
Zhen Wang,
Yulin Normal University, China

REVIEWED BY
P. E. Rajasekharan,
Indian Institute of Horticultural Research (ICAR), India
Xuejiao Huang,
Guangxi University, China
Zongrui Lai,
Beijing Forestry University, China

*CORRESPONDENCE
Zhengjie Zhu
zhuzhjie@163.com

†These authors have contributed equally to this work

RECEIVED 18 February 2025
ACCEPTED 15 April 2025
PUBLISHED 08 May 2025

CITATION
Yang C, Teng Z, Jin Z, Ouyang Q, Lv L, Hou X, Hussain M and Zhu Z (2025) Structure and composition of arbuscular mycorrhizal fungal community associated with mango. *Front. Plant Sci.* 16:1578936. doi: 10.3389/fpls.2025.1578936

Structure and composition of arbuscular mycorrhizal fungal community associated with mango

Cuifeng Yang[1,2,3†], Zheng Teng[1,2,3†], Zhibo Jin[1,2,3], Qiufei Ouyang[1,2,3], Lingling Lv[1,2,3], Xianbin Hou[1,2,3], Muzammil Hussain[1,2,3] and Zhengjie Zhu[1,2,3*]

[1]College of Agriculture and Food Engineering, Baise University, Baise, China, [2]Guangxi Key Laboratory of Biology for Mango, Baise, China, [3]College of Subtropical Characteristic Agricultural Industry, Baise, China

Mango (*Mangifera indica* L.) is an important fruit crop with significant economic value in tropical and subtropical areas globally. Arbuscular mycorrhizal fungal (AMF) symbiosis is vital for mango trees growth, and the detailed understanding of various (a)biotic factors that influence AMF community composition is crucial for sustainable crop production. To date, there is little information available on how do different seasons and plant age influence the AMF community composition associated with mango. Using high-throughput amplicon sequencing, we examined AMF community diversity and composition in the rhizosphere of mango from two distinct orchards during spring (C_BY and C_YL) and autumn (Q_BY and Q_YL), which differed in age (10 and 28 years). The results revealed a notable variation in the number of observed species between two 28-years-old mango orchards (C_BY28 vs C_YL28 and Q_BY28 vs Q_YL28) during both the spring and autumn seasons. However, the comparison of 10-years-old and 28-years-old mangoes showed no significant shift in the diversity and richness of AMF. At the taxonomic level, *Glomus* was the absolute dominant genus in AMF community. The correlation analysis between species abundance and soil nutrients showed that the level of phosphorus, potassium and their available forms (AP, AK) significantly affect AMF community. Furthermore, the P, AP, and AK contents were found positively correlated with the dominant AMF molecular virtual species *Sclerocystis sinuosa*. These findings indicate the response characteristics of mango rhizosphere AMF community to soil nutrients, providing scientific basis for precise regulation of soil environment to improve mango tree growth and production.

KEYWORDS

AMF community, mango, microbial diversity, planting years, seasonal dynamic, soil properties

1 Introduction

The agricultural economy on a global scale heavily depends on tropical fruits, and their development is influenced by several factors, notably the interplay between soil nutrients and native microbial communities. Arbuscular mycorrhizal fungi (AMF) are beneficial group of microorganisms commonly found in the soils of diverse ecosystems, capable of establishing symbiotic association with the root systems of many tropical fruit species. AMF can effectively promote the absorption and utilization of mineral nutrients by plants through the formation of a complex mycelial networks (Hartoyo and Trisilawati, 2021), which helps with the growth and development of tropical fruits, enhances plant resistance to biotic and abiotic stresses (Mickan et al., 2016; Boldt-Burisch et al., 2018), affects the secondary metabolism process of tropical fruits, and directly or indirectly affects the community structure, diversity, and productivity of different ecosystems (Meddad-Hamza et al., 2010; Zhang et al., 2015). AMF also provides a low-cost solution for stress resistant cultivation of tropical fruits under climate change and is currently a hot topic in exploring and utilizing beneficial microbial resources in tropical fruits. Studies have shown that AMF community composition is mainly influenced by factors such as management measures, host plants, and environmental conditions (Jia et al., 2023).

Mango (*Mangifera indica* L.) is an important fruit trees widely grown in tropical and subtropical regions (Xie et al., 2025). China is the world's second largest mango producing country (Guo et al., 2021), and Baise City, situated in the Guangxi Zhuang Autonomous Region of China, is a major hub for mango production with a total harvest of 1.22 million tons (Guo et al., 2021). The Baise mango is recognized as a national geographical indication agricultural product. However, the increase in human activities and non-scientific agricultural practices over an extended period has greatly affected the soil biodiversity in mango growing regions. For example, according to one regional study, the excessive use of fertilizers and traditional farming approaches have led to considerable harm to the soil ecosystem in mango production areas of Baise city (Ou et al., 2021). Generally, soil nutrients like nitrogen (N), phosphorus (P), potassium(K) and calcium (Ca) significantly alter the diversity and composition of AMF communities (de Pontes et al., 2017). Changes in soil pH may also directly and indirectly shift AMF diversity (Svenningsen et al., 2018). Therefore, the ongoing challenges to soil fertility threaten AMF community and sustainable mango production, significantly impeding the developmental progress of the mango industry (Govindan et al., 2020; Mohammed et al., 2022).

AMF communities associated with plants have direct and profound impact on the nutrient absorption efficiency, stress resistance, and ultimately fruit yield and quality of mangoes (Singh et al., 2024). Previous studies have identified a number of AMF taxa such as *Acaulospora*, *Diversispora*, *Glomus*, *Gigaspora*, *Paraglomus* and *Rhizophagus* from mango orchards using both traditional and high-throughput sequencing methods (Teixeira-Rios et al., 2018;Li et al., 2022). However, the questions regarding how the plants age and seasonal dynamics affect the diversity and composition of mango AMF community remains unanswered. Herein, we hypothesized that the age of mango trees and seasonal variation may significantly affect the structure and composition of AMF community. To test this hypothesis, we obtained rhizosphere samples from 10 and 28 years old mango plants across the spring and autumn seasons. Our specific objectives were to (a) assess the diversity and richness of AMF populations in two separate mango orchards in Baise city (b) decipher the structure and composition of the AMF community in the mango rhizosphere throughout different seasons and years of planting, and (c) understand how the structure of AMF community relates to the nutrient composition of the soil. This study offers valuable insights into the composition of AMF communities and their connection to soil health in mango orchards located in Baise city of the Guangxi Zhuang Autonomous Region of China.

2 Materials and methods

2.1 Sample collection

In November 2022 (autumn) and May 2023 (spring), the root samples with attached rhizosphere soil were collected from two mango orchards differed in age (10 and 28 years) located in Baise City, Guangxi Zhuang Autonomous Region, China. One orchards is situated in Baiyu Town (BY), Tianyang District (106°22′14″–107° 08′32″ E, 23°28′20″–24°06′55″ N) characterized by an average annual temperature ranging from 18 to 22 °C, yearly rainfall between 1,100 and 1,250 mm, a frost-free duration of 307 to 352 days, and a total annual sunshine of 1,906.6 hours. The second orchard is located in Yongle Town (YL), Youjiang District (106° 07′–106°56′ E, 23°33′–24°18′ N) characterized by an average annual temperature of 22 °C, total annual precipitation of 1,350 mm, a frost-free period of 360 days, and an annual sunshine duration of 1,633 hours. There is a significant heterogeneity in the geographical and climatic conditions between the two sampling sites, which is conducive to analyzing the construction of AMF communities and the temporal and spatial patterns of their responses to environmental factors. Five independent replicate samples were collected from 10-and 28-year-old mango plantations respectively (Supplementary Table 1), reducing the interference of microhabitat heterogeneity and meet the sample size requirements for subsequent statistical tests. The sample names in this study are as follow: C_BY10, 10yr old orchard in Baiyu Town during spring; C_BY28, 28yr old orchard in Baiyu Town during spring; C_YL10, 10yr old orchard in Yongle Town during spring; C_YL28, 28yr old orchard in Yongle Town during spring; Q_BY10, 10yr old orchard in Baiyu Town during autumn; Q_BY28, 28yr old orchard in Baiyu Town during autumn; Q_YL10, 10yr old orchard in Yongle Town during autumn; Q_YL28, 28yr old orchard in Yongle Town during autumn. In order to collect root samples through the five point sampling method, we first removed large gravel, dead branches, and leaves from the surface to ensure that the collected samples can truly reflect the rhizosphere soil conditions and avoid interference from

debris. Next, excavate the roots to a depth of 5-30 cm, and then gently knock off the root with attached rhizosphere soil that is tightly bound to the root system and place it in a sterile bag. After the soil was bought back to the laboratory, the rhizosphere soil was collected in accordance with the methods described by Hussain et al. (2024). It was then divided into two parts, with one part used for DNA extraction and subsequent AMF molecular identification, and the other part for the analysis of soil chemical properties.

2.2 Determination of soil chemical properties

The soil chemical properties were determined according to soil agrochemical analysis (Bao, 2000). Soil pH was determined by electrode method. The contents of total nitrogen (N), total phosphorus (P) and total potassium (K) in soil were determined by Kjeldahl method, perchloric acid sulfuric acid method and alkali fusion atomic absorption spectrometry, respectively. The contents of alkali hydrolyzed nitrogen (HN), available phosphorus (AP) and available potassium (AK) were determined by alkali hydrolysis diffusion method, sodium bicarbonate extraction - molybdenum antimony anti colorimetry method and ammonium acetate extraction - Flame photometric method, respectively. Organic matter (OM) content was determined by potassium dichromate external heating method.

2.3 DNA extraction, PCR amplification and Illumina sequencing

The DNA from rhizosphere soil was extracted using the cetyltrimethylammonium bromide (CTAB) method to examine AMF communities as described previously (Yurkov et al., 2023), due to its cationic detergent properties that effectively bind and precipitate polysaccharide-protein complexes, particularly suitable for complex soil environments containing humic acids and inhibitors. After adjusting the DNA concentration to 20 ng/μL, the AMF 18S rDNA region was amplified using the specific barcoded primers AMV4.5NF (5'-AAGCTCGT AGTTGAATTTCG-3') and AMDGR(5'- CCCAACTAT CCCTATTAATCAT-3') in a Veriti thermal cycler (Applied Biosystems). The PCR reaction mixture (20 μL) includes: 5 × fastpfu buffer 4.0 μL, 2.5 mmol/L dNTPs 2.0 μL, 5 μmol/L upstream and downstream primers 0.8 μL, fastpfu polymerase 0.4 μL, BSA 0.2 μL, template DNA 0.01 μL, ddH_2O make up to 20.0 μL. Amplification procedure: pre-denaturation at 95 °C for 3 min; 35 cycles were performed at 95 °C for 30 s, 55 °C for 30 s, and 72 °C for 45 s; extend at 72 °C for 10 min. The amplified product from PCR was purified with the PCR Clean-Up Kit (YuHua, Shanghai, China), and the final concentration of the DNA was determined by Qubit 4.0 (Thermo Fisher Scientific, USA). Finally, the paired-end sequencing was performed using the Illumina Nextseq 2000 platform by Majorbio Bio-Pharm Technology Co. Ltd. (Shanghai, China). The raw sequencing reads were deposited into the NCBI Sequence Read Archive (SRA) database (Accession Number: PRJNA1224724).

2.4 Bioinformatics analyses of amplicon sequencing

Quality control on double-ended raw sequencing data is carried out using the fastp software tool (https://github.com/OpenGene/fastp, Version 0.19.6). The sequencing reads were merged using FLASH (http://www.cbcb.umd.edu/software/flash, Version 1.2.11) and the resulting high-quality sequences were then de-noised using DADA2. The classification of amplicon sequence variants (ASVs) was carried out utilizing the Naive Bayes consensus taxonomy classifier that is integrated into QIIME2. The calculations for rarefaction curves and alpha diversity metrics, such as the Sobs and Shannon indices, were performed using Mothur version 1.30.1. The Wilcoxon rank sum test was employed to assess the differences in alpha diversity among the groups. To determine the relative significance of certainty and randomness in the AMF community assembly, we applied a zero model (999 randomizations) for calculating the β-nearest taxonomic unit index (β NTI) through the R package 'icamp'. The analysis of microbial typing conducted based on the proportion of the microbial community at a chosen classification tier, utilizing the Jensen Shannon Distance (JSD) for equidistant calculations and applying PAM (Partitioning Around Medoids) for clustering. The Calinski Harabasz index is employed to determine the ideal number of clusters (K), followed by principal coordinates analysis (PCoA, $K \geq 2$) for visualization purposes. This analysis is performed using R version 3.3.1 with the packages 'ade4', 'cluster', and 'clusterSim'. Venn diagram was created using the R package VennDiagrams. Circos diagrams was created using Circos-0.67-7 (http://circos.ca/). Species differential analysis was performed using R package 'stat' and the Wilxocon rank sum test was used to identify the differences in mean values of different groups. We then conducted a distance-based redundancy analysis (db-RDA) to assess the influence of soil chemical properties on the community structure of AMF in the soil. A numerical matrix was created by evaluating the correlation coefficient of environmental factors in relation to selected species and presented visually as a heatmap. The functional prediction of 18S rDNA sequencing reads was performed using PICRUSt2.

3 Results

3.1 Analysis of chemical properties of rhizosphere soil in mango orchard

The chemical properties of rhizosphere soil in mango orchards with different seasons, planting locations, and planting years exhibited strong heterogeneity (Supplementary Tables 2, 3). The differences in various indicators between spring (C_BY10, C_BY28, C_YL10 and C_YL28) and autumn (Q_BY10, Q_BY28, Q_YL10 and Q_YL28) did not show a clear consistent pattern, with only the

OM content in autumn being significantly lower than that in spring. For the same production area, the soil fertility varies with different planting years. The N and OM content in the 28 year old plantation (C_BY28) were significantly higher than those in the 10-year plantation (C_BY10). In Yongle Town, the K content in the 28 year old plantation (Q_YL28) was more than that in the 10-year plantation (Q_YL10). With an increasing planting year, the content of N, OM, K and other nutrients in the soil increased. There were differences in soil fertility indicators between mango orchards in Baiyu Town and Yongle Town. The soil pH of sample C_BY28 was higher than that of C_YL28. The N content of C_YL10 was more than that of C_BY10, and the N content of Q_YL28 was high than that of Q_BY28. The P content of Q_BY10 was more than that of Q_YL10. However, the K content in Yongle Town was significantly higher than that in Baiyu Town. In addition, the AP content in Baiyu Town in autumn was more than that in Yongle Town. After 10 years of planting, the AK content in Baiyu Town was high than that in Yongle Town. This indicates that the chemical properties of the rhizosphere soil in mango orchards vary depending on the planting location, which may be closely related to agronomic measures such as fertilization.

3.2 Alpha diversity, community structure and microbial typing analysis

The total reads retrieved from the sequencing data were enough to reflect the vast majority of microbial diversity information in the sample (Supplementary Figure 1). In addition, the Coverage Index of each sample was close to 1, indicating that the sequencing results covered all microbial groups in the sample, providing enough data for downstream analysis (Supplementary Figure 2). The findings from the Rank Abundance curve indicated that the different seasons (spring and autumn), planting years (10 years and 28 years), and locations (BY and YL) may have important impacts on the relative abundance distribution of microorganisms at the genus level (Supplementary Figure 3). The Sobs index values in C_YL28 was lowest as compared to C_BY28, indicating a relative significant different between two 28-years-old mango orchards (Figure 1A). The Sobs index values for sample Q_BY28 was also highest than that of Q_YL28, suggesting that despite the seasonal variations, these orchards hosted distinct groups of microbial species. Furthermore, the results of the Shannon index (Figure 1B) showed that the sample Q_BY28 had highest AMF diversity than that of C_YL28 and C_YL10, indicating that AMF diversity is relatively low and the evenness of species distribution is not uniform. The results of β-NTI analysis (β-Nearest Taxon Index analysis) showed that the range of β-NTI values for each sample was -1.22~1.71, within the range of |β-NTI |<2, indicating that stochastic processes dominate the assembly of AMF communities in the rhizosphere soil of mango orchards, and they may have different response modes when facing environmental changes (Figures 1C, D).

The results of microbial typing analysis at the genus level showed that the AMF community in the rhizosphere of mango orchards was mainly divided into two dominant types (type 1, type

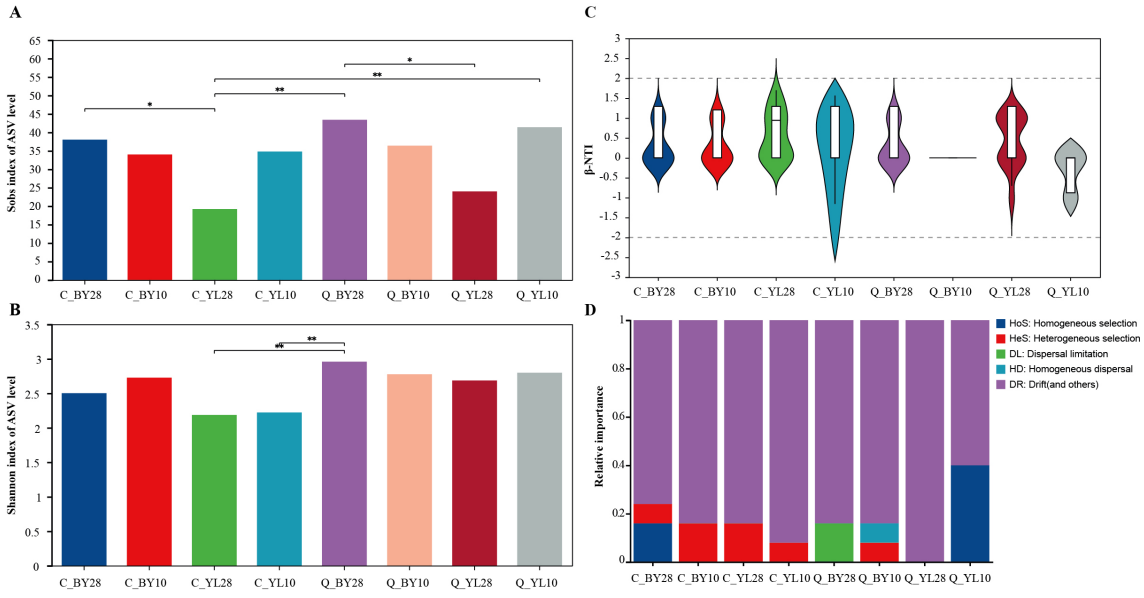

FIGURE 1
Diversity and community structure of AMF community in mango rhizosphere soil. **(A)** Sobs index of AMF in rhizosphere soil of mango orchard, **(B)** Shannon index of AMF in rhizosphere soil of mango orchard, and **(C)** Analysis of β-NTI community structure of AMF in rhizosphere soil of mango orchard. **(D)** Relative importance of different ecological processes of mango rhizosphere AMF community. Note: 0.01<P ≤ 0.05 is marked as *, 0.001<P ≤ 0.01 is marked as * *, the same applies below. C_BY10, 10yr old orchard in Baiyu Town during spring; C_BY28, 28yr old orchard in Baiyu Town during spring; C_YL10, 10yr old orchard in Yongle Town during spring; C_YL28, 28yr old orchard in Yongle Town during spring; Q_BY10, 10yr old orchard in Baiyu Town during autumn; Q_BY28, 28yr old orchard in Baiyu Town during autumn; Q_YL10, 10yr old orchard in Yongle Town during autumn; Q_YL28, 28yr old orchard in Yongle Town during autumn.

2). Within the confidence interval, the samples of type 1 were concentrated at the sampling point of YL origin, and the samples of type 2 were concentrated at the sampling point of BY origin, indicated that the sampling points of YL origin and BY origin each have one dominant microbial community (Figure 2). Among them, the sample size in type 1 was larger than that in type 2, suggesting that type 1 may contain some microbial genera with strong competitiveness, which may be in a relatively advantageous position in the community and play important roles in ecological processes such as nutrient transformation and organic matter decomposition. Type 2 may represent another microbial genus with different ecological strategies, with relatively low abundance in the community, but may still have irreplaceable functions in certain special ecological niches or specific ecological processes.

3.3 AMF community composition analysis in rhizosphere soil of mango orchard

AMF community in the rhizosphere soil of mango orchards shared three genera across samples, namely *Glomus*, *Sclerocystis*, and unclassified_f_*Glomeraceae* (Supplementary Figure 4A). There were no unique genera observed in each sample. While at the species level, there were a total of 5 dominant AMF molecular virtual species shared between samples, including sp.*VTX00387*, sp.*VTX00400*, unclassified_g_*Glomus*, *S. sinuosa*, and unclassified_f_*Glomeraceae* (Supplementary Figure 4B). The construction of the Circos plot at the genus level showed that the *Glomus* genus dominates the AMF community (Supplementary Figure 5A). The average relative abundance of *Glomus* and *Sclerocystis* was significantly different among the groups, with p-values of 0.01316 and 0.01922, respectively (Figure 3).

At the species level (Supplementary Figure 5B), the molecular virtual species sp.*VTX00387* was the main dominant species in sample C_YL10, with a sequence proportion of up to 61.94%. Further statistical analysis showed that the difference between sample C_YL10 and sample C_BY28 has reached an extremely significant level, which means that there was a fundamental difference in the existence of sp.*VTX00387* between these two samples. At the same time, there were significant differences between sample C_YL10 and samples C_BY10, Q_BY28, and Q_BY10; and between Q_YL10 and C_BY28, reflecting variation in the abundance or activity of the strain in these different sample environments (Figure 4A).

For *S. sinuosa*, sample Q_BY10 was a dominant sample, with a sequence proportion of 38.00% and there was a significant difference between sample Q_BY10 and samples C_YL10 and Q_YL10, indicating that the distribution of this species in different samples was not random, but was constrained by specific environmental conditions, resulting in significant differences in its proportion in different samples (Figure 4B). Further analysis revealed a negative correlation between the sequence proportions

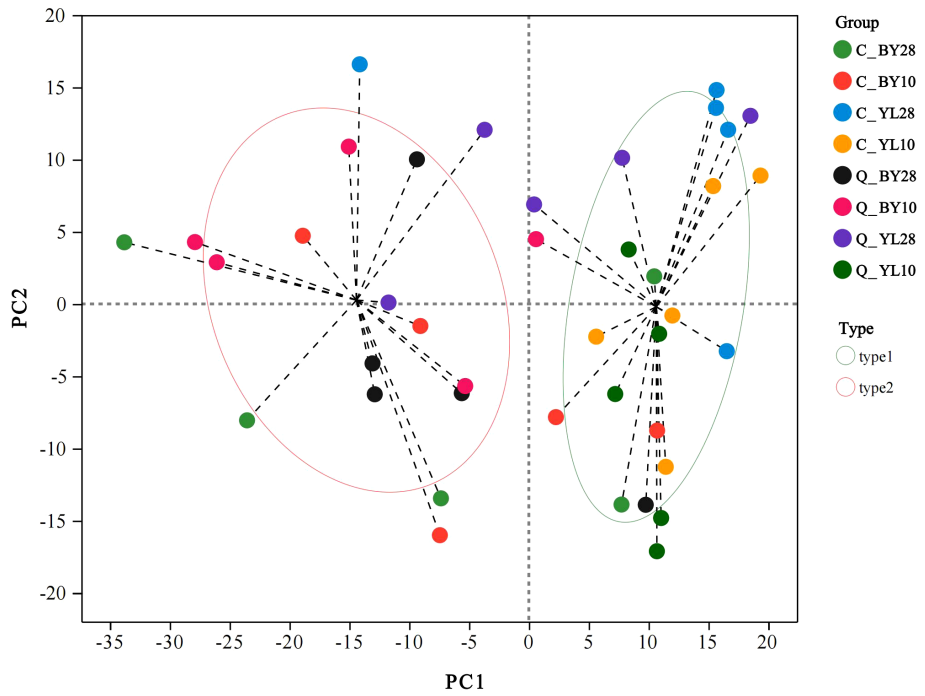

FIGURE 2
Microbial community typing analysis of AMF in rhizosphere soil of mango orchard. C_BY10, 10yr old orchard in Baiyu Town during spring; C_BY28, 28yr old orchard in Baiyu Town during spring; C_YL10, 10yr old orchard in Yongle Town during spring; C_YL28, 28yr old orchard in Yongle Town during spring; Q_BY10, 10yr old orchard in Baiyu Town during autumn; Q_BY28, 28yr old orchard in Baiyu Town during autumn; Q_YL10, 10yr old orchard in Yongle Town during autumn; Q_YL28, 28yr old orchard in Yongle Town during autumn.

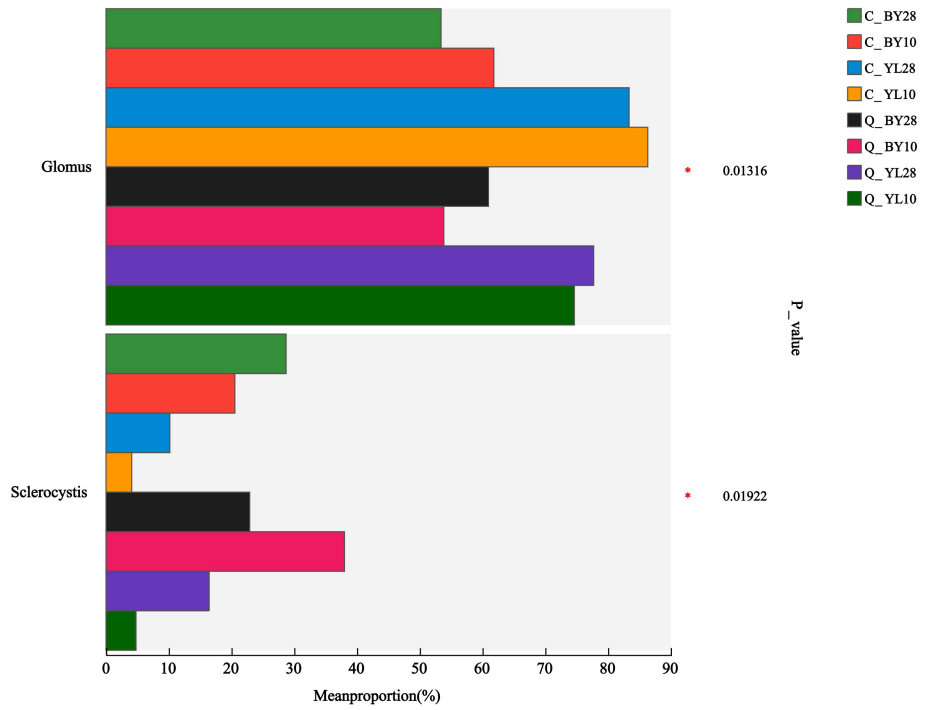

FIGURE 3
Differences in relative abundance of AMF in rhizosphere soil of mango orchard (genus level). C_BY10, 10yr old orchard in Baiyu Town during spring; C_BY28, 28yr old orchard in Baiyu Town during spring; C_YL10, 10yr old orchard in Yongle Town during spring; C_YL28, 28yr old orchard in Yongle Town during spring; Q_BY10, 10yr old orchard in Baiyu Town during autumn; Q_BY28, 28yr old orchard in Baiyu Town during autumn; Q_YL10, 10yr old orchard in Yongle Town during autumn; Q_YL28, 28yr old orchard in Yongle Town during autumn.

of sp.*VTX00387* and *S. sinuosa* in each sample. In the AMF microbial community of mango orchard rhizosphere soil, the proportions of sp.*VTX00387* and *S. sinuosa* were in a "competitive" state. When the proportion of sp.*VTX00387* decreased, the proportion of *S. sinuosa* increased (Figures 4A, B).

3.4 Correlation analysis of AMF in rhizosphere soil of mango orchard

At the species level, the db-RDA (distance-based redundancy analysis) analysis of AMF and soil chemical properties in the rhizosphere soil of mango orchards revealed that the two axes of RDA explained 20.78% of the variation in the AMF community, indicating a certain degree of correlation between soil chemical properties and the AMF community (Figure 5).

Further analysis reveals that the canonical Axis 1 (CAP1) coefficient of K was 0.9976, indicating that K had a strong explanatory power for changes in microbial community structure, explaining nearly 54.18% of the induced changes (Supplementary Table 4). Correlation analysis between AMF and soil chemical properties showed a positive correlation of sp.*VTX00387* with K content, and a negative correlation with P, AP, and AK contents (Figure 6). There was a positive correlation between *S. sinuosa* and the contents of P, AP, and AK, and a negative correlation between *S. sinuosa* and the K content.

3.5 Functional prediction of AMF in rhizosphere soil of mango orchard

Based on the 18S rDNA marker gene sequences, PICRUSt2 was used to predict the function of AMF in the rhizosphere soil of mango orchards (Figure 7). The results showed that the functions of each AMF sample were mainly enriched by the metabolic pathway 3.6.1.3 (Adenosine Triphosphatase, ATPase). From the perspective of correlation with soil elements, the ATPase function of sp.*VTX00387* was more focused on promoting the absorption, transport, and potassium-related metabolic processes of the K element, thus exhibiting a positive correlation with K content. The ATPase function of *S. sinuosa* was more conducive to the utilization and transformation of phosphorus elements and their related forms (such as AP and AK), and was positively correlated with the contents of P, AP, and AK. This difference in ATPase function towards different soil elements directly leads to their different strategies for resource acquisition.

4 Discussion

AMF enhances the absorption of water and nutrients by symbiotic plants through various pathways. In this study we found that N, K, OM and other nutrients content in the 28 year old plantation were significantly higher than those in the 10-year

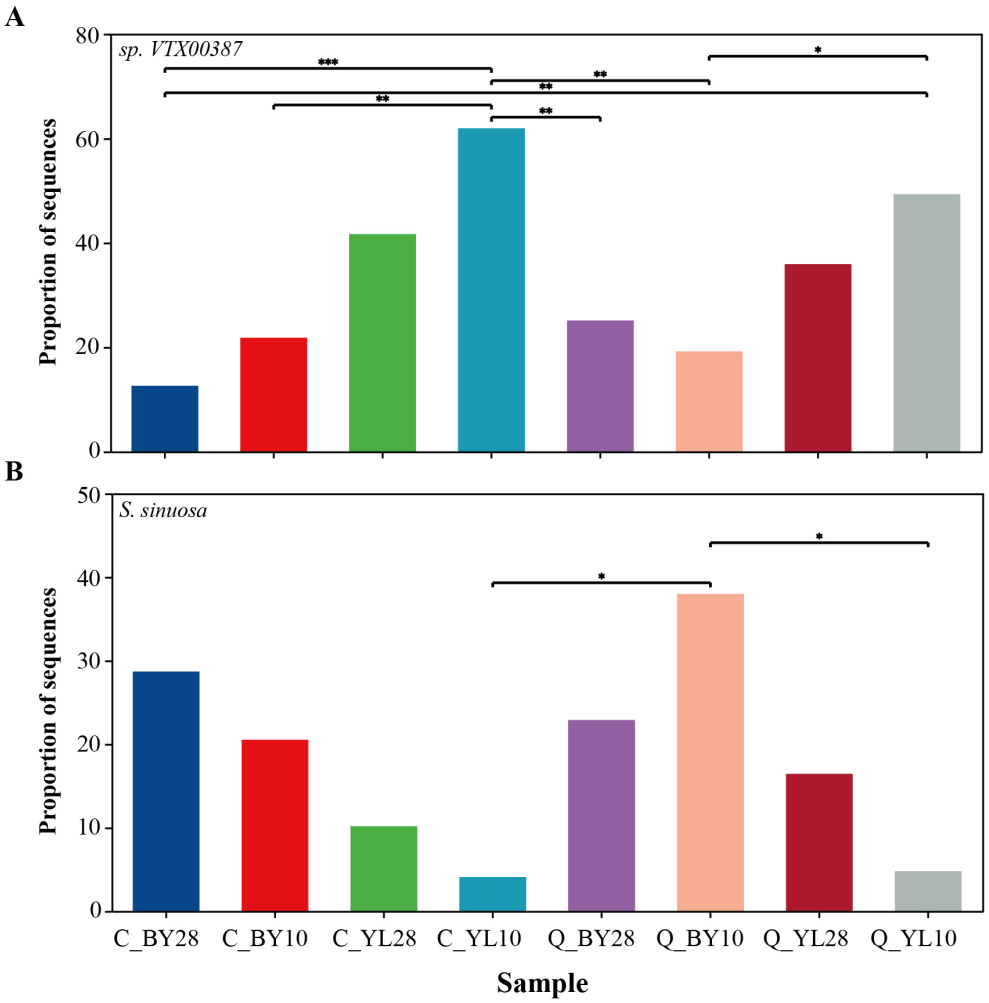

FIGURE 4
Proportion of sequences of two dominant AMF genera associated with mango rhizosphere soil. **(A)** The proportion of sequences of sp. VTX00387, and **(B)** S. sinuosa in mango rhizosphere soil. Note: 0.01<P ≤ 0.05 is marked as *0.001<P ≤ 0.01 is marked as **P ≤ 0.001 is marked as *** the same applies below. C_BY10, 10yr old orchard in Baiyu Town during spring; C_BY28, 28yr old orchard in Baiyu Town during spring; C_YL10, 10yr old orchard in Yongle Town during spring; C_YL28, 28yr old orchard in Yongle Town during spring; Q_BY10, 10yr old orchard in Baiyu Town during autumn; Q_BY28, 28yr old orchard in Baiyu Town during autumn; Q_YL10, 10yr old orchard in Yongle Town during autumn; Q_YL28, 28yr old orchard in Yongle Town during autumn.

plantation (Supplementary Table 3). AMF mycelium can extend into soil pores over time which is difficult for plant roots to reach, thereby establishing a mycorrhizal network and expanding the absorption range of plant roots. The hyphae of AMF have high affinity and can efficiently uptake phosphorus from soil, and transport phosphorus into plant cells through specific transport proteins. In addition, AMF can help plants absorb various nutrients such as N, zinc, and copper, resulting in improved plant growth (Govindan et al., 2020; Zhang et al., 2023). Leguminous plants have a high affinity for AMF and can quickly be infected and establish a good symbiotic relationship with AMF, thereby promoting the formation and function of mycorrhizal networks (Wu and Cui, 2016; Chen and Zeng, 2016). When facing pathogen invasion, microbes can also induce a series of defense responses in plants, activate the expression of defense related genes, synthesize and accumulate disease-related proteins, phytohormones and other substances, and enhance the plant's disease resistance (Ma et al., 2024; Ye et al., 2024; Hussain et al., 2025).

Currently, the development and utilization of AMF in mangoes is not comprehensive and systematic enough. This study utilized high-throughput amplicon sequencing to decipher AMF community in the rhizosphere soil of two mango orchards from different seasons and different planting years to obtain a comprehensive understanding of AMF community composition. The planting year has a certain impact on the diversity and structure of soil AMF communities. Previous studies showed that the number of AMF OTUs in the rhizospheric soil of three-year-old *Panax notoginseng* was significantly higher than that in the rhizospheric soils of one- and two-year-old *P. notoginseng* (Pei et al., 2023). Similarly, there were significant differences in the richness and community structure of root AMF in *P. notoginseng* at different planting ages. As the planting age increased, the AMF richness was

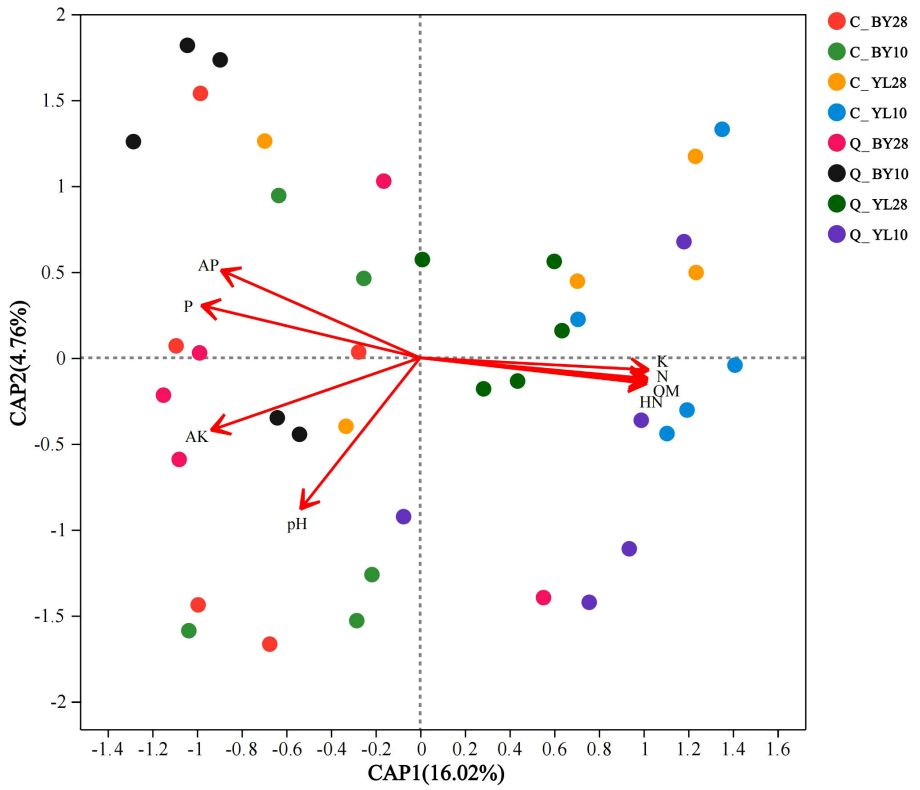

FIGURE 5
db-RDA analysis of AMF and soil chemical properties in the rhizosphere of mango orchard. C_BY10, 10yr old orchard in Baiyu Town during spring; C_BY28, 28yr old orchard in Baiyu Town during spring; C_YL10, 10yr old orchard in Yongle Town during spring; C_YL28, 28yr old orchard in Yongle Town during spring; Q_BY10, 10yr old orchard in Baiyu Town during autumn; Q_BY28, 28yr old orchard in Baiyu Town during autumn; Q_YL10, 10yr old orchard in Yongle Town during autumn; Q_YL28, 28yr old orchard in Yongle Town during autumn.

gradually decreased (Yang et al., 2023). We observed the absolute dominance of genus *Glomus* in AMF community (Figure 3), which was the dominant genus and the focus of functional AMF development in previously studies (Wang et al., 2011; Song et al., 2020). Chen et al. (2024) also previously found that the dominant AMF genus in the rhizosphere soil of lavender was *Glomus*, and its OTUs number gradually decreased with increasing planting years (Chen et al., 2024). *Glomus* is a common dominant genus in the rhizospheric soil of *Siraitia grosvenorii*, and its average relative abundance increases with the increase in the number of consecutive planting years (Yu et al., 2023). However, we found no significant effect of the planting years on the richness and diversity of AMF in mango rhizosphere soil. This indicates that the AMF community in mango rhizosphere soil can maintain a relatively stable state over a long period of time and did not experience drastic fluctuations due to the extension of planting years. This also implies that AMF has formed a stable adaptive mechanism during its long-term symbiotic evolution with mangoes, which can maintain population size and community structure through its own physiological regulation and ecological strategies.

In this study, *Glomus* had a relative abundance of 53.39% to 86.33% in the mango orchards (Figure 3). This may be due to the more diverse reproductive methods of *Glomus*, which gives it a stronger ability to infect plants compared to other genera (Hassan et al., 2011; Govindan et al., 2020; Silvana et al., 2020; Wang et al., 2021), indicating a closer mutualistic relationship between *Glomus* and mangoes compared to other genera. However, the results of dominant AMF species in the rhizosphere soil of mango orchards in different regions were not consistent. The dominant AMF molecular virtual species in the YL sampling point was sp. *VTX00387* belonging to *Glomus* genus, whereas, the dominant species of AMF at the BY sampling point was *S. sinuosa* in the genus *Sclerocystis* (Figure 4). These changes in species dominance could be related to different geographical environments or mango orchard management measures (Rasmussen et al., 2018). In addition, many AMF ASVs have not been identified to the species level, and most were belonged to unclassified_f_*Glomeraceae*, indicating that there may be new genera or species belonging to unclassified_f_*Glomeraceae* in the rhizosphere soil of mango orchards.

Geological and climatic conditions are known as the important determining factors affecting AMF communities. However, at the regional scale, soil type, soil pH, and ecological type are the main driving factors. Compared to biological factors (host species), abiotic factors are the most important driving factors determining AMF communities in semi-natural grassland ecosystems in Europe (Van Geel et al., 2017). Vast majority of the AMF studies are mainly performed on annual or perennial herbaceous plants, but there have been relatively less research on the AMF community in the

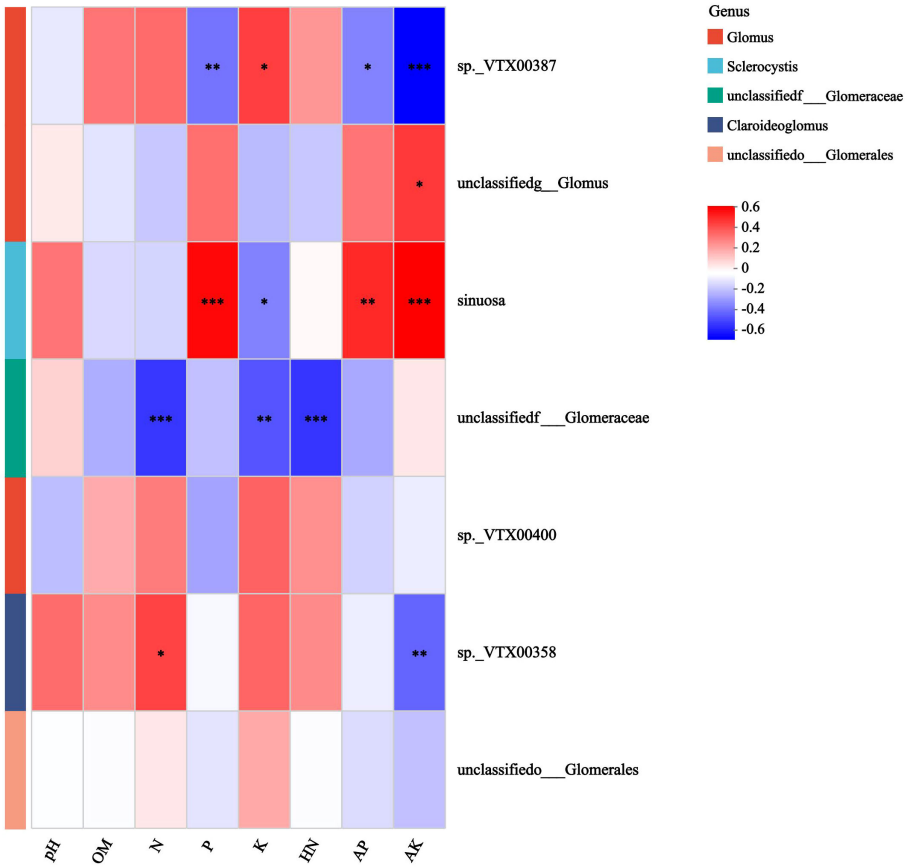

FIGURE 6
Spearman correlation heatmap of AMF and soil chemical properties in the rhizosphere of mango orchard. * 0.01 < P ≤ 0.05, ** 0.001 < P ≤ 0.01, *** P ≤ 0.001.

rhizosphere of woody plants, especially fruit trees (mangoes). In this study, there were significant differences in the richness and diversity of AMF in mango rhizosphere soil between sampling points in different regions. Our results found that P, K, AP, and AK had a significant impact on AMF diversity in mango rhizosphere soil (Figure 6; Supplementary Tables 2, 3). Among various types of AMF, sp.*VTX00387* showed a positive correlation with soil K content. This means that in areas with abundant soil K content, sp.*VTX00387* can more effectively utilize K elements to meet the needs of its own growth, metabolism, and reproduction, thereby occupying a relatively advantageous position in the microbial community. However, the strain showed a negative correlation with P, AP, and AK content. This phenomenon suggests that sp.*VTX00387* may face growth limitations or intense competitive pressure in soil environments with high P, AP, and AK contents. It is speculated that the reason for this may be that under conditions where these elements are abundant, other microorganisms (such as *S. sinuosa*) have higher utilization efficiency for P, AP, and AK, thereby compressing the living space of sp.*VTX00387* and leading to a decrease in its relative abundance in the corresponding area. On the contrary, *S. sinuosa* is positively correlated with the content of P, AP, and AK, which fully indicates its strong adaptability and competitive advantage in soil environments enriched with these elements, and can fully utilize these resources to maintain its own growth and reproduction. The negative correlation between *S. sinuosa* and K content indicates that it may be at a relative disadvantage in areas with higher K content. This may be due to the relatively weak ability of *S. sinuosa* in K uptake or metabolism, or it may be inhibited by competition from microorganisms with stronger K utilization abilities, such as sp.*VTX00387*. Previously, it was hypothesized that the chemical properties of rhizosphere, as a key ecological factor, have a complex impact on the types, diversity, and richness of AMF in mango rhizosphere soil (IIA, A. E. S, 2021; Zhao et al., 2024). Overall, the structure and composition of AMF community in mango rhizosphere soil were not affected by planting years and seasonal changes, but are mainly influenced by soil chemical properties.

This study found that the distribution pattern of AMF community structure in mango rhizosphere soil (such as dominant AMF molecular virtual species sp.*VTX00387* and *S. sinuosa*) is mainly driven by soil P, K and their available forms (AP, AK), rather than planting years or seasonal changes (Figure 6). These results conclusively provide a key ecological basis for the targeted development of AMF in microbial fertilizers. Soil nutrient characteristics should be the core decision-making parameters for microbial agent compatibility and application strategies. From the

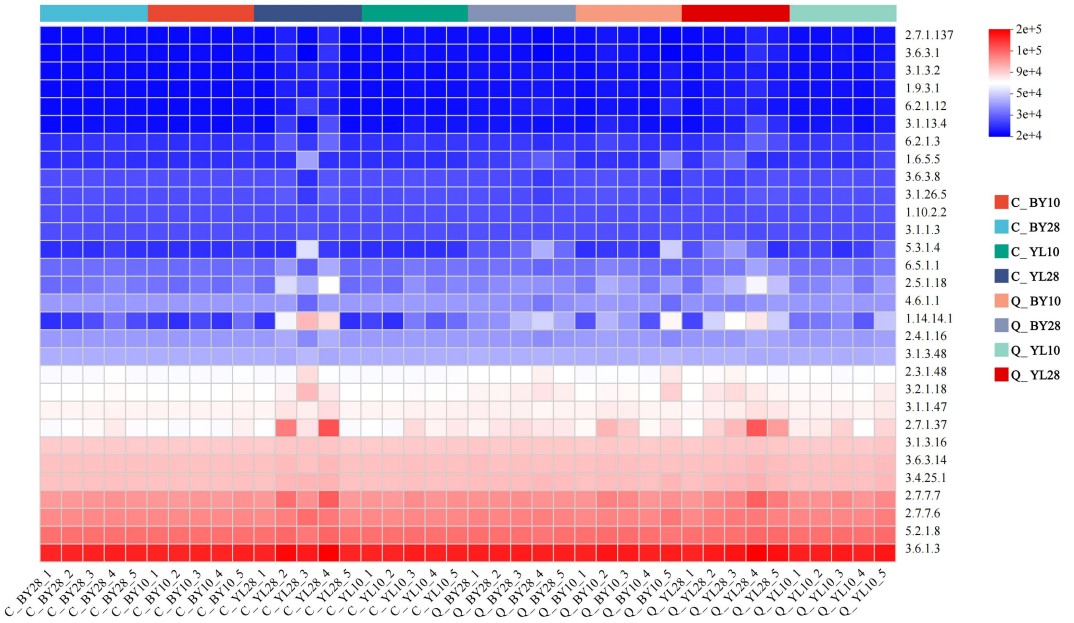

FIGURE 7
PICRUSt2 functional prediction heatmap of AMF in rhizosphere soil of mango orchard. C_BY10, 10yr old orchard in Baiyu Town during spring; C_BY28, 28yr old orchard in Baiyu Town during spring; C_YL10, 10yr old orchard in Yongle Town during spring; C_YL28, 28yr old orchard in Yongle Town during spring; Q_BY10, 10yr old orchard in Baiyu Town during autumn; Q_BY28, 28yr old orchard in Baiyu Town during autumn; Q_YL10, 10yr old orchard in Yongle Town during autumn; Q_YL28, 28yr old orchard in Yongle Town during autumn.

perspective of future microbial fertilizer development, sp.*VTX00387* can be developed into microbial fertilizers dominated by K elements. For soils with low K content, especially the red soils (pH4.5-5.5) widely distributed in the main mango-producing areas of southern China, the sp.*VTX00387* can be used as the microbial fertilizer component in a soil amendment. To address weak potassium retention capacity caused by the leaching of Ca^{2+} in acidic soils, the sp.*VTX00387* can be applied in conjunction with mineral fertilizer composed of calcium, magnesium and phosphate. Especially in soils with poor potassium mobility, AMF can overcome the diffusion limitations of potassium in the soil through the extension of mycelia, prevent secondary loss of K^+ resulting from factors like soil solution flow. Such strategy utilizing multi-level synergistic mechanism of activation-absorption-transport can rapidly transports the absorbed K^+ to the vicinity of the mango root system, making it available for absorption and utilization by the trees. It has the potential to systematically alleviate the supply-demand contradiction of K elements in the acidic soils of the mango-producing areas in southern China. Similarly, *S. sinuosa* can be developed to a microbial fertilizer with P as the main element, while balancing K. In some soils with high P contents but low utilization efficiency, such as those where long-term application of P fertilizer leads to its accumulation, the use of microbial fertilizers containing *S. sinuosa* can promote the transformation and utilization of insoluble P in the soil, improve the utilization efficiency of soil P resources, reduce P waste and environmental pollution (Cruz-Paredes et al., 2021). This addresses the issue of high phosphorus content and low utilization in acidic soil by relying on mycelial networks to achieve the synergy of phosphorus and potassium, providing microbial solutions for the sustainable nutrient management in southern China mango plantations. Although sp.*VTX00387* and *S. sinuosa* have shown clear correlation with soil P and K, their future commercialization still requires the establishment of a life cycle assessment system (LCA) for AMF functional strains, the development of soil nutrient AMF community, crop phenotype intelligent matching algorithms, and the precise release of microbial agents.

5 Conclusion

Our results showed that planting years and seasonal changes had minor impact on the structure and composition of AMF in mango rhizosphere soil, while soil chemical properties such as P, K, and their available content were major factors correlating with the AMF composition at two different mango orchards. A total of 733 ASVs were obtained from the rhizosphere soil of mango orchards, and 7 species of AMF belonging to 5 genera and 3 families were identified. Among them, *Glomus* was the absolute dominant genus in the mango AMF community, with a relative abundance of 53.39%~86.33%, followed by *Sclerocystis*. Differentiation analysis indicated that the molecular virtual species sp.*VTX00387* in the *Glomus* genus and *S. sinuosa* in the *Sclerocystis* genus were the dominant AMF species in the mango rhizosphere. The sp.*VTX00387* was positively correlated with K content and negatively correlated with P, AP, and AK. The high abundance of sp.*VTX00387* and *S. sinuosa* in the rhizosphere make them ideal candidate for specialized microbial fertilizers. This study provides a

theoretical basis and a reserve of strain resources for regulating nutrient dynamics in mango orchards to improve mango trees health and productivity.

Data availability statement

The datasets presented in this study can be found in online repositories. The names of the repository/repositories and accession number(s) can be found in the article/Supplementary Material.

Author contributions

CY: Data curation, Formal analysis, Investigation, Methodology, Project administration, Validation, Visualization, Writing – original draft, Writing – review & editing. ZT: Data curation, Formal analysis, Investigation, Methodology, Project administration, Validation, Visualization, Writing – original draft, Writing – review & editing. ZJ: Conceptualization, Data curation, Formal analysis, Investigation, Writing – review & editing. QO: Conceptualization, Data curation, Formal analysis, Writing – review & editing, Investigation. LL: Conceptualization, Data curation, Formal analysis, Writing – review & editing, Investigation. XH: Conceptualization, Data curation, Formal analysis, Writing – review & editing. MH: Conceptualization, Data curation, Formal analysis, Writing – review & editing. ZZ: Formal analysis, Funding acquisition, Methodology, Supervision, Writing – review & editing, Validation.

Funding

The author(s) declare that financial support was received for the research and/or publication of this article. This work was funded by the Guangxi Science and Technology Major Program (AA23062085), Guangxi Natural Science Foundation (2022GXNSFBA035458), the Guangxi Youth Talent Support Program (Zhengjie Zhu), Guangxi first-class discipline construction project (Agricultural Resources and Environment, Guijiao (2022) No. 1).

Acknowledgments

The authors would like to thanks the Guangxi Key Laboratory of Biology for Mango for their support.

Conflict of interest

The authors declare that the research was conducted in the absence of any commercial or financial relationships that could be construed as a potential conflict of interest.

Generative AI statement

The author(s) declare that no Generative AI was used in the creation of this manuscript.

Publisher's note

Supplementary material

The Supplementary Material for this article can be found online at: https://www.frontiersin.org/articles/10.3389/fpls.2025.1578936/full#supplementary-material

References

Bao, S. D. (2000). *Soil Agrochemical Analysis* (China: China Agricultural Press).

Boldt-Burisch, K., Naeth, M. A., Schneider, U., Schneider, B., and Hüttl, R. F. (2018). Plant growth and arbuscular mycorrhizae development in oil sands processing by -products. *Sci. Total Environ.* 621, 30–39. doi: 10.1016/j.scitotenv.2017.11.188

Chen, X., Wu'ern, A., Muguli, M., Bai, R., and Entmak, B. (2024). Evolution of fungal community structure in rhizosphere soil of lavender with different planting years. *J. Microbiol.* 44, 33–41. doi: 10.3969/j.issn.1005-7021.2024.02.003

Chen, X. Y., and Zeng, M. (2016). Effects of arbuscular mycorrhiza on physiological metabolism and protective enzyme system of kiwifruit. *South China Fruits* 45, 5. doi: 10.13938/j.issn.1007-1431.20150697

Cruz-Paredes, C., Diera, T., Davey, M., Rieckmann, M. M., and Jakobsen, I. (2021). Disentangling the abiotic and biotic components of AMF suppressive soils. *Soil Biol. Biochem.* 159, 108305. doi: 10.1016/j.soilbio.2021.108305

de Pontes, J. S., Oehl, F., Pereira, C. D., de Toledo MaChado, C. T., Coyne, D., da Silva, D. K. A., et al. (2017). Diversity of arbuscular mycorrhizal fungi in the Brazilian's Cerrado and in soybean under conservation and conventional tillage. *Appl. Soil Ecol.* 117, 178–189. doi: 10.1016/j.apsoil.2017.04.023

Govindan, M., Rajeshkumar, P. P., Varma, C. K. Y., Anees, M. M., Rashmi, C. R., and Nair, A. B. (2020). Arbuscular mycorrhizal fungi status of mango (Mangifera indica) cultivars grown in typic quartzipsamments soil. *Agric. Res.* 9, 188–196. doi: 10.1007/s40003-019-00432-8

Guo, Z., Yu, Z., Li, Q., Tang, L., and Luo, S. (2021). *Fusarium* species associated with leaf spots of mango in China. *Microb. Pathog.* 150, 104736. doi: 10.1016/j.micpath.2021.104736

Hartoyo, B., and Trisilawati, O. (2021). "Diversity of Arbuscular Mycorrhiza Fungi (AMF) in the rhizosphere of sugarcane," In *IOP Conference Series: Earth and Environmental Science IOP Publishing*, 653(1), 012066. doi: 10.1088/1755-1315/653/1/012066

Hassan, S. E. D., Boon, E., St-Arnaud, M., and Hijri, M. (2011). Molecular biodiversity of arbuscular mycorrhizal fungi in trace metal-polluted soils. *Mol. Ecol.* 20, 3469–3483. doi: 10.1111/j.1365-294x.2011.05142.x

Hussain, M., Adeel, M., and White, J. C. (2025). Nano-selenium: a novel candidate for plant microbiome engineering. *Trends Plant Sci.* doi: 10.1016/j.tplants.2025.02.002

Hussain, M., Xuan, P., Xin, Y., Ma, H., Zhou, Y., Wen, S., et al. (2024). Redundancy in microbiota-mediated suppression of the soybean cyst nematode. *Microbiome* 12, 125. doi: 10.1186/s40168-024-01840-x

IIA, A. E. S (2021). Effect of biochar rates on A-mycorrhizal fungi performance and maize plant growth, Phosphorus uptake, and soil P availability under calcareous soil conditions. *Commun. Soil Sci. Plant Anal.* 52, 815–831. doi: 10.1080/00103624.2020.1869766

Jia, T., Zhang, Y., Yao, Y., Wang, Y., Liang, X., Zheng, M., et al. (2023). Effects of AMF inoculation on the eco-physiological characteristics of Imperata cylindrica under differing soil nitrogen conditions. *Front. Plant Sci.* 14. doi: 10.3389/fpls.2023.1134995

Li, H., Jiang, S. T., Peng, H. Y., Gao, R. F., Zhang, J. L., Li, D. P., et al. (2022). Preliminary exploration of arbuscular mycorrhizal fungal resources in the rhizosphere soil of mango trees in Baise City, Guangxi. *Chin. J. Trop. Crops* 43, 2334–2344. doi: 10.3969/j.issn.1000-2561.2022.11.018

Ma, J., Zhao, Q., Zaman, S., Anwar, A., and Li, S. (2024). The transcriptomic analysis revealed the molecular mechanism of Arbuscular Mycorrhizal Fungi (AMF) inoculation in watermelon. *Sci. Hortic.* 332, 1–14. doi: 10.1016/j.scienta.2024.113184

Meddad-Hamza, A., Beddiar, A., Gollotte, A., Lemoine, M. C., and Gianinazzi, S. (2010). Arbuscular mycorrhizal fungi improve the growth of olive trees and their resistance to transplantation stress. *Afr. J. Biotechnol.* 9, 1159–1167. doi: 10.1186/1471-2164-11-131

Mickan, B. S., Abbott, L. K., Stefanova, K., and Solaiman, Z. M. (2016). Interactions between biochar and mycorrhizal fungi in a water-stressed agricultural soil. *Mycorrhiza* 26, 1–10. doi: 10.1007/s00572-016-0693-4

Mohammed, N. C., Nisy, S., Vishnu, N., Mohammed, A., Harikrishnan, M., Athira, M. M., et al. (2022). Comparative study on soil microbes from muthalamada mango farms. *Int. J. Res. Appl. Sci. Eng. Technol.* 10, 341–344. doi: 10.22214/ijraset.2022.41989

Ou, H. P., Peng, J. Y., Zhou, L. Q., Huang, J. S., Zhu, X. H., Zeng, Y., et al. (2021). Analysis of fertilization status and reduction potential of orchards in the main production area of baise mango. *J. South. Agric.* 52, 3375–3381. doi: 10.3969/j.issn.2095-1191.2021.12.021

Pei, Y., Yin, M., Li, Q. H., Zhang, Y. F., Zhong, Y., Chen, X., et al. (2023). Diversity and community structure of arbuscular mycorrhizal fungi (AMF) in the rhizospheric soil of panax notoginseng in different ages. *Eurasian Soil Sci.* 56, 329–339. doi: 10.1134/S1064229322602189

Rasmussen, P. U., Hugerth, L. W., Blanchet, F. G., Andersson, A. F., Lindahl, B. D., and Tack, A. J. (2018). Multiscale patterns and drivers of arbuscular mycorrhizal fungal communities in the roots and root-associated soil of a wild perennial herb. *New Phytol.* 220, 1248–1261. doi: 10.1111/nph.15088

Silvana, V. M., Carlos, F. J., Lucía, A. C., Natalia, A., and Marta, C. (2020). Colonization dynamics of arbuscular mycorrhizal fungi (AMF) in Ilex paraguariensis crops: Seasonality and influence of management practices. *J. King Saud Univ. Sci.* 32, 183–188. doi: 10.1016/J.JKSUS.2018.03.017

Singh, V. K., Soni, S. K., Shukla, P. K., Bajpai, A., and Laxmi, (2024). Application of paclobutrazol altered the soil bacterial diversity and richness of mango orchards: A metagenomic study. *Appl. Fruit Sci.* 66, 1163–1173. doi: 10.1007/s10341-024-01074-z

Song, F., Bai, F., Wang, J., Wu, L., Jiang, Y., and Pan, Z. (2020). Influence of citrus scion/rootstock genotypes on arbuscular mycorrhizal community composition under controlled environment condition. *Plants* 9, 901. doi: 10.3390/plants9070901

Svenningsen, N. B., Watts-Williams, S. J., Joner, E. J., Battini, F., Efthymiou, A., Cruz-Paredes, C., et al. (2018). Suppression of the activity of arbuscular mycorrhizal fungi by the soil microbiota. *ISME J.* 12, 1296–1307. doi: 10.1038/s41396-018-0059-3

Teixeira-Rios, T., da Silva, D. K. A., Goto, B. T., and Yano-Melo, A. M. (2018). Seasonal differences in arbuscular mycorrhizal fungal communities in two woody species dominating semiarid caatinga forests. *Folia Geobot.* 53, 191–200. doi: 10.1007/s12224-018-9314-7

Van Geel, M., Jacquemyn, H., Plue, J., Saar, L., and Ceulemans, T. (2017). Abiotic rather than biotic filtering shapes the arbuscular mycorrhizal fungal communities of European seminatural grasslands. *New Phytol.* 220, 1262–1272. doi: 10.1111/nph.14947

Wang, H. Q., Cheng, W., Hao, J., Mao, Y. Y., Lu, Q., Gu, T. Y., et al. (2021). Seasonal dynamics of arbuscular mycorrhizal fungi (AMF) communities in the roots and rhizosphere soil of Vetiveria zizanioides on coal gangue mountains in Guizhou. *Mycosystema* 40, 514–530. doi: 10.13346/j.mycosystema.200293

Wang, P., Liu, J. H., Xia, R. X., Wu, Q. S., Wang, M. Y., and Dong, T. (2011). Arbuscular mycorrhizal development, glomalin-related soil protein (GRSP) content, and rhizospheric phosphatase activity in citrus orchards under different types of soil management. *J. Plant Nutr. Soil Sci.* 174, 65–72. doi: 10.1002/jpln.200900204

Wu, X. Y., and Cui, X. Y. (2016). Effects of arbuscular mycorrhizal fungi on plant growth and fruit quality. *Tianjin Agric. Sci.* 22, 4. doi: 10.3969/j.issn.1006-6500.2016.06.028

Xie, X., Yang, Z., Li, D., Liu, Z., Li, X., and Zhu, Z. (2025). Proteomics analysis revealed the activation and suppression of different host defense components challenged with mango leaf spot pathogenalternaria alternata. *BMC Plant Biol.* 25, 1–13. doi: 10.1186/s12870-025-06250-1

Yang, S. L., Yin, M., Deng, L. J., Huang, B., Wang, Y. F., Huang, Y. R., et al. (2023). Diversity of arbuscular mycorrhizal fungi in the root system of Panax notoginseng at different ages and their correlation with soil physicochemical properties. *South. Agric. J.* 54, 3217–3227. doi: 10.3969/j.issn.2095-1191.2023.11.009

Ye, D., Zhou, X., Liu, X., Wang, W., Bian, J., and He, Z. (2024). Application of AMF Alleviates Growth and Physiological Characteristics of Impatiens walleriana under Sub - Low Temperature. *Horticulturae* 10, 856–870. doi: 10.3390/horticulturae10080856

Yu, L., Zhang, Z., Zhou, L., and Huang, K. (2023). Effects of altitude and continuous cropping on arbuscular mycorrhizal fungi community in siraitia grosvenorii rhizosphere. *Agriculture* 13, 1548. doi: 10.3390/agriculture13081548

Yurkov, A. P., Kryukov, A. A., Gorbunova, A. O., Kudriashova, T. R., Kovalchuk, A. I., Gorenkova, A. I., et al. (2023). Diversity of arbuscular mycorrhizal fungi in distinct ecosystems of the North Caucasus, a temperate biodiversity hotspot. *J. Fungi* 10, 11. doi: 10.3390/jof10010011

Zhang, Y. F., Mo, L. L., Liu, J. N., Niu, Y. F., Dong, C. L., Han, L., et al. (2015). Regulation of arbuscular mycorrhizal fungi on the growth and physiology of grape varieties with different growth vigor. *Hubei Agric. Sci.* 54, 6. doi: 10.14088/j.cnki.issn0439-8114.2015.20.032

Zhang, B., Shi, F., Zheng, X., Pan, H., Wen, Y., and Song, F. (2023). Effects of AMF compound inoculants on growth, ion homeostasis, and salt tolerance-related gene expression in oryza sativa L. Under salt treatments. *Rice* 16, 1–18. doi: 10.1186/s12284-023-00635-2

Zhao, W., Hu, X. N., Zheng, Y., Liang, N., Zheng, B., Wang, X. X., et al. (2024). Characteristics of the AMF community in the rhizosphere soil of maize and peanut and their responses to phosphate fertilizer. *Acta Agron. Sin.* 50, 2896–2907. doi: 10.3724/SP.J.1006.2024.43006

frontiers | Frontiers in Plant Science

TYPE Original Research
PUBLISHED 29 May 2025
DOI 10.3389/fpls.2025.1589266

OPEN ACCESS

EDITED BY
Rachana Singh,
Amity University, India

REVIEWED BY
Stanislav Kopriva,
University of Cologne, Germany
Gözde Merve Türksoy,
Max Planck Institute for Plant Breeding Research, in collaboration with reviewer SK
Jing Feng,
Guangxi Minzu University, China

*CORRESPONDENCE
Choong-Min Ryu
cmryu@kribb.re.kr

RECEIVED 07 March 2025
ACCEPTED 05 May 2025
PUBLISHED 29 May 2025

CITATION
Lee S-M, Yang H, Kong HG, Riu M and Ryu C-M (2025) Better than one: a synthetic community of Gram-positive bacteria protects pepper plants from aphid infestation through *de novo* volatile production. *Front. Plant Sci.* 16:1589266. doi: 10.3389/fpls.2025.1589266

Better than one: a synthetic community of Gram-positive bacteria protects pepper plants from aphid infestation through *de novo* volatile production

Sang-Moo Lee[1,2,3], Hyeonu Yang[1,2], Hyun Gi Kong[1,4], Myoungjoo Riu[1,2] and Choong-Min Ryu[1,2]*

[1]Molecular Phytobacteriology Laboratory, Infectious Disease Research Center, Korea Research Institute of Bioscience and Biotechnology (KRIBB), Daejeon, Republic of Korea, [2]Department of Biosystems and Bioengineering, Korea Research Institute of Bioscience and Biotechnology (KRIBB) School of Biotechnology, University of Science and Technology, Daejeon, Republic of Korea, [3]Institute of Agricultural Life Sciences, Dong-A University, Busan, Republic of Korea, [4]Department of Plant Medicine, College of Agriculture, Life and Environment Sciences, Chungbuk National University, Cheongju, Republic of Korea

Soil microbes offer various benefits to plants, including induced systemic resistance and growth promotion, with some functioning as biocontrol agents. Although the role of microbial consortium in microbiota function was recently elucidated, the production of a specific determinant through microbial cooperation for plant protection against insect infestation has not been demonstrated to date. Here, we report that a synthetic community (SynCom) comprising four Gram-positive bacteria could protect pepper plants from aphid infestation under greenhouse and field conditions. Headspace solid-phase microextraction-gas chromatography mass spectrometry analysis of the determinants produced by the four bacteria during co-cultivation led to the *de novo* detection of a volatile compound, 1-nonanol. Drench application of 1 mM 1-nonanol reduced aphid infestation. Taken together, our results suggest that SynCom and its volatile compound can effectively attenuate insect infestation. This is the first case study demonstrating how a volatile compound synthesized in the rhizosphere soil by bacteria protects plants against invasion by a sucking insect pest.

KEYWORDS

rhizobacteria, plant immunity, biological control, volatile, aphid, pepper

1 Introduction

In nature, microbial colonization in the rhizosphere soil facilitates plant adaptation to various environments by promoting plant growth (Zablotowicz et al., 1991; Hayat et al., 2010), enhancing abiotic stress tolerance (Yang et al., 2009), and defending plants against pathogen invasion (Kloepper et al., 2004; Berendsen et al., 2012; Kwak et al., 2018; Lee et al.,

2021). Certain rhizobacteria act as bioprotectants and biofertilizers by protecting plants from diseases and enhancing crop yield (Kloepper et al., 2004; Berg, 2009). Traditionally, beneficial bacterial species have been applied individually to agricultural fields; however, their effectiveness as bioprotectants and biostimulants has often been unstable. This instability under field conditions is attributed to the complex microbial interactions within natural communities (Martins et al., 2023). To address this issue, the co-inoculation of multiple bacterial species that mimic the natural microbiota, known as synthetic communities (SynComs), has recently been proposed (Vorholt et al., 2017; Durán et al., 2018; Martins et al., 2023).

The construction of SynComs can be achieved through the random selection of various natural isolates or through the integrated prediction of microbiota and plant phenotypes based on *in silico* approaches, such as metagenome sequencing (Martins et al., 2023). Accounting for microbial interactions is essential for SynCom construction. Microbial interactions among SynCom members, as well as those between SynCom members and native microbiota, play a crucial role in the overall functioning and stability of SynComs in nature (Lee et al., 2024). Recently, in addition to identifying keystone taxa important for the functionality and stability of SynComs, identifying rare taxa with relatively low abundance has been recognized as an essential consideration for ensuring the full activity of SynCom members (Jousset et al., 2017; Carlström et al., 2019; Lee et al., 2021; Xiong et al., 2021; Kim et al., 2023; Lee et al., 2024). In recent studies, diverse SynComs were constructed to investigate plant-microbiome interactions for causality determination, yet the chemical determinants underlying SynCom functionality remain largely unknown.

Microorganisms do not exist individually in nature, rather in multi-species communities, where biological diversity leads to chemical diversity (Martins et al., 2023). The chemicals produced by microbes include volatile and non-volatile secondary metabolites. A key feature of volatiles is their ability to travel long distances through air and soil, making them effective mediators of microbe-microbe or plant-microbe interactions (Ryu et al., 2003, 2004; Cernava et al., 2015; Silva Dias et al., 2021; Weisskopf et al., 2021). Bacterial volatiles, including 2,3-butanediol and acetoin, are known to promote plant growth and activate plant immunity (Garbeva and Weisskopf, 2020; Silva Dias et al., 2021; Gfeller et al., 2022; Almeida et al., 2023; Singh et al., 2024; Belt et al., 2025). For instance, 2,3-butanediol released by *Bacillus velezensis* strain GB03 (previously *Bacillus amyloliquefaciens*) was first reported to enhance plant growth and immunity in *Arabidopsis thaliana* (Ryu et al., 2003, 2004). Subsequent studies reported that bacterial volatile compounds protect host plants against microbial pathogens, including viruses, bacteria, and fungi, as well as insect pests (Cortes-Barco et al., 2010; Song and Ryu, 2013; Kong et al., 2018; Gfeller et al., 2022; Jung et al., 2023; Singh et al., 2024; Belt et al., 2025). Previously, most studies investigating the beneficial effects of volatiles focused on single bacterial species. Consequently, little is known about the biosynthesis of volatile compounds by SynCom for crop protection. However, a recent study reported differences in volatile composition between bacterial monocultures and mixed cultures (Schulz-Bohm et al., 2015). In addition, loss of the unique functionality of microbial volatiles was observed when specific taxa were absent from a microbial community (Hol et al., 2015). Thus, these data suggest the potential for the biosynthesis of specific volatile(s) that determine the functionality of SynCom.

Previously, based on the microbiome analysis of rhizosphere soil in tomato (*Solanum lycopersicum* L.) fields, we constructed a protective SynCom comprising four Gram-positive bacteria, namely, *Brevibacterium frigoritolerans* HRS1, *Bacillus niacini* HRS2, *Solibacillus silvestris* HRS3, and *Bacillus luciferensis* HRS4 (Lee et al., 2021). This SynCom efficiently reduced the occurrence of bacterial wilt disease, caused by *Ralstonia pseudosolanacearum*, in tomato by activating plant immunity (Lee et al., 2021). A complete combination of SynCom with keystone taxa and rare taxa can induce the full activation of plant immunity in tomato. However, the ability of SynCom to control naturally-occurring plant diseases and insect pests and the SynCom-derived determinants involved in this process remain largely unknown.

The aim of the present study is to investigate the biocontrol activity of the SynCom under field conditions. To validate this, we applied the SynCom to the root system of pepper plants instead of tomato plants, as tomatoes are generally cultivated in greenhouse conditions in S. Korea. Drenching application of SynCom effectively protects pepper (*Capsicum annum* L.) plants against aphid (*Myzus persicae* L.) infestation, even under field conditions. Compared with individual bacterium inoculations, the SynCom treatment showed higher biocontrol activity against aphid infestation in the field. The four bacterial species when used together as the SynCom specifically produced the volatile compound 1-nonanol. Thus, our data highlight the role of a specific combination of bacterial species (HRS1 + 2+3 + 4) in the production of a unique metabolite for host plant protection.

2 Materials and methods

2.1 Plant materials

Pepper (*Capsicum annum* L. cv. Bulkala) seeds were sown on autoclaved soilless potting medium (Punong, Co. Ltd., Gyeongju, South Korea), containing zeolite, perlite, colored dust, and lime (pH = 4.5–7.5), in a 50-hole plastic tray (28 cm × 54 cm × 5 cm). After 7 days, pepper seedlings were transplanted in new round pots (diameter = 10 cm, height = 8.5 cm) containing autoclaved soilless potting medium. Pepper plants were grown in an environmentally controlled growth room at 25°C under fluorescent lights (approximately 7,000 lux light intensity) and 12 h light/12 h dark cycle.

2.2 Evaluation of SynCom and 1-nonanol against aphid infestation in the greenhouse

Four different Gram-positive bacteria (*Brevibacterium frigoritolerans* HRS1, *Bacillus niacini* HRS2, *Solibacillus silvestris*

HRS3, and *Bacillus luciferensis* HRS4) were cultured as described previously. Briefly, four bacterial isolates were cultured on Tryptic Soy Agar (TSA, Difco Laboratories, Detroit, MI, USA) medium at 30 °C for 1 day and suspended in sterile distilled water (OD_{600} = 1.0). To prepare the SynCom suspension, the four strains were initially prepared at a higher concentration and then mixed in calculated volumes to achieve a final OD_{600} of 1.0 for each bacterium. To conduct the greenhouse experiment, 10 mL of the SynCom suspension was drenched into the root system of 3-week-old pepper plants twice a week, and the number of aphids on the aerial parts of each plant was counted at 0, 7, and 14 days after inoculation. Then, 10 mL of 1-nonanol at four different concentrations (1 µM, 10 µM, 100 µM, and 1 mM) was drenched into the root system of 3-week-old pepper plants. Drench application of 10 mL of 0.5 mM of benzothiadiazole (BTH) and sterile distilled water (SDW) served as positive and negative controls, respectively, and the number of aphids on the aerial parts of each plant was counted at 3, 4, 5, 6, and 7 days after inoculation.

Aphid (*Myzus persicae* L.) adults were obtained from the Department of Agro-Food Safety and Crop Protection, National Institute of Agricultural Sciences, Rural Development Administration, South Korea. Aphids were reared in a miniature plastic box (70 cm wide × 70 cm long × 80 cm tall). Then, 10 aphids were transferred onto the apex of freshly grown pepper plants using a small paint brush one week after the SynCom or 1-nonanol treatment.

2.3 Field trials

Field trials were conducted at Nonsan, Chungcheongnam-do, South Korea (36.23577°N, 127.18946°E). All necessary permits were obtained from landowners prior to the commencement of field trials. To evaluate the biocontrol activity of SynCom under typical field conditions, irrigation and fertilizer treatments were applied uniformly across all plots, including the negative control, by the farm owner, according to the environmental conditions at the experimental site throughout the entire trial period. Before transplanting, the furrows were covered with black polyethylene film to prevent weed growth. Pepper seedlings were planted 30 cm apart. After 30 days of growth, seedlings were irrigated with bacterial suspensions (OD_{600} = 1.0), 0.5 mM BTH, or SDW (100 mL per seedling) every 10 days, for a total of three times per month. To prepare the SynCom suspension (a mixture of HRS1, HRS2, HRS3, and HRS4), suspensions of all four strains were mixed, and the final OD_{600} of each bacteria was adjusted to 1.0. Each treatment was applied to four blocks, in a randomized block design (n = nine plants per treatment). For GC–MS analysis, we employed an Agilent 7890A series gas chromatograph (Agilent Technologies, Santa Clara, CA, United States).

To inoculate pepper plants, *Xanthomonas axonopodis* pv. *vesicatoria* (*Xav*) was cultured overnight at 28 °C in LB medium. At 2 weeks after inoculation, 500 µL of *Xav* (OD_{600} = 0.01) culture was pressure-infiltrated into the abaxial surface of pepper leaves using a needleless syringe. Seven days after inoculation, the severity of disease caused by *Xav* was recorded on a 0–5 scale, where 0 = no symptom; 1 = mild chlorosis; 2 = chlorosis; 3 = severe chlorosis and mild necrosis; 4 = necrosis; and 5 = necrosis with cell death (Kim et al., 2022). Each treatment was applied to four blocks, with five plants per treatment, in a randomized block design.

2.4 Evaluation of aphid infestation in pepper under field conditions

To evaluate the biological control activity of SynCom under field conditions, we measured the severity of aphid infestation at 4 weeks after treatment at the Nonsan field. The severity of aphid infestation was recorded on a 0–5 scale based on the distribution of aphids in the aboveground parts of the pepper: 0 = no infestation; 1 <25% of the pepper plant infested; 2 <50% of the pepper plant infested; 3 <75% of the pepper plant infested; 4 <100% of the pepper plant infested; and 5 = whole plant infested. Each treatment was replicated four or five times in a randomized block design (n = 36 plants per treatment).

2.5 Pepper fruit yield measurement

Fruit fresh weight per plant and number of pepper fruits per 20 plants in a row were measured at 16 weeks after transplanting, with four replications. Only red-colored fruits were harvested for market value. Total yield (g/plant) was estimated per treatment, and the total fruit weight per plant was calculated. In addition, the number of fruits per plant was recorded at each harvest, and the total harvest was then calculated as the number of fruits per plant.

2.6 Detection of *de novo* volatile compound production

Volatile compounds produced by the SynCom were identified by headspace solid-phase microextraction-gas chromatography mass spectrometry (HS-SPME-GC-MS). Briefly, 50 µL of each bacterial suspensions was inoculated on the TSA medium and cultured in 20-mL SPME vials at 30°C for 2 days. Suspension cultures of the four different bacterial species were mixed in different combinations (HRS1 + HRS2, HRS1 + HRS2 + HRS3, HRS1 + HRS2 + HRS4, and HRS1 + HRS2 + HRS3 + HRS4), and the final OD_{600} of each mixed bacterial species, as well as that of monocultures (HRS1, HRS2, HRS3, and HRS4), was adjusted to 1.0. The equipment condition of HS-SPME-GC-MS was modified using the method described previously (Song et al., 2019). Briefly, the fibers were conditioned in the GC injection port prior to use, according to the manufacturer's instructions. A manual holder was used to handle the fibers. Separation was performed using the

following program: initial temperature of 50°C with a 2-min hold, followed by ramping up to 220°C at a rate of 10°C/min with a 2-min hold. The split–splitless injection port was maintained at 280°C for volatile desorption in split mode, with a split ratio of 1:10. Helium was employed as the carrier gas at a constant flow rate of 1.0 mL/min. Volatile organic compounds (VOCs) were separated using a non-polar HP-5MS column (30 m × 0.25 mm × 0.25 μm, Hewlett Packard) with the following program: initial temperature of 40°C with a 3-min hold, followed by ramping up to 220°C at 10°C/min with a 2-min hold. The split–splitless injection port was set to 250°C in splitless mode. The MS parameters were set to the full-scan mode, with a range of 40–500 amu at a scan rate of 0.817 scan/s. The ion source temperature was 250°C, with an ionization energy of 70 eV and a mass transfer line temperature of 300°C. The retention time (tR) and mass spectrum of each VOC was compared with those of authentic standards and of volatiles from the National Institute of Standards and Technology (NIST) reference library. An in-house dedicated mass spectral library, containing the spectra of known compounds, was also used to verify the identity of the detected VOCs.

2.7 Expression analysis of defense-related marker genes in pepper leaves

Total RNA was isolated from pepper leaves collected at 8 days post-aphid inoculation, and first-strand cDNA was synthesized as previously described (Song et al., 2017). Quantitative real-time PCR (qRT-PCR) was carried out on the Chromo4 Real-Time PCR System (Bio-Rad, Hercules, CA, USA) using iQ™ SYBR® Green SuperMix (Bio-Rad), 10 pM sequence-specific primers (Supplementary Table 1) (Lee et al., 2012; Yi et al., 2013; Kong et al., 2018), and cDNA (template). The reaction conditions were as follows: an initial polymerase activation step at 95°C for 10 min, followed by 40 cycles of denaturation at 95°C for 30 s, annealing at 60°C for 30 s, and extension at 72°C for 30 s. Gene expression levels were calibrated and normalized against the mRNA level of *CaActin*.

2.8 Statistical analysis

Data were analyzed using analysis of variance (ANOVA) in JMP 4.0 software (SAS Institute Inc., Cary, NC, USA). Significant treatment effects were determined based on the F-value at a significance level of $p < 0.05$. When a significant F-value was obtained, *post hoc* pairwise comparisons were conducted using Fisher's protected least significant difference (LSD) or Tukey's honestly significant difference (HSD) test at $p < 0.05$. For ordinal disease severity measurements related to naturally occurring aphid infestations and *Xav* infections, statistically significant differences were assessed using the nonparametric Kruskal-Wallis test, followed by Dunn's *post hoc* test for multiple comparisons, implemented in R (http://www.r-project.org/).

3 Results

3.1 Gram-positive bacterial SynCom reduced aphid infestation in pepper

Previously, we designed a plant-protective SynCom comprising four Gram-positive bacterial species isolated from field upland soils (Lee et al., 2021). Since the drench application of SynCom systemically elicited induced resistance in tomato plants, we wanted to test whether the drench application of SynCom can protect economically important crop plants from insect pests. The roots of pepper plants grown under greenhouse conditions were drenched with the SynCom suspension, and the population of aphids on the aboveground plant parts was assessed (Figures 1A, B). Compared with the control, drenching with 0.5 mM BTH (positive control) reduced the aphid population size by 1.8- and 2.7-fold at 7 and 14 days post infestation, respectively (Figure 1C). Similar to BTH, the drench application of SynCom also reduced the population of aphids on pepper plants by 1.7- and 1.6-fold at 7 and 14 days post infestation, respectively (Figure 1C). However, unlike BTH, the SynCom treatment did not result in a growth penalty in pepper (Supplementary Figure 1).

SynCom activates the signaling of defense-related phytohormones, salicylic acid (SA) and jasmonic acid (JA), in tomato plants (Lee et al., 2021). To validate the activation of SA and JA signaling by SynCom treatment in pepper plants, we analyzed the expression patterns of defense-related marker genes involved in SA and JA signaling in pepper leaves at 24 hours post aphid inoculation (Figure 1D). Compared with the negative control, treatment with SynCom and BTH upregulated the expression of SA signaling marker gene *CaPR1* by 2.5-fold and 2.07-fold, respectively. In addition, SynCom treatment upregulated the expression of JA biosynthesis gene *CaLOX* by 2.74-fold compared to control, but not BTH treatment. However, the expression of JA responsive gene *CaPIN2* was downregulated by SynCom treatment compared to control. Thus, this result suggests that the SynCom treatment activates induced resistance in pepper plants against aphids.

3.2 SynCom enhanced resistance against aphids and *Xav* in pepper under field conditions

To test the disease control activity of the Gram-positive bacterial SynCom under field conditions, the roots of pepper plants grown at Nonsan, South Korea, were drenched with either individual bacterial suspensions or the SynCom suspension (Figures 2A, B). Among the bacterial treatments, only drenching with the SynCom suspension significantly reduced aphid infestation in pepper plants by 1.5-fold compared with the negative control (Figure 2B). In contrast, individual application of each strain did not lead to a significant reduction in aphid infestation compared with the negative control (Figure 2B). Meanwhile, treatment with BTH (positive control) reduced aphid infestation by 2.7-fold compared with the negative control (Figure 2B).

10.3389/fpls.2025.1589266

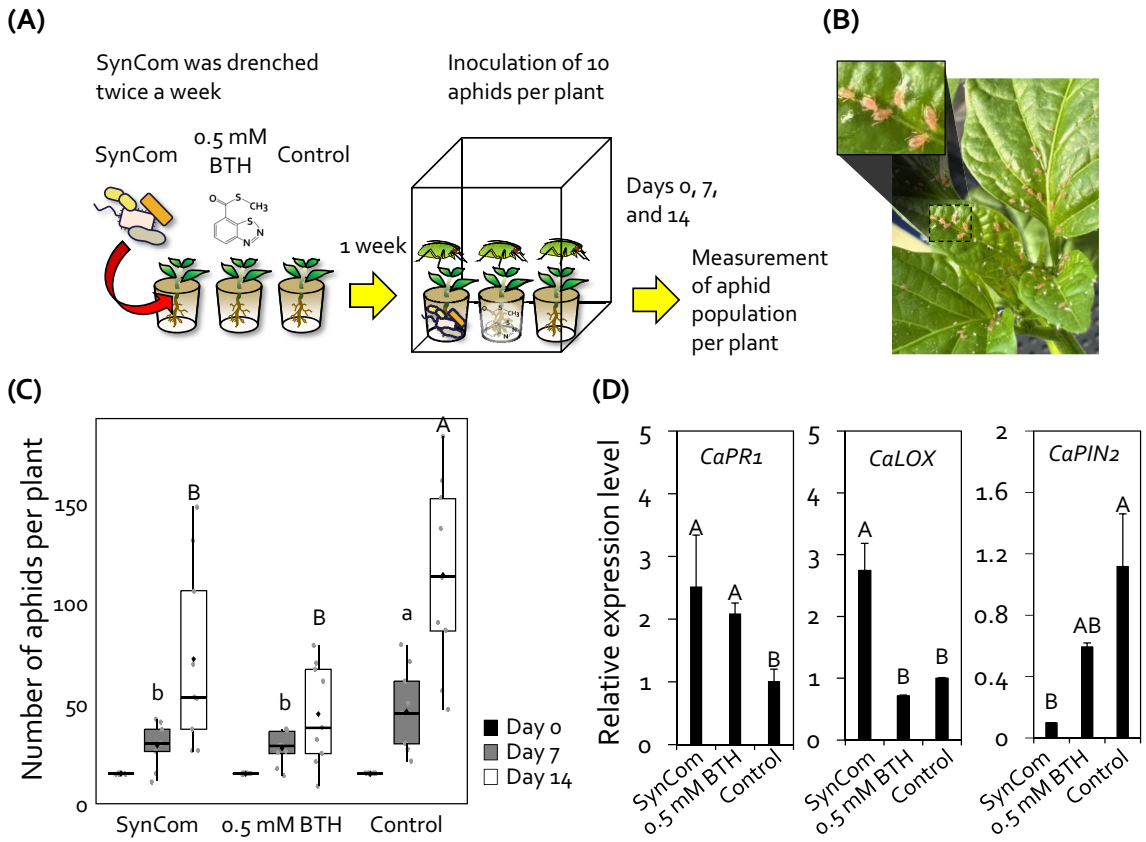

FIGURE 1
Synthetic community (SynCom) comprising four Gram-positive bacteria reduced aphid infestation in pepper plants. **(A)** Experimental procedure for the aphid control assay. SynCom (10 mL) was drenched into the root system of 3-week-old pepper plants twice a week. One week after the SynCom treatment, each pepper plant was inoculated with 10 aphids. The total population of aphids on the aerial parts of plants were counted at 0, 7, and 14 days post-inoculation. **(B)** Photograph showing aphid infestation on the aboveground parts of pepper plants at 14 days post-inoculation. **(C)** Total number of aphids on SynCom-treated pepper plants. SynCom, mixture of *Brevibacterium frigoritolerans* HRS1, *Bacillus niacini* HRS2, *Solibacillus silvestris* HRS3, *Bacillus luciferensis* HRS4; BTH, 0.5 mM benzothiadiazole (positive control); SDW, sterile distilled water (negative control). Data represent mean ± standard error of the mean (SEM; n = 18 replications per treatment). Different letters indicate significant differences between treatments ($P < 0.05$; least significant difference [LSD] test). Diamonds and bolded lines of the boxplot are the average and median of indicated values, respectively. **(D)** Relative expression levels of salicylic acid signaling marker gene (*CaPR*) and jasmonic acid signaling marker gene (*CaLOX* and *CaPIN2*) in the leaves of pepper plants treated with 1-nonanol at 24 hour post-inoculation with aphids. Data represent mean ± SEM. Different letters indicate significant differences between treatments ($P < 0.05$; LSD).

Previously, we showed that the activation of induced resistance against both aphids and *Xav* involves the same defense signaling pathways, including SA and JA signaling (Lee et al., 2012). Thus, SynCom-mediated induced resistance led us to hypothesize that the SynCom treatment can also elicit induced resistance against *Xav* infection in pepper. Indeed, drenching with SynCom reduced the symptoms of bacterial spot disease, caused by *Xav*, on the leaves of pepper plants under field conditions (Figure 2C). SynCom application notably reduced the severity of bacterial leaf spot on pepper leaves by 1.4-fold compared to the negative control (Figure 2C). In contrast, none of the individual SynCom strains showed a significant effect on disease severity (Figure 2C). BTH achieved a significant 1.6-fold reduction compared to negative control, and its disease control efficacy was comparable to that of SynCom (Figure 2C). Taken together, these results indicate that the combination of Gram-positive bacteria (SynCom) systemically protects pepper plants from attack by insect pests and bacterial pathogens.

3.3 SynCom treatment increased fruit yield

To investigate the effect of SynCom on the fruit yield of pepper plants, we measured the weight and number of fruits harvested from SynCom-treated pepper plants in the field at Nonsan in 2019 (Figures 3A, B). Drenching with SynCom enhanced the fruit number and weight per plant by 1.5- and 1.7-fold, respectively, compared with the negative control (Figures 3A, B). The drench application of HRS4 suspension also enhanced the fruit weight per plant by 1.7-fold, but not fruit number per plant, compared with the negative control (Figures 3A, B). Treatment with HRS1, HRS2, and HRS3 suspensions individually did not affect pepper fruit number

10.3389/fpls.2025.1589266

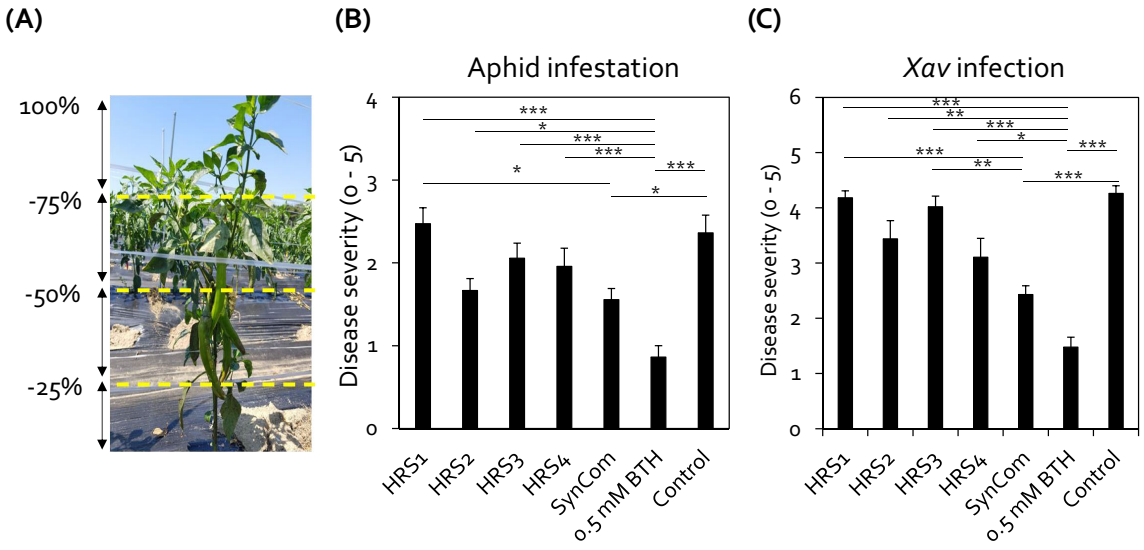

FIGURE 2
Drench application of SynCom protected pepper plants from aphid infestation and *Xanthomonas axonopodis* pv. *vesicatoria* (*Xav*) infection under field conditions. **(A)** Severity standard for aphid infestation in pepper plants in the field at Nonsan. Aphid infestation severity was recorded on a 0–5 scale, based on the proportion of aboveground tissues infested: 0 = no infestation; 1 = less than 25% of plant parts infested; 2 = 25–49% of plant parts infested; 3 = 50–74% infested; 4 = 75–99% infested; 5 = whole plant infested, resulting in plant death. **(B)** Severity of aphid infestation in pepper plants at 4 weeks after SynCom treatment. Data represent mean ± SEM of 10 plants with four block repeats (n = 40 replications per treatment). Asterisks indicate significant differences (*$P < 0.05$; **$P < 0.01$; ***$P < 0.001$; Dunn's test). **(C)** Drench application of SynCom protected pepper plants against *Xav* infection under field conditions. Data represent mean ± SEM of five plants with three block repeats (n = 15 replicates per treatment). Asterisks indicate significant differences (*$P < 0.05$; **$P < 0.01$; ***$P < 0.001$; Dunn's test). HRS1, *Brevibacterium frigoritolerans* HRS1; HRS2, *Bacillus niacini* HRS2; HRS3, *Solibacillus silvestris* HRS3; HRS4, *Bacillus luciferensis* HRS4; SynCom, mixture of HRS1–4; BTH, 0.5 mM benzothiadiazole (positive control); SDW, sterile distilled water (negative control).

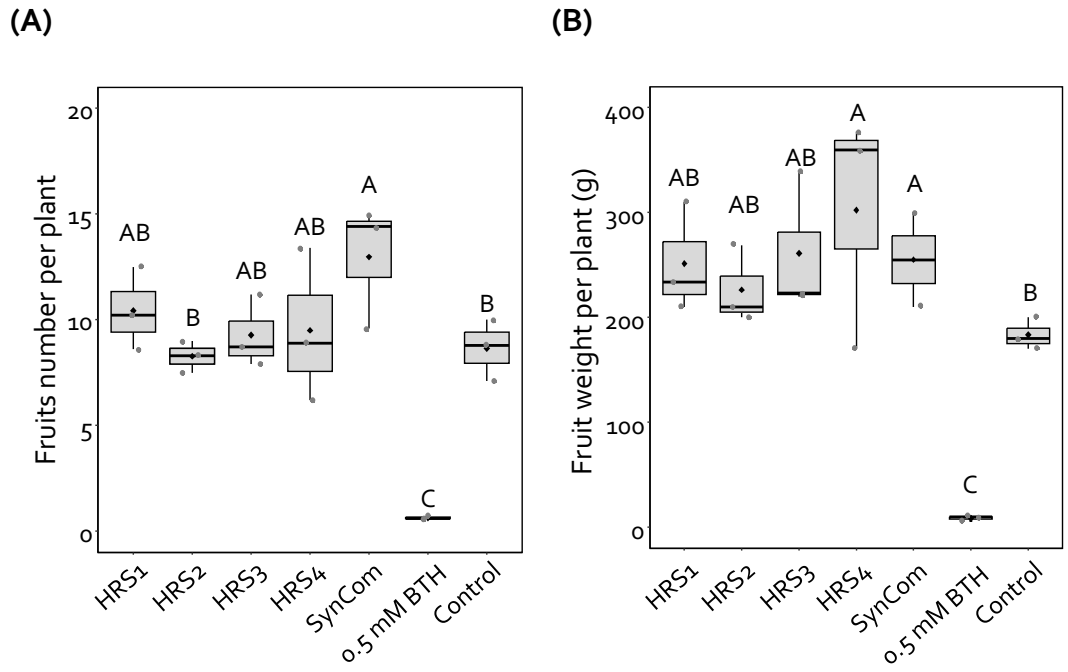

FIGURE 3
SynCom treatment increased pepper fruit yield. **(A, B)** Number **(A, B)** fresh weight of pepper fruits harvested from three blocks, each containing seven plants (n = 21), treated with Gram-positive bacterial species (either individually or as a mixture), BTH, and SDW. For each treatment, seven plants per block were measured and averaged, resulting in one value per block. Dots represent these block-level averages. HRS1, *Brevibacterium frigoritolerans* HRS1; HRS2, *Bacillus niacini* HRS2; HRS3, *Solibacillus silvestris* HRS3; HRS4, *Bacillus luciferensis* HRS4; SynCom, mixture of HRS1–4; BTH, 0.5 mM benzothiadiazole (positive control); SDW, sterile distilled water (negative control). Different letters indicate significant differences between treatments ($P < 0.05$; LSD). Diamonds and bolded lines of the boxplot are the average and median of indicated values, respectively.

and weight. Meanwhile, drenching with BTH significantly reduced the pepper fruit yield (Figures 3A, B). Thus, SynCom treatment increased the yield of pepper fruits under field conditions.

3.4 *De novo* production of 1-nonanol by the SynCom deterred aphid infestation in pepper

To identify the determinant eliciting plant immunity against aphid infestation, we analyzed the volatiles produced by SynCom bacteria by HS-SPME-GC-MS. Previously, various combinations (dual, triple, and quadruple mixes) were tested by supplementing the core strains HRS1 and HRS2 with HRS3 and/or HRS4, and the complete combination of all four strains (HRS1 + HRS2 + HRS3 + HRS4) most effectively suppressed disease development (Lee et al., 2021). Based on this, we analyzed the volatiles emitted by single strains or various combinations in which HRS1 and HRS2 were supplemented with HRS3 and/or HRS4 (Figure 4). We selected major compounds that were detected only in the SynCom treatment, with a match quality >90% and a peak area >1%, and were not detected in the control. 1-Butanol, 3-methyl-, Octyl chloroformate, (S)-(+)-6-Methyl-1-octanol, 1-Nonanol, and Cyclodecane were detected in SynCom (Supplementary Table 2, Supplementary Figure 2). Among five major candidates, the full SynCom (HRS1 + HRS2 + HRS3 + HRS4) treatment resulted in the production of the volatile compound 1-nonanol, with a 90% matching quality of its mass spectrum in the MS library, at levels higher than those produced in other treatments (i.e., individual or other combinatorial inoculations) (Figure 4). The volatile compound 1-nonanol was also detected in the HRS4 and HRS1 + 2+4 treatments, but its abundance in the SynCom treatment was 5.1- and 13.8-fold higher, respectively, at 13.6 min (Figure 4). Since the four bacterial strains were more effective in protecting pepper plants from aphids and *Xav* when used altogether than when used individually, we hypothesized that 1-nonanol generated by SynCom might be a key factor in reducing plant diseases.

To investigate the active concentration of 1-nonanol for controlling aphid infestation, we applied serially diluted concentration of 1-nonanol (1 mM, 100 µM, 10 µM, and 1 µM) to the pepper root system (Figure 5A). Drench application of 1 mM 1-nonanol significantly decreased the aphid population on pepper plants by 26.1%, 34.5%, 45.1%, 48.3%, and 38.9% at 3, 4, 5, 6, and 7 days post-inoculation, respectively compared with the negative control (Figure 5A). Significant reduction in aphid populations was also observed in the SynCom or BTH treatment at 4, 5, 6, and 7 days post-inoculation.

To investigate whether the SynCom-derived 1-nonanol activates defense signaling in pepper, we analyzed the expression

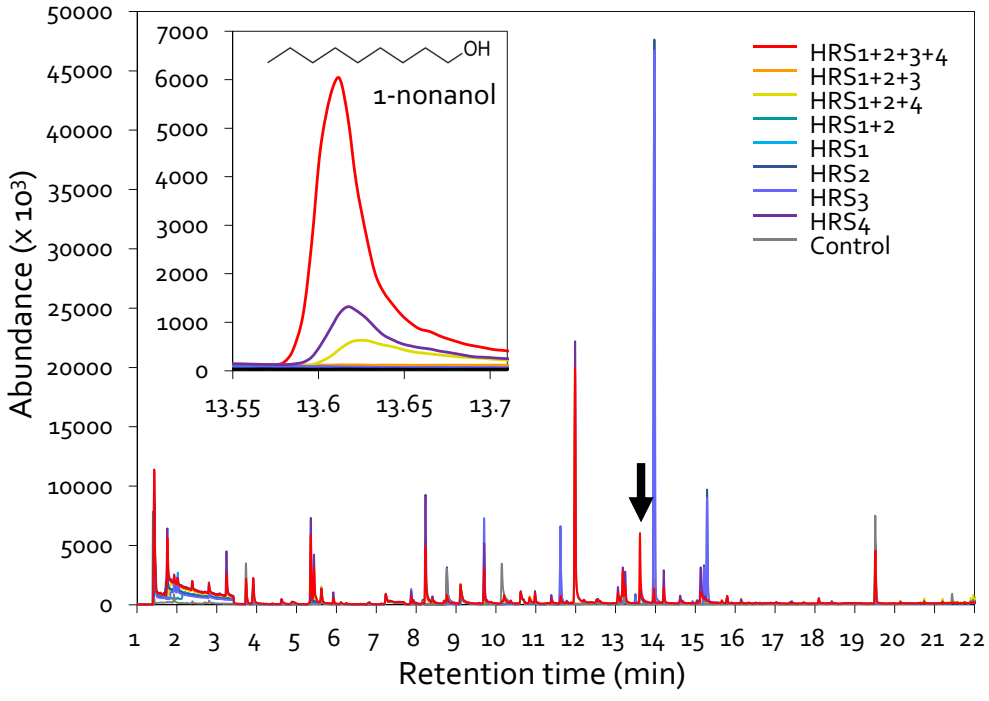

FIGURE 4
Chromatographic profiling of volatile organic compounds (VOCs) produced by Gram-positive bacteria. GC-MS of VOCs released by Gram-positive bacteria,either individually or in different combinations. The TSA medium was inoculated with bacterial suspensions in 20-mL SPME vials and incubated at 30°C for 2 days. The graph at the top left shows the peak of 1-nonanol. HRS1 + HRS2, mixture of *Brevibacterium frigoritolerans* (HRS1) and *Bacillus niacini* (HRS2); HRS1 + HRS2 + HRS3, mixture of HRS1, HRS2, and *Solibacillus silvestris* (HRS3); HRS1 + HRS2 + HRS4, mixture of HRS1, HRS2, and *Bacillus luciferensis* (HRS4); HRS1 + HRS2 + HRS3 + HRS4, mixture of all four SynCom strains. HRS1, HRS2, HRS3, and HRS4, single inoculations of SynCom strains; Control, Tryptic Soy Agar (negative control).

10.3389/fpls.2025.1589266

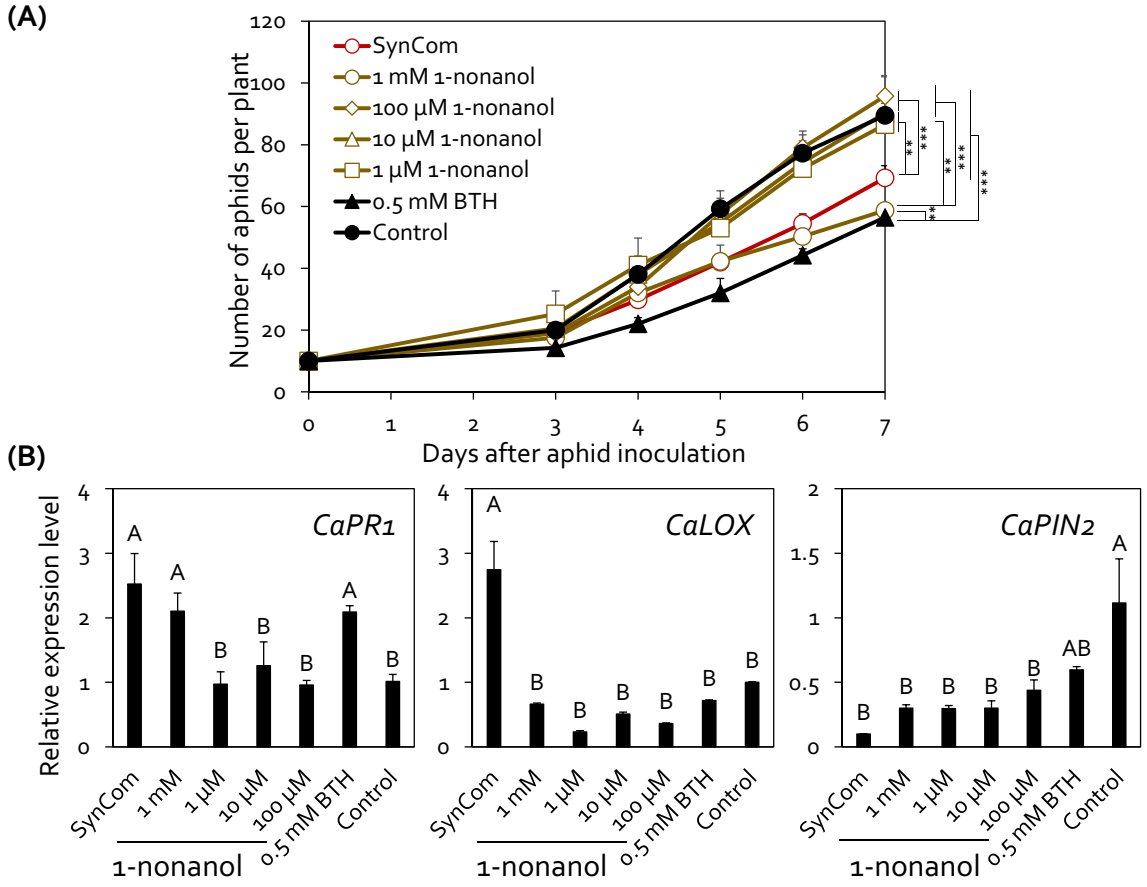

FIGURE 5
Exogenous 1-nonanol treatment protected pepper plants from aphid infestation. **(A)** Effect of 1-nonanol on aphid population size. The root system of pepper plants (n = 5) was drenched with 10 mL of 1-nonanol at different concentrations (1 µM, 100 µM, 10 µM, and 1 mM). The number of aphids on the aerial parts of pepper plants was counted at 3, 4, 5, 6, and 7 days post-inoculation. Comparison of treatments at different time points (Day 3 to Day 7) was performed using repeated measures ANOVA, with Group and Time as between-subjects and within-subjects factors, respectively, followed by Tukey's honestly significant difference (HSD) *post-hoc* tests for pairwise comparisons (*p < 0.05, **p < 0.01, ***p < 0.001). The experiment was repeated three times with similar results. **(B)** Relative expression levels of salicylic acid signaling marker gene (*CaPR*) and jasmonic acid signaling marker gene (*CaLOX* and *CaPIN2*) in the leaves of pepper plants treated with 1-nonanol at 24 hour post-inoculation with aphids. Data represent mean ± SEM. Different letters indicate significant differences between treatments (P < 0.05; LSD). SynCom, mixture of HRS1, HRS2, HRS3, and HRS4; 1mM, 100 µM, 10 µM, and 1 µM, 1-nonanol treated pepper; BTH, 0.5mM BTH treated pepper; Control, SDW treated pepper.

patterns of defense-related marker genes involved in SA and JA signaling in pepper leaves at 24 hours post-inoculation (Figure 5B). Compared with the negative control, treatment with SynCom and BTH upregulated the expression of SA signaling marker gene *CaPR1* by 2.52-fold, 2.09-fold, respectively. Treatment with 1 mM 1-nonanol and BTH upregulated the expression of SA signaling marker gene *CaPR1* by 2.10-fold, compared with the negative control. SynCom treatment activated the expression of the JA biosynthesis gene *CaLOX* by 2.74-fold compared to the control, but did not affect the expression of the JA responsive gene *CaPIN2*. However, except for SynCom, the expression of the JA marker genes *CaLOX* and *CaPIN2* did not up-regulated in any 1-nonanol treatments compared to negative control (Figure 5B). Meanwhile, unlike BTH, exogenous 1-nonanol treatment did not result in a growth penalty in pepper (Supplementary Figure 3). Taken together, these results suggest that the SynCom can activate SA-dependent induced resistance in pepper plants against aphids through the *de novo* synthesis of 1-nonanol.

4 Discussion

Rhizosphere microbiota benefit plants by enhancing their abiotic and biotic stress tolerance. While studies have explored the interactions among beneficial microbiota, the production of unique plant-protective determinants by these microbiota remains largely unknown. Here, we demonstrate that a Gram-positive SynCom and its *de novo* synthesized metabolite, 1-nonanol, protects pepper plants from aphid infestation under greenhouse and field conditions. The SynCom showed higher biocontrol activity against aphids and *Xav* compared with individual bacterial inoculations. We found that the volatile compound 1-nonanol, produced by the combination of all four Gram-positive positive bacteria (SynCom), reduced aphid infestation in pepper plants, demonstrating how this specific bacterial combination produces a unique metabolite to enhance plant defense.

Previously, the SynCom exhibited priming effects against *Ralstonia pseudosolanacearum* SL341, which causes bacterial wilt

disease in tomato (Lee et al., 2021). Consistent with this finding, when applied as a biocontrol agent in pepper, another *Solanaceae* crop, the SynCom exhibited strong disease control activity against aphids under both indoor and field conditions (Figures 1, 2). In alignment with previous data, the application of all four Gram-positive bacteria (SynCom) resulted in the highest biocontrol activity compared with individual bacterium inoculations and control (Figure 2, Lee et al., 2021). Similar to resistance against aphids, the SynCom treatment also protected pepper plants against the semibiotrophic bacterial pathogen *Xav* (Figure 2B). Since the SynCom treatment primed SA- and JA-dependent induced resistance against *R. pseudosolanacearum* in tomato and aphid in pepper plant (Lee et al., 2021, Figure 1D), it is likely that the induced resistance triggered by the SynCom used in this study shares similarities with that induced against other phytopthogens and herbivores, including the sucking insect-pest aphid, *Xav*, and *R. pseudosolanacearum* (Walling, 2000; Kaloshian and Walling, 2005; Pieterse et al., 2009; Lee et al., 2012, 2021). In comparison with immune chemical triggers such as BTH, which can lead to excessive immune activation and growth penalties in plants, the SynCom not only enhanced disease resistance but also increased pepper fruit yield, suggesting that SynCom can systemically elicit induced resistance without growth penalties (Figures 1, 2; Supplementary Figure 1).

Induced resistance triggered by SynCom may be a result of the production of 1-nonanol, which protects pepper plants against aphid infestation without any growth penalties (Figures 2, 4, 5, Supplementary Figure 3). Exogenous 1-nonanol application can systemically activate the expression of genes involved in defense phytohormone (JA and SA) signaling as well as oxidative stress responses in *Arabidopsis* and cotton plants (Gamboa-Becerra et al., 2022; Parmagnani et al., 2023; Ni et al., 2024). Consistently, treatment with either the SynCom or exogenous 1-nonanol activated the expression of SA signaling genes in pepper leaves following infestation by the sucking insect aphid (Figures 1D, 5B), suggesting that SynCom-derived 1-nonanol is a key metabolite that elicits SA-dependent immunity against aphids in pepper. Interestingly, only SynCom treatment, not exogenous 1-nonanol alone, induced the expression of the JA biosynthetic gene *CaLOX* (Figure 1D). These indicates that in addition to 1-nonaol, SynCom-derived other metabolites might contribute to the activation of a more complex plant immunity against not only sucking insect but also broad spectrum of phytopathogens (Lee et al., 2021, Figure 2). Thus, while 1-nonanol serves as a key metabolite, the SynCom might activate a more complex plant immunity against broad-spectrum phytopathogens and insect pests through the combined effect of multiple metabolite(s). Traditionally, a bottom-up approach has been used to construct a plant-protective SynCom, in which the microbial characteristics of random combinations of isolated bacteria are investigated via *in vitro* tests, including enzymatic activity and metabolite production assays (Marín et al., 2021; Martins et al., 2023). However, the SynCom constructed using the bottom-up approach exhibits unstable activity in field conditions, possibly because of the complexity of microbial interactions within natural communities. A multispecies combination does not always result in additive or synergistic effects, and the presence or absence of specific taxa is crucial for determining the activity of the SynCom (Sanchez-Gorostiaga et al., 2019; Marín et al., 2021). The SynCom used in this study was constructed using a top-down approach, based on the microbiome analysis of natural rhizosphere soil (Lee et al., 2021). Among the members of our SynCom, HRS1 and HRS2 play key roles in activating plant immunity; however, the full activation of induced resistance against bacterial wilt disease requires the support of minor helper strains including HRS3 and HRS4 (Lee et al., 2021). Consistently, in this study, the complete SynCom combination (HRS1 + HRS2 + HRS3 + HRS4) showed maximum disease control activity against aphids and *Xav* in pepper plants even under field conditions (Figures 1, 2). Interestingly, the emission of 1-nonanol was significantly higher in the SynCom treatment than in individual or partial combination treatments lacking HRS3 and/or HRS4 (i.e., dual or triple combinations), suggesting that minor helper strains such as HRS3 and HRS4 play a crucial role in volatile compound biosynthesis through microbial interactions within the SynCom (Figure 4). These results demonstrate that specific microbial combinations can maximize the production of unique metabolites, offering new evidence for microbial interdependency and syntrophic interaction (Zengler and Zaramela, 2018; Kost et al., 2023; Lee et al., 2024). Meanwhile, the 1-nonanol were also detected in single inoculation of HRS4 and in partial combinations that included HRS4, indicating that HRS4 strain is the key strain responsible for 1-nonanol production. The ability of 1-nonanol production has only been found in Gram-negative bacteria, such as *Pseudomonas aurantiaca* and *Erwinia amylovora*, and not in Gram-positive bacteria (Ni et al., 2022; Parmagnani et al., 2023). Therefore, our findings represent the first report about 1-nonanol emission from Gram-positive *Bacillus luciferensis* HRS4 and from a Gram-positive bacterial SynCom.

For decades, various microorganisms have been used individually as alternatives to synthetic pesticides. However their activity has mostly declined under field conditions, because the lack of consideration for interactions within microbial communities in nature (Lee et al., 2021; Martins et al., 2023; Lee et al., 2024). In this study, using the top-down approach, a specific combination of four Gram-positive bacteria was constructed, which demonstrated effective biocontrol activity in pepper plants not only in the greenhouse but also in the field. A specific combination of bacterial species in the SynCom can lead to the production of unique volatile compounds, in amounts greater than those produced by monocultures, to support plant health and growth. This finding provides new insights for the development of future biocontrol agents. However, further research is needed to address the following: (1) benefits provided by 1-nonanol to the SynCom in the field; (2) the mechanism of 1-nonanol-induced plant immune signaling against diverse phytopathogens and herbivores; and (3) how the SynCom-derived 1-nonanol influences native microbial communities under natural conditions. Further investigation using soil and leaf microbiome profiling could help evaluate the colonization capacity of SynCom members and their impact on native microbial communities. In addition, plant metabolomic

analyses, including volatile profiling, may offer deeper insights into the immune responses activated by SynCom or 1-nonanol treatment. Although previous studies have shown that the absence of SynCom increases plant disease susceptibility, the causes of SynCom dysbiosis remain unknown (Lee et al., 2021). Preventing the dysbiosis of protective microbiota or applying their active metabolites is essential for advancing biological control strategies (Chen et al., 2020; Lee et al., 2021; Arnault et al., 2023). Future efforts should focus on increasing the abundance of protective SynCom using probiotics or utilizing SynCom-derived metabolites, such as 1-nonanol, as postbiotics for agricultural applications.

Data availability statement

The raw data supporting the conclusions of this article will be made available by the authors, without undue reservation.

Author contributions

C-MR: Conceptualization, Funding acquisition, Supervision, Writing – original draft, Writing – review & editing. HY: Investigation, Visualization, Writing – review & editing. S-ML: Data curation, Investigation, Visualization, Writing – original draft, Writing – review & editing. HGK: Investigation, Visualization, Writing – review & editing. MR: Investigation, Writing – review & editing.

Funding

The author(s) declare that financial support was received for the research and/or publication of this article. This research was supported by grants from the Woo Jang-Coon Project (PJ01093904) of the Rural Development Administration (RDA), the National Research Foundation of Korea (NRF); a grant funded by the Korea government (MIST) (RS-2024–00336247 and RS-2023-00249410); the Cooperative Research Program for Agriculture Science and Technology Development (Project No. RS-2022-RD010288) of the Rural Development Administration, Republic of Korea; and the Korea Research Institute of Bioscience and Biotechnology (KRIBB) Research Initiative Program.

Conflict of interest

The authors declare that the research was conducted in the absence of any commercial or financial relationships that could be construed as a potential conflict of interest.

The author(s) declared that they were an editorial board member of Frontiers, at the time of submission. This had no impact on the peer review process and the final decision.

Generative AI statement

The author(s) declare that no Generative AI was used in the creation of this manuscript.

Publisher's note

Supplementary material

The Supplementary Material for this article can be found online at: https://www.frontiersin.org/articles/10.3389/fpls.2025.1589266/full#supplementary-material

References

Almeida, O. A. C., De Araujo, N. O., Mulato, A. T. N., Persinoti, G. F., Sforça, M. L., Calderan-Rodrigues, M. J., et al. (2023). Bacterial volatile organic compounds (VOCs) promote growth and induce metabolic changes in rice. *Front. Plant Sci.* 13. doi: 10.3389/fpls.2022.1056082

Arnault, G., Mony, C., and Vandenkoornhuyse, P. (2023). Plant microbiota dysbiosis and the anna karenina principle. *Trends Plant Sci.* 28, 18–30. doi: 10.1016/j.tplants.2022.08.012

Belt, K., Flematti, G. R., Bohman, B., Chooi, H., Roper, M. M., Dow, L., et al. (2025). Actinobacteria warfare against the plant pathogen *Sclerotinia sclerotiorum*: 2,4,6-Trimethylpyridine identified as a bacterial derived volatile with antifungal activity. *Microb. Biotechnol.* 18, e70082. doi: 10.1111/1751-7915.70082

Berendsen, R. L., Pieterse, C. M., and Bakker, P. A. (2012). The rhizosphere microbiome and plant health. *Trends Plant Sci.* 17, 478–486. doi: 10.1016/j.tplants.2012.04.001

Berg, G. (2009). Plant–microbe interactions promoting plant growth and health: Perspectives for controlled use of microorganisms in agriculture. *Appl. Microbiol. Biotechnol.* 84, 11–18. doi: 10.1007/s00253-009-2092-7

Carlström, C. I., Field, C. M., Bortfeld-Miller, M., Müller, B., Sunagawa, S., and Vorholt, J. A. (2019). Synthetic microbiota reveal priority effects and keystone strains in the *Arabidopsis* phyllosphere. *Nat. Ecol. Evol.* 3, 1445–1454. doi: 10.1038/s41559-019-0994-z

Cernava, T., Aschenbrenner, I. A., Grube, M., Liebminger, S., and Berg, G. (2015). A novel assay for the detection of bioactive volatiles evaluated by screening of lichen-associated bacteria. *Front. Microbiol.* 6. doi: 10.3389/fmicb.2015.00398

Chen, T., Nomura, K., Wang, X., Sohrabi, R., Xu, J., Yao, L., et al. (2020). A plant genetic network for preventing dysbiosis in the phyllosphere. *Nature* 580, 653–657. doi: 10.1038/s41586-020-2185-0

Cortes-Barco, A., Goodwin, P., and Hsiang, T. (2010). Comparison of induced resistance activated by benzothiadiazole,(2R, 3R)-butanediol and an isoparaffin mixture against anthracnose of *Nicotiana benthamiana*. *Plant Pathol.* 59, 643–653. doi: 10.1111/j.1365-3059.2010.02283.x

Durán, P., Thiergart, T., Garrido-Oter, R., Agler, M., Kemen, E., Schulze-Lefert, P., et al. (2018). Microbial interkingdom interactions in roots promote *Arabidopsis* survival. *Cell* 175, 973–983. e914. doi: 10.1016/j.cell.2018.10.020

Gamboa-Becerra, R., Desgarennes, D., Molina-Torres, J., Ramírez-Chávez, E., Kiel-Martínez, A. L., Carrión, G., et al. (2022). Plant growth-promoting and non-promoting rhizobacteria from avocado trees differentially emit volatiles that influence growth of *Arabidopsis thaliana*. *Protoplasma* 259, 1–20. doi: 10.1007/s00709-021-01705-2

Garbeva, P., and Weisskopf, L. (2020). Airborne medicine: bacterial volatiles and their influence on plant health. *New Phytol.* 226, 32–43. doi: 10.1111/nph.16282

Gfeller, A., Fuchsmann, P., De Vrieze, M., Gindro, K., and Weisskopf, L. (2022). Bacterial volatiles known to inhibit *Phytophthora infestans* are emitted on potato leaves by *Pseudomonas* strains. *Microorganisms* 10, 1510. doi: 10.3390/microorganisms10081510

Hayat, R., Ali, S., Amara, U., Khalid, R., and Ahmed, I. (2010). Soil beneficial bacteria and their role in plant growth promotion: A review. *Ann. Microbiol.* 60, 579–598. doi: 10.1007/s13213-010-0117-1

Hol, W. G., Garbeva, P., Hordijk, C., Hundscheid, M. P., Gunnewiek, P. J. K., Van Agtmaal, M., et al. (2015). Non-random species loss in bacterial communities reduces antifungal volatile production. *Ecology* 96, 2042–2048. doi: 10.1890/14-2359.1

Jousset, A., Bienhold, C., Chatzinotas, A., Gallien, L., Gobet, A., Kurm, V., et al. (2017). Where less may be more: How the rare biosphere pulls ecosystems strings. *ISME J.* 11, 853–862. doi: 10.1038/ismej.2016.174

Jung, S. H., Riu, M., Lee, S., Kim, J. S., Jeon, J. S., and Ryu, C. M. (2023). An anaerobic rhizobacterium primes rice immunity. *New Phytol.* 238, 1755–1761. doi: 10.1111/nph.18834

Kaloshian, I., and Walling, L. L. (2005). Hemipterans as plant pathogens. *Annu. Rev. Phytopathol.* 43, 491–521. doi: 10.1146/annurev.phyto.43.040204.135944

Kim, H., Kim, C., and Lee, Y.-H. (2023). The single-seed microbiota reveals rare taxa-associated community robustness. *Phytobiomes J.* 7, 324–338. doi: 10.1094/PBIOMES-10-22-0068-R

Kim, D., Riu, M., Oh, S.-K., and Ryu, C.-M. (2022). Extracellular self-RNA: A danger elicitor in pepper induces immunity against bacterial and viral pathogens in the field. *Front. Plant Sci.* 13. doi: 10.3389/fpls.2022.864086

Kloepper, J. W., Ryu, C.-M., and Zhang, S. (2004). Induced systemic resistance and promotion of plant growth by *Bacillus* spp. *Phytopathology* 94, 1259–1266. doi: 10.1094/PHYTO.2004.94.11.1259

Kong, H. G., Shin, T. S., Kim, T. H., and Ryu, C.-M. (2018). Stereoisomers of the bacterial volatile compound 2, 3-butanediol differently elicit systemic defense responses of pepper against multiple viruses in the field. *Front. Plant Sci.* 9. doi: 10.3389/fpls.2018.00090

Kost, C., Patil, K. R., Friedman, J., Garcia, S. L., and Ralser, M. (2023). Metabolic exchanges are ubiquitous in natural microbial communities. *Nat. Microbiol.* 8, 2244–2252. doi: 10.1038/s41564-023-01511-x

Kwak, M.-J., Kong, H. G., Choi, K., Kwon, S.-K., Song, J. Y., Lee, J., et al. (2018). Rhizosphere microbiome structure alters to enable wilt resistance in tomato. *Nat. Biotechnol.* 36, 1100–1109. doi: 10.1038/nbt.4232

Lee, S.-M., Kong, H. G., Song, G. C., and Ryu, C.-M. (2021). Disruption of firmicutes and actinobacteria abundance in tomato rhizosphere causes the incidence of bacterial wilt disease. *ISME J.* 15, 330–347. doi: 10.1038/s41396-020-00785-x

Lee, B., Lee, S., and Ryu, C.-M. (2012). Foliar aphid feeding recruits rhizosphere bacteria and primes plant immunity against pathogenic and non-pathogenic bacteria in pepper. *Ann. Bot.* 110, 281–290. doi: 10.1093/aob/mcs055

Lee, S.-M., Thapa Magar, R., Jung, M. K., Kong, H. G., Song, J. Y., Kwon, J. H., et al. (2024). Rhizobacterial syntrophy between a helper and a beneficiary promotes tomato plant health. *ISME J.* 18, wrae120. doi: 10.1093/ismejo/wrae120

Marín, O., González, B., and Poupin, M. J. (2021). From microbial dynamics to functionality in the rhizosphere: A systematic review of the opportunities with synthetic microbial communities. *Front. Plant Sci.* 12. doi: 10.3389/fpls.2021.650609

Martins, S. J., Pasche, J., Silva, H. A. O., Selten, G., Savastano, N., Abreu, L. M., et al. (2023). The use of synthetic microbial communities to improve plant health. *Phytopathology* 113, 1369–1379. doi: 10.1094/PHYTO-01-23-0016-IA

Ni, H., Kong, W.-L., Zhang, Y., and Wu, X.-Q. (2022). Effects of volatile organic compounds produced by *Pseudomonas aurantiaca* st-tj4 against *Verticillium dahliae*. *J. Fungi* 8, 697. doi: 10.3390/jof8070697

Ni, H., Kong, W.-L., Zhang, Q.-Q., and Wu, X.-Q. (2024). Volatiles emitted by *Pseudomonas aurantiaca* st-tj4 trigger systemic plant resistance to *Verticillium dahliae*. *Microbiol. Res.* 287, 127834. doi: 10.1016/j.micres.2024.127834

Parmagnani, A. S., Kanchiswamy, C. N., Paponov, I. A., Bossi, S., Malnoy, M., and Maffei, M. E. (2023). Bacterial volatiles (mvoc) emitted by the phytopathogen *Erwinia amylovora* promote arabidopsis thaliana growth and oxidative stress. *Antioxidants* 12, 600. doi: 10.3390/antiox12030600

Pieterse, C. M., Leon-Reyes, A., van der Ent, S., and Van Wees, S. C. (2009). Networking by small-molecule hormones in plant immunity. *Nat. Chem. Biol.* 5, 308–316. doi: 10.1038/nchembio.164

Ryu, C.-M., Farag, M. A., Hu, C.-H., Reddy, M. S., Kloepper, J. W., and Paré, P. W. (2004). Bacterial volatiles induce systemic resistance in *Arabidopsis*. *Plant Physiol.* 134, 1017–1026. doi: 10.1104/pp.103.026583

Ryu, C.-M., Farag, M. A., Hu, C.-H., Reddy, M. S., Wei, H.-X., Paré, P. W., et al. (2003). Bacterial volatiles promote growth in *Arabidopsis*. *Proc. Natl. Acad. Sci. U.S.A.* 100, 4927–4932. doi: 10.1073/pnas.0730845100

Sanchez-Gorostiaga, A., Bajić, D., Osborne, M. L., Poyatos, J. F., and Sanchez, A. (2019). High-order interactions distort the functional landscape of microbial consortia. *PloS Biol.* 17, e3000550. doi: 10.1371/journal.pbio.3000550

Schulz-Bohm, K., Zweers, H., De Boer, W., and Garbeva, P. (2015). A fragrant neighborhood: Volatile mediated bacterial interactions in soil. *Front. Microbiol.* 6. doi: 10.3389/fmicb.2015.01212

Silva Dias, B. H., Jung, S.-H., de Castro Oliveira, J. V., and Ryu, C.-M. (2021). C4 bacterial volatiles improve plant health. *Pathogens* 10, 682. doi: 10.3390/pathogens10060682

Singh, P., Singh, J., Ray, S., Vaishnav, A., Jha, P., Singh, R. K., et al. (2024). Microbial volatiles (mVOCs) induce tomato plant growth and disease resistance against wilt pathogen *Fusarium oxysporum* f. sp. *lycopersici*. *J. Plant Growth Regul.* 43, 3105–3118. doi: 10.1007/s00344-023-11060-6

Song, G. C., Choi, H. K., Kim, Y. S., Choi, J. S., and Ryu, C.-M. (2017). Seed defense biopriming with bacterial cyclodipeptides triggers immunity in cucumber and pepper. *Sci. Rep.* 7, 14209. doi: 10.1038/s41598-017-14155-9

Song, G. C., Riu, M., and Ryu, C.-M. (2019). Beyond the two compartments petri-dish: Optimising growth promotion and induced resistance in cucumber exposed to gaseous bacterial volatiles in a miniature greenhouse system. *Plant Methods* 15, 1–11. doi: 10.1186/s13007-019-0395-y

Song, G. C., and Ryu, C.-M. (2013). Two volatile organic compounds trigger plant self-defense against a bacterial pathogen and a sucking insect in cucumber under open field conditions. *Int. J. Mol. Sci.* 14, 9803–9819. doi: 10.3390/ijms14059803

Vorholt, J. A., Vogel, C., Carlström, C. I., and Müller, D. B. (2017). Establishing causality: Opportunities of synthetic communities for plant microbiome research. *Cell Host Microbe* 22, 142–155. doi: 10.1016/j.chom.2017.07.004

Walling, L. L. (2000). The myriad plant responses to herbivores. *J. Plant Growth Regul.* 19, 195–216. doi: 10.1007/s003440000026

Weisskopf, L., Schulz, S., and Garbeva, P. (2021). Microbial volatile organic compounds in intra-kingdom and inter-kingdom interactions. *Nat. Rev. Microbiol.* 19, 391–404. doi: 10.1038/s41579-020-00508-1

Xiong, C., He, J. Z., Singh, B. K., Zhu, Y. G., Wang, J. T., Li, P. P., et al. (2021). Rare taxa maintain the stability of crop mycobiomes and ecosystem functions. *Environ. Microbiol.* 23, 1907–1924. doi: 10.1111/1462-2920.15262

Yang, J., Kloepper, J. W., and Ryu, C.-M. (2009). Rhizosphere bacteria help plants tolerate abiotic stress. *Trends Plant Sci.* 14, 1–4. doi: 10.1016/j.tplants.2008.10.004

Yi, H.-S., Yang, J. W., and Ryu, C.-M. (2013). ISR meets SAR outside: Additive action of the endophyte *Bacillus pumilus* INR7 and the chemical inducer, benzothiadiazole, on induced resistance against bacterial spot in field-grown pepper. *Front. Plant Sci.* 4. doi: 10.3389/fpls.2013.00122

Zablotowicz, R. M., Tipping, E. M., Lifshitz, R., and Kloepper, J. W. (1991). "Plant growth promotion mediated by bacterial rhizosphere colonizers," in *The Rhizosphere and Plant Growth: Proceedings of a Symposium held May 8–11, 1989, at the Beltsville Agricultural Research Center*. Eds. D. L. Keister and P. B. Cregan (Springer, Beltsville, Maryland), 315–326.

Zengler, K., and Zaramela, L. S. (2018). The social network of microorganisms—how auxotrophies shape complex communities. *Nat. Rev. Microbiol.* 16, 383–390. doi: 10.1038/s41579-018-0004-5

frontiers | Frontiers in Plant Science

TYPE Original Research
PUBLISHED 13 June 2025
DOI 10.3389/fpls.2025.1611674

OPEN ACCESS

EDITED BY
Ajay Kumar,
Amity University, India

REVIEWED BY
Udai B. Singh,
National Bureau of Agriculturally Important Microorganisms (ICAR), India
Muhammad Abdullah Akber,
Lanzhou University, China

*CORRESPONDENCE
Dao-Jun Guo
Gdj0506@163.com
Dong-Ping Li
lidongping0201@126.com
Bin Yang
yangbinysz@163.com

RECEIVED 14 April 2025
ACCEPTED 05 May 2025
PUBLISHED 13 June 2025

CITATION
Guo D-J, Yang G-R, Singh P, Wang J-J, Lan X-M, Singh RK, Guo J, Dong Y-D, Li D-P and Yang B (2025) Comprehensive analysis of the physiological and molecular responses of phosphate-solubilizing bacterium *Burkholderia gladioli* DJB4–8 in promoting maize growth. *Front. Plant Sci.* 16:1611674. doi: 10.3389/fpls.2025.1611674

Comprehensive analysis of the physiological and molecular responses of phosphate-solubilizing bacterium *Burkholderia gladioli* DJB4–8 in promoting maize growth

Dao-Jun Guo[1,2,3]*, Guo-Rong Yang[4], Pratiksha Singh[3], Juan-Juan Wang[1,2], Xue-Mei Lan[5], Rajesh Kumar Singh[3], Jing Guo[2], Yu-Die Dong[2], Dong-Ping Li[1,2,3]* and Bin Yang[1,2]*

[1]Key Laboratory of Hexi Corridor Resources Utilization of Gansu, Hexi University, Zhangye, Gansu, China, [2]College of Life Sciences and Engineering, Hexi University, Zhangye, Gansu, China, [3]Guangxi Key Laboratory of Sugarcane Genetic Improvement, Guangxi Academy of Agricultural Sciences, Nanning, Guangxi, China, [4]College of Life Sciences, Sichuan Agricultural University, Ya'an, Sichuan, China, [5]College of Agriculture and Ecological Engineering, Hexi University, Zhangye, Gansu, China

Phosphorus (P) is one of the essential macroelements for the growth of maize. The deficiency of P in maize will result in adverse effects, including chlorosis and reduced yield. The Hexi Corridor in China serves as the principal region for seed maize production, with chemical phosphate fertilizer remaining the predominant source of P delivery for local maize cultivation. Nonetheless, the agricultural non-point source pollution resulting from the prolonged application of artificial phosphate fertilizers is intensifying. P in farmland soil often exists in an insoluble form, which plants cannot directly absorb and utilize. Phosphate-solubilizing bacteria (PSB) in the rhizosphere are a kind of plant growth-promoting rhizobacteria (PGPR) that can transform insoluble P in soil into soluble P for plants to absorb and utilize. Utilizing PGPR in agricultural production is an ecological approach to achieving sustainable development in agricultural practices and output. In this study, 41 strains of bacteria were isolated from the rhizosphere soil of four maize varieties. According to an *in vitro* plant growth-promoting (PGP) feature study and 16S RNA molecular identification, *Burkholderia gladioli* DJB4-8, among all strains tested, exhibited the highest *in vitro* PGP activity, with a phosphate-solubilizing ability of 8.99 mg/L. By scanning electron microscope (SEM) and green fluorescent protein (GFP) labeling technique, it was found that strain DJB4–8 formed a colonization symbiotic system with maize roots. The inoculation of maize Zhengdan 958 with strain DJB4–8 altered the plant's photosynthetic physiology and indole-3-acetic acid (IAA) level, and it also dramatically increased the plant's growth rate. The combined analysis of transcriptome and metabolomics showed that the key genes and metabolites in the interaction between strain DJB4–8 and maize were mainly concentrated in plant growth key pathways such as plant hormone signal transduction, phenylalanine, tyrosine and tryptophan biosynthesis, phenylalanine

metabolism, phenylpropane biosynthesis, pentose phosphate pathway, zeatin biosynthesis, amino sugar and nucleotide sugar metabolism, and glutathione metabolism. These findings shed light on the need for additional research into the mechanism of interaction between PSB and maize.

KEYWORDS

***Burkholderia gladioli* DJB4-8, phosphate-solubilizing bacteria, PGP, maize, transcriptome, metabolomics**

Introduction

The Hexi Corridor in China is the principal site for maize production, with approximately one million acres dedicated to seed maize cultivation (Chen et al., 2023). P is essential for the growth and development of maize, mainly in promoting cell division and differentiation, affecting photosynthesis and nutrient absorption, promoting root development and flowering and fruiting, and affecting the yield and quality of maize (Lambers, 2022; Richardson et al., 2009; Sadiq et al., 2017). P in the soil frequently exists in insoluble forms, such as calcium phosphate, rendering it inaccessible for direct absorption and utilization by plants (Johnston and Richards, 2003; Deng and Dhar, 2023; Olsen et al., 1983). P deficiency has become a critical limiting factor affecting local seed maize production. Currently, maize's primary source of P supply relies on chemical P fertilizers. Plant growth-promoting rhizobacteria (PGPR) are beneficial microorganisms that interact symbiotically with plants and positively affect plant growth (Bhattacharyya and Jha, 2012; Jha and Saraf, 2015; Parray et al., 2016). Phosphate-solubilizing bacteria (PSB) play a crucial role in the P cycle within the soil (Khan et al., 2009; Pande et al., 2017). PSB secrete abundant organic acids as metabolic byproducts and generate CO_2 through respiratory processes, which react with water in the soil to form carbonic acid. These acidic compounds dissolve insoluble phosphate minerals (e.g., calcium phosphate and aluminum phosphate) in the soil, releasing plant-available phosphate ions for uptake and enhancing P bioavailability in agricultural systems (Chen et al., 2006; Prijambada et al., 2009; Billah et al., 2019; Prager and Cisneros-Rojas, 2017). Regarding organic P compounds, PSB can release enzymes like phosphatase and phytase (Zhang et al., 2014; Rawat et al., 2021). These enzymes break down organic P compounds, such as phospholipids, phytic acid, and nucleic acids, and release phosphate and carbohydrates for use by crops (Pan and Cai, 2023; Prabhu et al., 2019; Alori et al., 2017). PSB can satisfy maize's P needs by creating a comparatively adequate phosphorus supply micro area surrounding the rhizosphere. It accelerates the use of P fertilizer and promotes maize growth and development (Ingle and Padole, 2017; Adnan et al., 2020). In addition to facilitating phosphorus activation in the soil, PSB also can enhance plant growth by modifying the type and quantity of root exudates, thereby augmenting the uptake of minerals such as potassium, calcium, manganese, iron, and zinc by plant roots (Yahya et al., 2021; Biswas et al., 2018). Additionally, PSB produce biocontrol chemicals that inhibit the growth of phytopathogens and lower the incidence of disease, such as cyanide, siderophores, lytic enzymes, and antibiotics. At the same time, they increase the surface area of plant roots by colonizing them, improving nutrient uptake efficiency (Mitra et al., 2020; Vassilev et al., 2006; Li et al., 2017). This collaborative association mitigates abiotic stress and rhizosphere acidification, enabling plants to acclimate to adverse environments while enhancing agricultural productivity and stress resilience (Dey et al., 2021; Vassilev et al., 2012).

Numerous soil types and biological settings are home to PSB, which include bacteria such as *Bacillus*, *Pseudomonas*, *Burkholderia*, *Erwinia*, *Agrobacterium*, *Serratia*, and *Flavobacterium*, and these microbes are essential to the cycling of soil P (Saeid et al., 2018; Soares et al., 2023; You et al., 2020). PSB has been found in the rhizosphere of economic crops such as soybeans, sweet potatoes, fruit trees, and vegetables, as well as cereal crops like wheat, maize, sugarcane, and rice (Shome et al., 2022; Marques et al., 2019; Wang et al., 2022; Sundara et al., 2002; Rahman et al., 2015). According to previous reports, *Pseudomonas fluorescens*, *Pseudomonas putida*, *Bacillus megaterium*, *Bacillus subtilis*, *Burkholderia cepacia*, *Serratia liquefaciens*, *Enterobacter cloacae*, *Arthrobacter* sp*haeroides*, *Arthrobacter globiformis*, and *Azotobacter chroococcum* are the main PSB found in the rhizosphere of maize (Vyas and Gulati, 2009; Ahmad et al., 2019; Zhao et al., 2014; Tang et al., 2020).

Leveraging the growth-promoting attributes of PSB to augment phosphorus uptake and use in maize, hence fostering maize development, represents an eco-friendly approach to reducing chemical fertilizer application in maize cultivation (Fathi, 2017). *Burkholderia* is a common rhizosphere bacterium with multifunctional growth-promoting potential, especially in maize and other gramineous crops (Gastélum et al., 2022; Elnahal et al., 2022). The combination of its phosphate-solubilizing ability and pleiotropic growth-promoting mechanism plays a vital role in improving the P utilization efficiency of maize, enhancing stress resistance, and promoting root development (Liu, 2021; Li et al., 2012). Particularly in low-phosphorus soil, *Burkholderia* sp. can raise the biomass by 15% to 30% and the amount of accessible P in the maize rhizosphere by 20% to 50%. For example, maize

production increased by 22% in the tropical red soil experiment (Pal et al., 2022). According to certain research, inoculating maize plants with PSB boosted their P intake by 29.74% (Vincze et al., 2024). PSB may also further enhance the nutritional status of maize, facilitating the absorption of additional elements like potassium and nitrogen (Sekhar et al., 2020). The primary focus of research on PSB in the maize rhizosphere is to isolate strains and evaluate their ability to stimulate growth. However, the mechanism of interaction between these bacteria and maize is poorly understood. Employing omics technologies, particularly transcriptomics and metabolomics, it is possible to discover differentially expressed genes and metabolites, build networks of gene–metabolite interactions, and uncover the functions and connections of important genes and metabolites in the interaction process (Yang et al., 2021). The basic objectives of this study were to identify and screen PSB from the rhizosphere soil of maize seed production in China's Hexi Corridor and i) investigate the plant growth-promoting (PGP) activity of the isolated PSB while conducting a phylogenetic analysis; ii) examine the morphological traits of the PSB strain *Burkholderia gladioli* DJB4–8 via scanning electron microscopy, development of green fluorescent protein (GFP) clone transformants of strain DJB4-8, and assessment of its colonization properties in maize; iii) assess agronomic characteristics, photosynthetic physiology, and biochemical enzyme activities of maize Zhengdan 958 following inoculation with strain DJB4-8; and iv) examine the interaction genes and metabolic variances between strain DJB4–8 and maize Zhengdan 958 utilizing transcriptomics and metabolomics. The results will provide a scientific basis for further study of the interaction mechanism between PSB and maize.

Materials and methods

Isolation of bacteria from rhizosphere soil of seed maize

Healthy seed maize plants were selected from various areas of China's Hexi Corridor's National Hybrid Seed Maize production base. After digging the maize roots, the loose soil was carefully shaken to remove it. A sterile brush was used to brush the soil 1–2 mm from the root surface. The soil samples were immediately taken to the lab in an ice box and kept at 4°C (less than 24 h). Four soil samples, each approximately 100 g, were collected. The collection of information for rhizosphere soil samples of seed maize is presented in Supplementary Table S1. One gram of rhizosphere soil was weighed and added to 9 mL of sterile normal saline (containing 0.05% Tween 80 for dispersion). Oscillates were vortexed for 2 min and allowed to stand for 30 s; the supernatant was taken as the stock solution (10^{-1} dilution) and then gradually diluted it to 10^{-2}, 10^{-3}, 10^{-4}, 10^{-5}, 10^{-6}, and 10^{-7}; 100 µL of each diluted soil solution was coated on the plate of PKO medium and cultured upside down at 32°C for 48 h. Subsequent to the growth of the colonies, the strains were purified based on the distinct colony morphologies. All strains were cultivated in two aliquots: one was supplemented with 20% glycerol and preserved at −80°C, while the other was maintained at 4°C.

Testing of PGP characteristics of maize rhizosphere soil bacteria

The activity of dissolved inorganic phosphate in maize rhizosphere bacteria for plant growth promotion was measured using a specialized Pikovskaya's agar culture plate; 5 µL of each test bacterial solution was placed in the middle of the plate. Each culture plate was sealed with a membrane and then placed flat in an incubator set at 32°C for 72 h prior to observation. The strain's phosphate-solubilizing ability was qualitatively indicated by the presence or absence of a colorless translucent circle, and the diameter of the circle was positively correlated with the ability. PSB's capacity to dissolve inorganic phosphate was quantitatively assessed using the molybdenum antimony colorimetric technique (Guo et al., 2023).

The colorimetric method of Nessler's reagent was utilized to determine whether the strains can produce ammonia. Culture media were created by dividing them into 15-mL vials and adding 10 g of peptone and 5 g of sodium chloride per liter. After dividing each vial into 9.5 mL of sterilized culture media, 10 µL of each test bacterial solution was added. Every culture bottle was put in an oscillating incubator with a consistent temperature. After 48 h of cultivation at 32°C and 110 rpm, 0.5 mL of Nessler's reagent was added and observed to see if the bacterial solution turned reddish brown instead of yellow. A change in hue indicates that the strain can produce ammonia, and the capacity to produce ammonia increases with color darkness.

The tested strains' capacity to secrete siderophores was assessed using the chrome azurol S (CAS) agar plate method (Milagres et al., 1999). The center of the CAS culture plate was inoculated with 5 µL of each test bacterial solution. Before being observed, each culture plate was placed flat in an incubator set at 32°C for 72 h after sealing it with a sealing film. The strain's capacity to secrete siderophores was shown by the presence or absence of the yellow halo, and the diameter of the yellow halo was positively connected with the strain's siderophore strength.

Culture plates were prepared for qualitative examination by adding 1-aminocyclopropyl-1-carboxylic acid (ACC) to Dworkin and Foster (DF) media (Li et al., 2011). After inoculating DF–ACC culture plates with the bacterial solution, they were incubated for 72 h at 32°C. The size of the bacterial circle positively correlates with the strain's capacity to use the ACC nitrogen source. The absence of a bacterial growth zone demonstrates the strain's incapacity to utilize ACC as a nitrogen source.

Identification and phylogenetic analysis of maize rhizosphere soil bacteria

The bacterial genomic DNA was extracted using a TIANamp Bacteria DNA Kit (TIANGEN Biotech Co., Ltd., Beijing, China) following the manufacturer's instructions. Each bacterium underwent PCR amplification of its 16S rRNA sequences. The primers and reaction parameters of the PCR conditions are presented in Supplementary Table S2. After acquiring the PCR

products, the SanPrep column DNA gel recovery kit (Shenggong Biotech Co., Shanghai, China) was employed. The kit's directions are referred to as the unique operation method. Following gel recovery and purification, the PCR product was identified using a 1.2% agarose gel to guarantee that only one band was sequenced. Shanghai Biotech Co., Ltd., completed the sequencing of bacterial 16S rRNA sequences. To obtain a login number, the sequencing data were compared and uploaded to the official website of the National Center for Biotechnology Information (NCBI). Next, sequences were grouped using the Mega7.0 software to produce a PSB strain 16S rRNA gene phylogenetic tree.

Colonization analysis of PSB in maize

Seedlings of the maize variety Zhengdan 958 were inoculated with strain DJB4–8 at a concentration of 1×10^6 CFU mL^{-1} and grown for 3 days. Sterile scissors were used to cut samples of the maize roots and stems, and absorbent paper was used to absorb the surface moisture. After being promptly fixed for 2 h using an electron microscope fixative, the samples were moved to 4°C for storage. The fixed samples for testing were washed three times for 15 min each using 0.1 M phosphoric acid buffer (Pb; pH 7.4). The samples were soaked in alcohol solutions for 15 min before being transferred to isoamyl acetate for 15 min. The samples were sprayed with gold for 30 s using the ion sputtering machine (Hitachi MC1000, Tokyo, Japan). After that, a scanning electron microscope (SEM; HITACHI SU8100) was used to collect the images.

Guo's approach (Guo et al., 2020) was used in three parent bindings to change strain DJB4-8's GFP into DJB4-8/pPROBE-pTetr-TT-gfp. Using sterile water as a control, Zhengdan 958 maize seedlings were inoculated with a concentration of 1×10^6 CFU mL^{-1} of the three parent conjugate transformant solutions. The seedlings were removed after 4 days of inoculation, and sterile water was used to wash the culture media and contaminants from the root surface. Using a fluorescence microscope, the maize roots were manually sliced to assess the colonization status of strain DJB4-8.

Agronomic traits and physiological and biochemical evaluation of maize after inoculation

The pot specifications for the inoculation experiment had a height of 18 cm, a bottom diameter of 18 cm, and an upper diameter of 25 cm. Each pot contained approximately 8 kg of soil. The maize variety was Zhengdan 958, and the inoculation concentration of the bacterial solution was 1×10^6 CFU mL^{-1}. Maize seedling cultivation used seedling trays: the cultivation tray was 40 cm long and 30 cm wide, with 50 seedling holes per tray and one seedling per hole. The seedling substrate was sterilized with high-pressure steam. Maize seeds were soaked in 1% carbendazim for 0.5 h before being transplanted into seedling trays. Under conventional management in greenhouse conditions, after the maize grew to two to three– leaves, maize seedlings with consistent growth were selected for inoculation and transplantation. After removing the maize seedlings from the seedling tray, the root maize matrix was rinsed with sterile water, and the roots were allowed to soak in the test bacterial solution for approximately 1 h. They were transferred to the container as the control group, and then the maize seedlings' roots were submerged in sterile water. Each of the 60 pots in the treatment and control groups had 30 pots and one maize seedling. Maize was merely irrigated and did not receive fertilizer while growing. The experimental facility was situated in Hexi University's maize-growing base. The maize plants were carefully uprooted from the growth medium, adhering rhizospheric soil particles were gently removed through manual agitation, and the root system was thoroughly rinsed with deionized water and allowed to air-dry at ambient temperature under laboratory conditions. The root, stem, and leaf weights were measured separately. The experiment was repeated three times, with three maize plants taken from each repetition for testing.

The growth hormone indole-3-acetic acid (IAA) in maize leaves was measured using high-performance liquid chromatography (HPLC); 0.2 g aliquot of the maize roots was accurately weighed and subjected to cryogenic grinding in a liquid nitrogen-chilled mortar. The resulting powder was homogenized with a pre-cooled methanol–acidic solution (70%–80% v/v, 4°C) and maintained at 4°C for 12 h to facilitate extraction. Following homogenization, the mixture underwent centrifugation at 12,000 rpm for 10 min (4°C). The supernatant was then collected under controlled temperature conditions and designated as the primary extract (first solution). After centrifuging the residue, 0.5 mL of a 70%–80% methanol solution was added, mixed well, and extracted for 2 h at 4°C; the second solution (the supernatant) was centrifuged, and then the supernatant was mixed twice. The supernatant was evaporated to one-third of its volume at 4°C and lowered pressure, and then an equivalent volume of petroleum ether was added. After two or three repetitions of extraction and decolorization, triethylamine was added after static stratification, and the pH was lowered to 8.0. The supernatant was put in the cross-linked polyvinylpyrrolidone (CTFA) and allowed to sit at room temperature for 20 min at 150 rpm. After adjusting the pH to 3.0, the supernatant was removed from the centrifuge, extracted three times using ethyl acetate, and then evaporated at 40°C with reduced pressure until dry. Vortex oscillation was used to dissolve the mobile phase solution after adding it. Under the following chromatographic conditions, the sample was passed through a needle filter, and a WuFeng LC-100 HPLC was used to identify it: mobile phase A of 100% methanol and B of 0.1% acetic acid aqueous solution (A:B = 55:45), with an injection volume of 20 µL, a column temperature of 30°C, a column size of 150 mm × 4.6 mm × 5 µm, and a detection wavelength of 254 nm. The standard curve for detecting endogenous hormone IAA in plants is shown in Supplementary Table S3.

Transcriptome analysis of maize inoculated with PSB

After 40 days of PSB inoculation, the maize root RNA was extracted using a kit (Omega Bio-Tek, Inc., Norcross, GA, US). For

the RNA extraction procedure, the kit instructions were consulted. Since 1% agarose gel electrophoresis was used to detect RNA integrity, and NanoDrop 2000 was used to detect RNA purity and concentration, it was appropriate for the RNA standard of transcriptome sequencing (OD260/OD230 value greater than 2.0, OD260/OD280 value between 1.8 and 2.2, and Rin value greater than 6.5).

The RNA library was created using the TruSeq^{TM} RNA sample preparation kit (Illumina, San Diego, CA, USA). The 200–300 bp cDNA enrichment fragment was recovered by 2% agarose gel electrophoresis. The sequencing platform utilizes Illumina NovaSeq 6000. The sequencing library quantitatively employs TBS380 (PicoGreen), and the sequencing read length was PE150. The specific sequencing of RNA-seq refers to the method proposed by Zhang et al. (2020). The processes of cDNA synthesis, library construction and sequencing, sequencing result calculation and assembly, screening of differentially expressed genes, and analysis of metabolic pathways followed those of Martin and Wang (2011). Using the maize inbred line B73 genome as a transcriptome annotation reference genome, the genes were analyzed and found to be significantly differentially expressed after screening using the Kyoto Encyclopedia of Genes and Genomes (KEGG) and Gene Ontology (GO). Utilizing the Goatools program (https://github.com/tanghaibao/GOatools), functional analysis was conducted on genes that exhibited substantial differential expression, and *p*-values were adjusted using the Sidak, Holm, Bonferroni, and false discovery procedures. p (pfdr) ≤ 0.05 is the *p*-value threshold for GO functional significance enrichment. KOBAS (http://kobas.cbi.pku.edu.cn/home.do) enriched the KEGG metabolic pathway. Several tests were run on the results using the Benjamini–Hochberg (BH) [false discovery rate (FDR)] method to control the false-positive rate.

For transcriptome validation, quantitative real-time PCR (qRT-PCR) was used to verify the accuracy of the data. Twelve significantly differentially expressed genes were randomly selected for qRT-PCR validation, with the glyceraldehyde-3-phosphate dehydrogenase gene (GAPDH) as an internal reference gene. The gene primer design software was Primer 5.0, and the sequence is presented in Supplementary Table S4. Using the remaining RNA from transcriptome sequencing, its quality was evaluated using NanoDrop 2000, and the RNA was reverse-transcribed into cDNA using the reverse transcription reagent (Takara, Dalian, China). The qRT-PCR instrument was LightCycler 480) II, and the relative gene expression level was determined using the $2^{-\Delta\Delta Ct}$ method (Fleige and Pfaffl, 2006).

Metabolome analysis of maize inoculated with strain DJB4-8

The collected maize root samples were stored on ice, and the metabolites were extracted with 50% methanol buffer. Then, the supernatant was transferred to a new 96-hole plate for mass spectrometry analysis. In addition, an equal amount of 10 μL diluent from the extracted mixture of each sample was obtained and mixed evenly as the quality control sample. All samples were collected using the LC–MS system following the manufacturer's instructions. An ultra-high-performance liquid chromatography (UPLC) system was used for chromatographic separation, and an Acquity UPLC T3 column was used for reversed-phase separation. The injection volume of each sample was 4 μL.

The metabolites eluted from the column were detected using a triple high-resolution tandem mass spectrometer 5600+. quadrupole-time of flight (Q-TOF) operates in positive ion and negative ion modes. The XCMS, CAMERA, and metaX tools in the R software (v3.5.2) were used to process the LC–MS raw data files after they were transformed into mzXML format. Combining m/z data with retention time (RT) allowed for the identification of each ion. The metabolites were annotated using the KEGG database, and the accuracy of metabolite identification was further verified using the internal metabolite fragment library. Peak intensity data underwent advanced preprocessing through Metax, followed by partial least squares–discriminant analysis (PLS-DA) to evaluate batch effects and identify outliers within the preprocessed dataset. Intergroup metabolite differences were statistically analyzed using Student's t-test, with *p*-values adjusted via the Benjamini–Hochberg FDR correction method. Subsequently, supervised PLS-DA was implemented in Metax to quantify variable importance in projection (VIP) scores and discriminate group-specific differentiating factors. The VIP's crucial value was set at 1.0 to select important metabolites.

Transcriptome and metabolome data were standardized through log2 transformation. The evaluation of correlation functions was based on the R language and normalized data Pearson's correlation analysis between differentially expressed genes (DEGs) and differentially accumulated metabolites (DAMs). KEGG signaling pathway enrichment analysis was performed using DEGs and DAMs with Pearson's correlation coefficient (PCC) ≥0.8. Then, the DEGs were mapped, and DAMs were grouped in the KEGG pathway diagram.

Data and statistical analyses

All data were analyzed using the SPSS 22.0 software for one-way analysis of variance (ANOVA) and Student's t-test. $p < 0.05$ means a significant difference, and $p < 0.01$ means a highly significant difference. The OmicStudio toolbox was used in bioinformatics analysis (https://www.omicstudio.cn/tool).

Results

Isolation and identification of bacteria from maize rhizosphere soil and their PGP activity

A total of 41 strains of bacteria were isolated and purified from the rhizosphere soil of four seed maize varieties. Among them, 20, 8, 9, and 4 strains were isolated from maize varieties Zhengdan 958,

Xianyu 335, Jingke 968, and Zhongdan 909, accounting for 48.78%, 19.51%, 21.95%, and 9.76%, respectively (Figure 1). Pikovskaya's plate test found that nine strains of bacteria had strong phosphate-solubilizing ability, accounting for 21.95% of the total strains, in terms of their ability to dissolve inorganic phosphates (Table 1). Furthermore, 12 strains (29.26%) had vigorous ammonia-producing activity and the capacity to secrete siderophores (Table 1). However, only two strains had vigorous growth activity on the medium with ACC as the sole nitrogen source (Table 1). By analyzing the PGP characteristics of all strains, strain DJB4–8 showed intense activity in all detection indexes, which has the potential for further development. At the same time, the 16S rRNA identification of all strains showed that there were 12 genera of bacteria in 41 strains, of which *Burkholderia* was the dominant genus, with 17 strains (41.46%). Nine strains with strong inorganic phosphate-solubilizing ability were used to create a phylogenetic tree using the MEGA7.0 software, which showed that the strains DJB4–8 and *B. gladioli* had high similarities (Figure 2). The 16S rRNA sequences of all strains were submitted to the NCBI GenBank, and the strain accession number was PP792774-792814 (Table 1).

Quantitative analysis of the ability of bacterial strains to dissolve inorganic phosphates

The molybdenum antimony colorimetric method was used to quantitatively analyze the dissolution ability of nine strains that were proven to have a strong ability to dissolve inorganic phosphate. The results showed that PSB had a range of 3.05 to 8.99 mg/L for this ability (Figure 3A). Among them, strain DJA1–9 had the lowest quantitative ability to dissolve inorganic phosphate, while strain DJB4–8 had the highest. Notably, strain DJB4–8 demonstrated the maximum phosphate solubilization capacity among tested isolates, with a halo zone diameter of 6.47 cm ($p < 0.01$ vs. controls), as quantified in Figure 3B. Strain DJB4–8 shows excellent potential for further research and use.

Colonization analysis of strain *B. gladioli* DJB4–8 in maize roots

The SEM imaging revealed the successful rhizospheric colonization of maize roots by strain DJB4-8 (Figures 4A–C). Complementary to these morphological observations, the GFP-tagged DJB4–8 derivatives demonstrated sustained endophytic colonization patterns within root cortical tissues by fluorescence microscopy (Figures 4D–F). This multimodal imaging evidence collectively confirms the establishment of functional symbiotic associations between DJB4–8 and *Zea mays* host plants.

Effect analysis of maize inoculated with strain *B. gladioli* DJB4-8

Strain DJB4–8 considerably enhanced the growth of maize following inoculation of maize Zhengdan 958 (Figure 5). The fresh weight of the roots, stems, and leaves and maize heights were assessed for 20 and 40 days following inoculation with strain

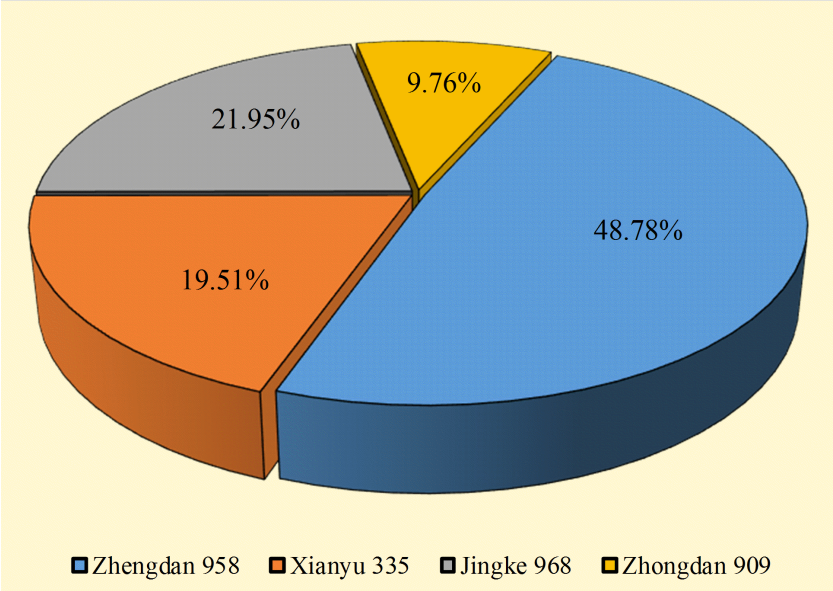

FIGURE 1
Isolation of bacterial strains from rhizosphere soil of four maize varieties.

10.3389/fpls.2025.1611674

TABLE 1 Molecular identification and PGP characteristics of rhizosphere soil bacteria from four maize varieties.

Isolations	Most similar strain	Similarity (%)	NCBI accession no.	Phosphate	Ammonia	Siderophore	DF–ACC
DJA1-2	*Chryseobacterium flavum*	100	PP792774	+++	+++	–	++
DJA1-3	*Stenotrophomonas* sp.	99.93	PP792775	–	+	++	+
DJA1-5	*Stenotrophomonas calcoaceticus*	99	PP792776	+++	+	+	+
DJA1-9	*Herbaspirillum* sp.	99.93	PP792777	+++	++	–	++
DJA1-12	*Agrobacterium deltaense*	100	PP792778	+++	–	–	++
DJA2-2	*Enterobacter cloacae*	99.79	PP792779	++	+++	+	–
DJA2-3	*Burkholderia* sp.	99.93	PP792780	+++	++	+	++
DJA2-5	*Enterobacter* sp.	100	PP792781	++	+	++	–
DJA2-7	*Acinetobacter* sp.	100	PP792782	+	+	–	+
DJA2-8	*Burkholderia* sp.	99.93	PP792783	++	++	+++	+
DJA2-9	*Agrobacterium* sp.	99.85	PP792784	–	+	–	+
DJA3-2	*Microbacterium* sp.	99.93	PP792785	–	+	–	+
DJA3-4	*Herbaspirillum seropedicae*	100	PP792786	+	++	++	+
DJA3-5	*B. gladioli*	100	PP792787	++	++	++	+
DJA4-2	*Enterobacter cancerogenus*	99.64	PP792788	++	++	–	+
DJA4-3	*Pantoea dispersa*	99.93	PP792789	++	++	+++	+
DJA4-5	*Herbaspirillum huttiense*	99.93	PP792790	+	+	+	+
DJA4-6	*B. gladioli*	100	PP792791	++	+++	+++	+
DJA4-9	*Enterobacter ludwigii*	99.86	PP792792	++	+++	+	+
DJA5-3	*Herbaspirillum* sp.	100	PP792793	++	+	–	++
DJB1-3	*Burkholderia* sp.	99.86	PP792794	+++	++	+++	+++
DJB1-4	*Burkholderia* sp.	99.93	PP792795	++	++	+	++
DJB1-6	*Burkholderia cenocepacia*	99.71	PP792796	++	+++	+++	++
DJB2-3	*B. cenocepacia*	99.64	PP792797	++	+++	+++	+
DJB2-8	*B. gladioli*	99.93	PP792798	++	+++	+	+
DJB4-5	*B. cenocepacia*	100	PP792799	++	+++	+++	++
DJB4-8	*B. gladioli*	99.93	PP792800	+++	+++	+++	+++
DJB5-1	*Burkholderia* sp.	99.45	PP792801	++	++	+++	+
DJC1-3	*Pantoea ananatis*	100	PP792802	++	++	+	+
DJC1-4	*Stenotrophomonas* sp.	99.93	PP792803	++	+	+	+
DJC2-3	*Serratia marcescens*	100	PP792804	+++	++	++	++
DJC3-1	*Herbaspirillum* sp.	99.93	PP792805	+	+	++	++
DJC3-2	*B. cenocepacia*	100	PP792806	+	+	+	+
DJC3-4	*Burkholderia* sp.	99.79	PP792807	++	+++	+++	+
DJC4-2	*Burkholderia* sp.	99.86	PP792808	++	+	+++	+
DJC4-3	*P. ananatis*	99.72	PP792809	++	+	–	+
DJC4-8	*Burkholderia* sp.	99.71	PP792810	–	+++	+++	+

(Continued)

TABLE 1 Continued

Isolations	Most similar strain	Similarity (%)	NCBI accession no.	Phosphate	Ammonia	Siderophore	DF–ACC
DJD1-1	*Sphingomonas* sp.	99.86	PP792811	++	++	–	+
DJD3-2	*Acinetobacter calcoaceticus*	100	PP792812	+++	++	++	+
DJD4-1	*Acidovorax avenae*	99.93	PP792813	++	+	–	+
DJD4-6	*Burkholderia cepacia*	99.86	PP792814	++	+++	++	+

The symbols "+++", "++", "+", and "–" correspond to strong, moderate, weak, and undetectable levels of PGP activity, respectively, as demonstrated by the bacterial strains under standardized assay conditions.
PGP, plant growth-promoting; NCBI, National Center for Biotechnology Information; ACC, 1-aminocyclopropyl-1-carboxylic acid.

DJB4-8. According to the results, inoculation treatment could significantly improve maize agronomic indicators. There was no significant difference in various agronomic indicators of maize at 20 days compared to the control group without inoculation, but significant differences were noted at 40 days (Figures 6A–D). Other physiological markers, such as intercellular CO_2, stomatal conductance, and transpiration, did not significantly change 20 days after inoculation with maize strain DJB4-8, with the exception of a notable increase in photosynthesis. Nonetheless, intercellular CO_2 and photosynthesis in maize increased dramatically 40 days after inoculation, although transpiration and stomatal conductance did not alter appreciably (Figures 6E–H). In maize Zhengdan 958 inoculated with strain DJB4-8, root growth hormone (IAA) was detected at 20 and 40 days. The results indicated that the inoculation of strain DJB4–8 significantly increased IAA in maize at both times, reaching 3.62 μg/g FW at 40 days (Figure 6I). The examination of the growth characteristics of maize Zhengdan 958 inoculated with strain DJB4–8 shows that inoculation with PSB strain DJB4–8 can greatly enhance physiological and biochemical markers and boost growth at 40 days.

Overall evaluation of transcriptome data and gene function annotation

A total of six maize root samples of maize Zhengdan 958 were sequenced at 40 days following the inoculation with PSB strain DJB4-8. The average comparison rate with maize reference genome B73_v4 was 80.46%, and the average percentages of sequencing quality indicators Q20 and Q30 were 97.89% and 93.63%, respectively, indicating that the quality of sequencing data was high (Supplementary Table S5), and the length distribution

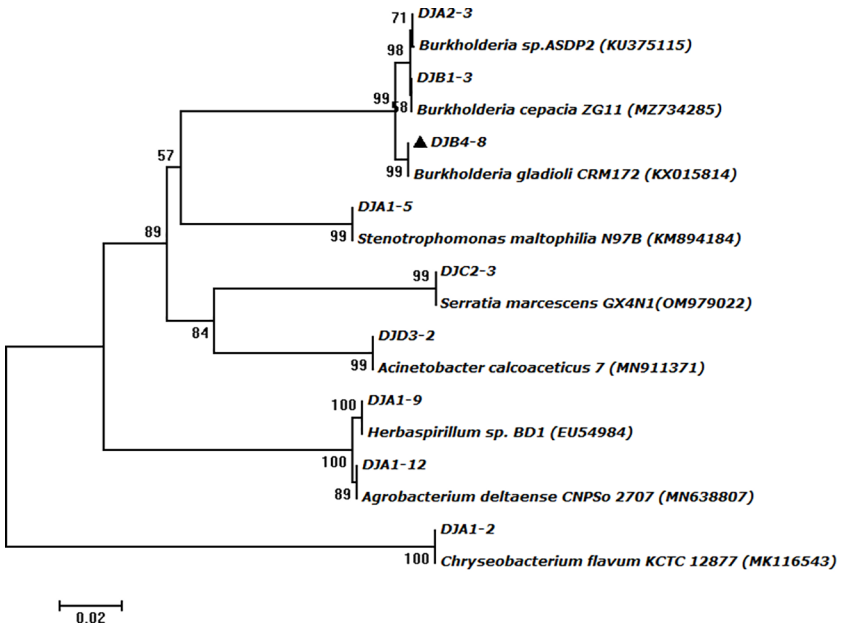

FIGURE 2
The phylogenetic tree was constructed based on the amplified 16S rRNA gene sequences of PSB strains from maize rhizosphere soil. PSB, phosphate-solubilizing bacteria.

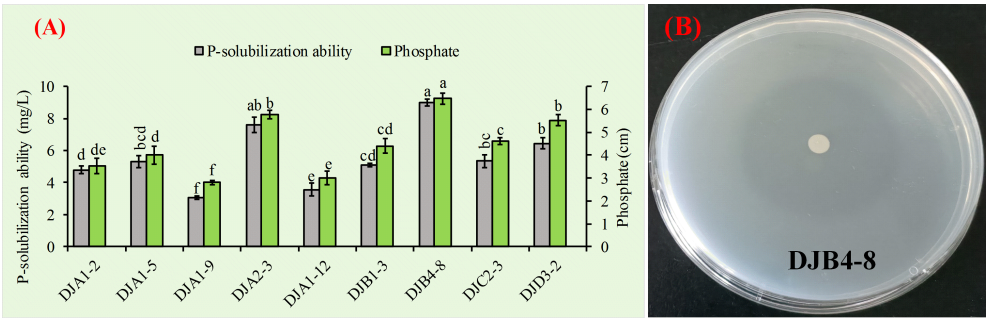

FIGURE 3
Assessment of phosphate-solubilizing capacity in PSB strains. **(A)** Quantitative determination of inorganic phosphate dissolution using the molybdenum-blue spectrophotometric method, demonstrating strain-specific solubilization efficiency. **(B)** Characterization of phosphate-releasing activity in the PSB strain DB4–8 through halo formation analysis on Pikovskaya's agar medium. PSB, phosphate-solubilizing bacteria. Different letters on the column indicate significant difference at 0.05 level. Student T-test was used for the determination of significant differences.

information of transcripts is shown in Supplementary Figure S1. The NCBI Sequence Read Archive (SRA) database received the original transcriptome sequencing data, and the accession number PRJNA1118104 was acquired. There were 22,750 genes in the inoculated treatment group and control group, accounting for 89.89% of the total number of genes, while 1,085 and 1,473 genes were unique to the inoculated treatment group and the control group, respectively (Supplementary Figure S2A). In addition, thermogram analysis showed that the samples in the same group were highly similar, indicating that the transcriptome sequencing data were highly repeatable (Supplementary Figure S2B). All genes were annotated in the public database, and the number of gene annotations in each database was obtained (Supplementary Figure S3).

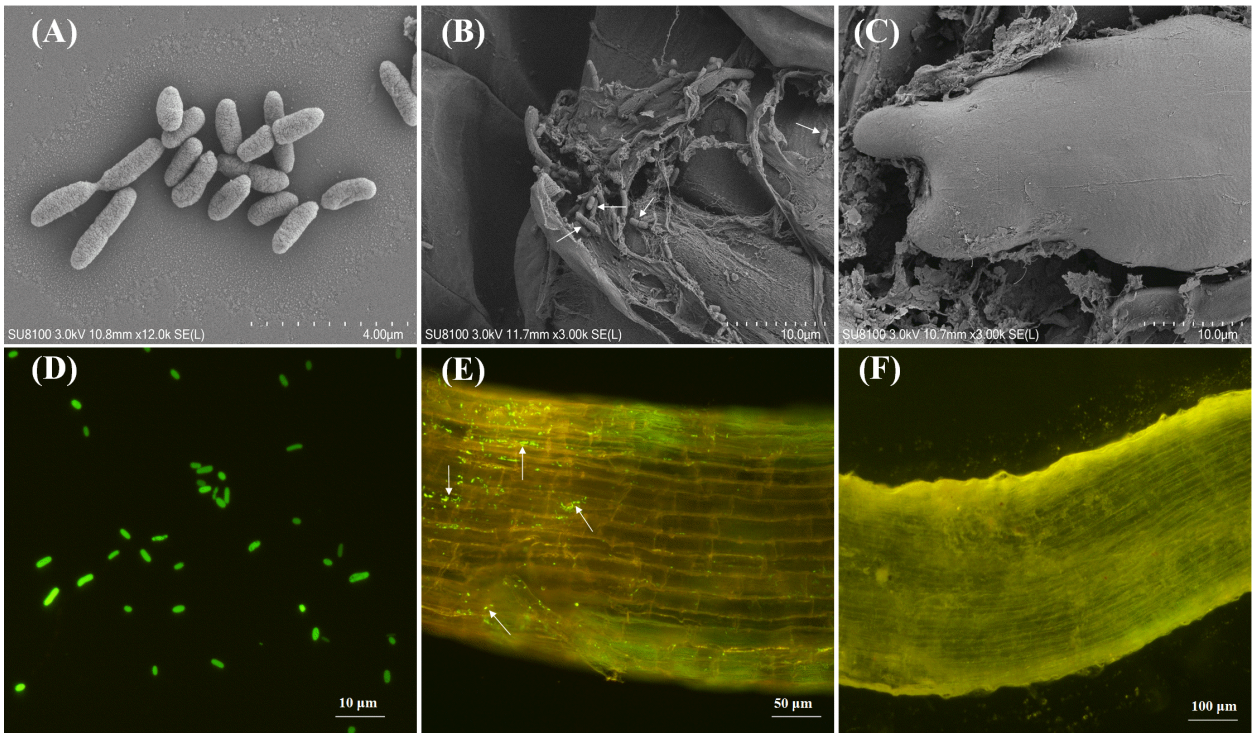

FIGURE 4
Using microscopic techniques to visualize DJB4–8 strain colonization dynamics in Zhengdan 958 maize root system. **(A)** SEM characterization of DJB4–8 colonial morphology. **(B)** SEM micrograph demonstrating successful rhizoplane colonization by DJB4–8 on Zhengdan 958 maize roots. **(C)** Comparative SEM analysis of root architecture in non-inoculated control plants. **(D)** Epifluorescence microscopic detection of GFP-expressing DJB4–8 colonies. **(E)** Spatial distribution pattern of GFP-tagged DJB4–8 colonizing Zhengdan 958 root tissues revealed by fluorescence microscopy. **(F)** Autofluorescence control imaging of uninoculated Zhengdan 958 root specimens. GFP, green fluorescent protein.

10.3389/fpls.2025.1611674

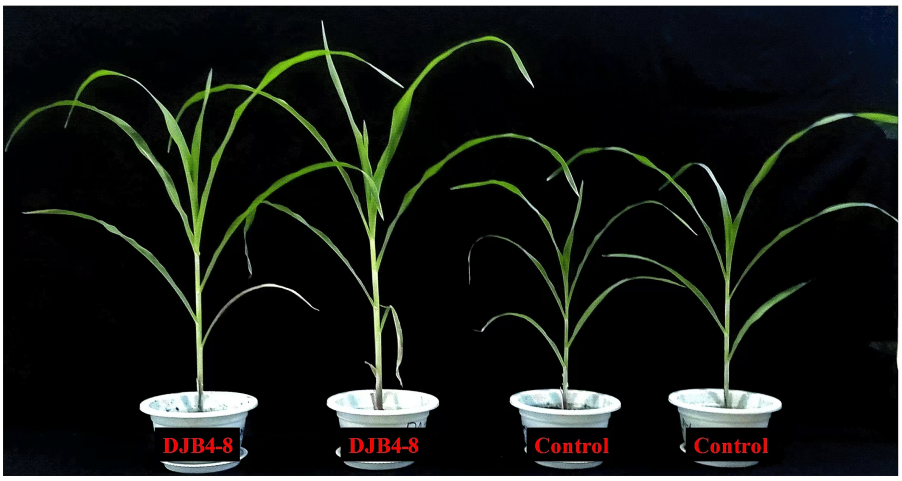

FIGURE 5
Growth status of strain DJB4–8 inoculated with maize Zhengdan 958 at 40 days.

Functional enrichment analysis of DEGs in maize inoculated with strain DJB4-8

The DEGs between the inoculated and the control groups were screened to examine the changes in gene expression brought about by the DJB4–8 inoculation of maize. This investigation identified 303 DEGs, of which 240 were downregulated and 63 were upregulated (Figure 7). Randomly selected 12 important genes with high and low expression in DEGs were chosen for expression verification using qRT-PCR. According to the findings, nine genes' expression trends aligned with RNA-seq. However, the expression trends of three genes (Zm00001eb382310,

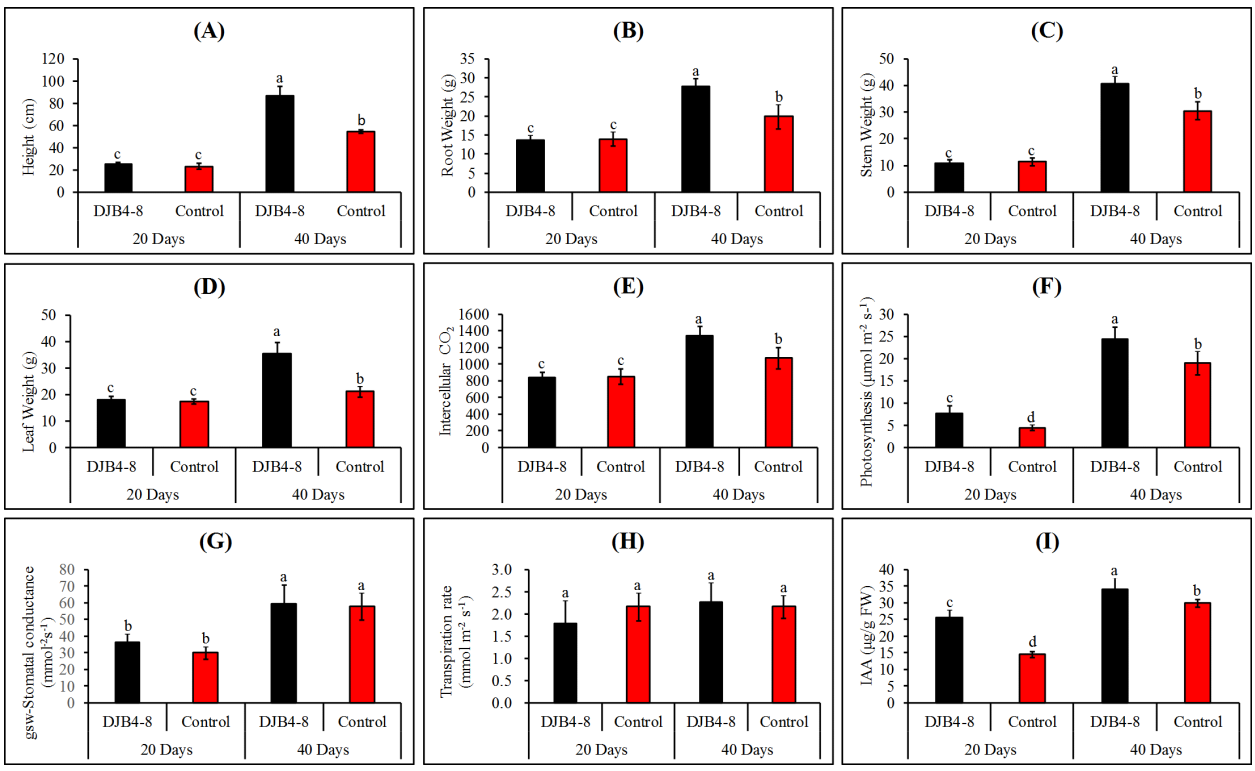

FIGURE 6
Determination of photosynthetic physiological indexes and IAA content of maize Zhengdan 958 inoculated with strain DJB4–8 at 20 and 40 days. **(A)** Height. **(B)** Root weight. **(C)** Stem weight. **(D)** Leaf weight. **(E)** Intercellular CO_2. **(F)** Photosynthesis. **(G)** Stomatal conductance (gsw). **(H)** Transpiration rate. **(I)** IAA content. IAA, indole-3-acetic acid. Different letters on the column indicate significant difference at 0.05 level. Student T-test was used for the determination of significant differences.

Zm00001eb264870, and Zm00001eb093660) did not align with RNA-seq (Supplementary Figure S4). Overall, the results of transcriptome sequencing were relatively reliable.

Using the GO database to annotate DEGs and conducting enrichment analysis separately, it was found that DEGs were mainly enriched in hydrolase activity, oxidoreductase activity, serine hydrolase activity, signaling receptor activity, carbohydrate phosphatase activity, nutrient reservoir activity, and glutathione transferase activity in terms of aspects of biological function. Biological processes (BPs) are mainly enriched in items such as response to stimulus, proteolysis, and defense response. Cellular components (CCs) are mainly enriched in the plasma membrane, extracellular region, etc. (Figure 8A). After annotating DEGs and conducting separate enrichment analyses using the KEGG database, it was discovered that DEGs were primarily enriched in metabolic pathways like glutathione metabolism (map00480), starch and sucrose metabolism (map00500), amino sugar and nucleotide sugar metabolism (map00520), and plant hormone signal transduction (map04075) (Figure 8B). The analysis of the predicted protein interaction network based on DEGs showed that genes such as trehalose biosynthesis process (Zm00001eb327900), cytoskeleton (Zm00001eb155540), xylan acetylation (Zm00001eb329480), synthesis (Zm00001 eb059380), and trehalose metabolism in response to stress (Zm00001eb 178890) play a decisive role in protein network interactions (Figure 9).

Metabolite identification and DAM analysis of maize inoculated with strain DJB4-8

In the metabolome data of the interaction between maize and strain DJB4-8, 3,069 and 5,740 metabolic ions were identified in cationic and anionic modes, respectively. Ultimately, 1,104 and 1,029 metabolites were identified, with 555 and 467 metabolites annotated to the KEGG database, respectively (Supplementary Table S6). PLS-DA indicates that under both anionic and cationic conditions, the greater the sample separation between the inoculation treatment group and the control group, the more significant the classification effect (Supplementary Figure S5). Meanwhile, the interpretability of components undefined d1 and two under cations was 23.8% and 16.2% (Supplementary Figure S5A), while under anions, it was 25.4% and 20.6% (Supplementary Figure S5B), respectively.

Orthogonal partial least squares–discriminant analysis (OPLS-DA) was utilized with univariate multiple analysis and t-test to screen for DAMs and perform significant difference analysis on the identified metabolic characteristics. Out of 115 DAMs screened in cationic conditions, 122 showed upregulation, and 33 showed downregulation (Figure 10A). After 169 DAMs were screened in anionic conditions, 103 showed upregulation, and 66 showed downregulation (Figure 10B). The OPLS-DA model analysis indicated significant differences between the groups. It revealed that the first predicted principal component release rate and the first orthogonal component release rate under cation were 19.10% and 20.90%, respectively (Figure 10C), while under anion, they were 19.70% and 25.60%, respectively (Figure 10D).

Metabolite enrichment analysis of metabolic differences in the interaction between maize and strain DJB4-8

Through KEGG pathway enrichment analysis of DAMs, the key metabolic pathways of maize-responsive strain DJB4–8 were further identified (Figure 11). The top 20 pathways with the highest enrichment level (lowest *p*-value) were selected from the KEGG database, such as biosynthesis of cofactors (map01240), glycerophospholipid metabolism (map00564), biosynthesis of various plant secondary metabolites (map00999), phenylpropanoid biosynthesis (map00940), and tyrosine metabolism (map00350), which are the metabolic pathways with higher enrichment levels (Figure 11A), indicating that metabolites in these pathways may play important roles in the interaction between maize and strain DJB4-8. Furthermore, clustering heatmaps and variable importance in projection analysis have shown that metabolites such as 2,6-diamino-

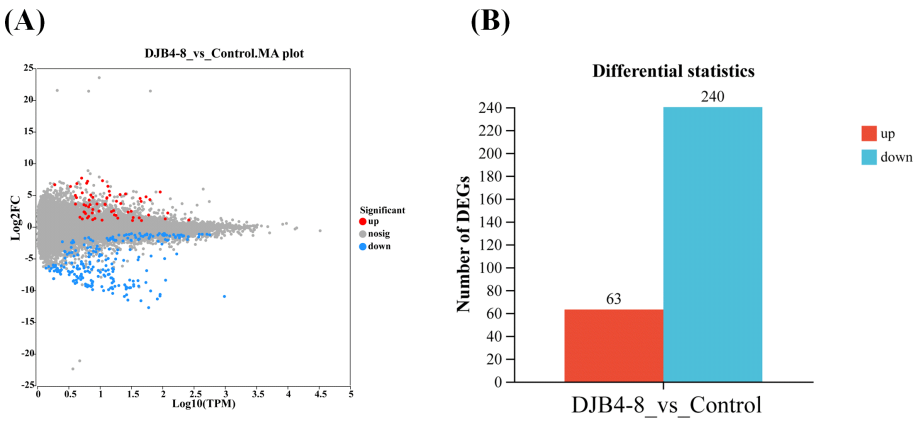

FIGURE 7
The DEGs in the root transcriptome of maize Zhengdan 958 inoculated with strain DJB4-8. **(A)** The Minus-versus-Add (MA) plot of gene transcriptome expressed genes. **(B)** The number of DEGs (bar). DEGs, differentially expressed genes.

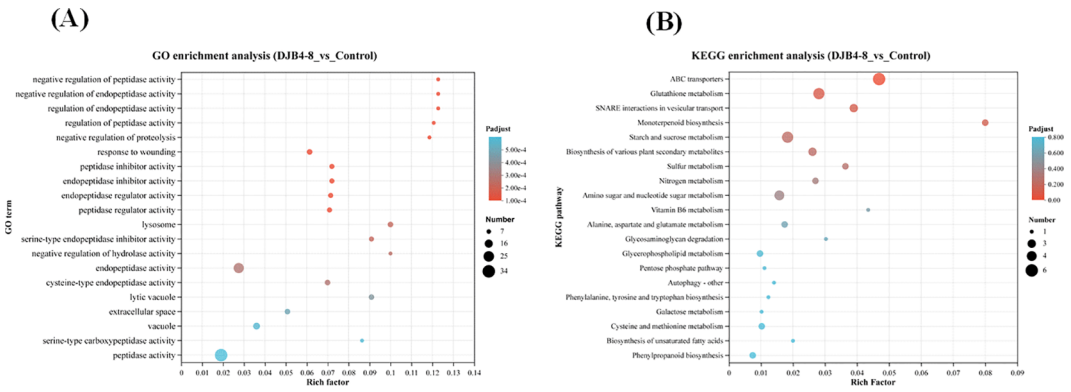

FIGURE 8
Functional enrichment analysis of maize transcriptome responses to DJB4–8 colonization. **(A)** Enrichment of DEGs in GO database. **(B)** Enrichment of DEGs in KEGG database. Note: The vertical axis represents the GO term/pathway name, and the horizontal axis represents the rich factor—the more significant the rich factor, the greater the degree of enrichment. The dot's size shows the number of genes in this GO term/pathway, and the dot's color reflects the various *p*-adjust ranges. DEGs, differentially expressed genes; KEGG, Kyoto Encyclopedia of Genes and Genomes.

9-(2-hydroxyethoxymethyl)purine, acevaltrate, and tricin are the main upregulated metabolites in DAMs, while (3*S*,5*R*,6*R*,7*E*)-3,5,6-trihydroxy-7-megastigmen-9-one, Fluoronaphthyridone, and others are the main downregulated metabolites in DAMs (Figure 11B).

Combined transcriptome and metabolome analysis of the interaction between maize and strain DJB4-8

The combined analysis of transcriptomics and metabolomics of the interaction between maize and strain DJB4–8 simultaneously locates DEGs and DAMs on the KEGG pathway map to better evaluate the relationship between genes and metabolites. The nine-quadrant plot analysis indicates a correlation between the transcriptome and metabolome data (Figure 12A). The response strain DJB4–8 of maize Zhengdan 958 has 23 and 34 transcriptome- and metabolome-associated genes and differential substances, respectively; KEGG has enriched multiple metabolic pathways, such as glutathione metabolism, starch and sucrose metabolism, biosynthesis of various plant secondary metabolites, amino sugar and nucleotide sugar metabolism, plant hormone signal transduction, and pentose phosphate pathway (Figure 12B). These metabolic pathways play important roles in various stages of plant growth.

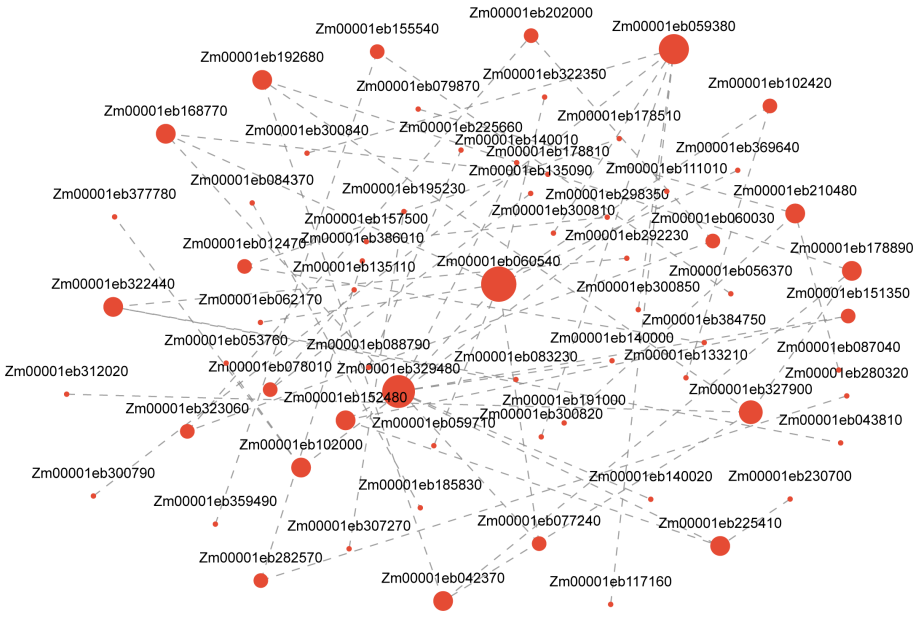

FIGURE 9
Analysis of protein network regulation predicted by DEGs. Note: Nodes represent genes, and edges represent interactions between two genes. The size of a node is proportional to its connectivity. DEGs, differentially expressed genes.

10.3389/fpls.2025.1611674

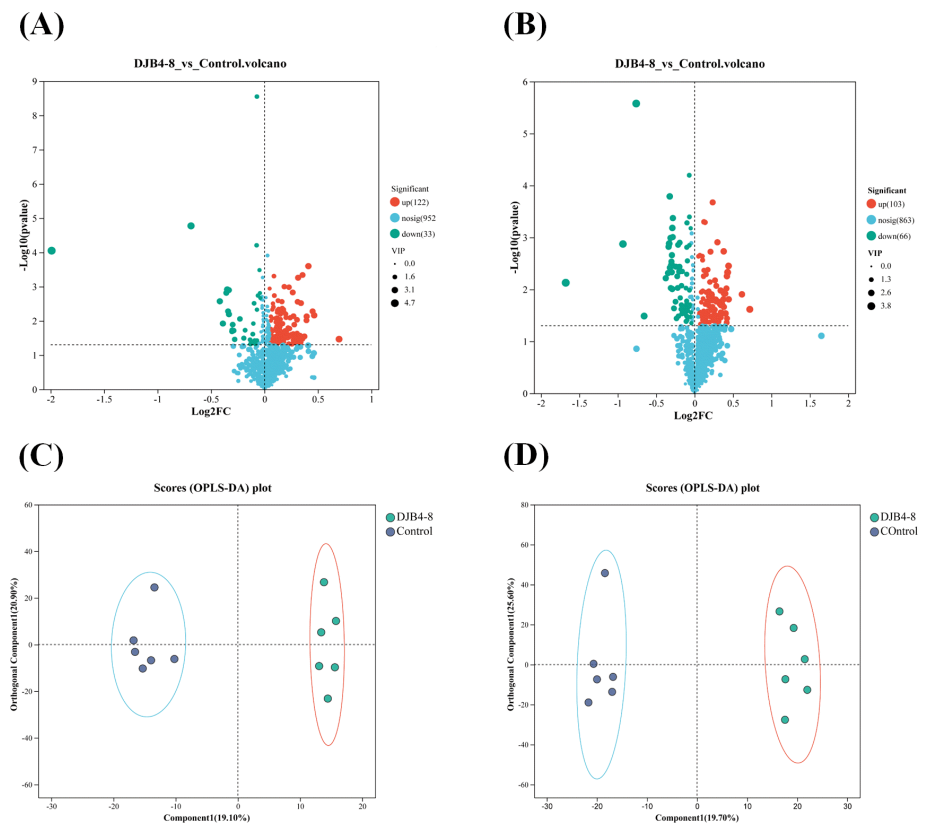

FIGURE 10
The DAMs in the root metabolome of maize Zhengdan 958 inoculated with strain DJB4-8. **(A)** DAMs in the metabolome under cationic conditions. **(B)** DAMs in the metabolome under anionic conditions. **(C)** OPLS-DA comparative analysis of metabolites under cationic conditions. **(D)** OPLS-DA comparative analysis of metabolites under anionic conditions. DAMs, differentially accumulated metabolites; OPLS-DA, orthogonal partial least squares–discriminant analysis.

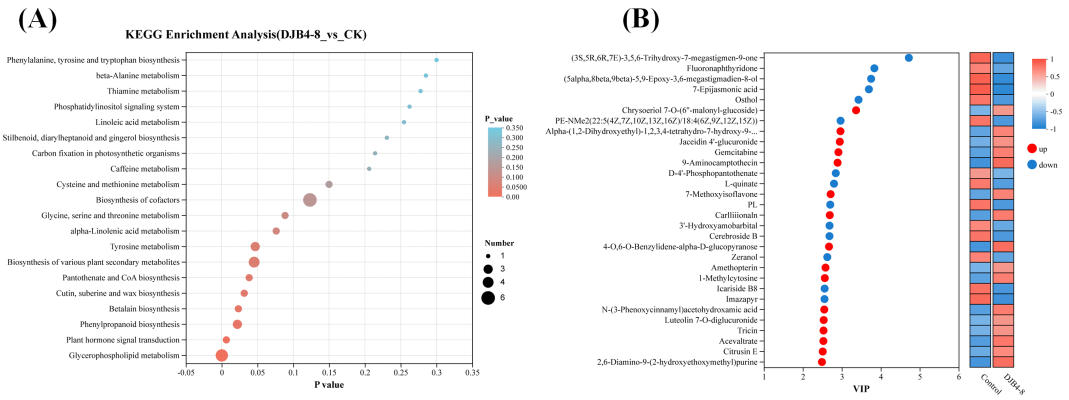

FIGURE 11
Enrichment of DAMs after strain DJB4–8 inoculated into maize. **(A)** Bubble diagram of DAMs enrichment in the KEGG database. **(B)** VIP analysis of metabolites. Note: In panel A, the abscissa denotes the enrichment ratio (metabolite set enrichment analysis score), while the ordinate specifies annotated KEGG pathways. Bubble diameter is proportional to metabolite set cardinality per pathway. Color gradient corresponds to the statistical significance level (–log10-transformed FDR-adjusted *p*-values). In panel B, the left ordinate displays metabolites ranked by variable importance in projection (VIP) scores derived from OPLS-DA modeling, with bubble size reflecting VIP magnitude. The right panel presents a hierarchical clustering heatmap of z-score normalized relative abundance, where columns represent experimental replicates, and rows indicate significantly regulated metabolites (VIP > 1.0, *q*-value < 0.05). DAMs, differentially accumulated metabolites; KEGG, Kyoto Encyclopedia of Genes and Genomes; FDR, false discovery rate; OPLS-DA, orthogonal partial least squares–discriminant analysis.

Discussion

Scientific researchers have always focused on improving crop yield and quality in agricultural production. With the deepening of microbiology research, using microbial resources to promote crop growth and enhance stress resistance has achieved rich research results in recent years (Guzmán et al., 2025; Sengupta and Gunri, 2015; Gupta et al., 2022; Adeleke and Babalola, 2021). As an important kind of PGPR, PSB can improve the content of available phosphorus in soil by dissolving insoluble phosphate in soil and then promoting crop growth (Panhwar et al., 2011; Ahemad, 2015). This study isolated 41 bacterial strains from the rhizosphere soil of four maize varieties. *B. gladioli* DJB4–8 was evaluated through *in vitro* analysis of plant growth-promoting characteristics and 16S rRNA molecular identification. Strain DJB4–8 exhibited the highest activity-promoting activity of any strain *in vitro*, and it could solubilize phosphate at a level of 8.99 mg/L, much greater than that of other strains. This outcome demonstrates the potential for *B. gladioli* DJB4–8 to be a superior PGPR. Similar to our study, Pande et al. (2017) isolated a PSB strain from the maize rhizosphere that exhibited potent *in vitro* PGP characteristics. Many PSB strains, such as *Pseudomonas aeruginosa*, *Enterobacter aerogenes*, and *Stenotrophomonas maltophilia*, have been screened (Panhwar et al., 2012; Sadiq et al., 2013; Amri et al., 2023). This greatly enriches the PGPR resource library and provides valuable microbial resources for the application of microorganisms in agricultural production. Compared with the reported PGPR, strain *B. gladioli* DJB4–8 exhibits a unique ecological niche preference. It possesses various PGP traits, including ammonia synthesis and iron excretion, and is capable of proliferating in a medium where ACC serves as the exclusive nitrogen source. Specifically, it possesses a high capacity to solubilize phosphorus (Table 1), indicating promise for study and use.

The prerequisite for the symbiotic system formed by PGPR and plants to exert its promoting effect is that microorganisms can successfully colonize plant tissues (Compant et al., 2010). This study integrated high-resolution surface morphology characterization using SEM and monitoring with GFP labeling to reveal the colonization pattern of PSB strain *B. gladioli* DJB4–8 in maize rhizosphere at a three-dimensional spatial scale. Strain DJB4–8 effectively infects the maize root surface and establishes a persistent symbiotic relationship by generating many microcolonies on maize Zhengdan 958 roots, as demonstrated by the SEM images. Certain studies have indicated that the preferential adhesion of bacterial cells to root hair regions and intercellular spaces of the root epidermis may correlate with their chemotactic responses and resilience to stressors, including drought and salinity (Kranawetter and Sumner, 2025; Verma et al., 2021). It may also promote the local enrichment of P through physical adsorption mechanisms (Liu et al., 2019; Sharma and Sharma, 2019). It is worth noting that GFP labeling showed clustering of strain DJB4–8 in the inner layer of maize roots (Figures 4E), suggesting that it may enter the plant's symbiotic system through intercellular hyphae or active transport. It provides a reference for studying cross-border interaction mechanisms in the *Burkholderia* genus. The rhizosphere microenvironment has also been shown to dramatically increase the expression level of the acid phosphatase gene (*phoA*) in the genome of certain PSB strains, improving their capacity to solubilize phosphate (Li et al., 2023b; Liu et al., 2020; Dey et al., 2021). At the same time, some PSB strains carry gene clusters encoding the Type III secretion system in their genomes, which may be involved in host-specific signal recognition (Preston et al., 2001; Stringlis et al., 2019). The symbiotic P release mechanism between strain DJB4–8 and maize still needs further research.

Both photosynthesis and respiration in plants depend on P. The carbon fixation mechanism and the photosynthetic electron transport chain are essential, facilitating the production of ATP and NADPH (Malhotra et al., 2018; Amthor, 2023). Photosynthesis and respiration intensity levels were significantly higher in maize Zhengdan 958 infected with the PSB strain DJB4–8 than in the control in this study. After 40 days of inoculation, it was noticed that maize's photosynthetic physiological activity changed significantly, possibly related to PSB's improvement of maize P

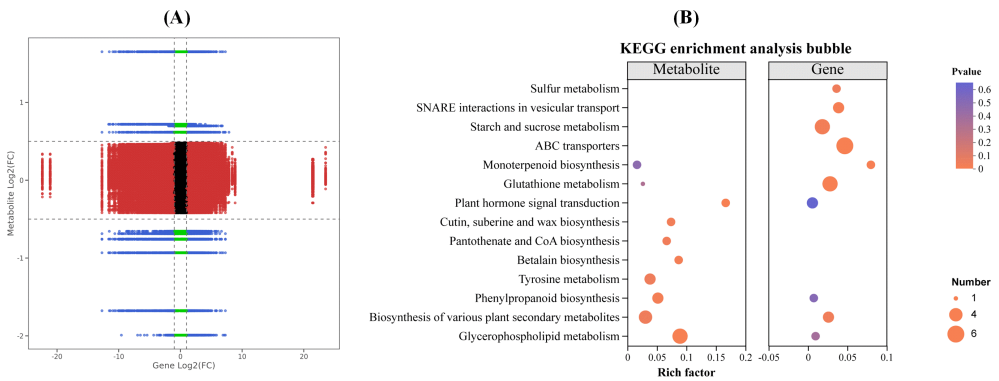

FIGURE 12
Combined analysis of transgenic and metabolome data after inoculation of strain DJB4–8 in maize. **(A)** Nine-quadrant plot of transcriptome and metabolome expression correlation. **(B)** KEGG enrichment bubble plot of transcriptome and metabolome. KEGG, Kyoto Encyclopedia of Genes and Genomes.

absorption. This study also found that after inoculation with strain *B. gladioli* DJB4-8, the IAA content in maize roots significantly increased, and the developmental pattern of maize roots was significantly altered considerably, increasing the fresh weight of maize roots. Quantitative analysis by HPLC showed that the IAA concentration secreted by DJB4–8 in the maize rhizosphere was as high as 34.03 mg/L, which was 1.14 times higher than that in the control group without inoculation ($p < 0.05$). Some scholars have detected high concentrations of IAA and tryptophan (Trp) in plant rhizosphere through targeted metabolomics. Combined with key genes for IAA synthesis annotated in the strain genome, such as *ipdC* and *aldH*, it has been confirmed that PGPR can synthesize IAA through dual channels of the indole-3-acetamide pathway and tryptophan-dependent pathway (Luziatelli et al., 2020; Li et al., 2018). This multi-pathway synergistic IAA synthesis strategy may help plants adapt to different growth environments. In this study, strain DJB4–8 significantly upregulates genes related to tryptophan synthesis in the transcriptome (map00400), which may be associated with PSB stimulation. Some research has found that PGPR stimulate plant tryptophan metabolism toward IAA synthesis by secreting small molecule metabolites such as IAA or inducing reactive oxygen species (ROS) signals (Deng et al., 2024; Mir et al., 2020). Additionally, after plant inoculation with PGPR, some hormones such as gibberellin drive stem elongation, and IAA enhances assimilate transport capacity, increasing aboveground biomass and maintaining growth through efficient phosphorus absorption, exhibiting a carbon–phosphorus synergistic optimization effect (Mogal et al., 2020). The transcriptome results of this study's interaction between strain DJB4–8 and maize revealed notable alterations in the expression levels of genes linked to the plant hormone signaling pathways in maize. It implies that strain DJB4–8 may impact maize growth and development by controlling the plant hormone signaling pathways.

The shikimic acid pathway produces phenylalanine, the precursor to the phenylpropane metabolic pathway. Several enzymes catalyze the synthesis of various secondary metabolites necessary for plant growth and development. In the phenylpropane metabolic cycle, lignin, the main component of plant cell walls, forms conduits, moves water and mineral components, and provides mechanical support for plants (Muro-Villanueva et al., 2019). It is a leading creator of systems for material transportation and plant support. Furthermore, this system produces flavonoid chemicals such as flavonoids, flavones, and isoflavones, which are essential for plant growth and development and can act as signaling molecules to help generate root nodules (Meng et al., 2022; Tohge et al., 2013; Wu et al., 2024). After inoculation with DJB4-8, key genes (Zm00001eb133780 and Zm00001eb286490) involved in the phenylpropanoid biosynthesis pathway in maize roots were significantly upregulated. This synergistic change suggests that DJB4–8 may indirectly regulate maize growth by regulating the phenylpropanoid pathway.

Zeatin, as one of the most active members of the cytokinin (CK) family, plays a core regulatory role in plant growth and development, stress response, and microbial interactions (Schäfer et al., 2015; Li et al., 2021). Zeatin drives the G1/S phase transition by activating cell cycle proteins (CycD3) to maintain cell activity (Lu et al., 2025). It can also delay leaf senescence by inhibiting the expression of SAG12 (senescence-related gene) while activating the expression of sucrose transporters (SUC2) to promote the transport of assimilates to grains (Wang et al., 2025; Swartzberg et al., 2011). Genes linked to the zeatin biosynthesis pathway in maize showed altered expression levels following inoculation with strain DJB4-8, suggesting that strain DJB4–8 may influence maize cell division and growth by controlling zeatin production. Glutathione is an important antioxidant that can eliminate free radicals in plants and protect cells from oxidative damage (Margis et al., 2008). This study found that after inoculation with strain DJB4-8, the expression levels of genes related to the glutathione metabolism pathway in maize changed, which may be related to the oxidative stress response triggered by the initial colonization of strain DJB4-8.

The pentose phosphate pathway (PPP) is key in plants' biosynthetic and energy metabolism processes (Kruger and Von Schaewen, 2003). Genes associated with the pentose phosphate system in maize exhibited changed expression levels when strain DJB4–8 was introduced. Strain DJB4–8 may regulate the pentose phosphate pathway, affecting energy metabolism and maize biosynthesis. Genes linked to the PPP, such as G6PD and 6PGD, were markedly elevated during the late contact stage (Barcia-Vieitez and Ramos-Martínez, 2014; Spielbauer et al., 2013). In addition to promoting phenylpropanoid production, the resultant NADPH may affect redox equilibrium by controlling the thioredoxin system (Zhang et al., 2024; Li et al., 2023c). This process of energy coupling across metabolic pathways may serve as a fundamental basis for enhancing host stress resistance by DJB4-8. After inoculation with PSB, the growth and development of maize were promoted. It may be related to the important role of NADPH and intermediates produced by the PPP in biosynthesis. As a reducing agent, NADPH participates in synthesizing biomolecules such as fatty acids, sterols, and nucleic acids, providing the necessary material and energy basis for the growth of maize plants. At the same time, the intermediate products produced by the PPP also provide raw materials for the synthesis of cell wall structural substances, enhancing the mechanical strength and stability of the cell wall and helping to improve the stress resistance of maize plants (Wurtele and Nikolau, 1986; Pugin et al., 1997).

Following the DJB4–8 inoculation of maize, transcriptome DEGs were enriched in KEGG for carbon amino sugar and nucleotide sugar metabolic pathways, which are centered around the *GFAT* and *GNA1* genes, and *UGD* and *UGP* gene clusters contribute to cell wall synthesis, glycosylation modification, and disease defense. Since nucleotide sugar synthesis is a high-energy process, PSB may raise ATP levels by improving phosphorus absorption, blocking the conformational sites of hexokinase (HXK), and encouraging carbon flow into nucleotide sugar metabolism (Reiter and Vanzin, 2001; Seifert, 2004; Bar-Peled and O'Neill, 2011). Research in the recent past has demonstrated that rhizosphere microorganisms can increase UDP glucuronic acid secretion and encourage microbial chemotaxis colonization (Velmourougane et al., 2017). The accumulation of compounds

like *N*-acetylglucosamine is advantageous for cell wall synthesis, maintaining cell osmotic balance, and boosting plant stress resistance (Yoo et al., 2021).

Metabolome analysis revealed that distinct metabolites in the interaction between maize and strain DJB4–8 were considerably enhanced in the glycerophospholipid metabolic pathway. This phenomenon suggests complex metabolic interactions between PSB and host plants, which may involve multiple biological processes such as phosphorus activation, cell membrane remodeling, signal transduction, and defense response (Li et al., 2022a). Glycerol phospholipids are the main components of precursors of signaling molecules and cell membranes, such as phosphatidic acid and phosphatidylinositol. Their metabolic changes may reflect the adaptive adjustment of plants to the action of microbial agents (Dedinaite and Campbell, 2000; Green et al., 2019). In the phospholipid metabolism pathway, phospholipid derivatives (phosphatidic acid) participate in the signal transmission of plant hormones (auxin and jasmonic acid). PSB may activate host defense enzymes [superoxide dismutase (SOD), peroxidase (POD), and catalase (CAT)] by secreting hormone analogs such as IAA, thereby regulating the expression of genes related to glycerophospholipid metabolism (Ge and Zhang, 2015). Simultaneously, glycerophospholipid metabolism interacts with channels like glycolysis and the tricarboxylic acid cycle (TCA), and its enrichment may be a result of plants modifying their energy allocation to accommodate the higher phosphorus absorption and utilization efficiency brought about by microbial agents (Li et al., 2023a, 2022b). The metabolic products of glycerophospholipids (phosphatidic acid) may optimize the plant's response to PSB promotion. These may function as second messengers and mediate the synergistic action of IAA signaling and the antioxidant enzyme system (Hou et al., 2024). This study indicates that strain DJB4–8 can promote maize root development by secreting IAA, which may enhance phosphorus absorption capacity, increase oxidative stress kinase activity during the maize seedling stage, reduce oxidative damage, and accelerate maize growth.

The biosynthesis of various plant secondary metabolites is another important metabolic pathway for enriching differential metabolites in this study's metabolome. Plant secondary metabolites (phenols, terpenes, and alkaloids) are important chemical mediators for plants to adapt to environmental stress, resist pathogen invasion, and interact with microorganisms (Firáková et al., 2007; Ko et al., 2010). Inoculating corn with PSB strain DJB4-8 may activate the secondary metabolic network of corn by regulating plant defense response, phosphorus utilization efficiency, or microbial host signaling communication. One important tactic that plants use to deal with biotic and abiotic stress is the manufacture of secondary metabolites, which may also contribute to promoting PSB. Some secondary metabolites (citric acid and malic acid) can directly chelate insoluble phosphorus in soil and synergistically improve phosphorus availability with organic acids secreted by PSB (Bai et al., 2024; Xia et al., 2024). In addition, secondary metabolites may optimize phosphorus absorption efficiency by regulating the expression of phosphorus transporters such as the PHT1 family. In the meantime, the activation of secondary metabolic pathways may reflect the redistribution of carbon sources in plants when phosphorus levels are high enough (Victor Roch et al., 2019; Zhao et al., 2024). It would balance stress resistance and growth promotion by directing photosynthetic products toward defense-related metabolism rather than necessary growth.

Tricin is a metabolite upregulated in DAMs discovered in this study (VIP = 2.53). Tricin is a flavonoid compound widely present in grasses. Tricin, as a flavonoid compound, has antioxidant activity and may protect maize cells from oxidative damage by scavenging free radicals or activating antioxidant enzyme systems such as SOD. Tricin may play a role in secondary metabolic processes in maize, like phenylpropanoid metabolism, which encourages the production of additional phenolic or flavonoid compounds—these metabolites, which help maize deal with biological stress, may be insect-resistant or antimicrobial (Santhoshkumar et al., 2025; Nephali et al., 2021).

This study elucidated the theoretical foundation of the interaction between *B. gladioli* DJB4–8 and maize, demonstrating that PSB modulate maize development via hormonal signals, phenylpropanoid production, redox equilibrium, and other mechanisms. In the future, we will focus on analyzing the spatiotemporal heterogeneity of the interaction between PSB and the maize rhizosphere at the single-cell level. Employing molecular marker technology to monitor the expression of pivotal genes dynamically facilitates a paradigm shift in plant–microbe interaction research from mere descriptive phenomena to precise regulation, hence offering theoretical and technical support for sustainable agriculture.

Conclusion

This research identified *B. gladioli* DJB4-8, a bacterium that promotes plant development and solubilizes phosphate, from the rhizosphere soil of maize. The strain can establish a persistent symbiotic association in maize roots, markedly enhancing agronomic characteristics and physiological photosynthesis while dramatically increasing the amount of the plant hormone IAA in maize roots. Combined transcriptome and metabolome analysis showed that the key genes and metabolites of maize Zhengdan 958 interacting with strain DJB4–8 were mainly enriched in the key metabolic pathways of plant growth. In conclusion, strain DJB4–8 has excellent potential for development and research. The pertinent research findings offer a theoretical framework for examining the interaction mechanism between PSB and maize, establishing a foundation for the application of PSB in maize cultivation.

Data availability statement

The datasets presented in this study can be found in online repositories. The names of the repository/repositories and accession number(s) can be found below: https://www.ncbi.nlm.nih.gov/, PRJNA1118104.

Author contributions

D-JG: Conceptualization, Funding acquisition, Methodology, Project administration, Resources, Validation, Visualization, Writing – original draft, Writing – review & editing. G-RY: Formal analysis, Investigation, Methodology, Software, Writing – original draft. PS: Data curation, Formal analysis, Methodology, Supervision, Validation, Writing – original draft. J-JW: Data curation, Formal analysis, Investigation, Writing – original draft. X-ML: Conceptualization, Investigation, Methodology, Writing – original draft. RS: Conceptualization, Data curation, Investigation, Methodology, Software, Writing – original draft, Writing – review & editing. JG: Investigation, Methodology, Writing – original draft. Y-DD: Investigation, Methodology, Writing – original draft. D-PL: Conceptualization, Investigation, Methodology, Resources, Validation, Visualization, Writing – original draft, Writing – review & editing. BY: Investigation, Resources, Software, Validation, Visualization, Writing – original draft, Writing – review & editing.

Funding

The author(s) declare that financial support was received for the research and/or publication of this article. This study was sponsored by the Science and Technology Planning Project of Gansu Province: Natural Science Foundation (No. 25JRRG036), Education and Technology Innovation Project of Gansu Province: College Faculty Innovation Fund Program (No. 2025A-178), and Startup fund for doctoral research of Hexi University (No. KYQD2024014) and New Agriculture Research and Reform Practice (2020103), and supported by Key Laboratory of Hexi Corridor Resources Utilization, Gansu Province (grant number: XZ2305).

Conflict of interest

The authors declare that the research was conducted in the absence of any commercial or financial relationships that could be construed as a potential conflict of interest.

Generative AI statement

The author(s) declare that no Generative AI was used in the creation of this manuscript.

Publisher's note

All claims expressed in this article are solely those of the authors and do not necessarily represent those of their affiliated organizations, or those of the publisher, the editors and the reviewers. Any product that may be evaluated in this article, or claim that may be made by its manufacturer, is not guaranteed or endorsed by the publisher.

Supplementary material

The Supplementary Material for this article can be found online at: https://www.frontiersin.org/articles/10.3389/fpls.2025.1611674/full#supplementary-material

References

Adeleke, B. S., and Babalola, O. O. (2021). The endosphere microbial communities, a great promise in agriculture. *Int. Microbiol.* 24, 1–17. doi: 10.1007/s10123-020-00140-2

Adnan, M., Fahad, S., Zamin, M., Shah, S., Mian, I. A., Danish, S., et al. (2020). Coupling phosphate-solubilizing bacteria with phosphorus supplements improve maize phosphorus acquisition and growth under lime induced salinity stress. *Plants-Basel* 9, 900. doi: 10.3390/plants9070900

Ahemad, M. (2015). Phosphate-solubilizing bacteria-assisted phytoremediation of metalliferous soils: a review. *3 Biotech.* 5, 111–121. doi: 10.1007/s13205-014-0206-0

Ahmad, M., Adil, Z., Hussain, A., Mumtaz, M. Z., Nafees, M., Ahmad, I., et al. (2019). Potential of phosphate solubilizing *Bacillus* strains for improving growth and nutrient uptake in mungbean and maize crops. *Pak. J. Agr. Sci.* 56, 283–289.

Alori, E. T., Glick, B. R., and Babalola, O. O. (2017). Microbial phosphorus solubilization and its potential for use in sustainable agriculture. *Front. Microbiol.* 8, 971. doi: 10.3389/fmicb.2017.00971

Amri, M., Rjeibi, M. R., Gatrouni, M., Mateus, D. M., Asses, N., Pinho, H. J., et al. (2023). Isolation, identification, and characterization of phosphate-solubilizing bacteria from Tunisian soils. *Microorganisms* 11, 783. doi: 10.3390/microorganisms11030783

Amthor, J. (2023). ATP yield of plant respiration: potential, actual and unknown. *Ann. Bot-London.* 132, 133–162. doi: 10.1093/aob/mcad075

Bai, K., Wang, W., Zhang, J., Yao, P., Cai, C., Xie, Z., et al. (2024). Effects of phosphorus-solubilizing bacteria and biochar application on phosphorus availability and tomato growth under phosphorus stress. *Bmc. Biol.* 22, 211. doi: 10.1186/s12915-024-02011-y

Barcia-Vieitez, R., and Ramos-Martínez, J. I. (2014). The regulation of the oxidative phase of the pentose phosphate pathway: new answers to old problems. *IUBMB Life.* 66, 775–779. doi: 10.1002/iub.1329

Bar-Peled, M., and O'Neill, M. A. (2011). Plant nucleotide sugar formation, interconversion, and salvage by sugar recycling. *Annu. Rev. Plant Biol.* 62, 127–155. doi: 10.1146/annurev-arplant-042110-103918

Bhattacharyya, P. N., and Jha, D. K. (2012). Plant growth-promoting rhizobacteria (PGPR): emergence in agriculture. *World J. Microb. Biot.* 28, 1327–1350. doi: 10.1007/s11274-011-0979-9

Billah, M., Khan, M., Bano, A., Hassan, T. U., Munir, A., and Gurmani, A. R. (2019). Phosphorus and phosphate solubilizing bacteria: Keys for sustainable agriculture. *Geomicrobiol. J.* 36, 904–916. doi: 10.1080/01490451.2019.1654043

Biswas, J. K., Banerjee, A., Rai, M., Naidu, R., Biswas, B., Vithanage, M., et al. (2018). Potential application of selected metal resistant phosphate solubilizing bacteria isolated from the gut of earthworm (*Metaphire posthuma*) in plant growth promotion. *Geoderma* 330, 117–124. doi: 10.1016/j.geoderma.2018.05.034

Chen, S., Liu, W., Morel, J., Parsons, D., and Du, T. (2023). Improving yield, quality, and environmental co-benefits through optimized irrigation and nitrogen management of hybrid maize in Northwest China. *Agr. Water Manage.* 290, 108577. doi: 10.1016/j.agwat.2023.108577

Chen, Y., Rekha, P., Arun, A., Shen, F., Lai, W.-A., and Young, C. C. (2006). Phosphate solubilizing bacteria from subtropical soil and their tricalcium phosphate solubilizing abilities. *Appl. Soil Ecol.* 34, 33–41. doi: 10.1016/j.apsoil.2005.12.002

Compant, S., Clément, C., and Sessitsch, A. (2010). Plant growth-promoting bacteria in the rhizo-and endosphere of plants: their role, colonization, mechanisms involved and prospects for utilization. *Soil Biol. Biochem.* 42, 669–678. doi: 10.1016/j.soilbio.2009.11.024

Dedinaite, A., and Campbell, B. (2000). Interactions between mica surfaces across triglyceride solution containing phospholipid and polyglycerol polyricinoleate. *Langmuir* 16, 2248–2253. doi: 10.1021/la991018u

Deng, L., and Dhar, B. R. (2023). Phosphorus recovery from wastewater via calcium phosphate precipitation: A critical review of methods, progress, and insights. *Chemosphere* 330, 138685. doi: 10.1016/j.chemosphere.2023.138685

Deng, C., Zeng, N., Li, C., Pang, J., Zhang, N., and Li, B. (2024). Mechanisms of ROS-mediated interactions between *Bacillus aryabhattai* LAD and maize roots to promote plant growth. *BMC Microbiol.* 24, 327. doi: 10.1186/s12866-024-03479-y

Dey, G., Banerjee, P., Sharma, R. K., Maity, J. P., Etesami, H., and Shaw, A. K. (2021). Management of phosphorus in salinity-stressed agriculture for sustainable crop production by salt-tolerant phosphate-solubilizing bacteria—A review. *Agronomy-Basel* 11, 1552. doi: 10.3390/agronomy11081552

Elnahal, A. S., El-Saadony, M. T., Saad, A. M., Desoky, E. S. M., El-Tahan, A. M., Rady, M. M., et al. (2022). The use of microbial inoculants for biological control, plant growth promotion, and sustainable agriculture: A review. *Eur. J. Plant Pathol.* 162, 759–792. doi: 10.1007/s10658-021-02393-7

Fathi, A. (2017). Effect of phosphate solubilization microorganisms and plant growth promoting rhizobacteria on yield and yield components of corn. *Sci. agricul.* 18, 66–69. doi: 10.15192/PSCP.SA.2017.18.3.6669

Firáková, S., Šturdíková, M., and Múčková, M. (2007). Bioactive secondary metabolites produced by microorganisms associated with plants. *Biologia* 62, 251–257. doi: 10.2478/s11756-007

Fleige, S., and Pfaffl, M. W. (2006). RNA integrity and the effect on the real-time qRT-PCR performance. *Mol. Aspects Med.* 27, 126–139. doi: 10.1016/j.mam.2005.12.003

Gastélum, G., Aguirre-von-Wobeser, E., de la Torre, M., and Rocha, J. (2022). Interaction networks reveal highly antagonistic endophytic bacteria in native maize seeds from traditional milpa agroecosystems. *Environ. Microbiol.* 24, 5583–5595. doi: 10.1111/1462-2920

Ge, H.-L., and Zhang, F.-L. (2015). The effects of composite photosynthetic bacterial inoculant PS21 on the biochemical characteristics of wheat seedlings under tetrabromobisphenol A stress. *Biotechnol. Biotec. Eq.* 29, 289–298. doi: 10.1080/13102818.2014.999298

Green, N. L., Euston, S. R., and Rousseau, D. J. C. (2019). Interfacial ordering of tristearin induced by glycerol monooleate and PGPR: A coarse-grained molecular dynamics study. *Colloid. Surface. B.* 179, 107–113. doi: 10.1016/j.colsurfb.2019.03.033

Guo, D.-J., Singh, R. K., Singh, P., Li, D.-P., Sharma, A., Xing, Y.-X., et al. (2020). Complete genome sequence of *Enterobacter roggenkampii* ED5, a nitrogen fixing plant growth promoting endophytic bacterium with biocontrol and stress tolerance properties, isolated from sugarcane root. *Front. Microbiol.* 11. doi: 10.3389/fmicb.2020.580081

Guo, D., Singh, P., Yang, B., Singh, R. K., Verma, K. K., Sharma, A., et al. (2023). Complete genome analysis of sugarcane root associated endophytic diazotroph *Pseudomonas aeruginosa* DJ06 revealing versatile molecular mechanism involved in sugarcane development. *Front. Microbiol.* 14. doi: 10.3389/fmicb.2023.1096754

Gupta, A., Singh, U. B., Sahu, P. K., Paul, S., Kumar, A., Malviya, D., et al. (2022). Linking soil microbial diversity to modern agriculture practices: a review. *Int. J. Env. Res. Pub. He.* 19, 3141. doi: 10.3390/ijerph19053141

Guzmán, Md. P.R., Díaz, I. F. C., and Molina, L. X. Z. (2025). Reflexions on the role, diversity, conservation and management of the genetic microbial resources in Agriculture. *Curr. Res. Microb. Sci.*, 100365. doi: 10.1016/j.crmicr.2025.100365

Hou, Y., Zeng, W., Ao, C., and Huang, J. (2024). Integrative analysis of the transcriptome and metabolome reveals *Bacillus atrophaeus* WZYH01-mediated salt stress mechanism in maize (*Zea mays* L.). *J. Biotechnol.* 383, 39–54. doi: 10.1016/j.jbiotec.2024.02.004

Ingle, K. P., and Padole, D. A. (2017). Phosphate solubilizing microbes: An overview. *Int. J. Curr. Microbiol. Appl. Sci.* 6, 844–852. doi: 10.20546/ijcmas.2017.601.099

Jha, C. K., and Saraf, M. (2015). Plant growth promoting rhizobacteria (PGPR): a review. *J. Agr. Res. Dev.* 5, 108–119. doi: 10.13140/RG.2.1.5171.2164

Johnston, A., and Richards, I. (2003). Effectiveness of different precipitated phosphates as phosphorus sources for plants. *Soil Use Manage.* 19, 45–49. doi: 10.1111/j.1475-2743.2003.tb00278.x

Khan, A. A., Jilani, G., Akhtar, M. S., Naqvi, S. M. S., and Rasheed, M. (2009). Phosphorus solubilizing bacteria: occurrence, mechanisms and their role in crop production. *J. Agric. Biol. Sci.* 1, 48–58.

Ko, W.-H., Tsou, Y.-J., Lin, M.-J., and Chern, L.-L. (2010). Activity and characterization of secondary metabolites produced by a new microorganism for control of plant diseases. *New Biotechnol.* 27, 397–402. doi: 10.1016/j.nbt.2010.05.014

Kranawetter, C., and Sumner, L. W. (2025). Differential root zone secretions and the role of root border cells in rhizosphere manipulation. *Phytochem. Rev.*, 1–20. doi: 10.1007/s11101-025-10084-y

Kruger, N. J., and Von Schaewen, A. (2003). The oxidative pentose phosphate pathway: structure and organisation. *Curr. Opin. Plant Biol.* 6, 236–246. doi: 10.1016/S1369-5266(03)00039-6

Lambers, H. (2022). Phosphorus acquisition and utilization in plants. *Annu. Rev. Plant Biol.* 73, 17–42. doi: 10.1146/annurev-arplant-102720-125738

Li, X., Cai, Q., Yu, T., Li, S., Li, S., Li, Y., et al. (2023c). ZmG6PDH1 in glucose-6-phosphate dehydrogenase family enhances cold stress tolerance in maize. *Front. Plant Sci.* 14. doi: 10.3389/fpls.2023.1116237

Li, Z., Chang, S., Lin, L., Li, Y., and An, Q. (2011). A colorimetric assay of 1-aminocyclopropane-1-carboxylate (ACC) based on ninhydrin reaction for rapid screening of bacteria containing ACC deaminase. *Lett. Appl. Microbiol.* 53, 178–185. doi: 10.1111/j.1472-765X.2011.03088.x

Li, M., Guo, R., Yu, F., Chen, X., Zhao, H., Li, H., et al. (2018). Indole-3-acetic acid biosynthesis pathways in the plant-beneficial bacterium *Arthrobacter pascens* ZZ21. *Int. J. Mol. Sci.* 19, 443. doi: 10.3390/ijms19020443

Li, D., Li, Z., Wu, J., Tang, Z., Xie, F., Chen, D., et al. (2022a). Analysis of outer membrane vesicles indicates that glycerophospholipid metabolism contributes to early symbiosis between *Sinorhizobium fredii* HH103 and soybean. *Mol. Plant Microbe In.* 35, 311–322. doi: 10.1094/MPMI-11-21-0288-R

Li, Y., Liu, X., Hao, T., and Chen, S. (2017). Colonization and maize growth promotion induced by phosphate solubilizing bacterial isolates. *Int. J. Mol. Sci.* 18, 1253. doi: 10.3390/ijms18071253

Li, N., Sheng, K., Zheng, Q., Hu, D., Zhang, L., Wang, J., et al. (2023b). Inoculation with phosphate-solubilizing bacteria alters microbial community and activates soil phosphorus supply to promote maize growth. Land. *Degrad. Dev.* 34, 777–788. doi: 10.1002/ldr.4494

Li, Z., Xu, C., Li, K., Yan, S., Qu, X., and Zhang, J. (2012). Phosphate starvation of maize inhibits lateral root formation and alters gene expression in the lateral root primordium zone. *BMC Plant Biol.* 12, 1–17. doi: 10.1186/1471-2229-12-89

Li, S.-M., Zheng, H.-X., Zhang, X.-S., and Sui, N. (2021). Cytokinins as central regulators during plant growth and stress response. *Plant Cell Rep.* 40, 271–282. doi: 10.1007/s00299-020-02612-1

Li, M., Zhou, J., Lang, X., Han, D., Hu, Y., Ding, Y., et al. (2022b). Integrating transcriptomic and metabolomic analysis in roots of wild soybean seedlings in response to low-phosphorus stress. *Front. Plant Sci.* 13, 1006806. doi: 10.3389/fpls.2022.1006806

Li, M., Zhou, J., Liu, Q., Mao, L., Li, H., Li, S., et al. (2023a). Dynamic variation of nutrient absorption, metabolomic and transcriptomic indexes of soybean (*Glycine max*) seedlings under phosphorus deficiency. *AoB Plants.* 15, plad014. doi: 10.1093/aobpla/plad014

Liu, D. (2021). Root developmental responses to phosphorus nutrition. *J. Integr. Plant Biol.* 63, 1065–1090. doi: 10.1111/jipb.13090

Liu, X., Jiang, X., He, X., Zhao, W., Cao, Y., Guo, T., et al. (2019). Phosphate-solubilizing Pseudomonas sp. strain P34-L promotes wheat growth by colonizing the wheat rhizosphere and improving the wheat root system and soil phosphorus nutritional status. *J. Integr. Plant Biol.* 38, 1314–1324. doi: 10.1007/s00344-019-09935-8

Liu, Y.-Q., Wang, Y.-H., Kong, W.-L., Liu, W.-H., Xie, X.-L., and Wu, X.-Q. (2020). Identification, cloning and expression patterns of the genes related to phosphate solubilization in *Burkholderia multivorans* WS-FJ9 under different soluble phosphate levels. *Amb Express* 10, 1–11. doi: 10.1186/s13568-020-01032-4

Lu, Z., Pan, Z., Chen, L., Chen, S., Tang, J., Cai, N., et al. (2025). Integrating analysis of nutrient elements, endogenous phytohormones, and transcriptomics reveals factors influencing variation of growth in height in *Pinus yunnanensis* Franch. *Plant Physiol. Bioch.*, 109866. doi: 10.1016/j.plaphy.2025.109866

Luziatelli, F., Ficca, A. G., Bonini, P., Muleo, R., Gatti, L., Meneghini, M., et al. (2020). A genetic and metabolomic perspective on the production of indole-3-acetic acid by *Pantoea agglomerans* and use of their metabolites as biostimulants in plant nurseries. *Front. Microbiol.* 11. doi: 10.3389/fmicb.2020.01475

Malhotra, H., Vandana,, Sharma, S., and Pandey, R. (2018). "Phosphorus nutrition: plant growth in response to deficiency and excess," in *Plant Nutrients and Abiotic Stress Tolerance* (Springer, Singapore), 171–190. doi: 10.1007/978-981-10-9044-8_7

Margis, R., Dunand, C., Teixeira, F. K., and Margis-Pinheiro, M. (2008). Glutathione peroxidase family-an evolutionary overview. *FEBS J.* 275, 3959–3970. doi: 10.1111/j.1742-4658.2008.06542.x

Marques, J. M., Mateus, J. R., da Silva, T. F., Couto, C. R. D. A., Blank, A. F., and Seldin, L. (2019). Nitrogen fixing and phosphate mineralizing bacterial communities in sweet potato rhizosphere show a genotype-dependent distribution. *Diversity-Basel* 11, 231. doi: 10.3390/d11120231

Martin, J. A., and Wang, Z. (2011). Next-generation transcriptome assembly. *Nat. Rev. Genet.* 12, 671–682. doi: 10.1038/nrg3068

Meng, J., Zhang, Y., Wang, G., Ji, M., Wang, B., He, G., et al. (2022). Conduction of a chemical structure-guided metabolic phenotype analysis method targeting phenylpropane pathway via LC-MS: *Ginkgo biloba* and soybean as examples. *Food Chem.* 390, 133155. doi: 10.1016/j.foodchem.2022.133155

Milagres, A. M., Machuca, A., and Napoleao, D. (1999). Detection of siderophore production from several fungi and bacteria by a modification of chrome azurol S (CAS) agar plate assay. *J. Microbiol. Meth.* 37, 1–6. doi: 10.1016/S0167-7012(99)00028-7

Mir, A. R., Siddiqui, H., Alam, P., and Hayat, S. (2020). Foliar spray of Auxin/IAA modulates photosynthesis, elemental composition, ROS localization and antioxidant machinery to promote growth of *Brassica juncea*. *Physiol. Mol. Biol. Pla.* 26, 2503–2520. doi: 10.1007/s12298-020-00914-y

Mitra, D., Anđelković, S., Panneerselvam, P., Senapati, A., Vasić, T., Ganeshamurthy, A., et al. (2020). Phosphate-solubilizing microbes and biocontrol agent for plant nutrition and protection: current perspective. *Commun. Soil Sci. Plan.* 51, 645–657. doi: 10.1080/00103624

Mogal, C. S., Jha, S., Suthar, H., Parekh, V., and Rajkumar, B. (2020). Efficiency of Plant Growth Promoting Rhizobacteria (PGPR) consortia for modulation of phytohormone and better nutrient acquisition. *Plantae Scientia*. 3, 20–29. doi: 10.32439/ps.v3i4.20-29

Muro-Villanueva, F., Mao, X., and Chapple, C. (2019). Linking phenylpropanoid metabolism, lignin deposition, and plant growth inhibition. *Curr. Opin. Biotech.* 56, 202–208. doi: 10.1016/j.copbio.2018.12.008

Nephali, L., Moodley, V., Piater, L., Steenkamp, P., Buthelezi, N., Dubery, I., et al. (2021). A metabolomic landscape of maize plants treated with a microbial biostimulant under well-watered and drought conditions. *Front. Plant Sci.* 12. doi: 10.3389/fpls.2021.676632

Olsen, S., Watanabe, F., and Bowman, R. (1983). Evaluation of fertilizer phosphate residues by plant uptake and extractable phosphorus. *Soil Sci. Soc Am. J.* 47, 952–958. doi: 10.2136/sssaj1983.03615995004700050022x

Pal, G., Saxena, S., Kumar, K., Verma, A., Sahu, P. K., Pandey, A., et al. (2022). Endophytic *Burkholderia*: Multifunctional roles in plant growth promotion and stress tolerance. *Microbiol. Res.* 265, 127201. doi: 10.1016/j.micres.2022.127201

Pan, L., and Cai, B. (2023). Phosphate-solubilizing bacteria: advances in their physiology, molecular mechanisms and microbial community effects. *Microorganisms* 11, 2904. doi: 10.3390/microorganisms11122904

Pande, A., Pandey, P., Mehra, S., Singh, M., and Kaushik, S. (2017). Phenotypic and genotypic characterization of phosphate solubilizing bacteria and their efficiency on the growth of maize. *J. Genet. Eng. Biotechn.* 15, 379–391. doi: 10.1016/j.jgeb.2017.06.005

Panhwar, Q. A., Othman, R., Rahman, Z. A., Meon, S., and Ismail, M. R. (2012). Isolation and characterization of phosphate-solubilizing bacteria from aerobic rice. *Afr. J. Biotechnol.* 11, 2711–2719. doi: 10.5897/AJB10.2218

Panhwar, Q., Radziah, O., Zaharah, A. R., Sariah, M., and Razi, I. M. (2011). Role of phosphate solubilizing bacteria on rock phosphate solubility and growth of aerobic rice. *J. Environ. Biol.* 32, 607–612. doi: 10.1007/s11852-010-0106-3

Parray, J. A., Jan, S., Kamili, A. N., Qadri, R. A., Egamberdieva, D., and Ahmad, P. (2016). Current perspectives on plant growth-promoting rhizobacteria. *J. Plant Growth Regul.* 35, 877–902. doi: 10.1007/s00344-016-9583-4

Prabhu, N., Borkar, S., and Garg, S. (2019). Phosphate solubilization by microorganisms: overview, mechanisms, applications and advances. *Adv.bio. Sci. Res.*, 161–176. doi: 10.1016/B978-0-12-817497-5.00011-2

Prager, S.-d., and Cisneros-Rojas, C. A. (2017). Organic acids production by rhizosphere microorganisms isolated from a Typic Melanudands and its effects on the inorganic phosphates solubilization. *Acta Agronómica.* 66, 241–247. doi: 10.15446/acag.v66n2.56148

Preston, G. M., Bertrand, N., and Rainey, P. B. (2001). Type III secretion in plant growth-promoting *Pseudomonas fluorescens* SBW25. *Mol. Microbiol.* 41, 999–1014. doi: 10.1046/j.1365-2958.2001.02560.x

Prijambada, I. D., Widada, J., Kabirun, S., and Widianto, D. (2009). Secretion of organic acids by phosphate solubilizing bacteria. *J. Trop. Soils.* 14, 245–251. doi: 10.5400/jts.2009.v14i3.245-251

Pugin, A., Frachisse, J.-M., Tavernier, E., Bligny, R., Gout, E., Douce, R., et al. (1997). Early events induced by the elicitor cryptogein in tobacco cells: involvement of a plasma membrane NADPH oxidase and activation of glycolysis and the pentose phosphate pathway. *Plant Cell.* 9, 2077–2091. doi: 10.1105/tpc.9.11.2077

Rahman, M. S., Quadir, Q. F., Rahman, A., Asha, M. N., and Chowdhury, M. A. K. F. (2015). Screening and characterization of Phosphorus solubilizing Bacteria and their effect on Rice seedlings. *Res. Agr. Livestock Fisheries.* 1, 27–35. doi: 10.3329/ralf.v1i1.22353

Rawat, P., Das, S., Shankhdhar, D., and Shankhdhar, S. (2021). Phosphate-solubilizing microorganisms: mechanism and their role in phosphate solubilization and uptake. *J. Soil Sci. Plant Nutt.* 21, 49–68. doi: 10.1007/s42729-020-00342-7

Reiter, W.-D., and Vanzin, G. F. (2001). Molecular genetics of nucleotide sugar interconversion pathways in plants. *Plant Cell Walls*, 95–113. doi: 10.1007/978-94-010-0668-2_6

Richardson, A. E., Hocking, P. J., Simpson, R. J., and George, T. S. (2009). Plant mechanisms to optimise access to soil phosphorus. *Crop Pasture Sci.* 60, 124–143. doi: 10.1071/cp07125

Sadiq, H. M., Jahangir, G. Z., Nasir, I. A., Iqtidar, M., and Iqbal, M. (2013). Isolation and characterization of phosphate-solubilizing bacteria from rhizosphere soil. *Biotechnol. Biotec. Eq.* 27, 4248–4255. doi: 10.5504/BBEQ.2013.0091

Sadiq, G., Khan, A. A., Inamullah, A. R., Fayyaz, H., Naz, G., Nawaz, H., et al. (2017). Impact of phosphorus and potassium levels on yield and yield components of maize. *Pure Appl. Biol.* 6, 1071–1078. doi: 10.19045/bspab.2017.600114

Saeid, A., Prochownik, E., and Dobrowolska-Iwanek, J. (2018). Phosphorus solubilization by *Bacillus* species. *Molecules* 23, 2897. doi: 10.3390/molecules23112897

Santhoshkumar, R., Parvathy, A. H., and Soniya, E. (2025). Modifications in Metabolomic Profile of *Andrographis paniculata* by Arsenic Tolerance *Herbaspirillum* sp.: Perception into Plant–Microbe Interactions. *J. Plant Growth Regul.*, 1–17. doi: 10.1007/s00344-025-11639-1

Schäfer, M., Brütting, C., Meza-Canales, I. D., Großkinsky, D. K., Vankova, R., Baldwin, I. T., et al. (2015). The role of cis-zeatin-type cytokinins in plant growth regulation and mediating responses to environmental interactions. *J. Exp. Bot.* 66, 4873–4884. doi: 10.1093/jxb/erv214

Seifert, G. J. (2004). Nucleotide sugar interconversions and cell wall biosynthesis: how to bring the inside to the outside. *Curr. Opin. Plant Biol.* 7, 277–284. doi: 10.1016/j.pbi.2004.03.004

Sekhar, M., Singh, V., Madhu, M., and Khan, W. (2020). Response of different levels of nitrogen, potassium and PSB on growth and yield attributes of greengram (*Vigna radiata* L.). *Int. J. Chem. St.* 8, 6–9. doi: 10.22271/chemi.2020.v8.i3a.9456

Sengupta, A., and Gunri, S. K. (2015). Microbial intervention in agriculture: an overview. *Afr. J. Microbiol. Res.* 9, 1215–1226. doi: 10.5897/AJMR2014.7325

Sharma, I. P., and Sharma, A. (2019). Mycorrhizal colonization and phosphorus uptake in presence of PGPRs along with nematode infection. *Symbiosis* 77, 185–187. doi: 10.1007/s13199-018-0576-x

Shome, S., Barman, A., and Solaiman, Z. M. (2022). Rhizobium and phosphate solubilizing bacteria influence the soil nutrient availability, growth, yield, and quality of soybean. *Agriculture-Basel* 12, 1136. doi: 10.3390/agriculture12081136

Soares, A. S., Nascimento, V. L., De Oliveira, E. E., Jumbo, L. V., Dos Santos, G. R., Queiroz, L. L., et al. (2023). *Pseudomonas aeruginosa* and *Bacillus cereus* isolated from Brazilian Cerrado soil act as phosphate-solubilizing bacteria. *Curr. Microbiol.* 80, 146. doi: 10.1007/s00284-023-03260-w

Spielbauer, G., Li, L., Römisch-Margl, L., Do, P. T., Fouquet, R., Fernie, A. R., et al. (2013). Chloroplast-localized 6-phosphogluconate dehydrogenase is critical for maize endosperm starch accumulation. *J. Exp. Bot.* 64, 2231–2242. doi: 10.1093/jxb/ert082

Stringlis, I. A., Zamioudis, C., Berendsen, R. L., Bakker, P. A., and Pieterse, C. M. (2019). Type III secretion system of beneficial rhizobacteria *Pseudomonas simiae* WCS417 and *Pseudomonas defensor* WCS374. *Front. Microbiol.* 10. doi: 10.3389/fmicb.2019.01631

Sundara, B., Natarajan, V., and Hari, K. (2002). Influence of phosphorus solubilizing bacteria on the changes in soil available phosphorus and sugarcane and sugar yields. *Field Crop Res.* 77, 43–49. doi: 10.1016/S0378-4290(02)00048-5

Swartzberg, D., Hanael, R., and Granot, D. (2011). Relationship between hexokinase and cytokinin in the regulation of leaf senescence and seed germination. *Plant Biol.* 13, 439–444. doi: 10.1111/j.1438-8677.2010.00376.x

Tang, A., Haruna, A. O., Majid, N. M. A., and Jalloh, M. B. (2020). Effects of selected functional bacteria on maize growth and nutrient use efficiency. *Microorganisms* 8, 854. doi: 10.3390/microorganisms8060854

Tohge, T., Watanabe, M., Hoefgen, R., and Fernie, A. R. (2013). The evolution of phenylpropanoid metabolism in the green lineage. *Crit. Rev. Biochem. Mol.* 48, 123–152. doi: 10.3109/10409238.2012.758083

Vassilev, N., Eichler-Löbermann, B., and Vassileva, M. (2012). Stress-tolerant P-solubilizing microorganisms. *Appl. Microbiol. Biot.* 95, 851–859. doi: 10.1007/s00253-012-4224-8

Vassilev, N., Vassileva, M., and Nikolaeva, I. (2006). Simultaneous P-solubilizing and biocontrol activity of microorganisms: potentials and future trends. *Appl. Microbiol. Biot.* 71, 137–144. doi: 10.1007/s00253-006-0380-z

Velmourougane, K., Prasanna, R., and Saxena, A. K. (2017). Agriculturally important microbial biofilms: present status and future prospects. *J. Basic. Microb.* 57, 548–573. doi: 10.1002/jobm.201700046

Verma, S. K., Sahu, P. K., Kumar, K., Pal, G., Gond, S. K., Kharwar, R. N., et al. (2021). Endophyte roles in nutrient acquisition, root system architecture development and oxidative stress tolerance. *J. Appl. Microbiol.* 131, 2161–2177. doi: 10.1111/jam.15111

Victor Roch, G., Maharajan, T., Ceasar, S. A., and Ignacimuthu, S. (2019). The role of PHT1 family transporters in the acquisition and redistribution of phosphorus in plants. *Crit. Rev. Plant Sci.* 38, 171–198. doi: 10.1080/07352689.2019.1645402

Vincze, É., Becze, A., Laslo, É., and Mara, G. (2024). Beneficial soil microbiomes and their potential role in plant growth and soil fertility. *Agriculture-Basel* 14, 152. doi: 10.3390/agriculture14010152

Vyas, P., and Gulati, A. (2009). Organic acid production *in vitro* and plant growth promotion in maize under controlled environment by phosphate-solubilizing fluorescent *Pseudomonas*. *Bmc. Microbiol.* 9, 1–15. doi: 10.1186/1471-2180-9-174

Wang, Z., Zhang, H., Liu, L., Li, S., Xie, J., Xue, X., et al. (2022). Screening of phosphate-solubilizing bacteria and their abilities of phosphorus solubilization and wheat growth promotion. *Bmc. Microbiol.* 22, 296. doi: 10.1186/s12866-022-02715-7

Wang, Y. B., Zou, Y. L., Wei, Y. T., and Meng, L. S. (2025). Crosstalk between ethylene and JA/ABA/sugar signalling in plants under physiological and stress conditions. *Mol. Plant Pathol.* 26, e70048. doi: 10.1111/mpp.70048

Wu, R., Qian, C., Yang, Y., Liu, Y., Xu, L., Zhang, W., et al. (2024). Integrative transcriptomic and metabolomic analyses reveal the phenylpropanoid and flavonoid biosynthesis of Prunus mume. *J. Plant Res.* 137, 95–109. doi: 10.1007/s10265-023-01500-5

Wurtele, E. S., and Nikolau, B. J. (1986). Enzymes of glucose oxidation in leaf tissues: the distribution of the enzymes of glycolysis and the oxidative pentose phosphate pathway between epidermal and mesophyll tissues of C3-plants and epidermal, mesophyll, and bundle sheath tissues of C4-plants. *Plant Physiol.* 82, 503–510. doi: 10.1104/pp.82.2.503

Xia, J., Nan, L., Wang, K., and Yao, Y. (2024). Comprehensive dissection of metabolites in response to low phosphorus stress in different root-type alfalfa at seedling stage. *Agronomy-Basel* 14, 1697. doi: 10.3390/agronomy14081697

Yahya, M., Islam, E. U., Rasul, M., Farooq, I., Mahreen, N., Tawab, A., et al. (2021). Differential root exudation and architecture for improved growth of wheat mediated by phosphate solubilizing bacteria. *Front. Microbiol.* 12. doi: 10.3389/fmicb.2021.744094

Yang, Y., Saand, M. A., Huang, L., Abdelaal, W. B., Zhang, J., Wu, Y., et al. (2021). Applications of multi-omics technologies for crop improvement. *Front. Plant Sci.* 12. doi: 10.3389/fpls.2021.563953

Yoo, J. Y., Ko, K. S., Vu, B. N., Lee, Y. E., Yoon, S. H., Pham, T. T., et al. (2021). N-acetylglucosaminyltransferase II is involved in plant growth and development under stress conditions. *Front. Plant Sci.* 12, 761064. doi: 10.3389/fpls.2021.761064

You, M., Fang, S., MacDonald, J., Xu, J., and Yuan, Z.-C. (2020). Isolation and characterization of *Burkholderia cenocepacia* CR318, a phosphate solubilizing bacterium promoting corn growth. *Microbiol. Res.* 233, 126395. doi: 10.1016/j.micres.2019.126395

Zhang, L., Fan, J., Ding, X., He, X., Zhang, F., and Feng, G. (2014). Hyphosphere interactions between an arbuscular mycorrhizal fungus and a phosphate solubilizing bacterium promote phytate mineralization in soil. *Soil Biol. Biochem.* 74, 177–183. doi: 10.1016/j.soilbio.2014.03.004

Zhang, Q., Tian, S., Chen, G., Tang, Q., Zhang, Y., Fleming, A. J., et al. (2024). Regulatory NADH dehydrogenase-like complex optimizes C4 photosynthetic carbon flow and cellular redox in maize. *New Phytol.* 241, 82–101. doi: 10.1111/nph.19332

Zhang, H., Zhang, J., Xu, Q., Wang, D., Di, H., Huang, J., et al. (2020). Identification of candidate tolerance genes to low-temperature during maize germination by GWAS and RNA-seq approaches. *BMC Plant Biol.* 20, 333. doi: 10.1186/s12870-020-02543-9

Zhao, R., He, F., Huang, W., Zhou, Y., Zhou, J., Chen, Q., et al. (2024). Dicranopteris dichotoma rhizosphere-derived Bacillus sp. MQB12 acts as an enhancer of plant growth via increasing phosphorus utilization, hormone synthesis, and rhizosphere microbial abundance. *Chem. Biol. Technol. Ag.*, 11. doi: 10.1186/s40538-024-00648-z

Zhao, K., Penttinen, P., Zhang, X., Ao, X., Liu, M., Yu, X. M., et al. (2014). Maize rhizosphere in Sichuan, China, hosts plant growth promoting *Burkholderia cepacia* with phosphate solubilizing and antifungal abilities. *Microbiol. Res.* 169, 76–82. doi: 10.1016/j.micres.2013.07.003

frontiers | Frontiers in Plant Science

TYPE Original Research
PUBLISHED 28 August 2025
DOI 10.3389/fpls.2025.1560550

OPEN ACCESS

EDITED BY
Manoj Kumar Solanki,
University of Silesia in Katowice, Poland

REVIEWED BY
Sami Abou Fayssal,
University of Forestry, Sofia, Bulgaria
Enrica Allevato,
University of Ferrara, Italy

*CORRESPONDENCE
Shuizhi Yang
yxz1967@sina.com
Binbin Huang
1049351830@qq.com

RECEIVED 17 January 2025
ACCEPTED 28 July 2025
PUBLISHED 28 August 2025

CITATION
Deng S, Huang B, Zeng B, Cao S, Gong B, Liao W, Zhang W, Luo S and Yang S (2025) Soybean green manure intercropping improves citrus quality by improving soil quality and altering microbial communities. *Front. Plant Sci.* 16:1560550. doi: 10.3389/fpls.2025.1560550

Soybean green manure intercropping improves citrus quality by improving soil quality and altering microbial communities

Sufeng Deng[1], Binbin Huang[2]*, Bin Zeng[1], Sheng Cao[1], Biya Gong[1], Wei Liao[1], Wen Zhang[1], Sainan Luo[1] and Shuizhi Yang[1]*

[1]Hunan Horticultural Research Institute, Yuelushan Laboratory, Changsha, China, [2]Hunan Provincial Engineering and Technology Research Center for Agricultural Microbiology Application, Hunan Institute of Microbiology, Yuelushan Laboratory, Changsha, China

Introduction: Intercropping leguminous green manure in orchards represents a widely adopted agroecological practice that concurrently influences soil physicochemical properties, microbial communities, and crop performance. However, the temporal mechanisms by which different durations of soybean green manure (SGM) intercropping regulate soil-plant-microbe interactions remain insufficiently understood. This study elucidates the impact of SGM intercropping duration on ecosystem functionality in citrus orchards.

Methods: A multi-year field experiment compared SGM intercropping durations (0-, 1-, and 2-year treatments). We assessed citrus fruit quality parameters (total soluble solids, TSS; sugar-acid ratio, TSS/TA) and soil properties (pH, available nitrogen, total nitrogen, available phosphorus, available potassium, and organic matter). Microbial community structure was analyzed via high-throughput sequencing. Spearman correlation analysis ($|\rho| \geq 0.8$, $p < 0.05$) delineated networks among intercropping duration, soil parameters, keystone microbial taxa (e.g., Proteobacteria, Acidobacteriota, Ascomycota), and fruit quality indicators.

Results: The two-year intercropping treatment (T2) significantly enhanced fruit quality: TSS increased by 11.66% and the sugar-acid ratio (TSS/TA) by 41.95% ($p < 0.05$). Soil properties improved markedly: pH rose by 0.42 units, while AN, TN, AP, AK, and OM increased by 41.80%, 9.15%, 16.78%, 100.50%, and 79.53%, respectively ($p < 0.05$). Microbial communities underwent structural reorganization, exhibiting increased α-diversity, enhanced network complexity, and selective enrichment of beneficial taxa including Actinobacteria, Mortierellales, and Ascomycota. Correlation networks revealed significant associations among intercropping duration, soil parameters, keystone microbes, and fruit quality.

Discussion: This study demonstrates that SGM intercropping enhances fruit quality through dual mechanisms: (1) amelioration of soil properties (pH elevation and improved nutrient availability), and (2) functional restructuring of

microbial communities. Notably, specific taxa such as Actinobacteria play pivotal roles in nutrient cycling. Our findings provide empirical evidence for microbiome-mediated optimization of soil functionality, offering a sustainable rehabilitation strategy for degraded orchards and reinforcing the scientific value of ecological intensification in perennial cropping systems.

KEYWORDS

soybean green manure (SGM) intercropping, citrus quality, soil quality, soil microbial communities, community diversity, keystone microbial taxa

Highlights

- Intercropping soybean green manure (SGM) enhanced the soil pH, organic matter content, and available nitrogen, available phosphorus, and available potassium concentrations.
- Intercropping SGM altered the soil microbial community composition and diversity, reconstructed co-occurrence networks, and enriched beneficial microbial taxa including *Actinobacteria*, *Proteobacteria*, *Ascomycota*, and *Mortierellales*.
- Intercropping SGM improved the citrus fruit quality, significantly increasing total soluble solid content (TSS) and TSS/titratable acidity ratio (TSS/TA).
- Citrus fruit quality exhibited strong correlations with intercropping duration (years), soil physicoproperties, and soil microbial community characteristics (diversity and specific microbial taxa).
- Intercropping SGM in orchards critically enhanced the soil quality and crop productivity, advancing sustainable agricultural practices.

1 Introduction

Citrus represents a significant economic fruit crop extensively cultivated in China, with documented planting areas and yields reaching 2.67 million hectares and over 600 million tonnes, respectively, in 2023 (Shen et al., 2024; National Bureau of Statistics of China, 2025). As a principal cultivar, navel orange (*C. sinensis* Osbeck) dominates production across key provinces including Jiangxi, Sichuan, Hubei, and Hunan (Yao et al., 2022; National Bureau of Statistics of China, 2025). Critical determinants of fresh fruit quality and commercial value encompass total soluble solids content (TSS), titratable acidity (TA), and sugar–acid ratio (TSS/TA) (Yu et al., 2015; Wu et al., 2021; Guo et al., 2023). The sensory quality and market value of navel oranges are largely determined by their TSS, TA, and TSS/TA, which collectively contribute to a balanced sweet–tart flavor profile. However, the accumulation of soluble sugars and total soluble solids (TSS) and the conversion of titratable acidity (TA) in fresh fruits are influenced by numerous factors, including the genetic characteristics of fruit trees, environmental variables (climate and soil conditions), and agricultural management practices (intercropping, crop rotation, no-till farming, and fertilization) as well as the timing of harvest (Li and Wan, 2006; Li C. et al., 2023; Yu et al., 2024). Intercropping has emerged as an efficacious approach for fostering the sustainable development of orchards and woodlands. This practice not only aids in minimizing the reliance on chemical fertilizers but also enhances crop yield and quality while simultaneously preserving the soil ecosystem (Li et al., 2020; Dong et al., 2021). The soil environment holds a pivotal position in determining the quality and productivity of orchards and woodlands, encompassing both the physical and chemical characteristics of the soil and the functional dynamics of the soil microbial community (Dong et al., 2021; Fu et al., 2023; Li C. et al., 2023).

Intercropping, a cornerstone of traditional Chinese agriculture with a history spanning over 2,000 years, has garnered significant attention due to its myriad benefits. These include mitigating crop competition for land, enhancing land utilization, stabilizing and augmenting yields per unit area, diminishing pest and disease issues, reducing agrochemical reliance, and fostering biodiversity (Li C. et al., 2023; Duan et al., 2024; Qin et al., 2024). Recently, the advancement and dissemination of modern orchard cultivation practices centered on wide-row, dense planting, mechanization, and intelligent, labor-saving technologies for citrus and other fruits in China have created conducive environments for orchard and woodland intercropping (Qin et al., 2024). Extensive literature attests to the prevalent practice of intercropping leguminous green manure in soil ecosystems, including farmland, orchards, and woodlands (Wang T. et al., 2022; Duan et al., 2024; Qin et al., 2024). Soybean and other leguminous crops, noted for their nitrogen-fixing capabilities, ease of cultivation, and management, are frequently employed as green manure or intercrops for balanced fertilization and soil amelioration (Jing et al., 2022; Yu et al., 2025). Research indicates that intercropping leguminous green manure in tea plantation woodlands alters the soil bacterial community, influencing amino acid metabolism and flavonoid biosynthesis, ultimately enhancing tea quality (Wang T. et al., 2022; Duan et al., 2024; Yu et al., 2025). This practice also modulated soil

physicochemical properties, boosted soil nutrient metabolism, and improved soil quality. Furthermore, soil microorganisms serve as vital bio-indicators reflecting soil health, plant growth, and development. They participated in nutrient cycling and impacted crop resistance to disease and stress, which was pivotal for fostering healthy crop growth, sustainable agricultural development, and ecosystem stability (Jing et al., 2022; Li C. et al., 2023). The structure and function of soil microbial communities were comprehensively influenced by soil properties, the soil environment, and agronomic practices (Jing et al., 2022; Wang T. et al., 2022; Duan et al., 2024; Yu et al., 2025). Studies highlighted the crucial role of soil fungal communities in regulating ecosystem services related to soil fertility, while bacterial communities were intimately linked to plant growth and soil properties (Read and Perez, 2003; Kyaschenko et al., 2017).

TCurrently, despite the fact that the utilization of chemical fertilizers can sustain the productivity of citrus navel orange orchards, the prolonged and excessive application of these fertilizers in orchards with acidified soils adversely affects the physicochemical properties of orchard soils, soil pH, and soil microbial communities (Lin et al., 2019; Wang Z. et al., 2022; Raiesi et al., 2024). Such practices are unsustainable for long-term development. To mitigate these issues, studies on intercropping leguminous green manures in orchards or woodlands have demonstrated that this practice can enrich soil nutrients, modulate soil properties and microbial communities, and enhance crop yield and quality (Wang T. et al., 2022; Wang Z. et al., 2022; Duan et al., 2024; Raiesi et al., 2024; Yu et al., 2025). Consequently, this study examined the effects of intercropping soybean green manure (SGM) in citrus orchards on orchard ecological functions (fruit yield and quality) and orchard soil ecosystems (soil properties, soil microbial communities) over different durations (0, 1, and 2 years). Additionally, the study evaluated the correlations between intercropping duration, citrus yield and quality, soil properties, and soil microbial communities. Ultimately, it is anticipated that the findings of this research will furnish theoretical backing for the establishment of a green manure model aimed at intercropping soybean in citrus orchards located in acid soil regions.

2 Materials and methods

2.1 Site description and experimental design

TThe citrus orchard experiment was situated in Houjiawan Village, Yongding District, Zhangjiajie City, Hunan Province, China (110°42′ E, 29°11′ N), within a subtropical mountain monsoon humid climate zone characterized by an average annual sunshine duration of 1,440 h, a mean temperature of 17°C, annual precipitation of 1,400 mm, and a frost-free period of 216–269 days. The gently sloping and flat orchard covered approximately 2 ha of uniform acidic brown soil, with 6-year-old Newhall navel orange trees (2022) spaced at 3 m × 4 m (row spacing). The experimental groups included T0 (control, no SGM intercropping or tillage in 2021–2022), T1 (no treatment in 2021, soybean intercropping and tillage in 2022), and T2 (two consecutive years of soybean intercropping and tillage in 2021 and 2022), each comprising five replicate plots of 20 trees (four rows × five trees/row) separated by two buffer tree rows to minimize cross-plot interference. Quarterly weed mowing was implemented, while the citrus trees received annual fertilization in April with 10 kg of organic fertilizer (2.5% N, 2.0% P_2O_5, 2.8% K_2O) and 2 kg of compound fertilizer (15-15-15, N–P_2O_5–K_2O) per tree, applied to 30-cm-deep furrows aligned with drip lines; for the soybean (*Glycine max L.* cv. Xiangchun 24) intercropping system, six rows were planted in 1.5-m-wide strips between citrus rows in March without supplemental fertilization, with residues mechanically processed into 3–5-cm segments and incorporated into topsoil (0–20-cm depth) via rotary tiller after fresh pod harvest in late July.

2.2 Soil sampling and DNA sequencing

On November 12, 2022 (fruit harvest date), soil samples were randomly collected from five points in each of the five experimental fields per treatment (totaling 15 samples), following modified protocols from Zhou et al. (2021) and Wu et al. (2024). The sampling avoided treatment edges and fertilizer application zones, specifically targeting the 5–15-cm depth within the 5–20-cm soil layer where citrus roots and soybean residues interact. All samples were immediately transported to the laboratory, where each was divided: one portion preserved for DNA extraction and sequencing, while the other was air-dried for physicochemical analysis.

TMicrobial DNA was extracted from soil samples using the E.Z.N.A.® Soil DNA Kit (Omega Bio-tek, Norcross, GA, USA) following the manufacturer's protocols. PCR amplification was conducted using the Takara ExTaq PCR kit (Takara Shuzo, Osaka, Japan) with specific primers: 338F (5′-ACTCCTACGGGAGGCAGCAG-3′) and 806R (5′-GGACTACHVGGGTWTCTAAT-3′) for bacterial 16S rRNA V3–V4 regions and ITS1F (5′-CTTGGTCATTTAGAGGAAGTAA-3′) and ITS2R (5′-GCTGCGTTCTTCATCGATGC-3′) for fungal ITS regions. The thermal cycling protocol consisted of initial denaturation at 95°C for 2 min, followed by 25 cycles of 95°C for 30 s, 55°C for 30 s, and 72°C for 30 s, with a final extension at 72°C for 10 min. PCR products were verified by 2% agarose gel electrophoresis, purified using a gel recovery kit, and sequenced on an Illumina MiSeq platform (Novogene, Beijing). The raw sequencing data were deposited in the NCBI Sequence Read Archive (accession: PRJNA957046).

2.3 Fruit yield and quality evaluation

At the stage of edible maturity (November 12), fruit sampling was performed using a stratified protocol: five fruits were randomly collected from different crown aspects of each tree, with three trees randomly selected per plot, yielding 15 fruits per plot across four replicate plots per treatment group, thus totaling 60 fruits per treatment. The yield and quality parameters of citrus were determined according to GB/T 12947-2008 (Fresh Citrus Fruits:

National Standards Information Public Service Platform) (China National Standardization Administration Committee, 2008) as briefly described below: single fruit weight (SFW) was directly measured using an electronic balance; yield per tree (YPT) was calculated by multiplying the mean SFW by the total fruit count per tree (field-recorded); and for quality assessment, 15 fruits per plot were pooled, peeled, and juiced with a mechanical extractor. Total soluble solids (TSS), expressed as a percentage (%) and representing water-soluble components (sugars, acids, vitamins, minerals), were measured using a handheld refractometer (PAL-BXIACID1, 0%–90%; Atago Co., Japan); titratable acidity (TA), quantifying total organic acids in the juice, was determined via the refractometer's acid titration mode; and the TSS/TA ratio was derived from the relative proportion of soluble solids to organic acids.

2.4 Analysis of soil physicochemical properties

The determination of soil chemical properties followed the procedures described in Soil Agrochemical Analysis edited by Bao SD (Bao, 2000), detailed as follows: Soil pH was measured using a pH meter with a soil-to-deionized water ratio of 1:2.5 (w/v). Organic matter content was determined via the potassium dichromate–sulfuric acid oxidation method. Total nitrogen was quantified using the Kjeldahl method, total potassium by flame photometry, and total phosphorus by molybdenum blue colorimetry. For available nutrients, alkali-hydrolyzable nitrogen was measured using the alkaline hydrolysis diffusion method, available potassium via neutral ammonium acetate extraction–flame photometry, and available phosphorus through sodium bicarbonate extraction–molybdenum antimony resistance colorimetry.

2.5 Soil microbial community analysis

The bioinformatics analysis of high-throughput sequencing results was performed following the methods described by Zhou et al. (2021) and Wu et al. (2024). Briefly, raw data were cleaned to remove assembly artifacts and then compared against the SILVA Database v138.1 and UNITE v7.2 Database for species annotation of bacteria and fungi, respectively. These results were further utilized for downstream analysis. Linear discriminant analysis effect size (LEfSe) with a linear discriminant analysis (LDA) threshold of 4.0 was employed to identify genus-specific microbes in each group. Phylogenetic tree diagrams were used to visualize differences in microbial communities from the phylum to species level. All of these data analyses were performed online on the NovoCloud Platform (https://magic.novogene.com) for both analysis and visualization.

2.6 Co-occurrence network analysis

The co-occurrence network analysis based on Spearman's correlation matrix was conducted using the "Hmisc" package (version 5.2.3) (Harrell, 2019) in R software. To ensure accuracy, amplicon sequence variants (ASVs) present in at least three subsamples within each group and with relative abundances >0.1% were included in the analysis. The results were filtered using thresholds of $|\rho|$ >0.8 and p <0.05. Network visualization was performed in Gephi (V0.9.2) (Bastian et al., 2009) with the Fruchterman Reingold layout and network topological parameters, which included nodes, edges, positive edges, negative edges, average degree, average clustering coefficient, and average path length, were calculated in Gephi.

2.7 Statistical analysis

Data processing was conducted using Excel 2020 software, with values in tables presented as means ± standard error. To analyze significant differences in soil properties and alpha diversity indices among all treatment groups, one-way analysis of variance (ANOVA) combined with Duncan's multiple-range test was employed. Statistical significance was determined at p-values <0.05. Additionally, analysis of similarity (ANOSIM) was performed to ascertain whether intergroup differences were significantly greater than intragroup variations. Venn diagrams were constructed using the R package "ggvenn" (version 0.1.9); note that a previous mention of "vegan" for this purpose was incorrect. Bacterial diversity analysis was facilitated by the R package "tidyverse" (version 2.0.0). Correlation analysis was carried out using the R package "Hmisc" (version 5.2.3), with subsequent network visualization performed in Cytoscape (version 3.5.0). Other data analyses and visualizations, including histograms of community composition, were executed on the Novogene Cloud Platform (https://magic.novogene.com).

3 Results

3.1 Citrus yield and quality

The effects of intercropping SGM with different years on citrus yield and quality parameters are presented in Table 1. As the years of intercropping SGM increase (0–2 years), the citrus trees showed progressive increases in yield per tree (YPT), single fruit weight (SFW), total soluble solids (TSS), and TSS/titratable acidity (TSS/TA) ratio. Conversely, titratable acidity (TA) exhibited a gradual decline. Crucially, significant improvements (p < 0.05) in fruit quality were observed exclusively for TSS and TSS/TA following 2 years of SGM intercropping (T2) that fruit TSS increased by 11.66% from 11.97% (T0) to 13.37% (T2) and TSS/TA rose markedly by 41.95% from 15.59 (T0) to 22.12 (T2). Although the YPT, SFW, and TA showed favorable directional changes (increases for YPT/SFW, decrease for TA), these alterations failed to reach statistical significance. So, the results indicate that intercropping SGM enhanced citrus fruit quality, with the most pronounced improvements in TSS and TSS/TA occurring specifically after 2 years of implementation (T2).

TABLE 1 Effect of SGM intercropping with different years on citrus yield and quality.

Treatments	Yield		Quality		
	Yield per tree (YPT), kg	Single fruit weight (SFW), g	Total soluble solid (TSS), %	Total acid (TA)	Solid–acid ratio (TSS/TA)
T0	27.79 ± 1.69 a	158.91 ± 7.37 a	11.97 ± 0.43 b	0.73 ± 0.08 a	15.59 ± 1.16 b
T1	28.90 ± 1.20 a	164.58 ± 7.54 a	12.61 ± 0.81 ab	0.70 ± 0.02 a	18.23 ± 1.26 b
T2	29.98 ± 2.08 a	167.79 ± 7.64 a	13.37 ± 0.56 a	0.66 ± 0.05 a	22.12 ± 3.79 a

The data shown are mean ± standard error. The lowercase letters denote significant differences between treatments as determined by Duncan's tests ($p < 0.05$).

3.2 Soil physicochemical properties

As shown in Table 2, intercropping SGM in citrus orchards differentially impacted soil physicochemical properties across treatment durations (0–2 years). The orchard soils exhibited acidity, with pH values ranging from 5.11 to 5.53. With increasing intercropping duration, significant enhancements ($p < 0.05$) were observed in soil pH, available nitrogen (AN), total nitrogen (TN), available phosphorus (AP), available potassium (AK), and organic matter (OM) content. However, no significant differences occurred in total phosphorus (TP) or total potassium (TK). Notably, at 1 year of SGM intercropping treatment (T1), significant increases ($p < 0.05$) were observed in soil pH (+0.26 units), available nitrogen (AN, +17.42%), available phosphorus (AP, +13.86%), available potassium (AK, +62.75%), and organic matter (OM, +28.52%). After 2 years of treatment (T2), further significant enhancements occurred in soil pH (+0.16 units), AN (+20.77%), AK (+23.20%), and OM (+39.69%). Cumulatively, the T2 treatment significantly improved the soil pH (+0.42 units), AN (+41.80%), total nitrogen (N, +9.15%), AP (+16.78%), AK (+100.50%), and OM (+79.53%) compared with the control (T0) ($p < 0.05$). Thus, SGM intercropping improved the soil physicochemical properties in citrus orchards, with particularly significant enhancements in soil pH and fertility indicators (AN, AK, AP, TN, OM) following 2 years of implementation.

3.3 Soil microbial composition and diversity

3.3.1 Soil microbial composition

A total of 1,168,771 and 1,068,647 high-quality bacterial and fungal sequences were obtained after sequencing and quality control, respectively. There were 59,960–72,770 and 55,850–83,106 valid reads obtained in bacterial and fungal ASVs, respectively. The corresponding rarefaction curves tended to nearly saturate at the selected sequencing depth (47,940 and 48,772 bacterial and fungal valid reads ASVs, respectively; Supplementary Figures S1, S2; Supplementary Tables S1, S2).

Among three different treatments, the dominant phyla (abundance in top 10) of soil bacterial communities (Figure 1a; Supplementary Table S3) were *Acidobacteriota* (34.03%–42.81%), *Proteobacteria* (28.54%–34.90%), *Chloroflexi* (6.52%–7.75%), *Actinobacteriota* (5.22%–7.29%), *Gemmatimonadota* (2.98%–3.80%), *Bacteroidota* (1.45%–2.48%), *Crenarchaeota* (1.41%–2.55%), *Myxococcota* (1.44%–1.92%), *Verrucomicrobiota* (1.30%–1.49%), and *WPS-2* (1.03%–1.41%). Soil fungal communities (Figure 1a; Supplementary Table S4) were dominated by *Ascomycota* (34.92%–72.71%), *Mortierellomycota* (2.95%–18.16%), *Basidiomycota* (4.75%–9.30%), *Rozellomycota* (0.11%–0.61%), *Kickxellomycota* (0.04%–0.32%), *Chytridiomycota* (0.06%–0.32%), *Mucoromycota* (0.08%–0.09%), *Glomeromycota* (0.02%–0.11%), *Zoopagomycota* (0.00%–0.01%), and *Aphelidiomycota* (0.00%–0.01%). The Venn analysis of soil microbial communities (Figure 1b; Supplementary Table S5) revealed that intercropping SGM (T1, T2) increased the number of ASVs in both bacterial and fungal communities compared to the control (T0). However, after 2 years of SGM intercropping (T2), the ASV richness of soil bacterial and fungal communities declined relative to T1, and it was still higher than in T0. A principal coordinates analysis (PCoA) of soil microbial β-diversity based on weighted UniFrac distances revealed distinct separation between T0 (control) and T2 (2-year SGM intercropping) treatments (Figure 1d). However, partial overlap persisted between T1 (1-year SGM intercropping) and both T0 and T2 groups, indicating incomplete community differentiation. The

TABLE 2 Effect of SGM intercropping with different years of treatment on soil properties.

Treatments	pH	Available nitrogen (AN)	Nitrogen (N)	Available phosphorus (AP)	Phosphorus (P)	Available potassium (AK)	Potassium (K)	Organic matter (OM)
		mg/kg	g/kg	mg/kg	g/kg	mg/kg	g/kg	g/kg
T0	5.11 ± 0.01 c	97.6 ± 8.85 c	1.53 ± 0.07 b	28.78 ± 0.26 b	2.11 ± 0.19 a	80.0 ± 14.76 c	13.20 ± 0.8 a	20.86 ± 2.7 c
T1	5.37 ± 0.03 b	114.6 ± 8.96 b	1.60 ± 0.05 ab	32.77 ± 1.51 a	2.10 ± 0.09 a	130.2 ± 7.33 b	12.92 ± 0.53 a	26.81 ± 4.05 b
T2	5.53 ± 0.02 a	138.4 ± 9.69 a	1.67 ± 0.09 a	33.61 ± 0.76 a	2.14 ± 0.07 a	160.4 ± 11.04 a	13.86 ± 0.76 a	37.45 ± 3.28 a

The data shown are mean ± standard error. The lowercase letters denote significant differences between treatments as determined by Duncan's tests ($p < 0.05$).

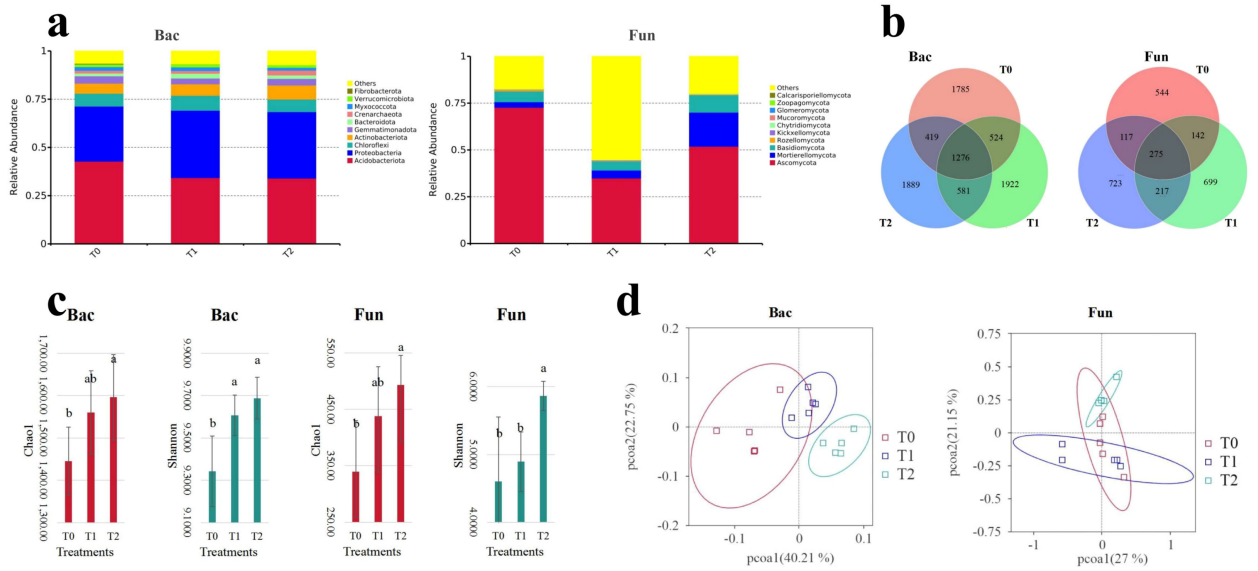

FIGURE 1
Soil bacteria (Bac) and fungal (Fun) communities of the top 10 phyla: relative abundance **(a)**, Veen analysis **(b)**, principal coordinate analysis **(c)**, and alpha-diversity **(d)**.

cumulative explanatory power of the first two principal coordinates (PCo1 + PCo2) approached or exceeded 50% of total variation, accounting for 62.96% (bacteria: 40.21% + 22.75%) and 48.15% (fungi: 27.00% + 21.15%) in bacterial and fungal communities, respectively. All of these findings demonstrate that SGM intercropping restructures soil microbial composition, with significantly more pronounced shifts in both bacterial and fungal community architecture following a 2-year implementation.

3.3.2 Soil microbial alpha diversity

Analyses of α-diversity indices (Chao1, observed species, Simpson, and Shannon) for soil bacterial and fungal communities revealed consistent increases under SGM intercropping treatments (T1, T2) compared to the monoculture control (T0) (Figure 1c; Supplementary Table S6). Notably, the T2 treatment (2-year intercropping) induced significant elevations ($p < 0.05$) in both Chao1 and Shannon indices for soil bacterial and fungal communities. In contrast, only the Simpson index of bacterial communities exhibited a significant enhancement ($p < 0.05$) following a 1-year intercropping (T1). Thus, intercropping SGM in citrus orchards enhanced the alpha diversity indices of soil bacterial and fungal communities, particularly after 2 years of implementation (T2) ($p < 0.05$).

3.4 Different taxon of soil bacterial and fungal communities

The unique ASV numbers of soil bacterial and fungal community are shown in Figure 1b. Compared to the no-intercropping treatment (T0), intercropping treatments (T1 and T2) increased the unique ASV numbers for both communities (Figure 1b; Supplementary Table S5). The number of unique ASVs increased as the intercropping years decreased, except for the fungal community, and this pattern was generally consistent with the overall changes in ASVs within the community.

The cladogram analysis (Figures 2a, c) showed the result of linear discriminant analysis effect size (LEfSe, LDA scores ≥ 4.0) and indicated the taxonomic component of bacterial and fungal microbial communities. It showed a better visualization of shifts in the bacterial and fungal community in citrus orchard soil, whether T0, T1, or T2 treatment. For soil bacterial community (Figure 2a), *Acidobacteria* (from phylum to genus) and *Proteobacteria* (from phylum to genus) were significantly enriched in T0 and T1 treatments, respectively. However, *Actinobacteriota* (the phylum) and Burkholderiales (from family to genus) were significantly enriched in T2 treatment. For soil fungal communities (Figure 2d), *Ascomycota* (the phylum and its order *Sordariomycetes*) and *Rutstroemiaceae* (from family to species) were significantly enriched in T0 treatment. *Fusarium solani* (the species) was significantly enriched in T1 treatment. *Mortierellomycota* (from phylum to genus) and *Dothideomycetes* (the class and its family *Lophiostomataceae*) were significantly enriched in T2 treatment.

The LEfSe analysis revealed differential microbial taxa across treatments (Figures 2b, d). In the soil bacterial community, 14 discriminative taxa were identified (LDA score ≥ 4.0), with enrichment patterns distributed as follows: five in T0 (control), six in T1 (intercropping = 1 year), and three in T2 (intercropping = 2 years). The predominant bacterial phyla were *Acidobacteriae* in T0, *Proteobacteria* in T1, and *Actinobacteriota* in T2. For fungal communities, 18 discriminative taxa were detected (LDA score ≥ 4.0), exhibiting distinct treatment enrichment: six in T0, one in T1, and 11 in T2. The predominant fungal taxa were *Ascomycota* in T0,

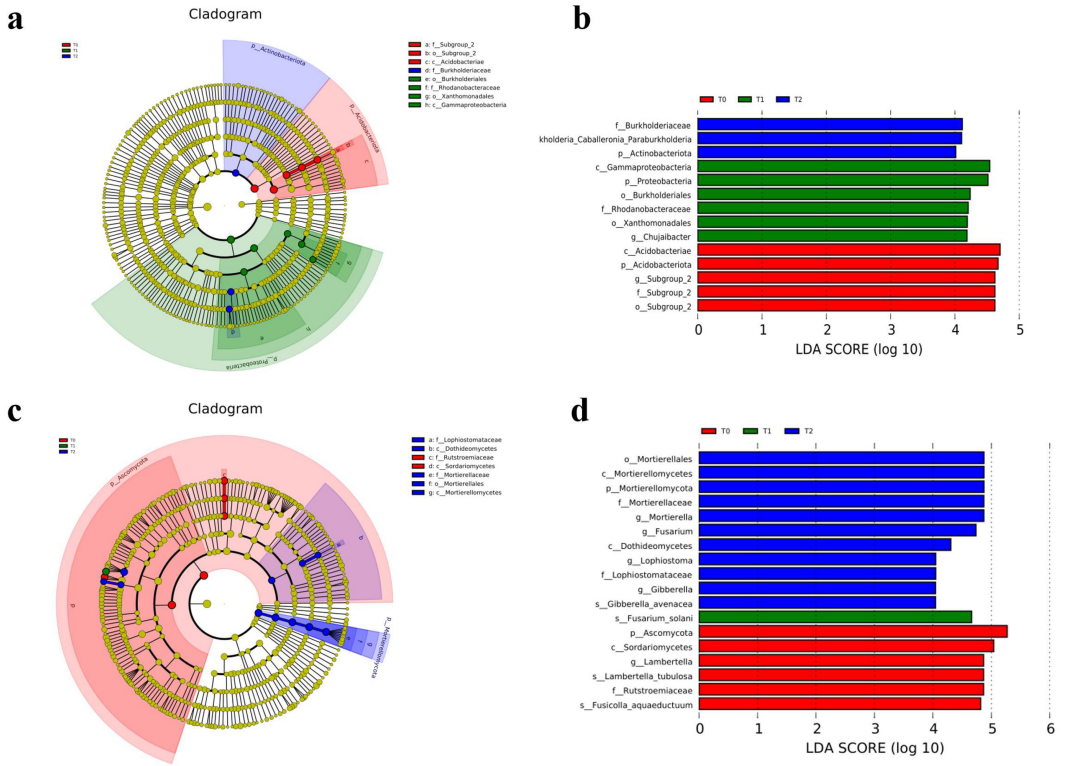

FIGURE 2
LEfSe and cladogram on different years of intercropping treatments of soil bacterial **(a, b)** and fungal **(c, d)** communities (LDA scores ≥4.0).

Fusarium solani (species taxon) in T1, and *Mortierellales* (order taxon) in T2.

3.5 Co-occurring network analysis

The co-occurrence network was used to analyze the co-occurrence characteristics of intercropping SGM treatments on soil microbial community in citrus orchards. Soil bacterial and fungal communities' ASVs with relative abundance ≥0.1% in three groups were constructed (Figure 3; Supplementary Table S7). The co-occurrence networks of soil bacterial and fungal communities exhibited increased node counts, link numbers, and structural complexity with extended intercropping duration (years) with SGM. Network connections shifted from predominantly positive links toward balanced positive–negative interactions (approaching 50%), indicating a transition from cooperative-dominant to cooperative-competitive dynamics, except for fungal communities in the T1 treatment. The average path length, inversely related to network compactness and stability (Li J. et al., 2023; Qiao et al., 2024), decreased progressively in bacterial networks (T0: 3.649; T1: 3.590; T2: 3.510), demonstrating enhanced cohesion and robustness over the intercropping chronosequence. Conversely, fungal networks displayed increased path lengths (T0: 1.444; T1: 1.725; T2: 3.651), reflecting gradual structural decentralization.

Elevated taxonomic diversity within these co-occurrence networks amplified complexity and critically supported soil microbial multifunctionality (Chen et al., 2022; Wang et al., 2023; Xiao et al., 2025). This complexity was evidenced by (i) increased node and link counts across bacterial and fungal networks (Supplementary Table S7; Figure 3) and (ii) declining proportional representation of dominant phyla alongside rising contributions from minor taxa. For bacterial networks (Supplementary Figure S3; Supplementary Table S8), nodes affiliated with *Acidobacteriota* decreased significantly (T0: 52.53% → T1: 44.70% → T2: 39.31%), whereas those assigned to *Proteobacteria* increased progressively (T0: 28.28% → T1: 34.09% → T2: 37.24%). Concurrently, the number of represented phyla expanded (T0: 9 → T1: 11 → T2: 11). Fungal networks exhibited parallel trends (Supplementary Figure S4; Supplementary Table S9).

Collectively, SGM intercropping in citrus orchards enhanced the structural complexity of soil microbial co-occurrence networks. Crucially, it increased species composition diversity within these networks, driving a shift from cooperation-dominated to balanced cooperative–competitive frameworks and reinforcing soil microbial community multifunctionality.

3.6 Correlations between soil properties and soil microorganisms

Distance-based redundancy analysis (db-RDA) was performed to assess the influence of soil properties on microbial communities (Figure 4). The first two axes collectively explained 55.93%

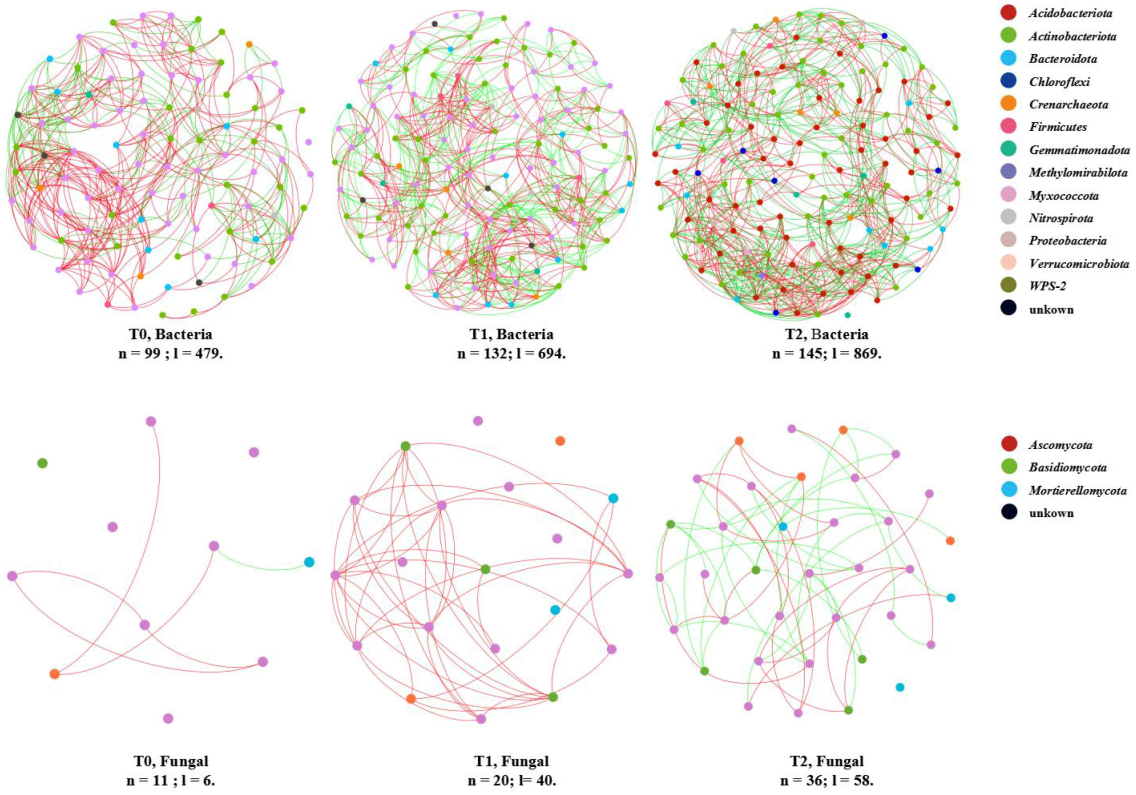

FIGURE 3
Co-occurring network of soil bacterial and fungal communities at ASV taxon. The nodes (n) are colored by phylum. The edges (l) show significant Spearman correlations ($|\rho| > 0.8$, $p < 0.05$), with red/green indicating positive/negative correlations.

(bacteria) and 58.98% (fungi) of community variation, indicating a robust model representation of environmental effects (>50% threshold). Bacterial and fungal communities exhibited directional succession along the dbRDA1 axis (left to right) with increasing SGM intercropping duration (0→1→2 years). Key drivers of community restructuring ($p < 0.05$, Supplementary Table S10) included soil pH, total nitrogen (N), available nitrogen (AN), available phosphorus (AP), available potassium (AK), and organic matter (OM). Notably, pH, AN, AK, and OM emerged as shared strong drivers for both communities ($p < 0.01$, r2 ≥ 0.8). In addition, acute angles between these factor vectors in ordination space implied synergistic interactions among dominant drivers.

Moreover, the correlation analysis between alpha diversity indices and the soil properties ae shown in Figure 5; Supplementary Table S11. For bacterial α-diversity, significant positive correlations were observed with soil pH, available nitrogen (AN), available phosphorus (AP), available potassium (AK), and organic matter (OM) ($p < 0.05$). The Shannon index exhibited particularly strong associations ($p < 0.01$) with soil pH ($\rho = 0.788$), AN ($\rho = 0.728$), AP ($\rho = 0.744$), and AK ($\rho = 0.781$). Similarly, fungal α-diversity showed significant positive correlations ($p < 0.05$) with soil pH, AN, AP, AK, and OM, with the Shannon index demonstrating robust linkages ($p < 0.01$) to AN ($\rho = 0.703$) and OM ($\rho = 0.776$). In contrast, total soil nitrogen (N), phosphorus (P), and potassium (K) displayed non-significant correlations ($p > 0.05$). Collectively, soil pH, available nutrients (AN, AP, AK), and OM emerged as key drivers shaping the α-diversity in both bacterial and fungal communities, particularly for the Shannon index. Notably, bacterial diversity displayed stronger correlations (higher coefficients, lower p-values) with soil pH, AN, AP, and AK than fungal diversity, whereas soil OM exerted a more pronounced influence (higher coefficient, lower p-value) on the fungal Shannon index.

Significant correlations (Spearman's $|\rho| \geq 0.6$, $p < 0.05$) between soil physicochemical properties and taxon-specific bacterial (Figure 2b) and fungal (Figure 2d) microbes are visualized in Figure 6. For bacteria (Figure 6a), soil pH, available nitrogen (AN), available phosphorus (AP), available potassium (AK), and organic matter (OM) exhibited strong positive correlations ($\rho \geq 0.8$, $p < 0.01$) with *Actinobacteriota* (Phylum), *Burkholderiales* (Order), *Burkholderiaceae* (Family), and *Burkholderia* (Genus). Conversely, these same soil parameters showed strong negative correlations ($\rho \leq -0.8$, $p < 0.01$) with *Subgroup 2* (Order to Genus). Additionally, *Acidobacteriae* (Class) was negatively correlated with AK ($-0.8 \leq \rho \leq -0.6$, $p < 0.05$). Among fungi (Figure 6b), 12 specific microbial taxa (including *Mortierellomycota, etc.*) demonstrated positive correlations ($\rho \geq 0.6$, $p < 0.05$) with soil properties, particularly showing strong positive associations ($\rho \geq 0.8$, $p < 0.01$) with soil pH, AN, AP, AK, and OM. In contrast, *Fusarium solani* (Species) displayed a negative correlation ($\rho \leq -0.6$, $p < 0.05$). Collectively,

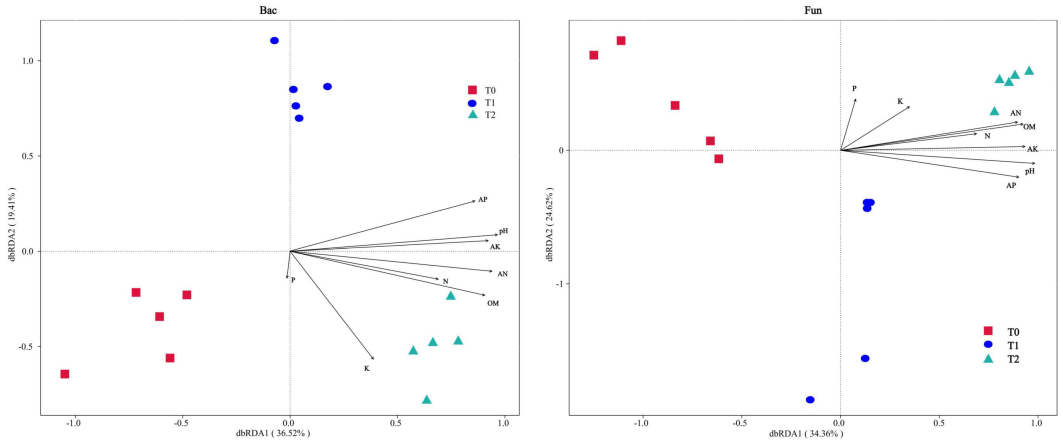

FIGURE 4
Distance-based redundancy analysis (dbRDA) for soil bacterial (Bac) and fungal (Fun) communities associated with soil properties at the ASV taxonomic level, respectively.

soil pH, OM, N, AN, AK, and AP emerged as key determinants governing the composition and abundance of some specific bacterial and fungal taxa in the soil ecosystem.

3.7 Correlations among the citrus yield and quality, soil properties, soil microorganism, and SGM intercropping years

The results of a network correlation analysis revealing multi-component interactions within the citrus orchard intercropped with SGM system are presented in Figure 7 (Spearman's $|\rho| \geq 0.8$, $p < 0.01$). As illustrated in Figure 7a, intercropping duration (years) exhibited numerous direct and indirect correlations with soil properties, the taxon-specific microbes, soil microbial diversity, and fruit quality. Overall, extremely strong positive correlations ($|\rho| \geq 0.9$, $p < 0.01$) were prevalent both among and within the core factors of intercropping duration (years), soil properties (specifically pH, available potassium, and available nitrogen), and some taxon-specific microbes. Notably, the taxon-specific microbes affiliated with *Acidobacteriota* and the titratable acidity (TA) index of fruit quality exhibited consistently negative correlations with all other analyzed factors, whereas all remaining correlations were positive. Additionally, soil properties and microbial factors exhibited several strong correlations ($|\rho| \geq 0.8$, $p < 0.01$) with soil microbial diversity. Analysis of factors directly and strongly correlated with fruit quality (Figure 7b, $|\rho| \geq 0.8$, $p < 0.01$) demonstrated that fruit quality was primarily influenced by three

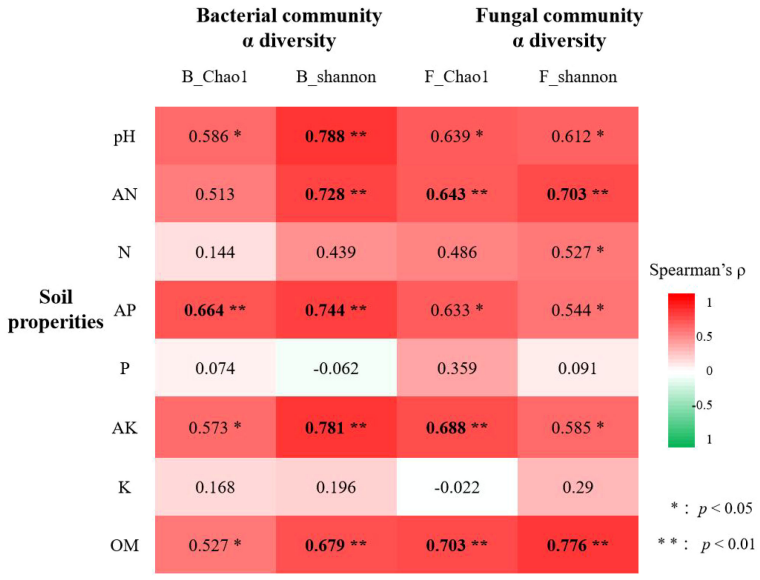

FIGURE 5
Correlations between soil properties and microbial α-diversity (Spearman's $|\rho| > 0.6$ in bold).

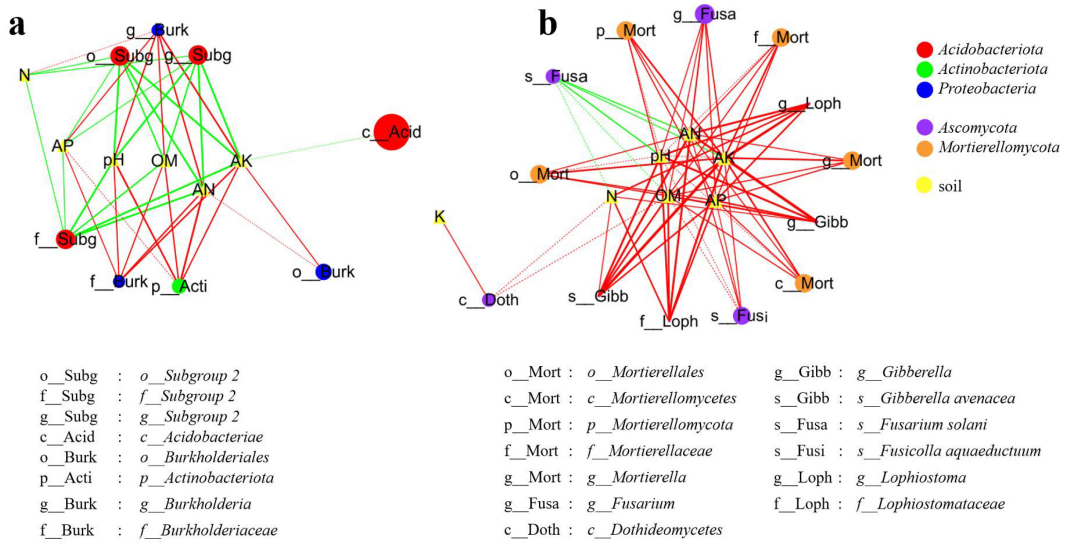

FIGURE 6
Correlations between soil properties and taxon-specific microbes (LEfSe, LDA ≥ 4.0; Spearman's $|\rho| \geq 0.6$ shown). The node size reflects microbial relative abundance. The solid line and dashed line represent $p < 0.01$ and $p < 0.05$, respectively; line with green (negative) and red (positive). The bold lines denote strong correlations ($|\rho| \geq 0.8$).

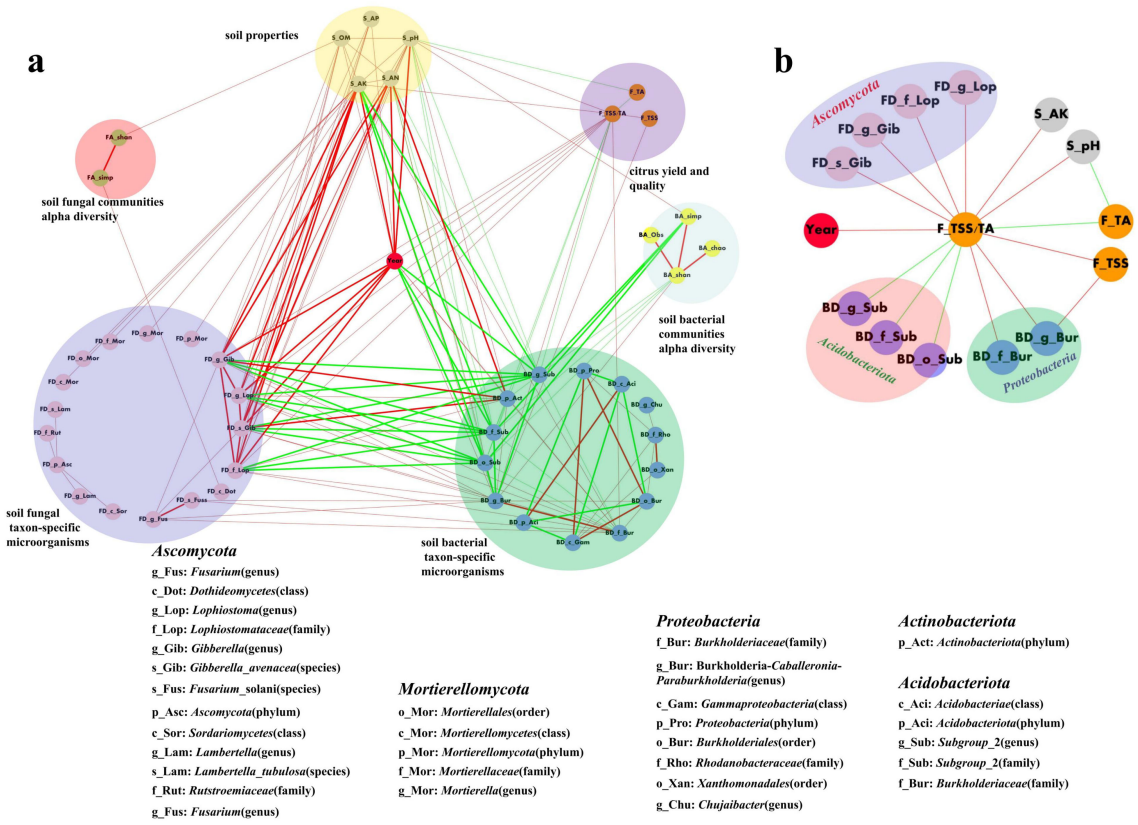

FIGURE 7
Correlation networks of **(a)** citrus yield/quality, soil properties, microbial α-diversity, and taxon-specific microbes (Spearman's $|\rho| \geq 0.8$, $p < 0.01$) and **(b)** key factors strongly correlated with citrus yield/quality ($|\rho| \geq 0.8$, $p < 0.01$). Red/green lines indicate positive/negative correlations; bold lines represent strong correlations ($|\rho| \geq 0.9$, $p < 0.01$).

external factors: intercropping duration (years), soil properties, and some taxon-specific microbes. Notably, certain taxa within the phylum *Acidobacteria* exhibited negative correlations with fruit quality. Additionally, the titratable acidity (TA) index of fruits showed negative correlations with both soil pH and the TSS/TA. In contrast, all other pairwise relationships among these factors demonstrated positive correlations.

This study demonstrated that citrus fruit quality was predominantly influenced by intercropping duration (years), key soil properties (pH and available potassium, AK), and specific soil microbial taxa (*Ascomycota*, *Acidobacteriota*, and *Proteobacteria*), exhibiting highly significant strong correlations ($|\rho| \geq 0.8$, $p < 0.01$).

4 Discussion

Cropping systems significantly influence orchard soil ecosystems by altering physical characteristics, chemical properties, and microbial communities—factors critically determining crop performance and quality (Wang T. et al., 2022; Li C. et al., 2023; Duan et al., 2024). This study specifically examined how SGM intercropping duration affects citrus yield/quality parameters and soil ecosystem dynamics (physicochemical properties and microbial structure), providing actionable insights for sustainable orchard management.

4.1 Effect of intercropping SGM on soil properties

Extensive research has documented the critical role of leguminous green manure incorporation in enhancing soil fertility and promoting nutrient transformation (Dong et al., 2021; Wang T. et al., 2022; Fu et al., 2023; Duan et al., 2024; Qin et al., 2024). The current investigation revealed that 1-year SGM intercropping significantly enhanced most soil physicochemical properties, with the exception of total N, P, and K content. Further improvements in soil pH and key nutrient indicators (AN, AK, AP, OM) were observed after 2 years of intercropping (T2) compared to the first year (T1) (Table 2). This finding aligns with established evidence demonstrating the nitrogen-fixing capacity of legume crops and their soil amelioration effects (Fu et al., 2023; Qin et al., 2024). The practice of intercropping SGM application effectively regulates soil nutrient conversion rates, leading to significant improvements in multiple soil parameters including pH, organic matter content, and AN, AK and AP, etc., ultimately enhancing crop yield and quality (Wang T. et al., 2022; Duan et al., 2024; Qin et al., 2024). The duration of SGM intercropping in orchards showed a positive correlation with the enhancement of essential nutrient conversion efficiency. These soil modifications, particularly the elevation of acidic soil pH and nutrient enrichment, subsequently influenced microbial community diversity and composition (Li et al., 2020; Fu et al., 2023; Qin et al., 2024). Consequently, SGM intercropping demonstrated substantial benefits for soil physicochemical properties in citrus orchards, with progressively more pronounced effects on soil pH neutralization and fertility improvement as intercropping duration (years) increased (Table 2).

4.2 Effect of intercropping SGM on soil microbial community

As the most biologically active and taxonomically diverse components of soil ecosystems, microorganisms perform indispensable ecological functions, including organic matter decomposition, biogeochemical cycling (Li et al., 2020; Adomako et al., 2022; Li C. et al., 2023), and modulation of plant growth and disease resistance (Shi et al., 2019; Philippot et al., 2024). Critical microbial community parameters—encompassing composition, α/β-diversity, phylogenetic structure, keystone taxon abundance, and co-occurrence network topology—serve as robust bioindicators for assessing soil ecosystem health and functional capacity (Li et al., 2020; Li C. et al., 2023; Li J. et al., 2023).

4.2.1 Effect on soil microbial community composition and diversity

Numerous studies have demonstrated that green manure intercropping significantly alters microbial community composition, diversity, and structure (Dong et al., 2021; Wang T. et al., 2022; Fu et al., 2023; Duan et al., 2024; Qin et al., 2024). The results demonstrated that SGM intercropping in citrus orchards induced marked changes in soil microbial communities and associated physicochemical properties (Figure 1). Taxonomic analysis identified *Acidobacteria*, *Proteobacteria*, *Chloroflexi*, *Actinobacteriota*, and *Gemmatimonadota* as dominant bacterial phyla, while *Ascomycota*, *Mortierellomycota*, and *Basidiomycota* predominated among fungi—consistent with global soil microbial distributions (Wang T. et al., 2022; Duan et al., 2024; Philippot et al., 2024). Notably, SGM intercropping practices induced differential shifts in microbial composition (Figure 1a) characterized by (i) increased *Actinobacteria* and decreased *Acidobacteria* in bacterial communities and (ii) elevated *Mortierellomycota* and reduced *Ascomycota* abundance in fungal populations (Figure 2). The results demonstrated that bacterial communities exhibited concurrent enrichment of *Actinobacteria* and *Proteobacteria* phyla alongside the depletion of *Acidobacteriota*, while fungal communities showed concomitant increases in *Mortierellomycota* abundance with reductions in *Ascomycota* (Figure 2).

Many researches have established soil pH and nutrient availability as primary determinants of microbial community dynamics (Kyaschenko et al., 2017; Lin et al., 2019; Wang Z. et al., 2022; Philippot et al., 2024; Raiesi et al., 2024). Our findings corroborated these observations, demonstrating that available nitrogen (AN), available phosphorus (AP), available potassium (AK), organic matter (OM), and pH constituted the key edaphic factors governing microbial succession following soybean green manure (SGM) incorporation (Figures 4, 5; Supplementary Table S10). The soil fertility index, which positively correlates with nutrient levels, emerged as a robust predictor of microbial diversity. Statistical analyses revealed

significant positive correlations ($p < 0.01$) between these soil parameters (particularly pH, AN, AP, AK, and OM) and both bacterial and fungal community diversity metrics (Figure 5). Consistent with previous reports (Duan et al., 2024; Xiao et al., 2025), soil properties exhibited stronger regulatory effects on bacterial communities, with pH, AN, AP, AK, and OM all showing substantial correlations ($\rho \geq 0.6$) with bacterial Shannon diversity. In contrast, fungal diversity demonstrated significant correlations ($\rho \geq 0.6$) only with AN and OM concentrations (Figure 5).

In total, the observed changes in soil properties (particularly pH and fertility indices) showed significant associations with alterations in soil microbial community composition and diversity under SGM intercropping systems in citrus orchards.

4.2.2 Effect on the co-occurrence network

The co-occurrence network analysis revealed that SGM intercropping in citrus orchards significantly enhanced the organizational complexity of soil microbial communities as evidenced by increased network nodes, connections, and species richness following SGM introduction (Figure 3; Supplementary Tables S8; S9). Research indicates that increases in node count, connectivity, and taxonomic richness within co-occurrence networks signify enhanced ecosystem health while simultaneously introducing novel ecological challenges. The core value of such network expansion lies in achieving equilibrium between functional augmentation and risk mitigation through structured development rather than pursuing quantitative complexity alone (Lei et al., 2023; Zhu et al., 2023; Qiao et al., 2024; Zhai et al., 2024).

A balance of positive and negative connections contributes to network stability (Luo et al., 2023). The study revealed a balanced distribution of positive and negative connections within the soil bacterial and fungal co-occurrence network following SGM intercropping, with this equilibrium being particularly pronounced under the 2-year intercropping regime (T2) (Figure 3; Supplementary Table S7). It is noteworthy that the negative connectivity number of the fungal co-occurrence network in the 1-year intercropped treatment was zero, which may be due to the *Fusarium* wilt disease of soybean in the 1-year intercropped SGM treatment group affecting the soil microflora fungal community environment (Figures 2c, d) (Zhou et al., 2022; Mendes et al., 2023). Despite the absence of documented *Fusarium* wilt cases in citrus to date, this potential pathogen requires increased attention. Furthermore, planting SGM in acid-biased environments tends to lead to the development of *Fusarium* wilt diseases in leguminous crops and has impacted the structure and network of soil fungal communities (Zhou et al., 2022; Du et al., 2024).

Small-world networks of interactions are characterized by short path lengths and have been shown to respond rapidly to disturbances in ecosystems (Zhou et al., 2010). This study showed that with increasing years of SGM intercropping, the average path length of bacterial co-occurrence networks decreased, while an opposite trend was observed in fungal communities (Supplementary Table S7). Therefore, intercropping soybean crops and using them as green manure led to an increase in the complexity of the bacterial and fungal communities in orchard soils, with enhanced internal interactions within the bacterial communities and weakened internal interactions within the fungal communities, which tended to be looser. These results are consistent with the results of Duan et al (Duan et al., 2024), who showed an increase in the interactions of bacterial networks and a strengthening of modularity of fungal networks and a loosening of internal interactions within the overall network after intercropping of a leguminous green manure in a tea garden.

4.2.3 Effect on soil-taxon-specific microbes

The SGM intercropping system induced distinct shifts in microbial community composition (Figure 1a), demonstrating selective recruitment of specific taxonomic groups (Figure 2). Notably, SGM treatment recruited *Actinobacteria* and *Proteobacteria* while reducing *Acidobacteria* in bacterial communities. Fungal communities exhibited increased *Mortierellomycota* abundance with concomitant reduction in *Ascomycota* populations (Figure 2).

The correlation analysis (Figure 6) between soil properties and taxon-specific microbes (Figure 2) revealed that *Actinobacteria*, *Proteobacteria*, *Mortierellomycota*, and *Ascomycetes* (excluding *Fusarium solani*) showed significant positive correlations with soil properties including pH, OM, AN, AP, AK, and N ($|\rho| \geq 0.6$, $p < 0.05$). In contrast, *Fusarium* and *Acidobacteria* exhibited opposite trends. Previous studies have demonstrated that *Acidobacteria* dominate in acidic soils, with their relative abundance increasing as pH decreases (Rousk et al., 2010; Zhao et al., 2025). These bacteria also play crucial roles in soil nutrient cycling and ecological function regulation. *Actinobacteria* and *Proteobacteria* contribute significantly to soil multifunctionality (Ma et al., 2022; Shi et al., 2025). *Proteobacteria* are particularly important for organic phosphorus activation (Chen et al., 2024) and community structure stabilization (Liu et al., 2025). *Actinobacteria* regulate microbial community structure, mediate nutrient transformation and plant uptake, and participate in organic pollutant degradation and heavy metal redox processes, making them essential for soil improvement, biomass maintenance, and pollutant remediation (Ma et al., 2022; Cui et al., 2023; Sun et al., 2024). *Ascomycetes* and other fungal groups serve as key indicators of soil health (Sun et al., 2024), while *Mortierellomycota* contribute to straw degradation and soil nutrient cycling through their ability to break down hemicellulose, cellulose, and lignin (Ning et al., 2022 2022). Notably, the 1-year intercropped SGM treatment group showed elevated recruitment of *Fusarium solani*, a known causal agent of soybean *Fusarium* wilt that often leads to significant crop losses (Ellis et al., 2016). Although no *Fusarium*-related disease symptoms were observed in citrus, soil acidification, barrenness, and nutrient imbalance have been identified as predisposing factors for soybean *Fusarium* wilt (Ning et al., 2020 2020; Osorio and Habte, 2014 2014). This may explain the establishment and dominance of *F. solani* in the T1 group, suggesting that *Fusarium* wilt in soybean crops intercropped with citrus warrants careful attention.

The SGM intercropping system demonstrated significant temporal effects on soil microbial community composition. Long-term SGM intercropping consistently enriched beneficial phyla including *Actinobacteria*, *Proteobacteria*, *Ascomycota*, and *Mortierellomycota* while reducing the relative abundance of *Acidobacteria*. This selective microbial recruitment pattern correlated with enhanced soil quality, greater microbial community functional versatility, and improved stability of the ecological network.

4.3 Effect of intercropping SGM on citrus quality

Intercropping with leguminous crops and green manure incorporation represent high-yielding, ecologically beneficial, and sustainable cultivation practices that enhance crop growth while improving the soil quality and microbial communities (Wang T. et al., 2022; Duan et al., 2024; Fan et al., 2025). Being consistent with this principle, the results of this study showed that SGM intercropping enhanced citrus fruit yield and quality parameters. Notably, after 2 years of implementation, this treatment significantly increased the total soluble solids (TSS) and the TSS/TA ratio in citrus fruits relative to the non-intercropped control (Table 1).

An analysis of factors exhibiting strong correlations with citrus fruit quality (Spearman coefficient $|\rho| \geq 0.8$, $p < 0.01$; Figure 7b) revealed that intercropping duration with SGM significantly and positively correlated with the TSS/TA ratio—a key indicator of flavor maturity in citrus. This aligns with documented evidence that long-term green manure application enhances fruit quality (Zhang et al., 2022; Yang et al., 2023). Concurrently, soil nutrient availability demonstrated strong positive correlations with multiple fruit quality parameters, consistent with established mechanisms whereby green manure improves edaphic conditions to elevate crop quality (Wang T. et al., 2022; Zhang et al., 2022; Duan et al., 2024). Contrastingly, titratable acidity (TA) showed a significant negative correlation with soil pH ($p < 0.01$). Critically, titratable acidity (TA) serves as a negative indicator of fresh fruit palatability (China National Standardization Administration Committee, 2008; Li et al., 2014; Yang et al., 2014), further corroborating the interdependent relationship between soil properties and sensory quality attributes. Notably, specific microbial taxa—predominantly affiliated with *Actinobacteria*, *Proteobacteria*, *Acidobacteriota*, and *Ascomycota*—exhibited robust correlations with quality indices (Figure 7). Previous studies have shown that *Proteobacteria* and *Ascomycota* are positively associated with crop performance (Ning et al., 2022; Wang T. et al., 2022; Duan et al., 2024). Despite the positive role of *Acidobacteria* in participating in nutrient activation and organic matter degradation, as well as in enhancing primary productivity, many *Acidobacteria* have been associated with oligotrophic strategies and have successfully proliferated in low-nutrient environments, especially with poor soil quality (Kielak et al., 2016; Stone et al., 2023). Collectively, these findings underscore that SGM intercropping synchronizes soil physicochemical properties, microbiome dynamics, and fruit quality optimization, with intercropping duration being a pivotal regulatory factor.

Therefore, this study underscored that the duration of sustained intercropping with SGM significantly impacts soil physicochemical properties and microbial communities within citrus orchards and consequently reveals intricate links to the formation of key fruit quality attributes in citrus.

In general, in this study, intercropping SGM contributed to improved soil physicochemical properties (Table 2) and modified soil microbial community structure (Figures 1–6), consequently enhancing citrus fruit quality (Table 1; Figure 7). However, due to the short duration (2 years) of the SGM treatment, the observed improvements in citrus fruit yield and titratable acidity (a key quality parameter in Table 1) were not statistically significant. Consequently, extending SGM intercropping beyond the current trial duration may augment beneficial effects on orchard ecological functions (fruit yield and quality) and soil ecosystem attributes (soil properties and microbial community structure), rendering these positive trends more pronounced.

5 Conclusion

This study revealed that soybean green manure (SGM) intercropping in acidified citrus orchards effectively modulated soil characteristics, reshaped microbial communities, enhanced biodiversity, optimized network complexity, and intensified microbial interactions, resulting in superior fruit quality. After 2 years of SGM intercropping, significant improvements were observed in orchard soil pH and fertility, along with the selective recruitment of beneficial microorganisms (*Proteobacteria*, *Actinobacteria*, *Ascomycota*, and *Mortierellomycota*), while reducing acidophilic *Acidobacteria* populations. These changes led to increased complexity in both bacterial and fungal communities, strengthened microbial network interactions, and consequent enhancement of fruit quality parameters. Importantly, significant correlations were established between fruit quality improvement and specific changes in soil physicochemical parameters, microbial community structure, and the recruitment of some keystone microbial taxa. These findings provide fundamental insights into the ecological mechanisms underlying soil environment improvement in acidified citrus orchards through green manure intercropping, suggesting this approach as a promising strategy for sustainable citrus production in acidic regions. Thus, future research should explore the long-term effects of SGM intercropping on citrus rhizosphere microbiome dynamics and soil carbon sequestration while evaluating its economic feasibility across different acidic soil types and climatic conditions.

Data availability statement

The original contributions presented in the study are publicly available. This data can be found here: National Center for

Biotechnology Information (NCBI) BioProject database under accession number: PRJNA957046.

Author contributions

SD: Conceptualization, Data curation, Methodology, Visualization, Writing – original draft, Writing – review & editing. BH: Conceptualization, Data curation, Methodology, Visualization, Funding acquisition, Writing – original draft, Writing – review & editing. BZ: Conceptualization, Methodology, Writing – original draft, Writing – review & editing. SC: Methodology, Writing – original draft, Writing – review & editing. BG: Methodology, Writing – original draft, Writing – review & editing. WL: Methodology, Writing – original draft, Writing – review & editing. WZ: Methodology, Writing – original draft, Writing – review & editing. SL: Methodology, Writing – original draft, Writing – review & editing. SY: Conceptualization, Funding acquisition, Methodology, Project administration, Supervision, Writing – original draft, Writing – review & editing.

Funding

The author(s) declare financial support was received for the research and/or publication of this article. This work was supported by the Central-level grassroots agricultural technology extension system reform and construction project - Joint construction of a county leading in agricultural technology modernization (2130106); Hunan Province Key Research and Development Project (2022NK2015; 2025AQ2028); Hunan Province Modern Agricultural Industry Technology System (HARS-09).

Conflict of interest

The authors declare that the research was conducted in the absence of any commercial or financial relationships that could be construed as a potential conflict of interest.

Generative AI statement

The author(s) declare that no Generative AI was used in the creation of this manuscript.

Any alternative text (alt text) provided alongside figures in this article has been generated by Frontiers with the support of artificial intelligence and reasonable efforts have been made to ensure accuracy, including review by the authors wherever possible. If you identify any issues, please contact us.

Publisher's note

Supplementary material

The Supplementary Material for this article can be found online at: https://www.frontiersin.org/articles/10.3389/fpls.2025.1560550/full#supplementary-material

References

Adomako, M., Roiloa, S., and Yu, F. (2022). Potential roles of soil microorganisms in regulating the effect of soil nutrient heterogeneity on plant performance. *Microorganisms* 10, 2399. doi: 10.3390/microorganisms10122399

Bao, S. D. (2000). *Soil and Agricultural Chemistry Analysis. 3rd ed.* (Beijing: Chinese Agriculture Press).

Bastian, M., Heymann, S., and Jacomy, M. (2009). "Gephi: an open source software for exploring and manipulating networks," *Proceedings of the Third International Conference on Weblogs and Social Media*, ICWSM 2009, San Jose, California, USA, pp. 4–6. doi: 10.13140/2.1.1341.1520

Chen, Q., Zhao, Q., Xie, B., Lu, X., Guo, Q., Liu, G., et al. (2024). Soybean(Glycine max)rhizosphere organic phosphorus recycling relies on acid phosphatase activity and specific phosphorus mineralizing related bacteria in phosphate deficient acidic soils. *J. Integr. Agric.* 23, 1685–1702. doi: 10.1016/j.jia.2023.09.002

Chen, W., Wang, J., Chen, X., Meng, Z., Xu, R., Duoji, D., et al. (2022). Soil microbial network complexity predicts ecosystem function along elevationg radients on the Tibetan Plateau. *Soil Biol. Biochem.* 172, 108766. doi: 10.1016/j.soilbio.2022.108766

China National Standardization Administration Committee. (2008). National public service platform for standards information. Available online at: https://openstd.samr.gov.cn/bzgk/gb/newGbInfo?hcno=23AEF842613A2444152B7F2FC91FA8EA (Accessed June 1, 2025).

Cui, X., Lin, X., Li, J., Zhang, H., and Han, Y. (2023). Diversity and functional properties of anticorrosive actinomycetes and their application in environmental remediation. *J. Microbiol.* 63, 1930–1943. doi: 10.13343/j.cnki.wsxb.20220941

Dong, N., Hu, G., Zhang, Y., Qi, J., Chen, Y., and Hao, Y. (2021). Effects of green-manure and tillage management on soil microbial community composition, nutrients and tree growth in a walnut orchard. *Sci. Rep.* 11, 16882. doi: 10.1038/s41598-021-96472-8

Du, L., Zhang, Z., Chen, Y., Wang, Y., Zhou, C., Yang, H., et al. (2024). Heterogeneous impact of soil acidification on crop yield reduction and its regulatory variables: A global meta-analysis. *Field Crops Res.* 319, 109643. doi: 10.1016/j.fcr.2024.109643

Duan, Y., Wang, T., Lei, X., Cao, Y., Liu, L., Zou, Z., et al. (2024). Leguminous green manure intercropping changes the soil microbial community and increases soil nutrients and key quality components of tea leaves. *Hortic. Res.* 11, uhae018. doi: 10.1093/hr/uhae018

Ellis, M. L., Lanubile, A., Garcia, C., and Munkvold, G. P. (2016). Association of putative fungal effectors in fusarium oxysporum with wilt symptoms in soybean. *Phytopathology* 106, 762–773. doi: 10.1094/PHYTO-11-15-0293-R

Fan, Z., Liu, P., Lin, Y., Qiang, B., Li, Z., and Cheng, M. (2025). Root plasticity improves the potential of maize/soybean intercropping to stabilize the yield. *Soil Tillage Res.* 251, 106553. doi: 10.1016/j.still.2025.106553

Fu, H., Chen, H., Ma, Q., Han, K., Wu, S., and Wu, L. (2023). Effect of planting and mowing cover crops as livestock feed on soil quality and pear production. *Front. Plant Sci.* 13, 1105308. doi: 10.3389/fpls.2022.1105308

Guo, H., Zheng, Y., Wu, D., Du, X., Gao, H., Ayyash, M., et al. (2023). Quality evaluation of citrus varieties based on phytochemical profiles and nutritional properties. *Front. Nutr.* 10, 1165841. doi: 10.3389/fnut.2023.1165841

Harrell, F. E. Jr. (2019). Hmisc: Harrell Miscellaneous. *R package version 4.8-0.* https://CRAN.R-project.org/package=Hmisc? (Accessed August 20, 2025).

Jing, J., Cong, W., and Bezemer, T. (2022). Legacies at work: plant-soil-microbiome interactions underpinning agricultural sustainability. *Trends Plant Sci.* 27, 781–792. doi: 10.1016/j.tplants.2022.05.007

Kielak, A. M., Barreto, C. C., Kowalchuk, G. A., Veen, J. A., and Kuramae, E. E. (2016). The ecology of acidobacteria: moving beyond genes and genomes. *Front. Microbiol.* 7, 00744. doi: 10.3389/fmicb.2016.00744

Kyaschenko, J., Clemmensen, K. E., Karltun, E., and Lindahl, B. D. (2017). Below-ground organic matter accumulation along a boreal forest fertility gradient relates to guild interaction within fungal communities. *Ecol. Lett.* 20, 1546–1555. doi: 10.1111/ele.12862

Lei, J., Liu, J., Liu, Z., Liang, A., Hu, X., Yu, Z., et al (2023). Conservation tillage enhances ecological network stability of fungal communities. *J. Microbiol.* 63, 2835–2847. doi: 10.13343/j.cnki.wsxb.20220820

Li, C., Hoffland, E., Kuyper, T. W., Yu, Y., Zhang, C., Li, H., et al. (2020). Syndromes of production in intercropping impact yield gains. *Nat. Plants* 6, 653–660. doi: 10.1038/s41477-020-0680-9

Li, C., Stomph, T. J., Makowski, D., Li, H., Zhang, C., Zhang, F., et al (2023). The productive performance of intercropping. *Proc. Natl. Acad. Sci. U S A.* 120, e2201886120. doi: 10.1073/pnas.2201886120

Li, W., Wang, L., Yuan, Q., Chen, S., Peng, Z., Bai, Z., et al. (2014). Analysis of soluble sugar and organic acid content of beef red vermilion orange fruits from different origins. J. *Jiangsu Agric. Sci.* 42, 255–258. doi: 10.15889/j.issn.1002-1302.2014.01.104

Li, Z., and Wang, Z. (2006). Research on the influencing factors of citrus quality. *J. South. Agric. Sci. J.* 37, 307–310. doi: 10.3969/j.issn.2095-1191.2006.03.029

Li, J., Zhao, J., Liao, X., Yi, Q., Zhang, W., Lin, H., et al. (2023). Long-term returning agricultural residues increases soil microbe-nematode network complexity and ecosystem multifunctionality. *Geoderma* 430, 116340. doi: 10.1016/j.geoderma.2023.116340

Lin, W., Lin, M., Zhou, H., Wu, H., Li, Z., and Lin, W. (2019). The effects of chemical and organic fertilizer usage on rhizosphere soil in tea orchards. *PloS One* 14, e0217018. doi: 10.1371/journal.pone.0217018

Liu, X., Wang, M., Liu, B., Chen, X., An, L., Nie, Y., et al. (2025). Keystone taxa mediate the trade-off between microbial community stability and performance in activated sludges. *Nat. Water*. 3, 723–733. doi: 10.1038/s44221-025-00451-6

Luo, H., Wang, C., Zhang, K., Ming, L., Chu, H., and Wang, H. (2023). Elevational changes in soil properties shaping fungal community assemblages in terrestrial forest. *Sci. Total Environ.* 900, 165840. doi: 10.1016/j.scitotenv.2023.165840

Ma, L., Zhang, C., Xu, X., Wang, C., Liu, G., Liang, C., et al. (2022). Different facets of bacterial and fungal communities drive soil multifunctionality in grasslands spanning a 3500km transect. *Funct. Ecol.* 36, 3120–3133. doi: 10.1111/1365-243.14220

Mendes, L. W., Raaijmakers, J. M., Hollander, M., Sepo, E., Gómez Expósito, R., Chiorato, A. F., et al. (2023). Impact of the fungal pathogen Fusarium oxysporum on the taxonomic and functional diversity of the common bean root microbiome. *Environ. Microbiome* 18, 1–17. doi: 10.1186/s40793-023-00524-7

National Bureau of Statistics of China (2025). *China Statistical Yearbook 2024: 12 Agriculture* (Beijing: China Statistics Press). Available online at: https://www.stats.gov.cn/sj/ndsj/2024/indexch.htm (Accessed August 20, 2025).

Ning, Q., Chen, L., Jia, Z., Zhang, C., Ma, D., Li, F., et al. (2020). Multiple long-term observations reveal a strategy for soil pH-dependent fertilization and fungal communities in support of agricultural production. *Agriculture Ecosyst. Environ.* 293, 106837. doi: 10.1016/j.agee.2020.106837

Ning, Q., Chen, L., Li, F., Zhang, C., Ma, D., Cai, Z., et al. (2022). Effects of mortierella on nutrient availability and straw decomposition in soil. *Acta Pedologica Sinica* 59, 206–217. doi: 10.11766/trxb202006020213

Osorio, N., and Habte, M. (2014). Soil phosphate desorption induced by a phosphate-solubilizing fungus. *Commun. Soil Sci. Plant Anal.* 45, 451–460. doi: 10.1080/00103624.2013.870190

Philippot, L., Chenu, C., Kappler, A., Rillig, M. C., and Fierer, N. (2024). The interplay between microbial communities and soil properties. *Nat. Rev. Microbiol.* 22, 226–239. doi: 10.1038/s41579-023-00980-5

Qiao, Y., Wang, T., Huang, Q., Guo, H., Zhang, H., Xu, Q., et al. (2024). Core species impact plant health by enhancing soil microbial cooperation and network complexity during community coalescence. *Soil Biol. Biochem.* 188, 109231. doi: 10.1016/j.soilbio.2023.109231

Qin, X., Zhang, S., Li, G., Zhang, W., Zhang, X., and Gao, W. (2024). Thoughts on the intercropping model of soybeans in orchards. *J. Chin. Fruit* 9, 117–120. doi: 10.16626/j.cnki.issn1000-8047.2024.09.017

Raiesi, T., Shiri, M., and Mousavi, S. (2024). The fruit quality and nutrient content of kiwifruit produced by organic versus chemical fertilizers. *J. Sci. Food Agric.* 104, 6821–6830. doi: 10.1002/jsfa.13511

Read, D., and Perez, M. (2003). Mycorrhizas and nutrient cycling in ecosystems – a journey towards relevance? *New Phytol.* 157, 475–492. doi: 10.1046/j.1469-8137.2003.00704.x

Rousk, J., Bååth, E., Brookes, P., Lauber, C. L., Lozupone, C., Caporaso, J. G., et al. (2010). Soil bacterial and fungal communities across a pH gradient in an arable soil. *ISME J.* 4, 1340–1351. doi: 10.1038/ismej.2010.58

Shen, Z., Han, T., Huang, J., Li, J., Daba, N. A., Gilbert, N., et al. (2024). Soil organic carbon regulation by pH in acidic red soil subjected to long-term liming and straw incorporation. *J. Environ. Manage* 367, 122063. doi: 10.1016/j.jenvman.2024.122063

Shi, W., Li, M., Wei, G., Tian, R., Li, C., Wang, B., et al. (2019). The occurrence of potato common scab correlates with the community composition and function of the geocaulosphere soil microbiome. *Microbiome* 7, 14. doi: 10.1186/s40168-019-0629-2

Shi, Y., Li, T., Zheng, L., Jing, X., Hussain, H. A., and Zhang, Q. (2025). Enhancing soil multifunctionality through restoring erosion environment and microbial functions combined with organic manure and straw mulching. *Agriculture Ecosyst. Environ.* 383, 109515. doi: 10.1016/j.agee.2025.109515

Stone, B. W. G., Dijkstra, P., Finley, B., Fitzpatrick, R., Foley, M. M., Hayer, M., et al. (2023). Life history strategies among soil bacteria—dichotomy for few, continuum for many. *ISME J.* 17, 611–619. doi: 10.1038/s41396-022-01354-0

Sun, X., Li, T., and Zhang, J. (2024). Soil health and microbial network analysis in a wheat-maize cropping system under different wheat yields. *Front. Agr. Sci. Eng.* 11, 615–625. doi: 10.15302/J-FASE-2024570

Wang, T., Duan, Y., Liu, G., Shang, X., Liu, L., Zhang, K., et al (2022). Tea plantation intercropping green manure enhances soil functional microbial abundance and multifunctionality resistance to drying-rewetting cycles. *Sci. Total Environ.* 810, 151282. doi: 10.1016/j.scitotenv.2021.151282

Wang, Z., Yang, T., Mei, X., Wang, N., Li, X., Yang, Q., et al. (2022). Bio-organic fertilizer promotes pear yield by shaping the rhizosphere microbiome composition and functions. *Microbiol. Spectr.* 10, e0357222. doi: 10.1128/spectrum.03572-22

Wang, X., Zhang, Q., Zhang, Z., Li, W., Liu, W., Xiao, N., et al. (2023). Decreased soil multifunctionality is associated with altered microbial network properties under precipitation reduction in a semiarid grassland. *Imeta* 2, e106. doi: 10.1002/imt2.106

Wu, S., Li, M., Zhang, C., Tan, Q., Yang, X., Sun, X., et al. (2021). Effects of phosphorus on fruit soluble sugar and citric acid accumulations in citrus. *Plant Physiol. Biochem.* 160, 73–81. doi: 10.1016/j.plaphy.2021.01.015

Wu, L., Ren, C., Jiang, H., Zhang, W., Chen, N., Zhao, X., et al. (2024). Land abandonment transforms soil microbiome stability and functional profiles in apple orchards of the Chinese Losses Plateau. *Sci. Total Environ.* 906, 167556. doi: 10.1016/j.scitotenv.2023.167556

Xiao, Y., Wang, J., Wang, B., Fan, B., and Zhou, G. (2025). Soil microbial network complexity predicts soil multifunctionality better than soil microbial diversity during grassland-farmland-shrubland conversion on the Qinghai-Tibetan Plateau. *Agriculture Ecosyst. Environment.* 379, 109356. doi: 10.1016/j.agee.2024.109356

Yang, R., Song, S., Chen, S., Du, Z., and Kong, J. (2023). Adaptive evaluation of green manure rotation for a low fertility farmland system: impacts on crop yield, soil nutrients, and soil microbial community. *CATENA*. 222, 106873. doi: 10.1016/j.catena.2022.106873

Yang, Y., Tang, N., Li, Z., and Huang, T. (2014). Study on quality changes during fruit development of five late-maturing citrus varieties. *Southwest China J. Agric. Sci.* 27, 263–267. doi: 10.16213/j.cnki.scjas.2014.01.070

Yao, F., Wen, L., Chen, R., Du, C., Su, S., Yan, M., et al. (2022). Enrichment characteristics and dietary evaluation of selenium in navel orange fruit from the largest navel orange-producing area in China (southern Jiangxi). *Front. Plant Sci.* 13, 880198. doi: 10.3389/fpls.2022.881098

Yu, X., Du, C., Wang, X., Gao, F., Lu, J., Di, X., et al. (2024). Multivariate analysis between environmental factors and fruit quality of citrus at the core navel orange-producing area in China. *Front. Plant Sci.* 15, 1510827. doi: 10.3389/fpls.2024.1510827

Yu, Q., Qiu, Z., Zhao, M., Lv, H., Sun, L., Wang, Y., et al. (2025). Trifolium intercropping promotes amino acid metabolism and suppresses flavonoid metabolism of tea plants. *Beverage Plant Res.* 5, e013. doi: 10.48130/bpr-0025-0003

Yu, Y., Xiao, G., Xu, Y., Wu, J., Fu, M., and Wen, J. (2015). Slight Fermentation with Lactobacillus fermentium Improves the Taste (Sugar: Acid Ratio) of Citrus (Citrus reticulata cv. chachiensis) Juice. *J. Food Sci.* 80, M2543–M2547. doi: 10.1111/1750-3841.13088

Zhai, C., Han, L., Xiong, C., Ge, A., Yue, X., Li, Y., et al. (2024). Soil microbial diversity and network complexity drive the ecosystem multifunctionality of temperate grasslands under changing precipitation. *Sci. total Environ*. 906, 167217. doi: 10.1016/j.scitotenv.2023.167217

Zhang, J., Nie, J., Cao, W., Gao, Y. J., Lu, Y. H., and Liao, Y. (2022). Long-term green manuring to substitute partial chemical fertilizer simultaneously improving crop productivity and soil quality in a double-rice cropping system. *Eur. J. Agron.* 142, 126641. doi: 10.1016/j.eja.2022.126641

Zhao, Y., Zhou, J., Chen, L., Li, S., Yin, Y., Jeyaraj, A., et al. (2025). Allelopathic effect of osmanthus fragrans changes the soil microbial community and increases the soil nutrients and the aroma quality of tea leaves. *J. Agric. Food Chem.* 73, 13818–13831. doi: 10.1021/acs.jafc.5c03692

Zhou, J., Deng, Y., Luo, F., He, Z., Tu, Q., and Zhi, X.. (2010). Functional molecular ecological networks. *mBio* 1, e00169–10. doi: 10.1128/mBio.00169-10

Zhou, Y., Tang, Y., Hu, C., Zhan, T., Zhang, S., Cai, M., et al. (2021). Soil applied Ca, Mg and B altered phyllosphere and rhizosphere bacterial microbiome and reduced Huanglongbing incidence in Gannan Navel Orange. *Sci. Total Environ.* 791, 148046. doi: 10.1016/j.scitotenv.2021.148046

Zhou, X., Wang, J., Liu, F., Liang, J., Zhao, P., Tsui, C. K. M., et al. (2022). Cross-kingdom synthetic microbiota supports tomato suppression of Fusarium wilt disease. *Nat. Commun.* 13, 7890. doi: 10.1038/s41467-022-35452-6

Zhu, W., Lu, X., Hong, C., Hong, L., Ding, J., Zhou, W., et al. (2023). Pathogen resistance in soils associated with bacteriome network reconstruction through reductive soil disinfestation. *Appl. Microbiol. Biotechnol.* 107, 5829–5842. doi: 10.1007/s00253-023-12676-0

frontiers | Frontiers in Plant Science

TYPE Mini Review
PUBLISHED 24 September 2025
DOI 10.3389/fpls.2025.1652366

OPEN ACCESS

EDITED BY
Zhen Wang,
Yunnan Agricultural University, China

REVIEWED BY
Adil Zahoor,
University of Arkansas, United States
Yohannes Ebabuye Andargie,
Kyungpook National University,
Republic of Korea

*CORRESPONDENCE
Birgit Wassermann
Birgit.wassermann@tugraz.at

†These authors have contributed equally to this work

RECEIVED 23 June 2025
ACCEPTED 12 August 2025
PUBLISHED 24 September 2025

CITATION
Bziuk N, Wassermann B, Bickel S, Omidvar R, Manica A and Berg G (2025) *Aureobasidium pullulans*: a microbiome-based perspective from global biomes to edible plant tissues. *Front. Plant Sci.* 16:1652366. doi: 10.3389/fpls.2025.1652366

Aureobasidium pullulans: a microbiome-based perspective from global biomes to edible plant tissues

Nina Bziuk[1,2†], Birgit Wassermann[1,2*†], Samuel Bickel[2], Reza Omidvar[3], Andrea Manica[3] and Gabriele Berg[2,4,5]

[1]Austrian Centre of Industrial Biotechnology (ACIB), Graz, Austria, [2]Institute of Environmental Biotechnology, Graz University of Technology, Graz, Austria, [3]SAN Agrow Holding GmbH, Herzogenburg, Austria, [4]Microbiome Biotechnology, Leibniz Institute for Agricultural Engeneering and Bioeconomy (ATB), Potsdam, Germany, [5]Institute for Biochemistry and Biology, University of Potsdam, Potsdam, Germany

Aureobasidium pullulans is a globally distributed fungus commonly found in plant-associated and anthropogenic environments. Known for its antagonistic activity against plant pathogens, it is widely used as a biocontrol agent in sustainable agriculture. Despite its prevalence in edible plant tissues and frequent environmental exposure, its broader role within microbiomes and potential relevance for human health remain underexplored. In this perspective article, we highlight the global distribution of *A. pullulans* based on publicly available sequencing data and examine its ecological function from a microbiome-based viewpoint. Our synthesis supports the view of *A. pullulans* as a safe, plant-beneficial symbiont with high value for sustainable crop protection and potential relevance for the One Health framework. Future microbiome research should further explore its functional roles within plant and human-associated microbiomes to better harness its benefits while ensuring biosafety across ecosystems.

KEYWORDS

one health, crop protection, global occurrence, *Aureobasidium pullulans*, edible microbiome

Introduction

The fungus *Aureobasidium pullulans* (De Bary) Arnaud, commonly known as the 'black yeast', was first described 150 years ago (Cooke, 1959). At that time, like the majority of microorganisms, *A. pullulans* was subjected to an anthropocentric perspective on the microbial world, i.e., the mere presence of a microorganism implies disease (Heidenreich et al., 1997). Though ahead of the times, Cooke discussed the ecological life history of *A. pullulans* in 1959 and highlighted that more intense studies may demonstrate its independence from saprobic and pathogenic strains (Cooke, 1959). The discovery of the

microbiome, a term first defined by Whipps et al. (1988) and newly conceptualized by Berg et al. (2020) has provided an alternative to the anthropocentric perspective on microbial life. Microorganisms are ubiquitous providers of key ecosystem services and are, thus, intrinsically associated with the health of eukaryotic hosts. This has led to the definition of the holobiont, which refers to a host organism together with all of its associated microorganisms, including bacteria, archaea, fungi, viruses, and protists, forming a complex ecological unit (Vandenkoornhuyse et al., 2015). This concept emphasizes that the biology, evolution, and health of the host cannot be fully understood without considering its microbial interactions and co-evolutionary dynamics. Furthermore, the microbiome interconnects holobionts; for example, plant-associated bacteria in food can withstand human digestion (Wicaksono et al., 2022) and may inhabit the human gut, representing an underexplored but important component of the exposome (Wicaksono et al., 2023a), which is defined as the sum of exposures to which an individual is subjected during their lifespan.

A. pullulans is a frequent member of the environmental microbiome. Due to its targeted antagonistic activity, the fungus can protect crops against various plant pathogens, such as *Monilinia laxa*, *Botrytis cinerea, Alternaria alternata, and Fusarium spp* (Zajc et al., 2020; Iqbal et al., 2021; Wachowska et al., 2021; Di Francesco et al., 2023). Initially, *A. pullulans* was categorized into four subspecies: *A. pullulans* var. *pullulans*, var. *melanogenum*, var. *subglaciale*, and var. *namibiae* (Zalar et al., 2008). However, significant genomic differences among these groups warranted their reclassification as four distinct species: *A. pullulans, A. subglaciale, A. namibiae*, and *A. melanogenum* (Gostinčar et al., 2014). This revised taxonomy is particularly important for biotechnological applications in agriculture, as it clearly distinguishes *A. melanogenum* – a species with strains that may possess pathogenic potential for humans – from the agriculturally relevant species *A. pullulans* (Gostinčar et al., 2014; Černoša et al., 2025). *A. pullulans* has been considered safe for various agricultural applications (European Food Safety Authority, 2013; Prasongsuk et al., 2018), and its unparalleled global distribution and use for a sustainable economy (Rensink et al., 2024) calls for studying it in relation to the One Health concept. The importance of *A. pullulans* as an effective biocontrol agent, as well as its applicability in diverse sectors of the sustainable food industry, has been comprehensively reviewed by Di Francesco and colleagues (Di Francesco et al., 2023). However, a microbiome-based perspective on the global and host-associated role of *A. pullulans* is still missing. In this perspective paper, we review the literature on *A. pullulans* occurrence from a microbiome-based perspective to gain new insights into its global prevalence in different biomes and the potential for human exposure by representing a common member of the edible plant microbiome.

A. pullulans is prevalent in anthropogenic environments

A. pullulans is known for its host- and non-host-associated lifestyles. The fungus has been detected in numerous ecosystems, ranging from soils (Ignatova et al., 2015; Ademakinwa and Agboola, 2016; Bennamoun et al., 2016), freshwater and marine environments (Gunde-Cimerman et al., 2000; Wang et al., 2009), deserts and drylands (Coleine et al., 2021), glaciers' ice and permafrost (Branda et al., 2010; Sannino et al., 2020), as well as in the air and atmosphere (Shelton et al., 2002; Griffin, 2007). *A. pullulans* survives in acidic and alkaline surroundings (Cooke, 1959), and saline soils (Bennamoun et al., 2016). Due to its prevalence in extreme habitats, the fungus was described as a polyextremotolerant microorganism (Gostinčar et al., 2023) because it can survive cold as well as hot temperatures up to 50° C (Zajc et al., 2020). However, *A. pullulans* does not grow well at 37°C (Zajc et al., 2020). Interestingly, the fungus does not show substantial specialization in any of these habitats at the genomic level (Gostinčar et al., 2019). Frequent recombination between *A. pullulans* strains could diminish the structuring of the global *A. pullulans* population (Gostinčar et al., 2019).

We conducted a taxonomy-based search for *A. pullulans* in the GlobalFungi database (Větrovský et al., 2020), which contains high-throughput sequencing metabarcoding studies, to illustrate its global distribution (Figure 1). We used two search terms to query the database: (i) an empty prompt to retrieve all samples and (ii) "*Aureobasidium pullulans*" to obtain samples where *A. pullulans* was detected. These two tables were merged, and a total of 57'184 samples were obtained (as of 02.11.2023). We included only samples from 515 studies that were not flagged as "manipulated", used non-nested primers (covering ITS1, ITS2, or full-length ITS), and contained at least 500 samples per study. This resulted in a total of (i) 50'084 total samples and (ii) 10'191 samples in which *A. pullulans* was detected. Due to the compositional nature of the sequencing data and the high variability among reads between the different primers (Supplementary Figures 1, 2), we used presence/absence to delineate the global distribution of *A. pullulans*. Nonetheless, with an increasing number of reads, the detection of *A. pullulans* was more likely, and this was reflected in an increased prevalence (Supplementary Figure 3). Hence, we used prevalence for the purpose of delineating the occurrence probability of *A. pullulans* globally.

Our analysis demonstrates that *A. pullulans* can occur in various environments. Although *A. pullulans* occurred on all continents, it was more often detected in anthropogenic environments (51% of n = 707 samples) and croplands (36%, n = 2'713) compared to natural environments (19%, n = 46'664). Interestingly, *A. pullulans* was most prevalent in atmospheric samples, including air and dust. The high prevalence in soil (24%, n = 28'433), organic matter (28%, n = 3043), and atmospheric samples (34%, n = 838) suggests that it is often present in our surroundings. Hence, we expect frequent human exposure to *A. pullulans* across different environments with a low risk for hazard incidents (Prasongsuk et al., 2018).

A. pullulans is an effective biological agent in agriculture

The prevalence of *A. pullulans* in croplands is likely attributable to its broad use as an effective biocontrol agent against bacterial and

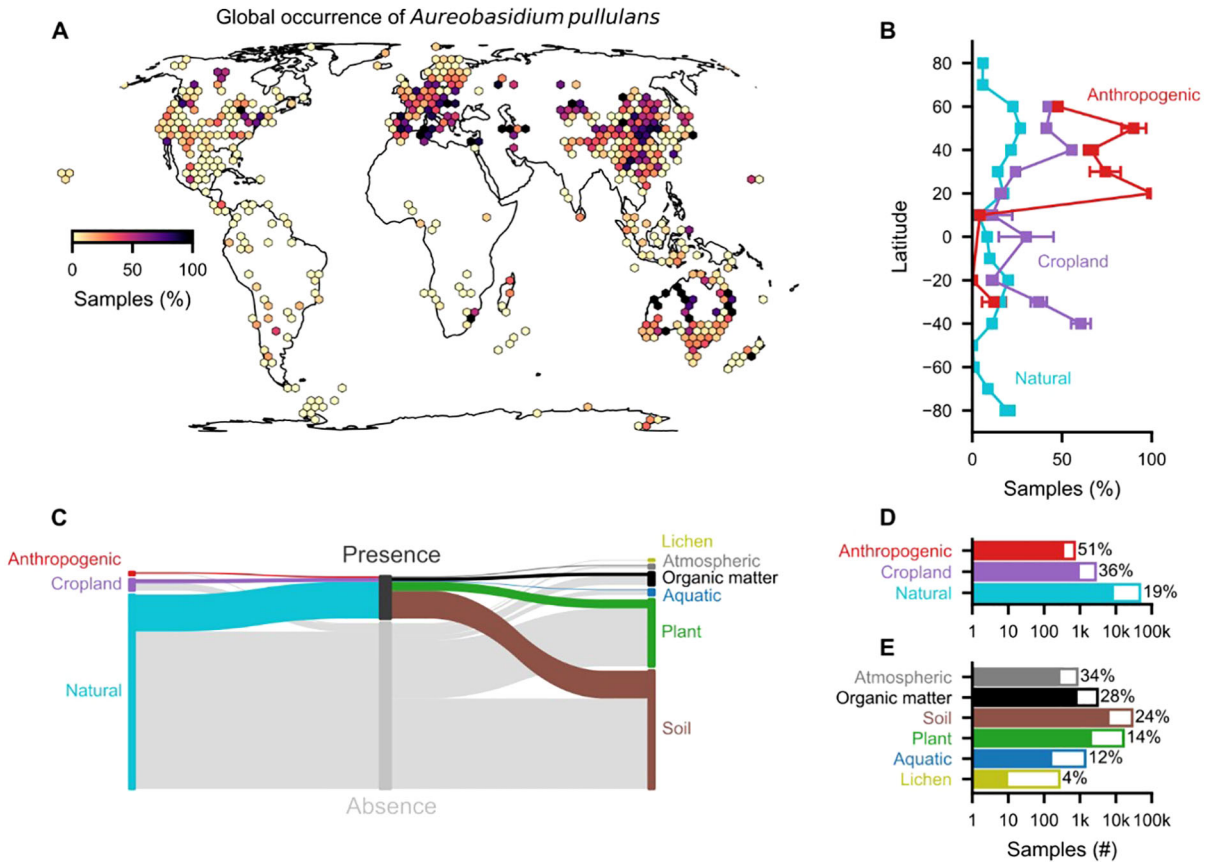

FIGURE 1
Global occurrence of *A. pullulans*. **(A)** Percentage of samples with *A. pullulans* out of 515 studies based on ITS sequences (ITS1, ITS2, full-length ITS), showing a total of 57'184 samples. **(B)** Latitudinal occurrence patterns in different environments (mean ± SE). **(C)** Distribution of samples with the presence/absence of *A. pullulans* in different environments and sample types. **(D)** Total number of samples in different environments and **(E)** sample types; percentages are represented by the colored part of the bars and indicate the fraction of samples with *A. pullulans*. The 50'084 samples were obtained from the GlobalFungi database (02.11.2023; Větrovský et al., 2020).

fungal phytopathogens. Several organic disease control products based on *A. pullulans* are already on the market (e.g., Boni Protect, Blossom Protect, Botector) and are highly promising alternatives to problematic chemicals in viticulture and horticulture, both pre- and postharvest. This is of high importance considering, for instance, the European Green Deal proposing a reduction of the use and risk of pesticides by 50% by 2030.

Over the past decades, *A. pullulans* strains have been applied as single organisms, and in combination with other organisms and chemical peptides (Zajc et al., 2020). Nevertheless, most studies focus on fruit crops, whereas the potential impact of *A. pullulans* on cereals and legumes is less explored. Pre-harvest applications have shown effectiveness against pathogens such as *Erwinia amylovora* in apples (Slack et al., 2019; Zeng et al., 2023), *Diplodia seriata* in grapevines (Pinto et al., 2018), and *Verticillium dahliae* in olive trees (López-Moral et al., 2021, 2022). Post-harvest studies have focused mainly on fruits, demonstrating biocontrol of *Botrytis cinerea* in strawberries, apples, and grapes (Schena et al., 2003; Mari et al., 2012; Iqbal et al., 2022), *Monilinia laxa* in stone fruits (Zhang et al., 2010; Di Francesco et al., 2018), or diverse *Penicillium* species in tropical and non-tropical fruits (Ippolito et al., 2000; Janisiewicz et al., 2000; Zhang et al., 2010, p. 20; Mari et al., 2012; Parafati et al., 2017), just to name some examples. In some cases, it has been used successfully in microbial consortia with *Bacillus subtilis* (Bellamy et al., 2022). In a recent study, *A. pullulans* was transmitted via bees to strawberry flowers, resulting in decreased strawberry post-harvest infections with *B. cinerea* (Iqbal et al., 2022). The potential impact of *A. pullulans* on insects and their microbiome has not been assessed so far (Davis and Landolt, 2013; Hung et al., 2015). Overall, *A. pullulans* is mainly used as a direct antagonist towards phytopathogens, and the main mode of action of *A. pullulans* is referred to as a competition for space and nutrients. However, *A. pullulans* might also have the ability, due to its wide genetic equipment, to induce systemic resistance in plants, which was shown lately by Zeng et al. (2023), demonstrating increased gene expression of pathogenesis-related genes. Further evidence for *A. pullulans*' broad spectrum application potential is given by its postulated function in abiotic stress management of coniferous trees under drought stress (Mannaa et al., 2023), underlining the global potential of *A. pullulans*.

Another important consideration for the use of biocontrol agents is their interaction with the native microbiome in plants

and soil, although this aspect has been less explored to date. A recent study showed that the dominance of *A. pullulans* on fruit surfaces resulted in a decreased abundance of naturally occurring phytopathogenic fungi and an increased proportion of bacteria with plant growth-promoting properties (Shi et al., 2022). Since the application and occurrence of *A. pullulans* seems to potentially result in benefits for the plant, we suggest that *A. pullulans* could be considered a fungal soterobiont. This term has recently been postulated to describe microorganisms – artificially applied or native to the plant – that can extend the host plant´s immune system by providing active protection against pathogens, which results in resistant phenotypes (Cernava and Berg, 2022). However, both genetic and functional aspects of *A. pullulans*, the host plant, and other members of the plant microbiota must be considered to build a comprehensive understanding of the dynamics within the holobiont.

A. pullulans is a native member of the plant and the edible microbiome

The native plant microbiome assists the host plant in acquiring nutrients, suppressing pathogens, enhancing stress tolerance, and regulating plant hormones (Sánchez-Cañizares et al., 2017; Berg et al., 2022; Gross, 2022). Thus, plants rely on their associated microbiota and are unlikely to survive without them under natural conditions (Paasch et al., 2023). *A. pullulans* displays a plethora of properties and was observed to natively colonize various plants, including wheat (Wachowska et al., 2020), apple (Abdelfattah et al., 2022), grapevine (Wassermann et al., 2021), olive trees (López-Moral et al., 2021), *Ficus* (Singh and Saini, 2008), wildflowers (Choudhury et al., 2011), and seeds of native alpine plants (Wassermann et al., 2019a). In addition, *A. pullulans* was frequently documented to occur in the edible parts of fresh produce, such as apples (Wassermann et al., 2019b; Abdelfattah et al., 2021; Zhimo et al., 2022), cherries (Schena et al., 2003; Molnárová et al., 2014), peaches (Zhang et al., 2010; Molnárová et al., 2014), citrus (Ferraz et al., 2016), and strawberries (Adikaram et al., 2002), and a large body of literature observed *A. pullulans* in berries of grapevine (Fleet, 2003; Martini et al., 2009; Verginer et al., 2010; Grube et al., 2011; Barata et al., 2012; Pinto et al., 2014). However, these observations are mainly based on PCR-based marker gene profiling or microbial cultivation methods, which do not provide direct information regarding actual microbial loads.

Based on the global data set, we found a wide range of sequence reads of *A. pullulans* across the different samples, reaching high percentages in certain samples (Supplementary Figure 2). However, microbiome-based quantitative data on the fungal plant microbiota remain limited. To estimate the load of *A. pullulans* in plant tissues, we analyzed a previously published dataset on the apple microbiome (Abdelfattah et al., 2022). The data includes marker gene sequences (ITS) and quantitative real-time PCR (ITS gene copy numbers (GCN) per centimeter of shoot length) measurements for the endophytic microbiota of 61 apple accessions from 11 *Malus* species. The total fungal load ranged from 10^6 GCN cm^{-1} to 10^9 GCN cm^{-1} in domesticated apples (Abdelfattah et al., 2022), and *A. pullulans* sequences accounted for 36% to 51% of all fungal GCN in these samples, indicating that the fungus is a native and significant member of the apple microbiome. This example supports *A. pullulans*' environmental prevalence and shows its potential for host interaction, as microbial abundance is a key determinant of ecological relevance and functional impact on the host (Lloréns-Rico et al., 2021).

In general, while all niche-specific microbiota play a functional role for the plant (Trivedi et al., 2020), and for humans as consumers, microbes associated with the edible parts of a plant can pose health benefits and risks (Berg et al., 2015; Kim et al., 2020). The risks are deeply studied, yet human pathogens causing food-borne outbreaks, as well as opportunistic pathogens that cause healthcare-associated infections (Mehta et al., 2017), are still of global concern, accelerated by the drivers of the Anthropocene (Flandroy et al., 2018). However, edible plants are colonized by a huge diversity of microorganisms, and only a very small fraction may have adverse impacts on healthy humans (Berg et al., 2015). Those microbes represent the edible plant microbiome and are an important component of the exposome (Berg et al., 2015; Wicaksono et al., 2023a). Studies suggest that the edible microbiome may positively impact the gut microbiome and human health. Fruit and vegetable-derived bacteria are, despite their low abundance, consistently present in the human gut, enriching the functional diversity of the gut microbiota due to the presence of genes associated with benefits for human health (Wicaksono et al., 2023b). Besides bacteria, eukaryotic organisms are important components of the gut microbiome (Zhang et al., 2022); yet, to our knowledge, no comparable studies on fruit- and vegetable-transmitted fungi in the human gut have been conducted so far (Laforest-Lapointe and Arrieta, 2018). Nonetheless, *A. pullulans* has been detected in stool samples of healthy humans (Maas et al., 2023). In addition, it is known that fungal β-glucans play an important role in the human immune system (Zhang et al., 2022) and also the compounds produced by *A. pullulans* may have potential health benefits for humans (Ikewaki et al., 2023; Raghavan et al., 2023). Analyzing the diversity of fungi and other eukaryotes in the human gut and whether they are delivered via plant consumption will help uncover those microorganisms' roles for host health.

Conclusion

A. pullulans is a globally distributed fungus commonly found in anthropogenic environments and croplands. Research indicates that *A. pullulans* pose minimal health risks to humans (Gostinčar et al., 2014). Yet, given its widespread occurrence in food and the

environment, animal and human exposure is probable, necessitating comprehensive risk assessments to ensure safety. The fungus's beneficial properties for plants, including pathogen suppression and crop protection, along with its native abundance in wild plants and crops, underscore its potential relevance for future agricultural practices aligned with the One Health framework. Future research should focus on its interaction with the native plant and the environmental microbiome. Further, its role within the human exposome and gut microbiome needs to be explored to better understand its interactions and any potential health implications.

Author contributions

NB: Writing – original draft, Writing – review & editing. BW: Writing – original draft, Writing – review & editing. SB: Writing – original draft, Writing – review & editing. RO: Writing – review & editing. AM: Writing – review & editing. GB: Writing – review & editing.

Funding

The author(s) declare financial support was received for the research and/or publication of this article. The COMET center: acib: Next Generation Bioproduction is funded by BMIMI, BMWET, SFG, Standortagentur Tirol, Government of Lower Austria aund Vienna Business Agency in the framework of COMET -Competence Centers for Excellent Technologies. The COMET-Funding Program is managed by the Austrian Research Promotion Agency FFG. This work was supported by TU Graz Open Access Publishing Fund.

Conflict of interest

Author RO and AM were employed by the company SAN Agrow Holding GmbH.

The remaining authors declare that the research was conducted in the absence of any commercial or financial relationships that could be construed as a potential conflict of interest.

Generative AI statement

The author(s) declare that no Generative AI was used in the creation of this manuscript.

Any alternative text (alt text) provided alongside figures in this article has been generated by Frontiers with the support of artificial intelligence and reasonable efforts have been made to ensure accuracy, including review by the authors wherever possible. If you identify any issues, please contact us.

Publisher's note

Supplementary material

The Supplementary Material for this article can be found online at: https://www.frontiersin.org/articles/10.3389/fpls.2025.1652366/full#supplementary-material

References

Abdelfattah, A., Freilich, S., Bartuv, R., Zhimo, V. Y., Kumar, A., Biasi, A., et al. (2021). Global analysis of the apple fruit microbiome: are all apples the same? *Environ. Microbiol.* 23, 6038–6055. doi: 10.1111/1462-2920.15469

Abdelfattah, A., Tack, A. J. M., Wasserman, B., Liu, J., Berg, G., Norelli, J., et al. (2022). Evidence for host–microbiome co-evolution in apple. *New Phytol.* 234, 2088–2100. doi: 10.1111/nph.17820

Ademakinwa, A. N., and Agboola, F. K. (2016). Biochemical characterization and kinetic studies on a purified yellow laccase from newly isolated Aureobasidium pullulans NAC8 obtained from soil containing decayed plant matter. *J. Genet. Eng. Biotechnol.* 14, 143–151. doi: 10.1016/j.jgeb.2016.05.004

Adikaram, N. K. B., Joyce, D. C., and Terryc, L. A. (2002). Biocontrol activity and induced resistance as a possible mode of action for Aureobasidium pullulans against grey mould of strawberry fruit. *Australas. Plant Pathol.* 31, 223–229. doi: 10.1071/AP02017

Barata, A., Malfeito-Ferreira, M., and Loureiro, V. (2012). The microbial ecology of wine grape berries. *Int. J. Food Microbiol.* 153, 243–259. doi: 10.1016/j.ijfoodmicro.2011.11.025

Bellamy, S., Shaw, M., and Xu, X. (2022). Field application of Bacillus subtilis and Aureobasidium pullulans to reduce Monilinia laxa post-harvest rot on cherry. *Eur. J. Plant Pathol.* 163, 761–766. doi: 10.1007/s10658-022-02508-8

Bennamoun, L., Hiligsmann, S., Dakhmouche, S., Ait-Kaki, A., Labbani, F.-Z., Nouadri, T., et al. (2016). Production and Properties of a Thermostable, pH—Stable Exo-Polygalacturonase Using Aureobasidium pullulans Isolated from Saharan Soil of Algeria Grown on Tomato Pomace. *Foods* 5, 72. doi: 10.3390/foods5040072

Berg, G., Erlacher, A., and Grube, M. (2015). "The edible plant microbiome: importance and health issues," in *Principles of Plant-Microbe Interactions* (Springer International Publishing, Cham), 419–426. doi: 10.1007/978-3-319-08575-3_44

Berg, G., Rybakova, D., Fischer, D., Cernava, T., Vergès, M.-C. C., Charles, T., et al. (2020). Microbiome definition re-visited: old concepts and new challenges. *Microbiome* 8, 103. doi: 10.1186/s40168-020-00875-0

Berg, G., Kusstatscher, P., Wassermann, B., Cernava, T., and Abdelfattah, A.. (2022). "Beneficial microbes for agriculture," in *Good Microbes in Medicine, Food Production, Biotechnology, Bioremediation, and Agriculture*, eds. F. J. De Bruijn, H. Smidt, L. S. Cocolin, M. Sauer, D. Dowling and L. Thomashow (Wiley), 427–443. doi: 10.1002/9781119762621.ch34

Branda, E., Turchetti, B., Diolaiuti, G., Pecci, M., Smiraglia, C., and Buzzini, P. (2010). Yeast and yeast-like diversity in the southernmost glacier of Europe (Calderone Glacier, Apennines, Italy). *FEMS Microbiol. Ecol.* 72, 354–369. doi: 10.1111/j.1574-6941.2010.00864.x

Cernava, T., and Berg, G. (2022). The emergence of disease-preventing bacteria within the plant microbiota. *Environ. Microbiol.* 24, 3259–3263. doi: 10.1111/1462-2920.15896

Černoša, A., Gostinčar, C., Holcar, M., Kostanjšek, R., Lenassi, M., and Gunde-Cimerman, N. (2025). The impact of Aureobasidium melanogenum cells and extracellular vesicles on human cell lines. *Sci. Rep.* 15, 1413. doi: 10.1038/s41598-024-84189-3

Choudhury, A. R., Saluja, P., and Prasad, G. S. (2011). Pullulan production by an osmotolerant Aureobasidium pullulans RBF-4A3 isolated from flowers of Caesulia axillaris. *Carbohydr. Polymers* 83, 1547–1552. doi: 10.1016/j.carbpol.2010.10.003

Coleine, C., Stajich, J. E., de los Ríos, A., and Selbmann, L. (2021). Beyond the extremes: Rocks as ultimate refuge for fungi in drylands. *Mycologia* 113, 108–133. doi: 10.1080/00275514.2020.1816761

Cooke, W. (1959). An ecological life history of Aureobasidium pullulans (de Bary) Arnaud. *Mycopathologia Mycologia Applicata* 12, 1–45. doi: 10.1007/BF02118435

Davis, T. S., and Landolt, P. J. (2013). A survey of insect assemblages responding to volatiles from a ubiquitous fungus in an agricultural landscape. *J. Chem. Ecol.* 39, 860–868. doi: 10.1007/s10886-013-0278-z

Di Francesco, A., Mari, M., Ugolini, L., and Baraldi, E. (2018). Effect of Aureobasidium pullulans strains against Botrytis cinerea on kiwifruit during storage and on fruit nutritional composition. *Food Microbiol.* 72, 67–72. doi: 10.1016/j.fm.2017.11.010

Di Francesco, A., Zajc, J., and Stenberg, J. A. (2023). Aureobasidium spp.: diversity, versatility, and agricultural utility. *Horticulturae* 9, 59. doi: 10.3390/horticulturae9010059

European Food Safety Authority (2013). Conclusion on the peer review of the pesticide risk assessment of the active substance Aureobasidium pullulans (strains DSM 14940 and DSM 14941). *EFSA J.* 11. doi: 10.2903/j.efsa.2013.3183

Ferraz, L. P., da Cunha, T., da Silva, A. C., and Kupper, K. C. (2016). Biocontrol ability and putative mode of action of yeasts against Geotrichum citri-aurantii in citrus fruit. *Microbiological Res.*, 188–189, 72–79. doi: 10.1016/j.micres.2016.04.012

Flandroy, L., Poutahidis, T., Berg, G., Clarke, G., Dao, M.-C., Decaestecker, E., et al. (2018). The impact of human activities and lifestyles on the interlinked microbiota and health of humans and of ecosystems. *Sci. Total Environ.* 627, 1018–1038. doi: 10.1016/j.scitotenv.2018.01.288

Fleet, G. (2003). Yeast interactions and wine flavour. *Int. J. Food Microbiol.* 86, 11–22. doi: 10.1016/S0168-1605(03)00245-9

Gostinčar, C., Ohm, R. A., Kogej, T., Sonjak, S., Turk, M., Zajc, J., et al. (2014). Genome sequencing of four Aureobasidium pullulans varieties: biotechnological potential, stress tolerance, and description of new species. *BMC Genomics* 15, 549. doi: 10.1186/1471-2164-15-549

Gostinčar, C., Turk, M., Zajc, J., and Gunde-Cimerman, N. (2019). Fifty *Aureobasidium pullulans* genomes reveal a recombining polyextremotolerant generalist. *Environ. Microbiol.* 21, 3638–3652. doi: 10.1111/1462-2920.14693

Gostinčar, C., Stajich, J. E., and Gunde-Cimerman, N. (2023). Extremophilic and extremotolerant fungi. *Curr. Biol.* 33, R752–R756. doi: 10.1016/j.cub.2023.06.011

Griffin, D. W. (2007). Atmospheric movement of microorganisms in clouds of desert dust and implications for human health. *Clin. Microbiol. Rev.* 20, 459–477. doi: 10.1128/CMR.00039-06

Gross, M. (2022). How plants grow their microbiome. *Curr. Biol.* 32, R97–R100. doi: 10.1016/j.cub.2022.01.044

Grube, M., Schmid, F., and Berg, G. (2011). Black fungi and associated bacterial communities in the phyllosphere of grapevine. *Fungal Biol.* 115, 978–986. doi: 10.1016/j.funbio.2011.04.004

Gunde-Cimerman, N., Zalar, P., Hoog, S., and PlemenitaÅš, A. (2000). Hypersaline waters in salterns â&128;&147; natural ecological niches for halophilic black yeasts'. *FEMS Microbiol. Ecol.* 32, 235–240. doi: 10.1111/j.1574-6941.2000.tb00716.x

Heidenreich, M. C. M., Corral-Garcia, M. R., Momol, E. A., and Burr, T. J. (1997). Russet of Apple Fruit Caused by Aureobasidium pullulans and Rhodotorula glutinis. *Plant Dis.* 81, 337–342. doi: 10.1094/PDIS.1997.81.4.337

Hung, K. Y., Michailides, T. J., Millar, J. G., Wayadande, A., and Gerry, A. C. (2015). House fly (Musca domestica L.) attraction to insect honeydew. *PloS One* 10, e0124746. doi: 10.1371/journal.pone.0124746

Ignatova, L. V., Brazhnikova, Y. V., Berzhanova, R. Z., and Mukasheva, T. D. (2015). Plant growth-promoting and antifungal activity of yeasts from dark chestnut soil. *Microbiological Res.* 175, 78–83. doi: 10.1016/j.micres.2015.03.008

Ikewaki, N., Sonoda, T., Kurosawa, G., Iwasaki, M., Devaprasad Dedeepiya, V., Senthilkumar, R., et al. (2023). Beta 1,3-1,6 glucans produced by two novel strains of aureobasidium pullulans exert immune and metabolic beneficial effects in healthy middle-aged Japanese men: results of an exploratory randomized control study. *J. Aging Res. Lifestyle* 12, 61–71. doi: 10.14283/jarlife.2023.11

Ippolito, A., El Ghaouth, A., Wilson, C. L., and Wisniewski, M. (2000). Control of postharvest decay of apple fruit by Aureobasidium pullulans and induction of defense responses. *Postharvest Biol. Technol.* 19, 265–272. doi: 10.1016/S0925-5214(00)00104-6

Iqbal, M., Jamshaid, M., Zahid, M. A., Andreasson, E., Vetukuri, R. R., and Stenberg, J. A. (2021). Biological control of strawberry crown rot, root rot and grey mould by the beneficial fungus Aureobasidium pullulans. *BioControl* 66, 535–545. doi: 10.1007/s10526-021-10083-w

Iqbal, M., Jützeler, M., França, S. C., Wäckers, F., Andreasson, E., and Stenberg, J. A. (2022). Bee-vectored *Aureobasidium pullulans* for biological control of Gray Mold in strawberry. *Phytopathology®* 112, 232–237. doi: 10.1094/PHYTO-05-21-0205-R

Janisiewicz, W. J., Tworkoski, T. J., and Sharer, C. (2000). Characterizing the mechanism of biological control of postharvest diseases on fruits with a simple method to study competition for nutrients. *Phytopathology®* 90, 1196–1200. doi: 10.1094/PHYTO.2000.90.11.1196

Kim, J., Yoon, S.-J., Park, Y.-J., Kim, S.-Y., and Ryu, C.-M. (2020). Crossing the kingdom border: Human diseases caused by plant pathogens. *Environ. Microbiol.* 22, 2485–2495. doi: 10.1111/1462-2920.15028

Laforest-Lapointe, I., and Arrieta, M.-C. (2018). Microbial eukaryotes: a missing link in gut microbiome studies. *mSystems* 3, e00201–e00217. doi: 10.1128/mSystems.00201-17

Lloréns-Rico, V., Vieira-Silva, S., Gonçalves, P. J., Falony, G., and Raes, J. (2021). Benchmarking microbiome transformations favors experimental quantitative approaches to address compositionality and sampling depth biases. *Nat. Commun.* 12. doi: 10.1038/s41467-021-23821-6

López-Moral, A., Agustí-Brisach, C., and Trapero, A. (2021). Plant biostimulants: new insights into the biological control of verticillium wilt of olive. *Front. Plant Sci.* 12. doi: 10.3389/fpls.2021.662178

López-Moral, A., Llorens, E., Scalschi, L., García-Agustín, P., Trapero, A., and Agustí-Brisach, C. (2022). Resistance induction in olive tree (Olea europaea) against verticillium wilt by two beneficial microorganisms and a copper phosphite fertilizer. *Front. Plant Sci.* 13. doi: 10.3389/fpls.2022.831794

Maas, E., Penders, J., and Venema, K. (2023). Fungal-bacterial interactions in the human gut of healthy individuals. *J. Fungi* 9, 139. doi: 10.3390/jof9020139

Mannaa, M., Han, G., Jung, H., Park, J., Kim, J.-C., Park, A. R., et al. (2023). Aureobasidium pullulans Treatment Mitigates Drought Stress in Abies koreana via Rhizosphere Microbiome Modulation. *Plants* 12, 3653. doi: 10.3390/plants12203653

Mari, M., Martini, C., Spadoni, A., Rouissi, W., and Bertolini, P. (2012). Biocontrol of apple postharvest decay by Aureobasidium pullulans. *Postharvest Biol. Technol.* 73, 56–62. doi: 10.1016/j.postharvbio.2012.05.014

Martini, M., Musetti, R., Grisan, S., Polizzotto, R., Borselli, S., Pavan, F., et al. (2009). DNA-Dependent Detection of the Grapevine Fungal Endophytes Aureobasidium pullulans and Epicoccum nigrum. *Plant Dis.* 93, 993–998. doi: 10.1094/PDIS-93-10-0993

Mehta, S. R., Johns, S., Stark, P., and Fierer, J. (2017). Successful treatment of Aureobasidium pullulans central catheter-related fungemia and septic pulmonary emboli. *IDCases* 10, 65–67. doi: 10.1016/j.idcr.2017.08.017

Molnárová, J., Vadkertiová, R., and Stratilová, E. (2014). Extracellular enzymatic activities and physiological profiles of yeasts colonizing fruit trees. *J. Basic Microbiol.* 54, S74–S84. doi: 10.1002/jobm.201300072

Paasch, B. C., Sohrabi, R., Kremer, J. M., Nomura, K., Cheng, Y. T., Martz, J., et al. (2023). A critical role of a eubiotic microbiota in gating proper immunocompetence in Arabidopsis. *Nat. Plants* 9, 1468–1480. doi: 10.1038/s41477-023-01501-1

Parafati, L., Vitale, A., Restuccia, C., and Cirvilleri, G. (2017). Performance evaluation of volatile organic compounds by antagonistic yeasts immobilized on hydrogel spheres against gray, green and blue postharvest decays. *Food Microbiol.* 63, 191–198. doi: 10.1016/j.fm.2016.11.021

Pinto, C., Pinho, D., Sousa, S., Pinheiro, M., Egas, C., and Gomes, A. C. (2014). Unravelling the diversity of grapevine microbiome. *PloS One* 9, e85622. doi: 10.1371/journal.pone.0085622

Pinto, C., Custódio, V., Nunes, M., Songy, A., Rabenoelina, F., Courteaux, B., et al. (2018). Understand the potential role of *Aureobasidium pullulans*, a resident microorganism from grapevine, to prevent the infection caused by *Diplodia seriata*. *Front. Microbiol.* 9, 3047. doi: 10.3389/fmicb.2018.03047

Prasongsuk, S., Lotrakul, P., Ali, I., Bankeeree, W., and Punnapayak, H. (2018). The current status of Aureobasidium pullulans in biotechnology. *Folia Microbiologica* 63, 129–140. doi: 10.1007/s12223-017-0561-4

Raghavan, K., Dedeepiya, V. D., Yamamoto, N., Ikewaki, N., Sonoda, T., Iwasaki, M., et al. (2023). Benefits of gut microbiota reconstitution by beta 1,3–1,6 glucans in subjects with autism spectrum disorder and other neurodegenerative diseases. *J. Alzheimer's Dis.* 94, S241–S252. doi: 10.3233/jad-220388

Rensink, S., Van Nieuwenhuijzen, E. J., Sailer, M. F., Struck, C., and Wösten, H. A. B. (2024). Use of Aureobasidium in a sustainable economy. *Appl. Microbiol. Biotechnol.* 108, 202. doi: 10.1007/s00253-024-13025-5

Sánchez-Cañizares, C., Jorrín, B., Poole, P. S., and Tkacz, A. (2017). Understanding the holobiont: the interdependence of plants and their microbiome. *Curr. Opin. Microbiol.* 38, 188–196. doi: 10.1016/j.mib.2017.07.001

Sannino, C., Borruso, L., Mezzasoma, A., Battistel, D., Zucconi, L., Selbmann, L., et al. (2020). Intra- and inter-cores fungal diversity suggests interconnection of different habitats in an Antarctic frozen lake (Boulder Clay, Northern Victoria Land). *Environ. Microbiol.* 22, 3463–3477. doi: 10.1111/1462-2920.15117

Schena, L., Nigro, F., Pentimone, I., Ligorio, A., and Ippolito, A. (2003). Control of postharvest rots of sweet cherries and table grapes with endophytic isolates of Aureobasidium pullulans. *Postharvest Biol. Technol.* 30, 209–220. doi: 10.1016/S0925-5214(03)00111-X

Shelton, B. G., Kirkland, K. H., Flanders, W. D., and Morris, G. K. (2002). Profiles of airborne fungi in buildings and outdoor environments in the United States. *Appl. Environ. Microbiol.* 68, 1743–1753. doi: 10.1128/AEM.68.4.1743-1753.2002

Shi, Y., Yang, Q., Zhao, Q., Dhanasekaran, S., Ahima, J., Zhang, X., et al. (2022). Aureobasidium pullulans S-2 reduced the disease incidence of tomato by influencing the postharvest microbiome during storage. *Postharvest Biol. Technol.* 185, 111809. doi: 10.1016/j.postharvbio.2021.111809

Singh, R. S., and Saini, G. K. (2008). Pullulan-hyperproducing color variant strain of Aureobasidium pullulans FB-1 newly isolated from phylloplane of Ficus sp. *Bioresource Technol.* 99, 3896–3899. doi: 10.1016/j.biortech.2007.08.003

Slack, S. M., Outwater, C. A., Grieshop, M. J., and Sundin, G. W. (2019). Evaluation of a contact sterilant as a niche-clearing method to enhance the colonization of apple flowers and efficacy of Aureobasidium pullulans in the biological control of fire blight. *Biol. Control* 139, 104073. doi: 10.1016/j.biocontrol.2019.104073

Trivedi, P., Leach, J. E., Tringe, S. G., Sa, T., and Singh, B. K. (2020). Plant–microbiome interactions: from community assembly to plant health. *Nat. Rev. Microbiol.* 18, 607–621. doi: 10.1038/s41579-020-0412-1

Vandenkoornhuyse, P., Quaiser, A., Duhamel, M., Le Van, A., and Dufresne, A. (2015). The importance of the microbiome of the plant holobiont. *New Phytol.* 206, 1196–1206. doi: 10.1111/nph.13312

Verginer, M., Leitner, E., and Berg, G. (2010). Production of volatile metabolites by grape-associated microorganisms. *J. Agric. Food Chem.* 58, 8344–8350. doi: 10.1021/jf100393w

Větrovský, T., Morais, D., Kohout, P., Lepinay, C., Algora, C., Awokunle Hollá, S., et al. (2020). GlobalFungi, a global database of fungal occurrences from high-throughput-sequencing metabarcoding studies. *Sci. Data* 7, 228. doi: 10.1038/s41597-020-0567-7

Wachowska, U., Kwiatkowska, E., and Pluskota, W. (2021). Alternaria alternata as a Seed-Transmitted Pathogen of Sida hermaphrodita (Malvaceae) and Its Suppression by Aureobasidium pullulans. *Agriculture* 11, 1264. doi: 10.3390/agriculture11121264

Wachowska, U., Stuper-Szablewska, K., and Perkowski, J. (2020). Yeasts isolated from wheat grain can suppress fusarium head blight and decrease trichothecene concentrations in bread wheat and durum wheat grain. *Polish J. Environ. Stud.* 29, 4345–4360. doi: 10.15244/pjoes/118427

Wang, W. L., Chi, Z. M., Chi, Z., Li, J., and Wang, X. H. (2009). Siderophore production by the marine-derived Aureobasidium pullulans and its antimicrobial activity. *Bioresource Technol.* 100, 2639–2641. doi: 10.1016/j.biortech.2008.12.010

Wassermann, B., Cernava, T., Müller, H., Berg, C., and Berg, G. (2019a). Seeds of native alpine plants host unique microbial communities embedded in cross-kingdom networks. *Microbiome* 7, 108. doi: 10.1186/s40168-019-0723-5

Wassermann, B., Korsten, L., and Berg, G. (2021). Plant health and sound vibration: analyzing implications of the microbiome in grape wine leaves. *Pathogens* 10, 63. doi: 10.3390/pathogens10010063

Wassermann, B., Kusstatscher, P., and Berg, G. (2019b). Microbiome response to hot water treatment and potential synergy with biological control on stored apples. *Front. Microbiol.* 10. doi: 10.3389/fmicb.2019.02502

Whipps, J., Lewis, K., and Cooke, R. (1988). "Mycoparasitism and plant disease control," in *Fungi in biological control systems* (Manchester University Press), 161–187.

Wicaksono, W. A., Buko, A., Kusstatscher, P., Cernava, T., Sinkkonen, A., Laitinen, O. H., et al. (2023a). Impact of cultivation and origin on the fruit microbiome of apples and blueberries and implications for the exposome. *Microbial Ecol.* 86, 973–984. doi: 10.1007/s00248-022-02157-8

Wicaksono, W. A., Buko, A., Kusstatscher, P., Sinkkonen, A., Laitinen, O. H., Virtanen, S. M., et al. (2022). Modulation of the food microbiome by apple fruit processing. *Food Microbiol.* 108, 104103. doi: 10.1016/j.fm.2022.104103

Wicaksono, W. A., Cernava, T., Wassermann, B., Abdelfattah, A., Soto-Giron, M. J., Toledo, G. V., et al. (2023b). The edible plant microbiome: evidence for the occurrence of fruit and vegetable bacteria in the human gut. *Gut Microbes* 15, 2258565. doi: 10.1080/19490976.2023.2258565

Zajc, J., Černoša, A., Di Francesco, A., Castoria, R., Curtis, F. D., Lima, G., et al. (2020). Characterization of aureobasidium pullulans isolates selected as biocontrol agents against fruit decay pathogens. *Fungal Genom. Biol.* 10, 163. doi: 10.35248/2165-8056.20.10.163

Zalar, P., Gostinčar, C., De Hoog, G. S., Uršič, V., Sudhadham, M., and Gunde-Cimerman, N. (2008). Redefinition of Aureobasidium pullulans and its varieties. *Stud. Mycology* 61, 21–38. doi: 10.3114/sim.2008.61.02

Zeng, Q., Johnson, K. B., Mukhtar, S., Nason, S., Huntley, R., Millet, F., et al. (2023). *Aureobasidium pullulans* from the fire blight biocontrol product, blossom protect, induces host resistance in apple flowers. *Phytopathology®* 113, 1192–1201. doi: 10.1094/PHYTO-12-22-0452-R

Zhang, D., Spadaro, D., Garibaldi, A., and Gullino, M. L. (2010). Efficacy of the antagonist Aureobasidium pullulans PL5 against postharvest pathogens of peach, apple and plum and its modes of action. *Biol. Control* 54, 172–180. doi: 10.1016/j.biocontrol.2010.05.003

Zhang, F., Aschenbrenner, D., Yoo, J. Y., and Zuo, T. (2022). The gut mycobiome in health, disease, and clinical applications in association with the gut bacterial microbiome assembly. *Lancet Microbe* 3, e969–e983. doi: 10.1016/s2666-5247(22)00203-8

Zhimo, V. Y., Kumar, A., Biasi, A., Abdelfattah, A., Sharma, V. K., Salim, S., et al. (2022). Assembly and dynamics of the apple carposphere microbiome during fruit development and storage. *Front. Microbiol.* 13. doi: 10.3389/fmicb.2022.928888

frontiers | Frontiers in Plant Science

TYPE Original Research
PUBLISHED 30 September 2025
DOI 10.3389/fpls.2025.1650792

OPEN ACCESS

EDITED BY
Zhen Wang,
Yunnan Agricultural University, China

REVIEWED BY
Kankan Zhao,
University of California, San Diego, United States
Pooja Sharma,
Dr. Yashwant Singh Parmar University of Horticulture and Forestry, India

*CORRESPONDENCE
Gang Zhang
jay_gumling2025@163.com
Yimin Li
liyimintt@163.com

RECEIVED 20 June 2025
ACCEPTED 08 September 2025
PUBLISHED 30 September 2025

CITATION
Wang Y, Yan F, Liang Y, Hu X, Gao J, Zhang M, Yan Y, Zhang G and Li Y (2025) Comparative analysis of rhizosphere microbial communities and secondary metabolites in cultivated *Rheum officinale* from different regions of China.
Front. Plant Sci. 16:1650792.
doi: 10.3389/fpls.2025.1650792

Comparative analysis of rhizosphere microbial communities and secondary metabolites in cultivated *Rheum officinale* from different regions of China

Yan Wang[1,2,3], Feng Yan[2,3], Yujie Liang[1], Xiaochen Hu[1,2], Jing Gao[1,2,3], Mingying Zhang[1,2,3], Yonggang Yan[1,2], Gang Zhang[1,2,3]* and Yimin Li[1,2,3]*

[1]Key Laboratory for Research and Development of "Qin Medicine" of Shaanxi Administration of Traditional Chinese Medicine, Shaanxi University of Chinese Medicine, Xi'an, China, [2]College of Pharmacy and Shaanxi Qinling Application Development and Engineering Center of Chinese Herbal Medicine, Shaanxi University of Chinese Medicine, Xi'an, China, [3]State Key Laboratory of Research and Development of Characteristic Qin Medicine Resources (Cultivation), Shaanxi University of Chinese Medicine, Xianyang, China

Rheum officinale Baill., a medicinal herb rich in anthraquinones and tannins, exhibits region-specific variation in bioactive compound accumulation. Given the well-documented pharmacological properties of *R. officinale* Baill. including its laxative, antibacterial, anti-inflammatory and regulating intestinal function, this study integrated Illumina sequencing of rhizosphere microbiomes, HPLC quantification of 10 active components (e.g., rhein, physcion), and soil analysis across three cultivation regions Shaanxi (ZB), Hubei (HB), Chongqing (CQ). Results demonstrated significant regional disparities: ZB showed highest rhein and catechin levels, while CQ accumulated more physcion. Microbial diversity followed the order ZB>HB>CQ, with *Proteobacteria* and *Ascomycota* dominating bacterial and fungal communities, respectively. Soil pH, moisture (SWC), and Zn/Cu content strongly correlated with microbial structure. Notably, *Rokubacteriales* was significantly positively associated with anthraquinones accumulation. These findings suggest that soil properties modulate microbial communities, which in turn regulate secondary metabolite biosynthesis through nutrient cycling (e.g., nitrogen/phosphorus metabolism). This study elucidates the tripartite interaction of soil-microbe-metabolite networks in *R. officinale* Baill., providing insights for geoherbalism optimization. Future research will focus on optimizing *R. officinale* Baill. cultivation through soil condition management to enhance both quality and yield.

KEYWORDS

16S rRNA sequencing, fungal ITS high-throughput sequencing, *Rheum officinale* Baill., secondary metabolites, soil properties

Introduction

Rheum officinale Baill. as a tall perennial herbaceous plant, its dried roots and rhizomes are known as the Chinese herbal medicine rhubarb (Chinese Pharmacopoeia Commission, 2025). The main chemical constituents include anthraquinones, anthrones, stilbenes, phenylbutanones, polysaccharides, tannins, and volatile oils (Cao et al., 2017). The laxative activity of *R. officinale* Baill. is primarily attributed to its anthraquinones derivatives (rhein, aloe-emodin) and anthrone glycosides (sennoside) (Duval et al., 2016; Takayama et al., 2012; Feng et al., 2013). The growing medicinal demand for *R. officinale* Baill. has outpaced wild supply, necessitating large-scale cultivation. While intensive farming system are now established in China's major production regions, persistent monoculture challenges have emerged. Notably, soil-borne diseases (particularly root rot) have increased substantially due to continuous cropping issues, threatening industry sustainability (Lin et al., 2024; Xu et al., 2025). Research confirms these agricultural problems correlate strongly with soil microbiome alterations, where pathogenic bacterial/fungi and nutrient imbalances directly impact plant health (Pang et al., 2022; Bi et al., 2023). Beneficial secondary metabolites (such as medicinal plant active ingredients, microbial functional compounds, plant polyphenols, etc.) have exploded in market demand in recent years due to their high application value in medicine, food and health care, etc.; The contradiction between insufficient adaptation of production scale and demand expansion is continuing to give birth to deepening basic research in this field.

Rhizosphere microorganisms are often termed the plant's 'second genome'. In natural environment, plant roots harbor a diverse community of microorganisms within and surrounding the root system, collectively known as the rhizosphere microbiome, which includes bacteria and fungi (Luo et al., 2024). This microbiome accompanies plants throughout their life cycle, interacts closely with them, and plays a vital role in the growth, development, and secondary metabolite accumulation of medicinal plants (Yuan et al., 2022; Peng et al., 2020). Among these microorganisms are plant growth-promoting rhizobacteria (PGPR). PGPR constitute a core functional group that directly or indirectly sustain plant growth and soil health through mechanisms such as promoting nutrient uptake, secreting plant hormones, enhancing tolerance to abiotic stresses, and suppressing pathogenic microorganisms (Jabborova et al., 2024; Vaghela and Gohel, 2023). Certain rhizobacteria directly promote plant growth by secreting plant hormones or influencing the plant's own hormone synthesis. Among them, phosphate-solubilizing bacteria (*Bacillus*, *Pseudomonas*, *Enterobacter* and *Escherichia*) represent the most dominant phosphorus-transforming groups in soil (Wang et al., 2023; Pang et al., 2024). Nitrogen-fixing bacteria such as *Klebsiella* and *Rhodococcus* can convert atmospheric nitrogen into ammonia, increasing soil nitrogen content and thereby promoting the growth of medicinal plants and the accumulation of their active ingredients (Shi et al., 2023). For instance, the latest research has found that *Paraburkholderia*, a probiotic flora in *Coptis chinensis*, can promote plant growth, activate immune responses, inhibit the main pathogens of coptis root rot, and significantly improve the overall health of plants (Cao et al., 2025), while *Streptomyces* TM32 from the rhizosphere of *Curcuma longa* exhibits potent antimicrobial effects against plant pathogens (Nakaew et al., 2019). Additionally, *Burkholderia* from the rhizosphere of *Baphicacanthus cusia*, as well as *Pseudomonas* and *Pantoea* strains from the rhizosphere of *Salvia miltiorrhiza*, can also directly participate in indigo biosynthesis and phenolic compound accumulation (Zeng et al., 2018; You et al., 2017).

Rhizosphere fungi are another important group within rhizosphere microorganisms, and their diversity plays a crucial role in stabilizing soil ecosystems, promoting plant growth, and directly participating in nutrient cycling between soil and plants, thereby making significant contributions to soil ecology (Adedayo and Babalola, 2013). Functionally, they are categorized into saprophytic fungi and symbiotic mycorrhizal fungi: beneficial fungi can enhance plant root activity, promote growth, and improve disease resistance, whereas harmful fungi may induce plant diseases or even lead to plant mortality (Finzi Razavi et al., 2016; Li Destri Nicosia et al., 2015). Among them, arbuscular mycorrhizal (AM) fungi form symbiotic associations with most terrestrial plants. By assisting hosts in absorbing water and mineral nutrients such as phosphorus (while acquiring organic nutrients from the hosts), they significantly influence plant secondary metabolism (Jiang et al., 2017; Welling et al., 2016; Kapoor et al., 2017). For instance, in *Salvia miltiorrhiza*, synthetic communities composed of fungi can significantly promote plant growth and improve the quality and yield of medicinal materials (Jia et al., 2024). Moreover, AM fungi are closely associated with the synthesis of phenolic compounds (Rosa-Mera et al., 2011). In addition, *Aspergillus flavus* can convert soluble arsenic into insoluble forms, reducing its toxicity to soil organisms to ensure plant growth (Mohd et al., 2019). In summary, the community diversity and functional specificity of rhizosphere microorganisms are the core research targets for elucidating the mechanisms underlying the growth regulation of medicinal plants and the accumulation of their active ingredients. Related research in this field has provided an important theoretical basis for the optimization of medicinal plant cultivation and the utilization of microbial resources.

This study investigated the relationship between rhizosphere microorganisms and *R. officinale* Baill. Using the second-generation NovaSeq platform for PE250 amplicon sequencing, we characterized bacterial and fungal communities in the 3-year-old plants. Our analysis focused on two key aspects: how these rhizosphere microorganisms influence soil physicochemical properties, and their impact on the accumulation of active components in medicinal plant *R. officinale* Baill.

Materials and methods

Sample collection

Field sample was conducted in November 2023 across three major *Rheum officinale* producing regions: Shaanxi, Hubei and

Chongqing. At each location, we collected three-year-old plants along with their rhizosphere soil (Li et al., 2021). Geographic coordinates for all sampling sites (longitude and latitude information) were recorded using Global Positioning System (GPS) (Supplementary Table S1). The study employed a replicated sampling design with three sampling points per region, each comprising three biological *R. officinale* Baill. replicates, yielding a total of nine sample batches. Notably, Zhenba County in Shaanxi Province served as a key sampling site due to its provincial recognition as a genuine producing area. All samples were collected from established medicinal cultivation bases. Three-year-old plants showing no visible signs of damage or disease were carefully selected (Figure 1, Supplementary Figure S1).

For soil sampling, the soil adhering to the roots of *R. officinal* was collected by gentle shaking, and rhizosphere soil samples tightly bound to the fibrous roots were carefully collected using sterilized brushes (Supplementary Figure S2). The frozen soil samples were dispatched to Shanghai Paisno Biotechnology Co., Ltd. for the detection of microbial diversity. Meanwhile, the remaining soil samples were air-dried to remove impurities, passed through a 20-mesh sieve, and then subjected to the determination of soil physical and chemical properties.

Determination of 10 secondary metabolites in *R. officinale* Baill.

The high-performance liquid chromatography (HPLC) analysis was performed according to an established method for *R. officinale* Baill (Li et al., 2025), enabling simultaneous quantification of ten bioactive components: gcatechin, catechin, sennoside B, chrysophanol-8-*O*-glucoside, emodin-8-*O*-glucoside, aloe-emodin, rhein, emodin, chrysophanol and physcion. The fresh *R. officinale* Baill. herbs underwent the following steps. The workflow is summarized in the schematic below (Jiang et al., 2025), illustrating the key steps from sample preparation to chromatographic analysis (Supplementary Figure S3). First, the coarse outer skin was carefully scraped off. The peeled *R. officinale* Baill. was then sliced into 3.0 cm pieces. These slices were air-dried for seven consecutive days and subsequently dried in an electric blast drying oven at 50°C for seven days. Finally, the dried *R. officinale* Baill. slices were pulverized and sieved through a No. 4 sieve (with an inner diameter of sieve hole of 250 μm) to acquire samples appropriate for liquid phase detection. Precisely, 100 mg of each powdered sample was transferred to a 50 mL stoppered flask, mixed with 4.5 mL methanol, and weighed. After 30 minutes of ultrasonication (500W, 40kHz), samples were returned to room temperature, reweighted to compensate for solvent lose, then centrifuged at 11260 xg for 10 minutes. The supernatant was filtered through a 0.22 μm membrane. The reference substances were purchased from Chengdu Desite Biotechnology Co., Ltd. Individual reference standards were accurately weighed and dissolved in methanol to prepare10 mL stock solutions. A mixed working standard solution was prepared by combining 1.0 mL aliquots of each primary standard, followed by ten-fold dilution with methanol. All standard solutions were stored at 4 °C. Separation was achieved using a Maple Unitary C18 column (5 μm, 4.6 × 250 mm) with a binary mobile phase system: (A) methanol and (B) 0.2% phosphoric acid in water. The analysis was conducted at 30 °C with a flow rate of 1.0 mL/min, detection wavelength of 260 nm, and injection volume of 10 μL. Gradient elution was performed according to program Supplementary Table S2.

Determination of soil physicochemical properties

Soil pH was measured with a Sardolus PB-10 pH meter. Total Nitrogen (TN) content was determined through sulfuric acid-catalyzed digestion. Flame photometric was used to quantify total Potassium (TK) content. For phosphorus analysis, total Phosphorus

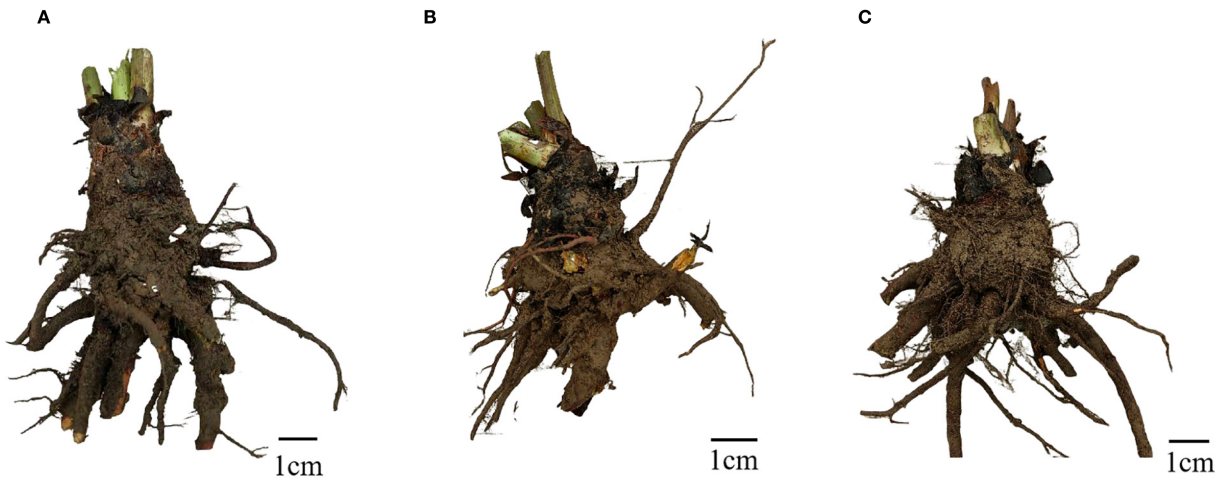

FIGURE 1
Sample photos of *R. officinale* Baill. from different origins. **(A)** ZB; **(B)** HB; **(C)** CQ.

(TP) and available Phosphorus (AP) were determined using the NaOH fusion method followed by molybdenum-antimony anti-colorimetric method. Soil organic carbon and organic matter were determined via the potassium dichromate-concentrated sulfuric acid external heating method. Ammonium nitrogen (NH_4^+-N) and Nitrate nitrogen (NO_3-N) was analyzed utilizing the potassium chloride extraction method. Soil Moisture Content (SWC) was determined gravimetrically by oven drying. Micronutrients analysis such as iron (Fe), manganese (Mn), zinc (Zn) and copper (Cu) was performed using acid extraction followed by atomic absorption spectrophotometry (Bao, 2000). All soil physical and chemical properties analyses were conducted by Yangling Xinhua Ecological Technology Co., Ltd.

Soil DNA extraction, PCR amplification, Illumina sequencing, and data processing

Total soil DNA was extracted using the OMEGA Soil DNA Kit (D5635-02) (OMEGA Bio-tek, USA), with extraction quality verified by 0.8% agarose gel electrophoresis. For bacterial community analysis, the V3-V4 hypervariable region of 16S rRNA gene was amplified using universal primers 338F: (5'-ACTCCTACGGGAGGCAGCAG-3') and 806R: (5'-GGACTACHVGGGTWTCTAAT-3'), with diluted DNA as template. Fungal community analysis targeted the ITS1 region using primers ITS1F(5'-GGAAGTAAAAGTCGTAACAAGG-3') and ITS2R(5'-GCTGCGTTCTTCATCGATGC-3') (Shanghai Paisano Biotechnology Co., Ltd., Shanghai). PCR products were purified using the Axygen Gel Recovery Kit (OMEGA, USA), followed by library preparation with the TruSeq Nano DNA LT Library Prep Kit (Illumina). Paired-end (2 × 250 bp) sequencing was performed on the Illumina MiSeq platform (Illumina, San Diego, CA) at Shanghai Personalbio Technology Co., Ltd.

Statistical analysis of data

The paired-end sequencing was conducted using the NovaSeq 6000 SP Reagent Kit (500 cycles) (Illumina Shanghai Personalbio Technology Co., Ltd., Shanghai). Raw sequence data were demultiplexed using the demux plugin, followed by primer removal with cutadapt plugin. Subsequent processing included quality filtering, denoising, read merged and chimera removal using DADA2 plugin to generate amplicon sequence variation (ASVs). The ASVs were using MAFFT, and phylogenetic trees with constructed with FastTree2. Bioinformatic analyses were primarily performed in QIIME2 and R (Bokulich et al., 2018). Alpha diversity indices (Chao1 index and Shannon index) were calculated from the ASV table and visualized as boxplots. Microbial taxonomic composition and relative abundance were analyzed using MEGAN and GraPhlAn (Asnicar et al., 2015; Huson et al., 2011). Beta diversity was assessed through principal coordinates analysis (PCoA) based on the Bray-curtis dissimilarity matrices, with community composition differences visualized in two-dimensional sorting plots. Statistical analyses were conducted by using SPSS26.0 for one-way ANOVA, Kruskal-Wallis and Duncan's multiple comparison test (α=0.05). GraphPad Prism 8 software was used for plotting.

Results

The content of bioactive ingredients in *R. officinale* Baill. exhibits interregional variations

To investigate the phytochemical variability of medicinal *R. officinale* Baill. from different geographical origins, we quantitatively analyzed ten characteristic bioactive ingredients using HPLC (Supplementary Figure S4). Comparative analysis revealed significant compositional variations in six components including rhein (Figure 2A), chrysophanol-8-*O*-glucoside (Figure 2B), catechin (Figure 2C), emodin-8-*O*-glucoside (Figure 2D), gallic acid (Figure 2E) and physcion (Figure 2F), whereas the remaining four components exhibited relatively Table Sconcentrations without statistically significant difference (Supplementary Figure S5). Specifically, *R. officinale* Baill. from ZB exhibited significantly higher levels of rhein (3.50 × CQ, 1.85 × HB), chrysophanol-8-*O*-glucoside (2.89 × CQ, 1.54 × HB), catechin (3.30 × CQ, 1.48 × HB) and emodin-8-*O*-glucoside (1.36 × CQ, 1.61 × HB) but lower gallic acid content compared to other regions. Conversely, CQ showed the highest physcion content (1.63 × ZB, 1.56 × HB). No significant interregional differences were observed for sennoside B, emodin, aloe-emodin, or chrysophanol. These findings demonstrate distinct chemotypic profiles associated with geographical origins, which may influence the pharmacological properties of *R. officinale* Baill. products.

Analysis of the composition and diversity of fungal and bacterial colonies in rhizosphere soil

To investigate the potential correlation between rhizosphere microbial communities and phytochemical variations in *R. officinale* Baill., we performed comprehensive analysis of bacterial and fungal populations in the rhizosphere soils from different cultivation regions. Microbial community analysis was performed on nine rhizosphere soil samples collected from three geographic regions using Illumina HiSeq high-throughput sequencing. The rarefaction curves of ITS (Supplementary Figure S6A) and 16S rRNA (Supplementary Figure S6B) sequencing demonstrated the continuous emergence of novel operational taxonomic units (OTUs) with increasing sequencing effort, indicating previously uncharacterized microbial diversity. Curve plateauing at sufficient sequencing depth, suggesting adequate coverage of extant microbial diversity with samples (Good's coverage >99%). For fungi, the sequencing depth ranges from 0 to 60,000 reads, and the effective sequencing depth (saturation depth) is 10,000–60,000 reads. For

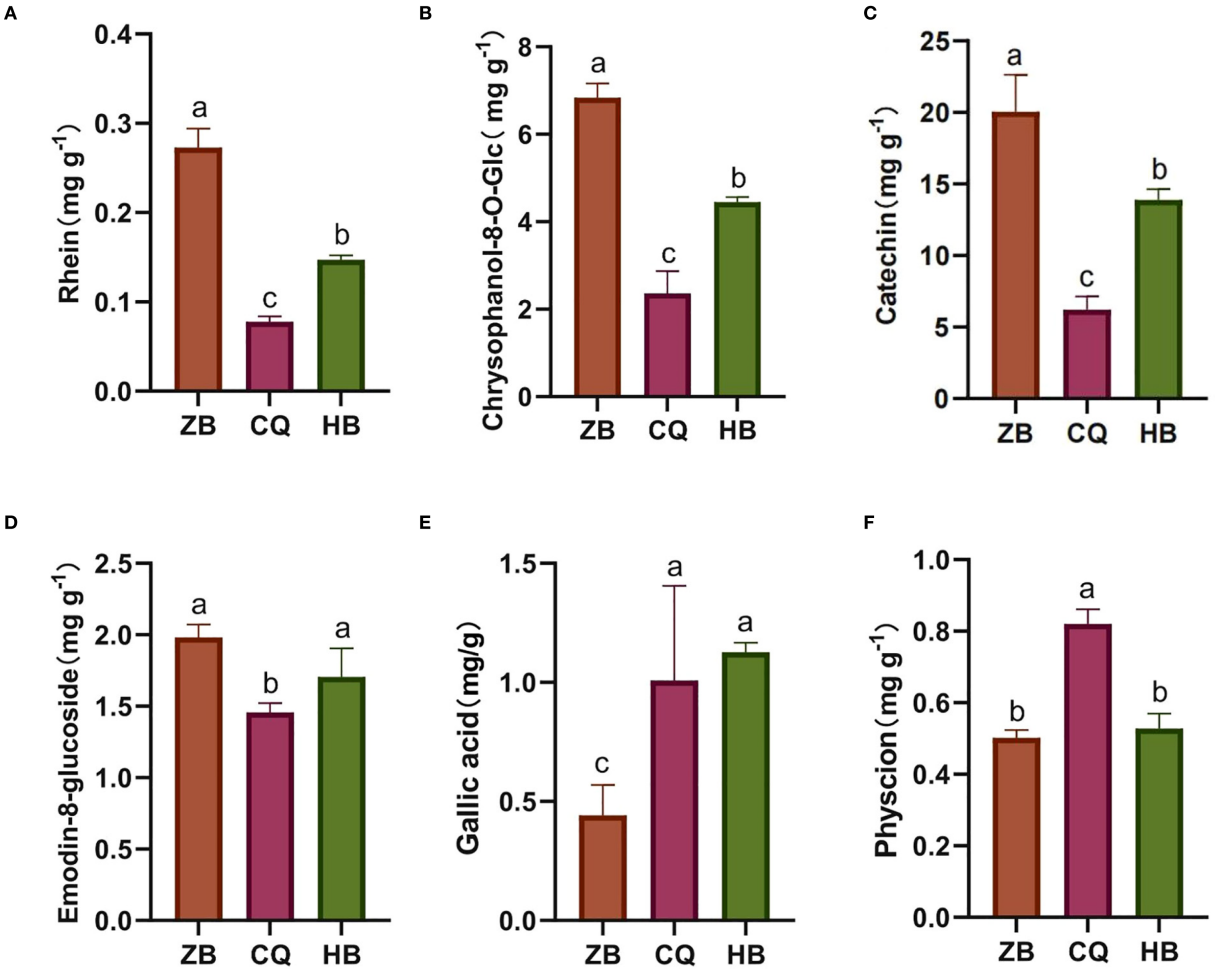

FIGURE 2
(A-F) is the numbering of the active ingredients in *R. officinale* Baill. The content of 6 effective components in *R. officinale* Baill. from 3 origins. The abscissa is the sample grouping, and the ordinate is the content of the components. Data are the mean of three replicates ± SE (standard error); different letters indicate significant differences at $p < 0.05$ according to analysis of variance (ANOVA).

bacteria, the sequencing depth ranges from 0 to 25,000 reads, with a saturation depth of 5,000–10,000 reads. The asymptotic behavior of the curves confirms that the sequencing depth achieved was sufficient to capture the majority of bacterial and fungal diversity present in the samples, while further sequencing would primarily reveal rare taxa.

Microbial community analysis was conducted at 97% sequence similarity threshold to determine operational OTUs in rhizosphere soil of *R. officinale* Baill. from three regions. Venn diagram analysis revealed distinct distribution patterns of shared and unique OTUs. For the fungal community (Figure 3A), there were a total of 1891 OTUs in the three regions, and only 52 OTUs were shared among all three regions, ZB region exhibited the highest diversity with 842 total OTUs, accounting for 44.53% of the total. While, HB region contained 643 total OTUs, accounting for 34.00%. And CQ region showed 616 total OTUs, accounting for 26.97%. For the bacterial community, a total of 13,360 OTUs were present in the three regions, of which 126 OTUs were common to all regions (Figure 3B). The samples from ZB demonstrated maximum diversity, with a total of 6364 OTUs, accounting for 47.63% of the total. Whereas, samples form HB contained 4625 OTUs, accounting for 34.62%, and samples from CQ showed only 2623 OTUs, accounting for 13.63%. The overall microbial diversity followed a consistent regional pattern: ZB>HB>CQ ($p<0.05$), indicating significantly higher microbial diversity in ZB rhizosphere soils compared to other regions.

Alpha diversity analysis was performed to assess microbial community characteristics across different regions. The Chao1 index, which estimates species richness, showed higher values corresponding to greater community richness. The Shannon index, incorporating both species richness and evenness, indicated higher community diversity with increasing values. Both indices followed the same trend: ZB (fungi: Chao1 = 377.92, Shannon=6.01; bacteria: Chao1 = 3274.80, Shannon=10.55) > HB (fungi: Chao1 = 289.33, Shannon=4.36; bacteria: Chao1 = 2247.59, Shannon=10.10) > CQ (fungi: Chao1 = 262.11, Shannon=5.72; bacteria: Chao1 = 1419.09, Shannon=8.73). According to bacterial communities, significant regional variations were detected in both Chao1 ($P<0.05$) and Shannon indices ($P<0.05$) (Figure 3C). Chao1 index ranking: ZB>CQ>HB. Shannon index pattern: CQ>HB>ZB.

10.3389/fpls.2025.1650792

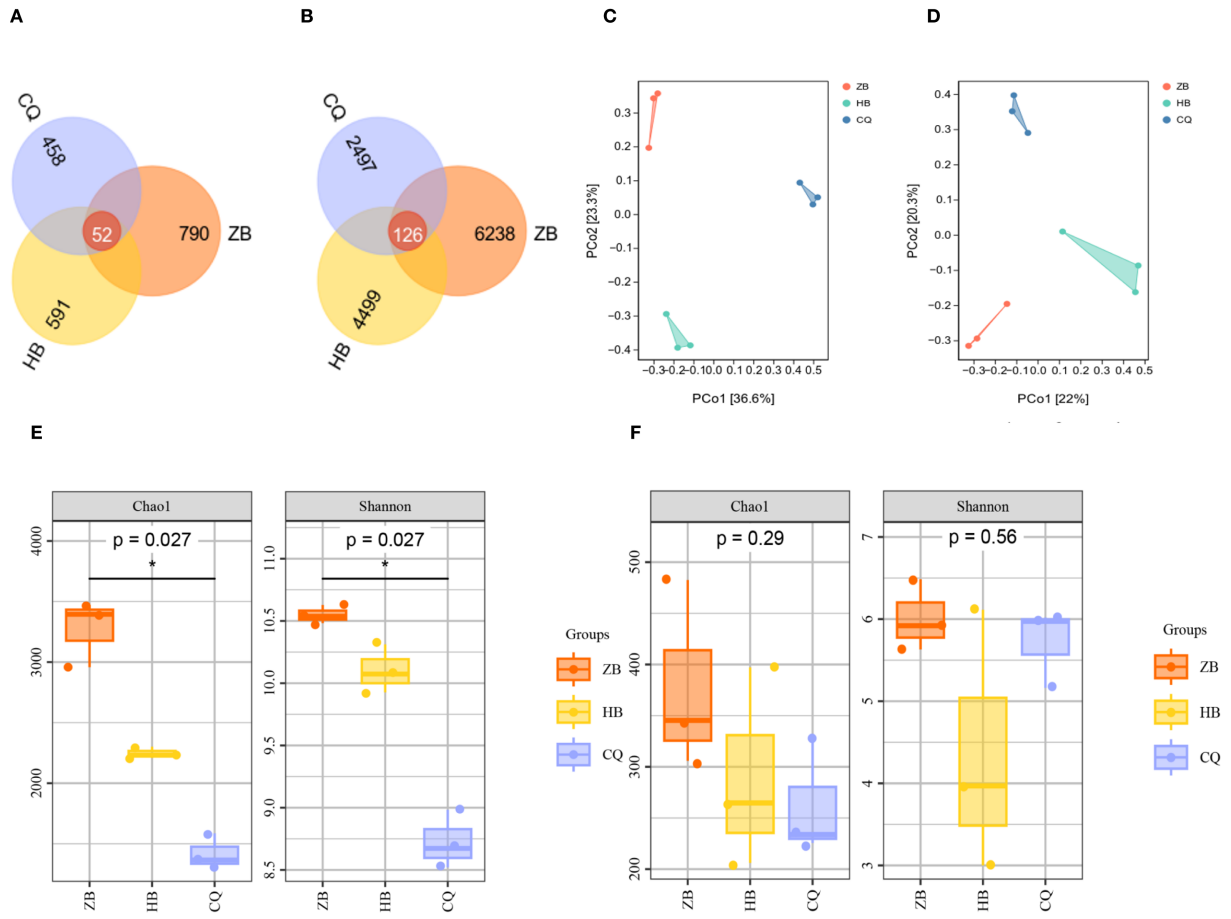

FIGURE 3
Venn diagrams depicting fungi **(A)** and bacteria **(B)** in the rhizosphere soil of *R. officinale* Baill. across three regions. PCoA analysis of fungi **(C)** and bacteria **(D)** in rhizosphere soil of *R. officinale* Baill. among three regions. α diversity analysis of bacteria **(E)** and fungi **(F)** in the rhizosphere soil of *R. officinale* Baill. in three regions. The Venn diagram shows the number of OTUs common and unique to the three regions, with different colors representing different regions. Each point in the PCoA diagram represents a sample, and the dots of different colors indicate different groupings. The percentage in the coordinate axis bracket represents the proportion of the sample difference data (distance matrix) that the corresponding coordinate axis can interpret. Box plots visually compare diversity between groups. α diversity index reflects the species richness and uniformity in the sample. Higher index values indicate higher microbial community complexity.

Regarding fungal communities, no statistically significant differences were detected in either Chao1 ($P > 0.05$) or Shannon ($P > 0.05$) (Figure 3D) indices among regions. These results demonstrate distinct spatial patterns in microbial diversity, with fungal communities showing consistent richness-diversity.

Principal Component Analysis (PCA) was employed to assess beta diversity patterns among sampling regions. For fungal communities (Figure 3E), the first two principal coordinates (PCo1 and PCo2) explained 42.03% of total variation (PCo1:22%; PCo2 20.3%). Bacterial communities (Figure 3F) showed stronger separation, with PCo1 (36.6%) and PCo2 (23.3%) collectively accounting for 59.9% of observed variation. This indicates that the selected principal components are effective in capturing the major patterns of difference in the raw data. In the PCoA diagram, the soil samples of ZB, HB and CQ were distributed in different quadrants and were far away from each other, indicating that there was significant spatial heterogeneity in the composition of fungal and bacterial communities in rhizosphere soil in the three regions.

Composition of fungal and bacterial communities

We further analyzed bacterial and fungal communities in *R. officinale* Baill. rhizosphere soils in Baill. three regions. Microbial abundance data were normalized during analysis, and species were matched in the NCBI database. Based on the horizontal abundance data of soil fungi in ZB, HB and CQ, the predominant fungal phylum across all regions was *Ascomycota*, accounting for 73.08%-92.14% of total fungal sequences. Secondary phyla included *Basidiomycota* (2.27%-15.30%), *Rozellomycota* (0.22%-1.52%) and *Mortierellomycota* (0.33%-3.79%), while other phyla each represented was less than 0.1% (Figure 4A). This consistent dominance pattern suggests *Ascomycota*'s ecological adaptation to the studied rhizosphere environments. However, in accordance with the bacterial community structure, the regional variations in the composition bacterial phyla were more pronounced. The horizontal abundance distribution of soil bacteria phyla in the

three regions was as follows: *Proteobacteria* (30.20%) and *Acidobacteria* (20.30%) were the dominant phyla in ZB samples, followed by *Actinobacteriota* (11.71%), *Chloroflexi* (4.41%), *Verrucomicrobiota* (3.26%), *Bacteroidota* (2.97%) and *Gemmatimonadota* (6.22%). *Proteobacteria* (37.39%) and *Actinobacteriota* (18.11%) were the dominant categories in HB samples, followed by *Acidobacteria* (16.11%), *Chloroflexi* (5.72%), *Gemmatimonadota* (5.98%), *Verrucomicrobiota* (2.23%) and *Bacteroidota* (5.23%). *Proteobacteria* (26.77%) and *Acidobacteriota* (21.27%) were the dominant phyla in the CQ sample, followed by *Gemmatimonadota* (9.31%), *Verrucomicrobiota* (3.01%), *Chloroflexi* (19.69%), *Bacteroidota* (1.08%) and *Myxococcota* (1.74%) (Figure 4A). The microbial communities were predominantly composed of known beneficial taxa, including plant-growth promoting *Proteobacteria* and organic matter-degrading *Acidobacteria* in bacteria, along with *Ascomycota* in fungi. The differential abundance patterns suggest region-specific environmental selection pressures shaping microbial community assembly.

The top 10 soil fungal genus in ZB, HB and CQ were *Penicillium*, *Humicola*, *Fusarium*, *Longitudinalis*, *Staphylotrichum*, *Varicosporellopsis*, *Solicoccozyma*, *Oidiodendron*, *Saitozyma* and *Trichoderma* (Figure 4B). Among them, *Penicillium* (5.59%) was the most abundant in ZB, *Humicola* (41.13%) was the most abundant in HB, and *Penicillium* (10.75%) was the most abundant in CQ. Notably, *Fusarum* showed significant regional variation (CQ:6.40% > HB:2.86 > ZB: 2.11%). Eight of the den dominant fungal genera are known beneficial microorganisms, with *Trichoderma* and *Penicillium* being particularly notable for their plant-growth promoting properties. The top 10 species of soil bacteria were *JG30-KF-AS9*, *SC-I-84*, *Sphingomonas*, *Subgroup_2*, *Rokubacteriales*, *Vicinamibacteraceae*, *Gemmatimonas*, *RB41*, *KD4–96* and *Candidatus_Solibacter*. *Rokubacteriales* (4.84%) and *SC-I-84* (4.67%) were the dominant genera in ZB, *Sphingomonas* (6.87%) and *SC-I-84* (6.55%) were dominant in HB, and *JG30-KF-AS9* (14.56%) and *Subgroup_2* (7.29%) were dominant in CQ (Figure 4B). Ecologically significant beneficial genera including *Rokubacteriales*, *Sphingomonas* and *Gemmatimonas* showed higher relative abundance in ZB and HB (8.24%-8.89%) compared to CQ (2.72%). This distribution pattern potential functional differences in microbial-mediated soil processes across regions.

Correspondence analysis on soil microorganisms from three different *R. officinale* Baill. cultivation regions

The soil samples from the three regions were roughly divided into three quadrants, indicating that there were some differences in the composition of fungal and bacterial communities among different soil samples. Among the fungal communities, the ZB region was dominated by *Penicillium* and *Humicola* (Figure 5A). *Penicillium* and *Humicola* were significantly enriched in the HB region. In the CQ area, *Solicoccozyma* and *Varicosporellopsis* are dominant. Among the physicochemical properties, the arrow of Cu was the longest and pointed to the negative direction of the RDA1 axis, indicating that it had the greatest impact on the community. The direction was consistent with the distribution of CQ samples, *Solicoccozyma* and *Varicosporellopsis*, indicating that Cu

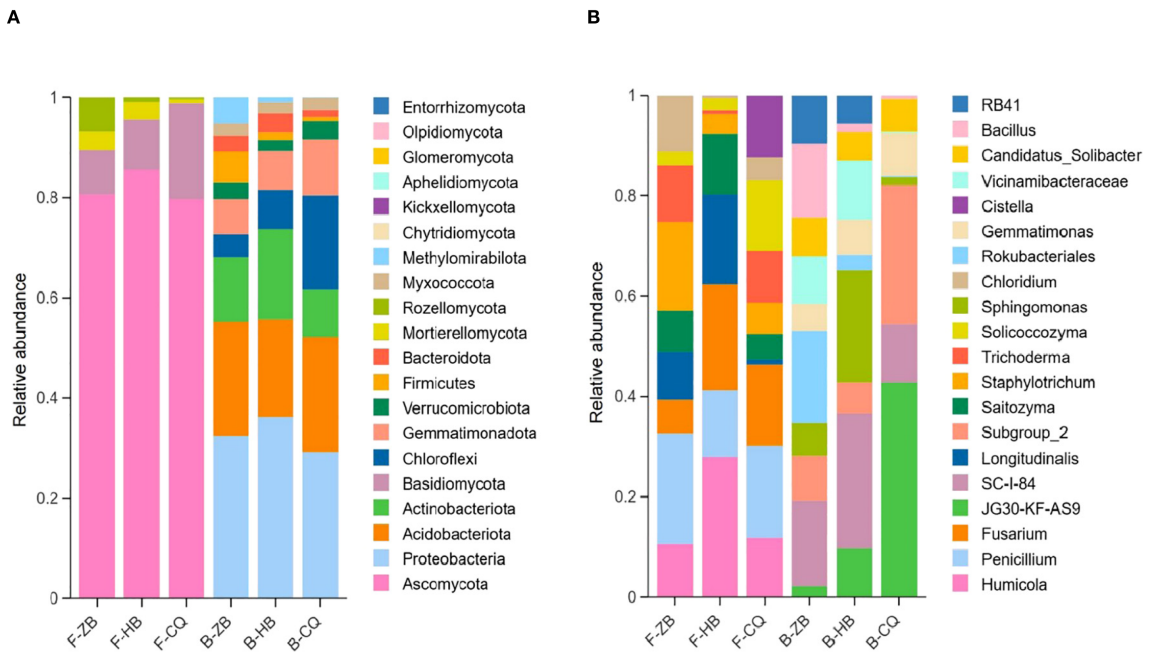

FIGURE 4
Relative abundance of fungi at the phylum **(A)** and genus **(B)** levels in the cultivated soil of *R. officinale* Baill. from three origins. F, fungi; B, bacteria. The picture shows the top 10 taxa by relative abundance at the phylum and genus level. The colors distinguish between microbial taxa, while the x-axis indicates the sample name and the y-axis indicates the relative abundance (%).

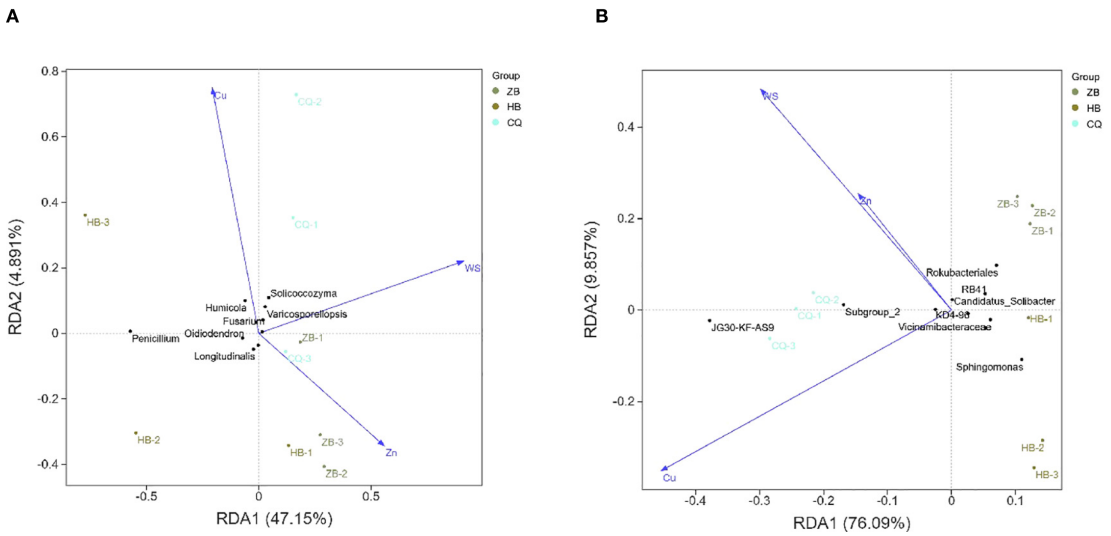

FIGURE 5
Redundancy analysis (RDA) of soil fungi **(A)** and bacteria **(B)** communities of *R. officinale* Baill. cultivated in three different locations and their environmental factors. The percentage of coordinate axes in the graph represents the degree of difference in the raw data it can interpret, with dots representing different samples and different colors representing different groupings. Arrows indicate environmental factors, and the length represents the degree to which the corresponding environmental factors are related to microorganisms. The angle between the arrows indicates the correlation between the two, with the acute angle positively correlated and the obtuse angle negatively correlated.

significantly affected the enrichment of CQ samples and *Solicoccozyma* and *Varicosporellopsis*. The WS pointed to the positive direction of the RDA2 axis, which was close to the CQ sample, which may have a certain effect on the fungal community in the CQ area. Zn points to the positive direction of the RDA1 axis, which is correlated with the distribution trend of the ZB group. In the bacterial community, the Cu arrow was the longest and pointed to the negative direction of the RDA1 axis, which was the most influential factor (Figure 5B). The direction was highly consistent with the distribution of CQ samples and *JG30-KF-AS9*, indicating that Cu may significantly affect the enrichment of CQ samples and *JG30-KF-AS9*. The arrows of Zn and WS are shorter and have a weaker influence. Zn points to the positive direction of the RDA1 axis, which is correlated with the distribution trend of samples in the ZB group. Taken together, the influencing factors of fungal and bacterial communities were about the same.

Correlation analysis of soil microorganisms and bioactive components of *R. officinale* Baill.

Correlation analysis between soil factors and the active ingredient content in *R. officinale* Baill. was performed using SPSS software (version 27). It was performed between the top ten most abundant soil microorganisms (bacteria and fungi) and ten active ingredients in *R. officinale* Baill (Tohge, 2020). Firstly, the normality test of the data is carried out, and the Spearman correlation analysis method is selected to test the initial correlation coefficient and p-value according to the results. In order to control the risk of false positives caused by multiple comparisons, FDR correction was further used to process the p-value to more reliably identify the key soil factors affecting the formation of active ingredients in wolfberry. Fungal correlation showed that there were no fungi significantly associated with the ten active ingredients among the top 10 fungi in abundance ($p>0.05$) (Figure 6A). In the composition of the bacterial community, there was a significant correlation between two bacteria and the components (Figure 6B). *Rokubacteriales* was significantly positively correlated with rhein and emodin-8-*O*-glucoside ($p<0.05$), and *JG30-KF-AS9* was significantly negatively correlated with rhein, catechin, and chrysophanol-8-*O*-glucoside ($p<0.01$), and positively correlated with physcion ($p<0.05$).

Differences in physicochemical properties of rhizosphere soil of *R. officinale* Baill. in different production areas

To explore whether the differences in soil are related to the variations in the components of *R. officinale* Baill., we conducted test on various physical and chemical indicators of the soil.

Significant regional variations in soil physicochemical properties were observed among the three study areas (Table 1). Soil pH analysis revealed neutral conditions in ZB (pH 6.5-7.5), while HB and CQ exhibited acidic soils (pH 4.5-5.5). Trace element analysis demonstrated distinct distributions patterns: iron (Fe) concentrations were markedly elevated in HB (6.78 × ZB, 1.38 × CQ; $p<0.01$), whereas ZB showed the highest manganese (Mn) levels (5.91× HB, 1.20× CQ; $p<0.01$). CQ soils contained significantly greater Copper (Cu) (2.01 × ZB, 1.24 × HB; $p<0.05$), while Zinc (Zn) showed no significant interregional differences.

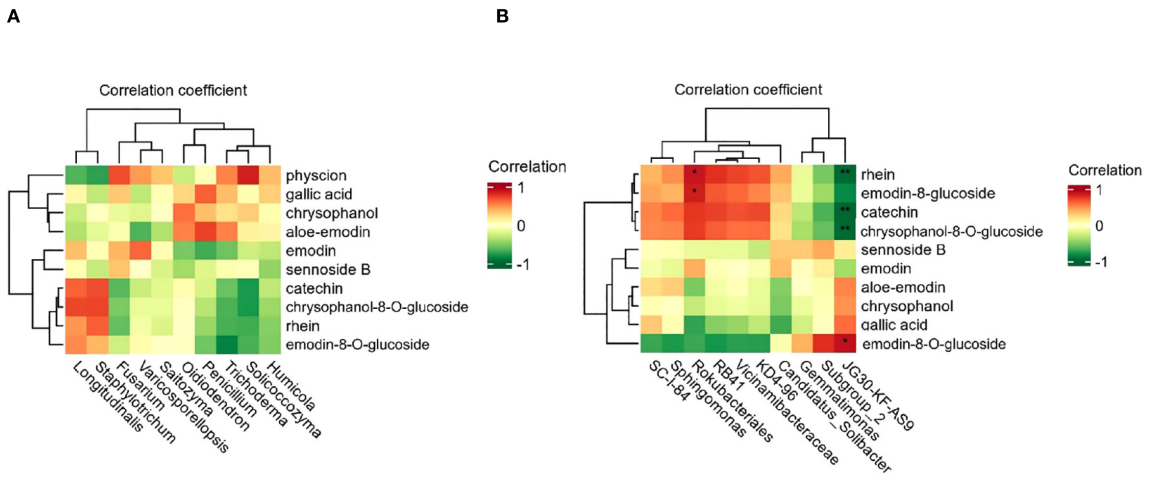

FIGURE 6
Correlation analysis between the content of active ingredients in *R. officinale* Baill. and the levels of fungi **(A)** and bacteria **(B)** in the cultivation soil. The abscissa in the figure represents the microbial species, and the ordinate is the ten active ingredients. The color of the square represents the level of the correlation coefficient.

Nutrient analysis revealed HB's superior fertility, with significantly higher concentrations of total nitrogen (TN: 1.65 × ZB, 1.95 × CQ), organic matter (OM: 2.04 × ZB, 2.48 × CQ), available phosphorus (AP: 7.74 × ZB, 8.46 × CQ), and total phosphorus (TP: 2.57 × ZB, 1.92 × CQ; all $p<0.01$). CQ exhibited the highest total potassium (TK: 1.45 × ZB, 1.12 × HB; $p<0.05$) and ammonium nitrogen (NH_4^+-N: 6.48 × ZB, 1.53 × HB; $p<0.01$). ZB showed predominant nitrate nitrogen (NO_3^--N: 2.93 × HB, 8.01 × CQ; $p<0.01$), while water-soluble content (SWC) was significantly lower in HB compared to other region.

Correlation analysis of soil physical and chemical properties and bioactive components of *R. officinale* Baill.

The correlation between soil properties and the active ingredients of *R. officinale* Baill. was further discussed, and the p-value was FDR corrected (Figure 7; Supplementary Table S3). The results showed that Zn, Mn, TN, OM, AP, TP and SWC were not significantly correlated with the 10 active ingredients. Specifically, pH was significantly positively correlated with gallic acid, catechin, chrysophanol-8-*O*-glucoside, and rhein ($P<0.05$); Fe and gallic acid, chrysophanol-8-*O*-glucoside and rhein were significantly positively correlated. Cu, NH_4^+-N and NO_3-N were significantly positively correlated with catechin, chrysophanol-8-*O*-glucoside, emodin-8-*O*-glucoside and rhein. TK and catechin, chrysophanol-8-*O*-glucoside, emodin-8-*O*-glucoside and rhein were significantly positively correlated. AK was significantly positively correlated with physcion.

Discussion

A growing body of research has shown that *R. officinale* Baill. has a variety of pharmacological properties, including anti-inflammatory, anticancer, antibacterial, and antiviral, and can also be used as an expectorant. It has been recognized as effective in treating a variety of conditions, including stomach pain, nausea, and vomiting (Keshavarzi et al., 2021). The medicinal properties of *R. officinale* Baill. stem from the synergistic effects of several active ingredients (Supplementary Table S4). Gallic acid and catechin belong to tannins, sennoside B belongs to dianthranone, chrysophanol-8-*O*-glucoside and emodin-8-*O*-glucoside belong to conjugated anthraquinone, and aloe-emodin, rhein, emodin, chrysophanol and physcion belong to free anthraquinone. According to the results of HPLC analysis, there exist distinct regional patterns in bioactive compound accumulation. Specifically, ZB region exhibited the highest concentrations of tannins (gallic acid, catechin), dianthrones (sennoside B), and conjugated anthraquinones (chrysophanol-8-*O*-glucoside, emodin-8-*O*-glucoside). Conversely, free anthraquinone (aloe-emodin, rhein, emodin, chrysophanol, physcion) were minimally abundant in ZB but reached peak levels in CQ region. Studies have revealed that the pharmacological effect of tannins predominantly manifest as astringency and antidiarrheal properties (Xu et al., 2024). Regarding anthone, its pharmacological effects mainly include laxative and promoting of bile secretion. When combined with anthraquinone, it exhibits a potent laxative effect. Moreover, it also possesses antioxidant functions. Free anthraquinone is associated with various effect such as antibacterial, anti-inflammatory, antitumor and antioxidant effects (Xiang et al., 2020). The pronounced inter-regional variability in active ingredients profiles underscore the significant impact of geographical factors on secondary metabolite biosynthesis in *R. officinale* Baill (Komatsu et al., 2006). These suggest that origin-specific quality variations may influence clinical efficacy.

Soil physicochemical properties serve as critical determinants of medicinal plant yield and quality through their influence on plant growth, nutrient uptake, secondary metabolism and microbial interaction (Lv G. et al., 2024). Through the association of soil

10.3389/fpls.2025.1650792

TABLE 1 Soil physicochemical properties.

Index	ZB	HB	CQ
pH	6.1333 ± 0.0907	5.13 ± 0.01	4.82 ± 0.0529
Zn	2.3091 ± 0.1865	2.2122 ± 0.0538	2.3133 ± 0.0578
Fe	14.1382 ± 1.3556	95.927 ± 3.7401	69.6704 ± 2.978
Mn	62.2394 ± 2.8578	10.5285 ± 0.2194	51.728 ± 0.8646
Cu	0.9123 ± 0.073	1.4753 ± 0.0413	1.8363 ± 0.068
TN	1.7973 ± 0.0491	2.9649 ± 0.0966	1.5225 ± 0.0144
OM	29.6375 ± 0.4334	60.4537 ± 0.6611	24.335 ± 0.3768
AP	23.0333 ± 0.9793	178.1667 ± 5.8126	21.0667 ± 0.3253
TP	0.5906 ± 0.0121	1.5155 ± 0.0147	0.7906 ± 0.0076
TK	15.4504 ± 0.4246	20.0417 ± 0.1015	22.4769 ± 0.3172
AK	241.3333 ± 6.4291	260.5581 ± 3.8116	147.3333 ± 6.6583
NH_4^+-N	3.9781 ± 0.411	16.8209 ± 0.5874	25.783 ± 0.9739
NO_3^--N	36.2577 ± 1.8023	12.3743 ± 1.0447	4.5264 ± 0.4299
SWC	33.228 ± 1.5133	28.1955 ± 0.3253	33.3004 ± 0.7698

physicochemical properties with active components, it was discovered that pH exhibited a strong correlation with the content of ten active components. In contrast, TN, AK, and heavy metal ions in soil were only correlated with specific individual components. Thus, we hypothesized that soil pH might be the core factor driving the quality variation of *R. officinale* Baill., consistent with observations in other medicinal species. Study revealed that soil stands as one of the crucial determinants of *Panax notoginseng* production, and soil physicochemical properties and soil microbiome have high contributions to the biomass and saponins of *Panax notoginseng* (Xia et al., 2024). Specific pH conditions proved beneficial for the synthesis and accumulation of THSG and total anthraquinones in *Polygonum multiflorum*, thereby enhancing the quality of the medicinal material (Wu et al., 2023). Enhanced medicinal quality of *Astragalus mongholicus* correlates with improved soil quality, particularly pH, soil organic matter (SOM), and calcium content (STCa). These factors directly regulate the biosynthesis of key bioactive compounds including asragalosides (I, II, and IV) and calycosin (Sun et al., 2020). Similar studies in *Lycium barbarum* found that soil pH mediates the accumulation of fruit flavonoids and total sugars, demonstrating both direct and indirect regulatory effects (Liu et al., 2022). It is worth noting that correlation analysis only provides preliminary insights into the

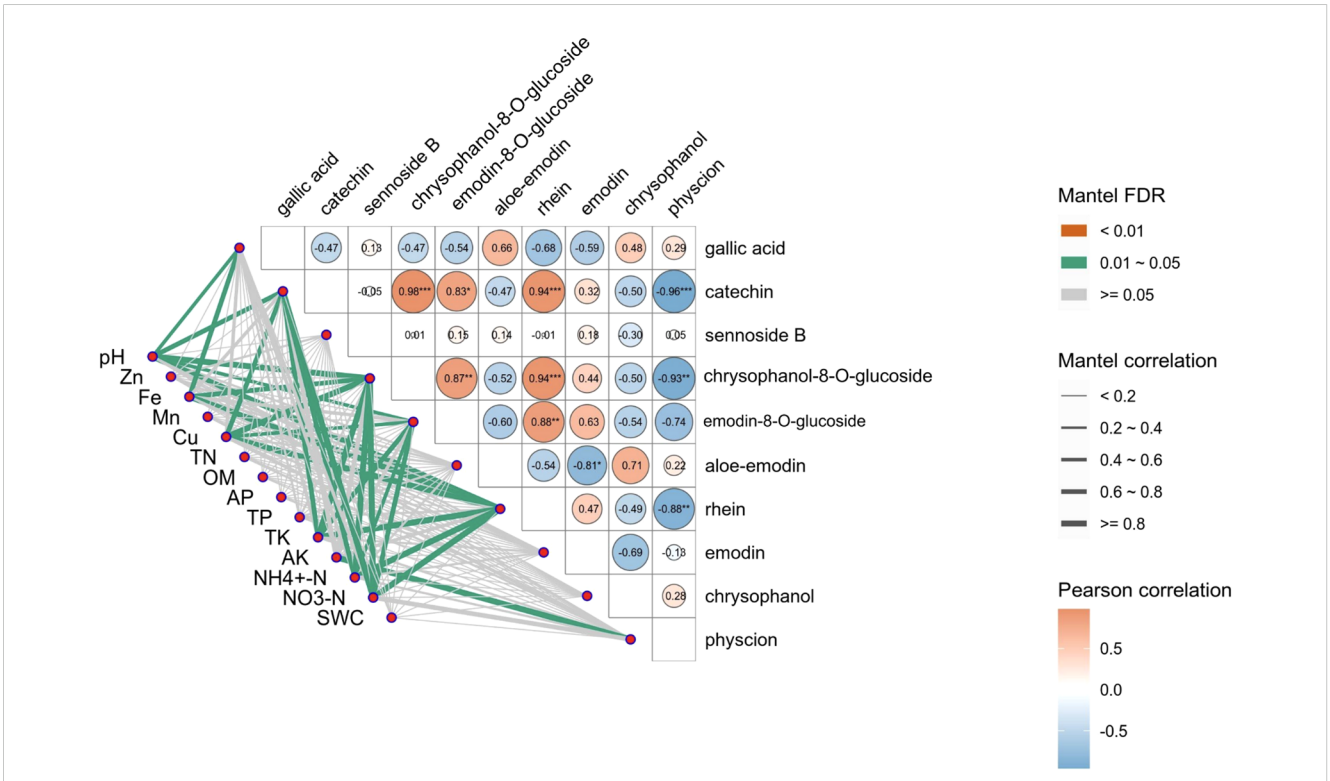

FIGURE 7
Correlation analysis between the content of active ingredients in *R. officinale* Baill. and soil properties. The lower left line represents the Mantel test results of soil physical and chemical properties and active ingredients. The thickness of the line represents the overall correlation coefficient, and the color of the line represents the significance test result of the correlation coefficient. The triangle is a heat map of correlations between substances, with cell color blocks indicating the size of the correlation coefficient, red indicating positive correlation, and blue indicating negative correlation.

potential association between soil physicochemical factors, active ingredients and microorganisms, but cannot establish a causal mechanism between the two, so the results need to be interpreted with caution.

Rhizosphere microorganisms can directly or indirectly regulate the accumulation process of plant active ingredients by building an "interaction network" with plant roots (Lv J. et al., 2024). In terms of nutrient uptake enhancement, nitrogen-fixing microorganisms can convert N_2 in the air into ammonia nitrogen available to plants, and efficiently supplement nitrogen for plants. In addition, these microorganisms can synthesize plant hormones such as indoleacetic acid (IAA) to promote root growth, and cytokinins to enhance leaf photosynthesis and fruit development. At the same time, microorganisms can also regulate the physical and chemical properties of rhizosphere soil and create a suitable microenvironment for the accumulation of active ingredients (Hacquard et al., 2017; Zhong et al., 2022). Analysis of soil samples from different *R. officinale* Baill. cultivation regions revealed significant correlations between microbial community characteristics and specific environmental, with copper (Cu), zinc (Zn) and water content (WC) emerging as primary determinant. Heavy metal contamination, originating from mineral mining, fossil fuel combustion, and industrial/agricultural activities, has been documented to alter soil physicochemical properties and disrupt microbial composition and community structure through cadmium (Cd), arsenic (As), and Cu accumulation (Perveen et al., 2017). Experimental evidence demonstrates a concentration-dependent relationship between Cu exposure and microbial diversity reduction. Biolog analysis indicate an inverse correlation between $CuCl_2$ concentration (0, 10, 20, 100 and 300 μmol/L) and Shannon diversity indices, confirming Cu's suppressive effect on microbial diversity (Woźniak et al., 2019; Kong et al., 2006). In addition, it has been found that Cu has a particularly significant effect on the composition of rhizosphere bacterial communities, which may be due to the fact that Cu can not only destroy the cellular structure and function of microorganisms, but also change the spatial conformation of proteins by binding to specific proteins, produce harmful clumps, interfere with the functions of key proteins, lead to cellular metabolic disorders and signal transduction obstruction, enter a toxic stress state, and eventually die (An et al., 2023). In this study, Cu exhibited the strongest pronounced effects observed in the CQ region. This spatial pattern suggests localized Cu accumulation may drive significant microbiome alteration in CQ soils. In contrast, Zn and water content demonstrated comparatively weaker impacts on microbial communities. These results are only derived from high-throughput data analysis. The specific mechanisms still need to be further verified through experiments.

Fusarium, a prevalent pathogenic genus among the dominant fungi taxa, exhibits significant phytotoxicity toward medicinal plants. For example, in *Panax ginseng*, *Fusarium* can cause root rot, leading to root decay, which affects the ginseng's absorption of water and nutrients, and in severe cases, the entire plant can die (Jun et al., 2022). When *Salvia miltiorrhiza* is infected by *Fusarium*, the content of effective components such as tanshinone will decrease significantly, thus affecting the medicinal value of Danshen (Yang et al., 2020). In medicinal plants like *Atractylodes macrocephala*, root rot and wilt diseases often occur, leading to poor growth, reduced yield, and diminished quality (Huang et al., 2021). Our data revealed a negative correlation between *Fusarium* and catechin levels, suggesting potential suppression of catechin biosynthesis, possibly through interference with phenylpropanoid pathway enzymes. This provides us with a clue that when *Fusarium* infects the plants, it may reduce the medicinal quality of *R. officinale* Baill. by directly or indirectly affecting the synthesis of catechin. Subsequently, molecular techniques can be combined with plant pathology methods for verification. As a beneficial fungus, *Trichoderma* can solubilize poorly soluble nutrients such as phosphorus and potassium in the soil by secreting organic acids, enzymes, and other substances. It converts these nutrients into forms that can be absorbed by plants, thereby enhancing the medicinal plants' ability to absorb and utilize these nutrients and promoting plant growth and development. For instance, during the cultivation of *Astragalus membranaceus*, it facilitates plant growth by dissolving soil nutrients, promoting root elongation, and generating hormone-like substances (He et al., 2022). Correlation analysis revealed a modest positive association between *Trichoderma* and the concentration of physcion and aloe-emodin. This pattern suggests that *Trichoderma* might contribute to enhanced synthesis or accumulation of physcion and aloe-emodin. Conversely, *Trichoderma* exhibited significant negative correlations with emodin-8-*O*-glucoside, rhein, and chrysophanol-8-*O*-glucoside, indicating potential inhibitory effects on these metabolites. Regarding *Penicillium*, evidence suggests this fungal genus promotes growth and secondary metabolism in medicinal plants. For instance, mono-inoculation of the endophytic fungus *Penicillium steckii* in *Tripterygium wilfordii* significantly increased triptolide and tripterine production (Song et al., 2020). Based on this functional analogy, *Penicillium* may similarly facilitate aloe-emodin in *R. officinale* Baill. All correlation analyses were interpreted with careful consideration of inherent observational limitations. While these analyses reveal significant associations between microbial communities and metabolic profiles, they do not establish direct causation. To validate these findings and elucidate mechanistic relationships, we propose employing complementary experimental approaches, including microbial isolation of key operational taxonomic units, controlled co-cultivation systems integrating isolated microbes with plant tissues, and Table Sisotope-assisted metabolic tracing to quantify microbial contributions. This multi-approach will bridge the gap between correlative observations and causative inferences.

Notably, among the top ten bacteria phyla in relative abundance, many remain understudied regarding their functional roles. The bacteria taxa most strongly associated with bioactive components in *R. officinale* Baill. include *Rokubacteriales*, *JG30-KF-AS9*, *RB41*, *Subgroup_2* and. *RB41* belongs to the phylum *Acidobacteria*, which contributes significantly to soil carbon cycling. *Acidobacteria* generally account for approximately 20% of

soil bacterial communities (Jones et al., 2009) and carry out ecologically beneficial functions including plant polymers degradation, iron cycling, and single-carbon compound metabolism (Pankratov et al., 2012; Lu et al., 2010). *RB41* and *Rokubacteriales* are significantly positively correlated with catechin, chrysophanol-8-*O*-glucoside, emodin-8-*O*-glucoside, and rhein, indicating that bacteria from these two genera may promote the accumulation of these four components. *Subgroup_2* and *JG30-KF-AS9* are extremely significantly positively correlated with physcion, suggesting that bacteria from these two genera may promote the synthesis and accumulation of physcion, while being negatively correlated to varying degrees with emodin-8-*O*-glucoside, rhein, catechin, and chrysophanol-8-*O*-glucoside, possibly inhibiting the synthesis and accumulation of these four components. Due to the limited sample size (N = 3), the statistical power of our analyses may be insufficient to detect subtle effects or interactions. Correlation analysis only provides preliminary insights into the potential association between soil physicochemical factors, active ingredients and microorganisms, but cannot establish a causal mechanism between the two, so the results need to be interpreted with caution.

While these correlation analysis provide preliminary insights into potential microbe-metabolite relationships in *R. officinale* Baill., their inherent limitations warrant cautious interpretation. Correlative data alone cannot establish causal mechanisms and may reflect indirect associations influenced by unmeasured environmental variables or microbial interactions. To validate the proposed roles of *RB41*, *Rokubacteriales*, *Subgroup_2*, and *JG30-KF-AS9* in metabolite modulation, targeted experimental approaches are recommended. For instance, *in vitro* co-culture assays with isolated bacterial strains and *R. officinale* Baill. tissues/cell lines to directly quantify effects on specific metabolite accumulation.

Data availability statement

The datasets presented in this study are publicly available. This data can be found here: https://www.ncbi.nlm.nih.gov, accession numbers PRJNA1288235 and PRJNA1320834.

Author contributions

YW: Methodology, Formal analysis, Investigation, Writing – original draft. FY: Writing – review & editing, Software, Conceptualization. YJL: Investigation, Data curation, Methodology, Writing – review & editing, Conceptualization. XH: Writing – review & editing. JG: Visualization, Writing – review & editing, Project administration, Investigation. MZ: Writing – review & editing, Methodology, Investigation. YY: Conceptualization, Writing – review & editing, Supervision. GZ: Project administration, Writing – review & editing, Funding acquisition. YML: Funding acquisition, Visualization, Writing – review & editing, Project administration.

Funding

The author(s) declare financial support was received for the research and/or publication of this article. This work was supported by the National Natural Science Foundation of China (82104334, 81973430); Youth Innovation Team Research Project of Shaanxi Provincial Education Department (24JP043); Shaanxi Provincial Department of Education Service Local Special Plan Project (24JC030); The Key Research and Development Program of Xianyang (L2023-ZDYF-SF-017).

Conflict of interest

The authors declare that the research was conducted in the absence of any commercial or financial relationships that could be construed as a potential conflict of interest.

Generative AI statement

The author(s) declare that no Generative AI was used in the creation of this manuscript.

Any alternative text (alt text) provided alongside figures in this article has been generated by Frontiers with the support of artificial intelligence and reasonable efforts have been made to ensure accuracy, including review by the authors wherever possible. If you identify any issues, please contact us.

Publisher's note

Supplementary material

The Supplementary Material for this article can be found online at: https://www.frontiersin.org/articles/10.3389/fpls.2025.1650792/full#supplementary-material

SUPPLEMENTARY FIGURE 1
Schematic diagram of the sample preparation and HPLC analysis procedure.

SUPPLEMENTARY FIGURE 2
The content of four effective components in *R. officinale* Baill. sourced from three locations shows no obviously variations: sennoside B (A), emodin (B), aloe-emodin (C), chrysophano (D). Data are the mean of three replicates ± SE (standard error); different letters indicate significant differences at $p < 0.05$ according to analysis of variance (ANOVA). ZB for Zhenba, Shaanxi. CQ for Chongqing. HB for Hubei.

SUPPLEMENTARY FIGURE 3
Rhubarb plants from three medicinal rhubarb cultivation bases. A: ZB; B: HB; C: CQ.

SUPPLEMENTARY FIGURE 4
Soil sample for fungal ITS and bacterial 16S sequencing from three regions. ZB for Zhenba, Shaanxi. CQ for Chongqing. HB for Hubei.

SUPPLEMENTARY FIGURE 5
HPLC chromatograms of *R. officinale* Baill. from three production areas.

SUPPLEMENTARY FIGURE 6
Dilution curves of fungal ITS (A) and bacterial 16S (B) sequencing in soil samples. The abscissa is the flattening depth, and the ordinate is the alpha diversity index calculated 10 times.

References

Adedayo, A. A., and Babalola, O. O. (2013). Fungi that promote plant growth in the rhizosphere boost crop growth. *J. Fungi (Basel)* 9, 239. doi: 10.3390/jof9020239

An, Q. R., Li, Y. Y., Zheng, N., Ma, J., Hou, S. N., Sun, S. Y., et al. (2023). Influence of cadmium andcopper mixtures to rhizosphere bacterial communities. *SoilEcol. Lett.* 5, 94–107. doi: 10.1007/s42832-021-0128-9

Asnicar, F., Weingart, G., Tickle, T. L., Huttenhower, C., and Segata, N. (2015). Compact graphical representation of phylogenetic data and metadata with GraPhlAn. *PeerJ* 3, e1029. doi: 10.7717/peerj.1029

Bao (2000). *Soil Agrochemical Analysis. 3rd* (Beijing, China: Agriculture Press), 22–239.

Bi, Y. M., Zhang, X. M., Jiao, X. L., Li, J. F., Peng, N., Tian, G. L., et al. (2023). The relationship between shifts in the rhizosphere microbial community and root rot disease in a continuous cropping American ginseng system. *Front. Microbiol.* 14. doi: 10.3389/fmicb.2023.1097742

Bokulich, N. A., Kaehler, B. D., Ram, R. J., Matthew, D., Evan, B., Rob, K., et al. (2018). Optimizing taxonomic classification of marker-gene amplicon sequences with qiime 2's q2-feature-classifier plugin. *Microbiome* 6, 90. doi: 10.1186/s40168-018-0470-z

Cao, Y. J., Pu, Z. J., Tang, Y. P., Shen, J., Chen, Y. Y., Kang, A., et al. (2017). Advances in bio-active constituents, pharmacology and clinical applications of rhubarb. *Chin. Med.* 12, 36. doi: 10.1186/s13020-017-0158-5

Cao, X., Yuan, Q., Hu, C., Zhang, H., Sun, X., Yan, B., et al. (2025). Wild wisdom meets cultivation: comparative rhizomicrobiome analysis unveils the key role of *Paraburkholderia* in growth promotion and disease suppression in *Coptis chinensis*. *Microbiome* 13, 150. doi: 10.1186/s40168-025-02136-4

Chinese Pharmacopoeia Commission (2025). *Pharmacopoeia of the People's Republic of China, vol. I* Vol. 24 (Beijing: China Pharmaceutical Science and Technology Press).

Duval, J., Pecher, V., Poujol., M., and Lesellier, E. (2016). Research advances for the extraction, analysis and uses of anthraquinones: a review. *Ind. Crops Prod.* 94, 812–833. doi: 10.1016/j.indcrop.2016.09.056

Feng, T. S., Yuan, Z. Y., Yang, R. Q., Zhao, S., Lei, F., Xiao, X. Y., et al. (2013). Purgative components in rhubarbs: adrenergic receptor inhibitors linked with glucose carriers. *Fitoterapia* 91, 236–246. doi: 10.1016/j.fitote.2013.09.020

Finzi Razavi, B. S., Zarebanadkouki, M., Blagodatskaya, E., and Adrien, C. (2016). Rhizosphere shape of lentil and maize:spatial distribution of enzyme activities. *Soil Biol. Biochem.* 96, 229–237. doi: 10.1016/j.soilbio.2016.02.020

Hacquard, S., Spaepen, S., Garrido-Oter, R., and Schulze-Lefert, P. (2017). Interplay between innate immunity and the plant microbiota. *Annu. Rev. Phytopathol.* 55, 565–589. doi: 10.1146/annurev-phyto-080516-035623

He, C., Liu, C., Liu, H. F., Wang, W. Q., Hou, J. L., and Li, X. N. (2022). Dual inoculation of dark septate endophytes and *Trichoderma viride* drives plant performance and rhizosphere microbiome adaptations of *Astragalus mongholicus* to drought. *Environ. Microbiol.* 24, 324–340. doi: 10.1111/1462-2920.15878

Huang, X. G., Li, M. Y., Yan, X. N., Yang, J. S., Rao, M. C., and Yuan, X. F. (2021). The potential of *Trichoderma brevicompactum* for controlling root rot on *Atractylodes macrocephala*. *Can. J. Plant Pathol.* 43, 794–802. doi: 10.1080/07060661.2021.1933602

Huson, D. H., Mitra, S., Ruscheweyh, H. J., Weber, N., and Schuster, S. C. (2011). Integrative analysis of environmental sequences using MEGAN4. *Genome Res.* 21, 1552–1560. doi: 10.1101/gr.120618.111

Jabborova, D., Mamarasulov, B., Davranov, K., Enakiev, Y., Bisht, N., Singh, S., et al. (2024). Diversity and plant growth properties of rhizospheric bacteria associated with medicinal plants. *Indian J. Microbiol.* 64, 409–417. doi: 10.1007/s12088-024-01275-w

Jia, H. M., Zheng, C. W., Wu, Y. R., Wang, H., and Yan, Z. Y. (2024). Metabolomic approach reveals the mechanism of synthetic communities to promote high quality and high yield of medicinal plants—danshen (*Salvia miltiorrhiza* Bge.). *Chem. Biol. Technol. Agric.* 11, 120. doi: 10.1186/s40538-024-00651-4

Jiang, S., Li, H., Zhang, L., Mu, W., Zhang, Y., Chen, T., et al. (2025). Generic Diagramming Platform (GDP): a comprehensive database of high-quality biomedical graphics. *Nucleic Acids Res.* 52, 1670–1676. doi: 10.1093/nar/gkae973

Jiang, Y., Wang, W., Xie, Q., Liu, N., Liu, L., Wang, D., et al. (2017). Plants transfer lipids to sustain colonization by mutualistic mycorrhizal and parasitic fungi. *Science* 356, 1172–1175. doi: 10.1126/science.aam9970

Jones, R. T., Robeson, M. S., Lauber, C. L., Hamady, M., Knight, R., and Fierer, N. (2009). A comprehensive survey of soil acidobacterial diversity using pyrosequencing and clone library analyses. *ISME J.* 3, 442–453. doi: 10.1038/ismej.2008.127

Jun, W., Shi, F., Baohui, L. U., Lina, N. Y., Xue, W., Yan, J. Z., et al. (2022). Fusarium oxysporum f. sp. ginseng, a new forma specialis causing Fusarium root rot of Panax ginseng. *Phytopathol. Mediterr.* 61, 417–429. doi: 10.36253/phyto-13723

Kapoor, R., Anand, G., Gupta, P., and Mandal, S. (2017). Insight into the mechanisms of enhanced production of valuable terpenoids by arbuscular mycorrhiza. *Phytochem. Rev.* 16, 677–692. doi: 10.1007/s11101-016-9486-9

Keshavarzi, Z., Shakeri, F., Maghool, F., Jamialahmadi, T., Johnston, T. P., and Sahebkar, A. (2021). A review on the phytochemistry, pharmacology, and therapeutic effects of rheum ribes. *Adv. Exp. Med. Biol.* 1328 (56), 447–461. doi: 10.1007/978-3-030-73234-9_30

Komatsu, K., Nagayama, Y., Tanaka, K., Ling, Y., Cai, S. Q., Omote, T., et al. (2006). Comparative study of chemical constituents of rhubarb from different origins. *Chem. Pharm. Bull. (Tokyo)* 54, 1491–1499. doi: 10.1248/cpb.54.1491

Kong, W. D., Zhu, Y. G., Fu, B. J., Marschner, P., and He, J. Z. (2006). The veterinary antibiotic oxytetracycline and Cu influence functional diversity of the soil microbial community. *Environ. pollut.* 143, 129–137. doi: 10.1016/j.envpol.2005.11.003

Li, S. Z., Deng, Y., Du, X. F., Wu, Y., He, Q., Wang, Z., et al. (2021). Sampling cores and sequencing depths affected the measurement of microbial diversity in soil quadrats. *Sci. Total Environ.* 50, 144966. doi: 10.1016/j.scitotenv.2021.144966

Li, Y. M., Wang, X. R., Yang, G., Yan, T. T., Hu, X. C., Peng, L., et al. (2025). Profiling the accumulation of ten bioactive compounds in *Rheum officinale* across different growth years using integrated HPLC and transcriptomic approaches. *Med. Plant Biol.* 4, e022. doi: 10.48130/mpb-0025-0020

Li Destri Nicosia, M. G., Mosca, S., Mercurio, R., and Schena, L. (2015). Dieback of *Pinus nigra* Seedlings Caused by a Strain of *Trichoderma viride*. *Plant Dis.* 99, 44–49. doi: 10.1094/PDIS-04-14-0433-RE

Lin, Y., Cai, Y., Hu, F., Wang, J. Y., Jiang, H. L., Zhou, S. S., et al. (2024). Study on the correlation of Rhubarb root rot disease with soil nutrients and microbial community composition. *J. Southwest Univ. Nat. Sci. Ed.* 46, 70–83. doi: 10.13718/j.cnki.xdzk.2024.03.006

Liu, S. Y., Wang, Q. Q., Lei, Y. H., Wang, S. S., Chen, K. L., Li, Y., et al. (2022). Elucidating the interaction of rhizosphere bacteria and environmental factors in influencing active ingredient content of Lycium barbarum fruit in China. *J. Appl. Microbiol.* 132, 3783–3796. doi: 10.1111/jam.15502

Lu, S., Gischkat, S., Reiche, M., Akob, D. M., Hallberg, K. B., and Küsel, K. (2010). Ecophysiology of Fe-cycling bacteria in acidic sediments. *Appl. Environ. Microbiol.* 76, 8174–8183. doi: 10.1128/AEM.01931-10

Luo, C., He, Y., and Chen, Y. (2024). Rhizosphere microbiome regulation: Unlocking the potential for plant growth. *Curr. Res. Microb. Sci.* 8, 100322. doi: 10.1016/j.crmicr.2024.100322

Lv, G., Li, Z., Zhao, Z., Liu, H., Li, L., and Li, M. (2024). The factors affecting the development of medicinal plants from a value chain perspective. *Planta* 259, 108. doi: 10.1007/s00425-024-04380-8

Lv, J., Yang, S., Zhou, W., Liu, Z., Tan, J., and Wei, M. (2024). Microbial regulation of plant secondary metabolites: Impact, mechanisms and prospects. *Microbiol. Res.* 283, 127688. doi: 10.1016/j.micres.2024.127688

Mohd, S., Kushwaha, A. S., Shukla, J., Mandrah, K., Shankar, J., Arjaria, N., et al. (2019). Fungal mediated biotransformation reduces toxicity of arsenic to soil dwelling microorganism and plant. *Ecotoxicol. Environ. Saf.* 176, 108–118. doi: 10.1016/j.ecoenv.2019.03.053

Nakaew, N., Lumyong, S., Sloan, W. T., and Sungthong, R. (2019). Bioactivities and genome insights of a thermotolerant antibiotics-producing *Streptomyces* sp. TM32 reveal its potentials for novel drug discovery. *Microbiologyopen* 8, e842. doi: 10.1002/mbo3.842

Pang, F., Li, Q., Solanki, M. K., Wang, Z., Xing, Y. X., and Dong, D. F. (2024). Soil phosphorus transformation and plant uptake driven by phosphate-solubilizing microorganisms. *Front. Microbiol.* 15. doi: 10.3389/fmicb.2024.1383813

Pang, Z., Mao, X., Xia, Y., Xiao, J., Wang, X., Xu, P., et al. (2022). Multiomics reveals the effect of root rot on polygonati rhizome and identifies pathogens and biocontrol strain. *Microbiol. Spectr.* 10, e0238521. doi: 10.1128/spectrum.02385-21

Pankratov, T. A., Kirsanova, L. A., Kaparullina, E. N., Kevbrin, V. V., and Dedysh, S. N. (2012). Telmatobacter bradus gen. nov., sp. nov., a cellulolytic facultative anaerobe from subdivision 1 of the Acidobacteria, and emended description of Acidobacterium capsulatum Kishimoto et al., 1991. *Int. J. Syst. Evol. Microbiol.* 62, 430–437. doi: 10.1099/ijs.0.029629-0

Peng, Z., Guo, X. Z., Xu, Y., Liu, D. H., Wang, H. Y., Guo, L. P., et al. (2020). Advances in interaction between medicinal plants and rhizosphere microorganisms. *Chin. J. Chin. Mater. Med.* 45, 2023–2030. doi: 10.19540/j.cnki.cjcmm.20200302.116

Perveen, I., Raza, M. A., Sehar, S., Naz, I., Young, B., and Ahmed, S. (2017). Heavy metal contamination in water,soil,and milk of the industrial area adjacent to Swan River, Islamabad, Pakistan. *HERA* 23, 1564–1572. doi: 10.1080/10807039.2017.1321956

Rosa-Mera, C. J. D. L., Ferrera-Cerrato, R., Alejandro, A. A., Sánchez-Colín, M. J., and Muñoz-Muñiz, O. D. (2011). Arbuscular mycorrhizal fungi and potassium bicarbonate enhance the foliar content of the vinblastine alkaloid in *Catharanthus roseus*. *Plant Soil.* 349, 367–376. doi: 10.1007/s11104-011-0883-y

Shi, Z., Guo, X., Lei, Z., Wang, Y., Yang, Z., Niu, J., et al. (2023). Screening of high-efficiency nitrogen-fixing bacteria from the traditional Chinese medicine plant Astragalus mongolicus and its effect on plant growth promotion and bacterial communities in the rhizosphere. *BMC Microbiol.* 23, 292. doi: 10.1186/s12866-023-03026-1

Song, H., Liu, J., Song, P., Feng, L., Wu, C. Z., and Hong, W. (2020). Effects of inoculation with endophytic fungi and endophytic bacteria on growth and accumulation of secondary metabolites in tripterygium wilfordii. *J. Trop. Subtrop. Bot.* 28, 347–355. doi: 10.11926/jtsb.4176

Sun, H., Jin, Q., Wang, Q., Shao, C., Zhang, L. L., Guan, Y. M., et al. (2020). Effects of soil quality on effective ingredients of *Astragalus mongholicus* from the main cultivation regions in China. *Ecol. Indic.* 114, 106296. doi: 10.1016/j.ecolind.2020.106296

Takayama, K., Tsutsumi, H., Ishizu, T., and Okamura, N. (2012). The influence of rhein 8-*O*-β-D-glucopyranoside on the purgative action of sennoside a from rhubarb in mice. *Biol. Pharm. Bull.* 35, 2204–2208. doi: 10.1248/bpb.b12-00632

Tohge, T. (2020). From fruit omics to fruiting omics: systematic studies of tomato fruiting by metabolic networks. *Mol. Plant* 13, 1114–1116. doi: 10.1016/j.molp.2020.07.012

Vaghela, N., and Gohel, S. (2023). Medicinal plant-associated rhizobacteria enhance the production of pharmaceutically important bioactive compounds under abiotic stress conditions. *J. Basic Microbiol.* 63, 308–325. doi: 10.1002/jobm.202200361

Wang, C., Pan, G., Lu, X., and Qi, W. (2023). Phosphorus solubilizing microorganisms: potential promoters of agricultural and environmental engineering. *Front. Bioeng. Biotechnol.* 11. doi: 10.3389/fbioe.2023.1181078

Welling, M. T., Liu, L., Rose, T. J., Waters, D. L., and Benkendorff, K. (2016). Arbuscular mycorrhizal fungi: effects on plant terpenoid accumulation. *Plant Biol. (Stuttg)* 18, 552–562. doi: 10.1111/plb.12408

Woźniak, M., Gałązka, A., Tyśkiewicz, R., and Jaroszuk-Ściseł, J. (2019). Endophytic bacteria potentially promote plant growth by synthesizing different metabolites and their phenotypic/Physiological profiles in the biolog GEN III microPlate™ Test. *Int. J. Mol. Sci.* 20, 5283. doi: 10.3390/ijms20215283

Wu, Y., Leng, F., Liao, M., Yu, Y., Chen, Z., Wei, S., et al. (2023). Characterization of the physiological parameters, effective components, and transcriptional profiles of *Polygonum multiflorum* Thunb. Under pH stress. *Plant Physiol. Biochem.* 37, 108279. doi: 10.1016/j.plaphy.2023.108279

Xia, Q., Wang, B., Liu, Z., Wei, F. G., Yang, S. Z., Li, X. C., et al. (2024). Deciphering the key soil microbial taxa that contribute to saponin accumulation in a geo-authentic Sanqi ginseng production area: Evidence from four different varieties. *Appl. Soil Ecol.* 201, 105470. doi: 10.1016/j.apsoil.2024.105470

Xiang, H., Zuo, J., Guo, F., and Dong, D. (2020). What we already know about rhubarb: a comprehensive review. *Chin. Med.* 15, 88. doi: 10.1186/s13020-020-00370-6

Xu, R., Chen, W., Chen, S., Wang, X., Xu, J., Zhang, Y., et al. (2025). Unraveling the rhubarb (*Rheum officinale* baill.) root and rhizosphere microbial communities in response to pathogen exposure. *Mol. Biotechnol.* 32, 1–11. doi: 10.1007/s12033-025-01367-y

Xu, H., Wang, W., Li, X., Li, Y., Jiang, Y., Deng, C., et al. (2024). Botany, traditional use, phytochemistry, pharmacology and clinical applications of rhubarb (Rhei radix et rhizome): A systematic review. *Am. J. Chin. Med.* 52, 1925–1967. doi: 10.1142/S0192415X24500757

Yang, J., Wang, F., Wen, Y., Gao, S., Lu, C., Liu, Y., et al. (2020). First report of *Fusarium proliferatum* causing root rot disease in *Salvia miltiorrhizae* in China. *Plant Dis.* 105, 1210–1210. doi: 10.1094/PDIS-09-20-1908-PDN

You, H., Yang, S., Zhang, L., Hu, X., and Li, O. (2017). Promotion of phenolic compounds production in Salvia miltiorrhiza hairy roots by six strains of rhizosphere bacteria. *Eng. Life Sci.* 18, 160–168. doi: 10.1002/elsc.201700077

Yuan, Y., Zuo, J., Zhang, H., Meng, T. Z., and Sian, L. (2022). The Chinese medicinal plants rhizosphere: Metabolites, microorganisms, and interaction. *Rhizosphere* 22, 100540. doi: 10.1016/j.rhisph.2022.100540

Zeng, M., Zhong, Y., Cai, S., and Diao, Y. (2018). Deciphering the bacterial composition in the rhizosphere of *Baphicacanthus cusia* (NeeS) Bremek. *Sci. Rep.* 8, 15831. doi: 10.1038/s41598-018-34177-1

Zhong, Y., Xun, W., Wang, X., Tian, S., Zhang, Y., Li, D., et al. (2022). Root-secreted bitter triterpene modulates the rhizosphere microbiota to improve plant fitness. *Nat. Plants* 8, 887–896. doi: 10.1038/s41477-022-01201-2

frontiers | Frontiers in Plant Science

TYPE Original Research
PUBLISHED 14 November 2025
DOI 10.3389/fpls.2025.1678786

OPEN ACCESS

EDITED BY
Zhen Wang,
Yunnan Agricultural University, China

REVIEWED BY
Mubashar Raza,
Xinjiang Academy of Agricultural Sciences, China
Shayan Syed,
Lithuanian Research Centre for Agriculture and Forestry, Lithuania

*CORRESPONDENCE
Yun Li
gxuliyun@gxu.edu.cn
Pingwu Liu
hnulpw@hainanu.edu.cn

†These authors have contributed equally to this work

RECEIVED 03 August 2025
ACCEPTED 21 October 2025
PUBLISHED 14 November 2025

CITATION
Umer M, Anwar N, Mubeen M, Li Y, Alsyaad KM, Ahmed AE and Liu P (2025) Functional genome analysis reveals that serine carboxypeptidase *Bd-SCP10* mediates vegetative growth, pathogenicity, and stress tolerance in *Botryosphaeria dothidea*. *Front. Plant Sci.* 16:1678786. doi: 10.3389/fpls.2025.1678786

Functional genome analysis reveals that serine carboxypeptidase *Bd-SCP10* mediates vegetative growth, pathogenicity, and stress tolerance in *Botryosphaeria dothidea*

Muhammad Umer[1†], Naureen Anwar[2†], Mustansar Mubeen[3], Yun Li[4*], Khalid M. Alsyaad[5], Ahmed Ezzat Ahmed[5,6] and Pingwu Liu[1*]

[1]School of Breeding and Multiplication (Sanya Institute of Breeding and Multiplication), College of Tropical Agriculture and Forestry, Hainan University, Sanya, Hainan, China, [2]Department of Biological Sciences, Faculty of Science and Technology, Virtual University, Lahore, Pakistan, [3]Department of Plant Pathology, College of Agriculture, University of Sargodha, Sargodha, Pakistan, [4]College of Agriculture, Guangxi University, Nanning, China, [5]Department of Biology, College of Science, King Khalid University, Abha, Saudi Arabia, [6]Prince Sultan Bin Abdelaziz for Environmental Research and Natural Resources Sustainability Center, King Khalid University, Abha, Saudi Arabia

Introduction: *Botryosphaeria dothidea* (*B. dothidea*) is a catastrophic fungal pathogen that threatens fruit production worldwide. Secreted peptidases like serine carboxypeptidases (*SCPs*) are well known to be involved in fungal virulence, but their role in *B. dothidea* is unknown.

Methodology: Here, we identified and functionally characterized *Bd-SCP10*, a homolog of *SCPs* found in *B. dothidea*, which is a member of the S10 family, using a split marker strategy for gene knockout and complementation.

Results: Mutants exhibited substantial phenotypic changes, including reduced radial growth and compromised biomass production, as well as altered pathogenicity and stress tolerance in response to multiple stress conditions. In contrast, complementation restored these traits, suggesting a functional role of *Bd-SCP10*. Particularly, *Bd-SCP10* contributes to maintaining growth, cell wall integrity and adaptation to host-induced stresses, highlighting its involvement in fungal survival and pathogenicity.

Discussion: This study provides the first functional evidence that secreted peptidases in *B. dothidea* are a key factor in vegetative growth, pathogenicity, and stress tolerance. The identification and functional characterization of *Bd-SCP10* led us to believe that it is a promising molecular target for eco-friendly strategies to manage diseases caused by *B. dothidea* and related pathogens.

KEYWORDS

***Botryosphaeria dothidea*, eco-friendly disease control strategies, functional genomics, pathogenicity, serine carboxypeptidase S10 family**

1 Introduction

B. dothidea infects many woody plants worldwide and damages most parts of plants, including leaves, fruits, branches, and stems. It can cause fruit rot, leaf spot, twig dieback, and stem and branch canker diseases, leading to the death of infected trees (Jash et al., 2025). It has caught the attention of fruit tree pathologists, as it can infect most economically significant fruit trees, such as apples, pears, grapes, peaches, and blueberries, and cause severe diseases resulting in substantial annual losses. In China, apple white rot caused by *B. dothidea is* considered as one of the most destructive diseases (Dong and Guo, 2020). Raindrops facilitated the spread of fungal conidia to the host tissue surface, and conidia primarily form a germ tube and appressorium. After the development of the appressoria appressorium, it begins to invade cells and expand inside the cell, then infects the cells and absorbs nutrients from the infected tissues (Kim et al., 2016). Eco-friendly strategies for disease control measures are still unknown for this devastating fungal pathogen. That is why it is necessary to explore sustainable approaches. The host defense system is considered the first line of defense against fungal invasion, and the plant cell wall can provide an adequate defense against fungal attacks (Looi et al., 2017; Munzert and Engelsdorf, 2025). Alternatively, fungal pathogens employ a range of strategies, including physical, enzymatic (such as hemicellulase, cutinase, pectinase, cellulase, lipases, secreted peptidases, and degradative enzymes), and chemical effectors to overcome barriers during invasion and infection (Zhao et al., 2013; Rauwane et al., 2020). Comparative genomic analysis of *B. dothidea* has suggested that virulence- and pathogenicity-related genes are involved in regulating metabolic pathways associated with the production of various enzymes, including those involved in plant cell wall degradation, biosynthesis, cytochrome P450, carbohydrate-active, and secreted peptidases (Wang et al., 2018). Plant cell wall degrading and secreted peptidases are considered the most important factors related to pathogenicity, and the former have been well characterized as responsible for virulence in many phytopathogenic fungi. While the latter remains enigmatic (Wang et al., 2018; Munzert and Engelsdorf, 2025). *SCPs* are proteolytic enzymes belonging to the peptidase S10 family, characterized by a conserved Ser–Asp–His catalytic triad (Oda et al., 2022) and hydrolyze peptide bonds from the C-terminus of peptides and proteins (Semenova et al., 2020), thereby contributing to protein processing, nutrient acquisition, and regulation of cellular functions (Chen et al., 2022). In fungi, *SCPs* are often secreted into the extracellular environment, where they interact with host proteins and cell wall components, facilitating the release of nutrients and promoting host colonization. Beyond their housekeeping functions, *SCPs* are increasingly recognized as essential virulence factors (Muszewska et al., 2017; Da Silva, 2018; Madhu et al., 2020). They vary in their characteristics, including substrate selectivity, active site, and catalytic mechanism, and are also involved in a wide range of complex physiological activities (Da Silva et al., 2006; Dong et al., 2021). Generally, fungal pathogens secrete peptidases to modify spore production and germination and these enzymes act as virulence regulators (Krishnan et al., 2018; Yang et al., 2023). In addition, fungal peptidases can inhibit the host defense system by modifying and inactivating protein components of the protection machinery of the host (Xia, 2004; Shi et al., 2025). *Fusarium graminearum*, *FgSCP* was shown to be essential for fungal growth, toxin biosynthesis, stress tolerance, pathogenicity, and suppression of host immunity (Liu et al., 2024). Similarly, in *Penicillium expansum*, secretome profiling identified a *PeBgl1* and *PeSCP* as enzymes required for virulence on apple fruit, emphasizing their direct role in host invasion (Wang et al., 2025). Several old studies have also shown the importance of secreted peptidases in the regulation of virulence in fungal pathogens, e.g., *SsNEP2* in *Sclerotinia sclerotiorum* (Yang et al., 2022), *BcCGF1* in *Botrytis cinerea* (Zhang et al., 2020a), *CpSge1* in *Cryphonectria parasitica* (Lin et al., 2025b), *Fospc2* in *Fusarium odoratissimum* (Yang et al., 2023), and *GcStuA* in *Glomerella cingulate* (Chethana et al., 2021). These findings highlight the functional role of *SCPs* as key modulators of fungal physiology, managing growth, stress adaptation, and host immune suppression. Although the recognized roles of *SCPs* in other phytopathogenic fungi are well understood, their functional role in *B. dothidea* remains largely unknown. Therefore, identifying the function of *Bd-SCP10* offers a key step toward understanding the mechanisms of pathogenicity and will help in developing innovative, eco-friendly strategies for disease control in fruit crops.

2 Materials and methods

2.1 Strains and cultural conditions

The *B. dothidea* wildtype strain (Bd-wt) was generously provided by Hafiz Husnain Nawaz (Hainan University, Haikou, China). For colony morphology analysis, the control [CK, representing uninoculated potato dextrose agar medium (PDA)] and Bd-wt were cultured and replicated 6 times on PDA for 5 days (d) at 25°C (Wei et al., 2019).

2.2 Nucleic acid manipulations and polymerase chain reaction

Fungal gDNA was isolated from 5 d old mycelium through the 2X Cetyltrimethylammonium bromide (CTAB) method (Jasim et al., 2024). The verification and identification of mutants and complementary strains were performed as previously described through polymerase chain reaction (PCR) (Huang et al., 2017a).

2.3 Bioinformatics analysis

The full-length nucleotide sequence of the *Bd-SCP10* gene, along with upstream and downstream flanking sequences, was downloaded from *B. dothidea* (ASM1106463v1, GenBank: GCA_011064635.1, https://www.ncbi.nlm.nih.gov/assembly/GCA_011064635.1/). Oligo primer analysis v. 7.0 (Molecular Biology Insights, Inc., Colorado, USA) was used to design the primers. For phylogenetic analysis, the protein sequence of *Bd-*

SCP10 (GenBank: KAF4310043.1) was obtained from NCBI, and the homologs of *SCPs* in 12 other phytopathogenic fungi were identified via MEROPS (https://www.ebi.ac.uk/Tools/services/web/toolresult.ebi?jobId=ncbiblast-I20210421-144041-0569-47522791-p2m) (Rawlings, 2020), followed by the multiple sequence alignment with Clustal Omega (https://www.ebi.ac.uk/Tools/msa/clustalo/). Finally, the phylogenetic tree was generated using MEGA software v. 7.0 (Kumar et al., 2016; Ahmad et al., 2021) with the neighbor-joining (NJ) method. The dendrograms were based on clustered homologs, determined through bootstrap analysis (with 1000 replicates), and displayed replication percentages on the respective branches. ORFFINDER (https://www.ncbi.nlm.nih.gov/orffinder/) was used for the analysis of the open reading frame (ORF) (Varabyou et al., 2023), and the protein domain was predicted using Pfam (https://pfam.xfam.org/) (Savojardo et al., 2021).

2.4 Targeted knockout of the *Bd-SCP10* gene from a wildtype strain

The deletion of the *Bd-SCP10* gene was conducted using a split marker strategy, in which the selectable marker HYG replaced the targeted gene (Yuan et al., 2023). Briefly, in the first round of PCR, the fragment of the upstream flanking sequence (UPS) of *Bd-SCP10* (887 base pairs (bp) was amplified with Up-F and Up-R primers, while the downstream flanking sequence (DNS) of 789 bp was amplified with Dn-F and Dn-R primers. On the other hand, the pCX62 plasmid (Lin et al., 2025a) was used to amplify the HYG resistance cassette for a 767 bp HY fragment with HYG-F/HY-R primers and a 931 bp YG fragment with HYG-R/YG-F primers. In the second round or fusion PCR, the Up-F/HY-R primers were used to fuse the UPS fragment with the HY fragment, while the Dn-R/YG-F primers were used to fuse the DNS fragment with the YG fragment through splicing of overlapped sequence extension, and templates were used in equal proportion in fusion PCR. Fusion PCR cycling conditions were conducted initially at 95 °C for 5 minutes (min), followed by 35 cycles of 95 °C for 30 seconds (s), 60 °C for 45 s, and 72 °C for 90 s, and finally at 72 °C for 10 min. The products of fusion PCR were transformed through the PEG-mediated transformation method (Zhang et al., 2022) into the protoplasts (2×10^7 cells/mL) isolated from 5 d old mycelium of Bd-wt using the previously described method (Ning et al., 2022). The transformants were cultured on PDA supplemented with 50 μg/mL hygromycin B (HYG; Roche, USA), and the developed colonies were randomly selected and verified by standard PCR using the two sets of primers *Bd-SCP10*-F/*Bd-SCP10*-R and HYG-F/HYG-R.

2.5 Complementation of the *Bd-SCP10* gene

The complementation of the mutant *ΔBd-SCP10a* was achieved by inserting the Bd-SCP10 gene, along with a NEO resistance cassette, into the knockout mutant through a split marker strategy (Gravelat et al., 2012). The first-round PCR was briefly conducted to amplify the 47 bp upstream flanking region (UPS) together with the full length of the *Bd-SCP10* gene, resulting in a 2800 bp amplified fragment and the 832 bp amplified fragment of the downstream flanking region (DNS). Then, the pSELECT-neo plasmid (InvivoGen, USA) was used to amplify the NEO drug cassette for the NE fragment (975 bp) with NEO-F/NE-R primers and the EO fragment (543 bp) with NEO-R/EO-F primers. In the second round or fusion PCR, the cycling conditions were kept the same as those used for deleting the targeted gene. The corresponding primers UP-F/NE-R were used for the fusion of the UPS fragment with the NE fragment. In contrast, the Dn-R/EO-F primers fused the DNS fragment with the EO fragment by splicing an overlapped extension. The products of fusion PCR were transformed through the PEG-mediated transformation method (Zhang et al., 2022) into the protoplasts (1×10^5 cells/mL) isolated from 5 d old mycelium of mutant *ΔBd-SCP10*a using the previously described method (Ning et al., 2022). Finally, the complementary transformants were screened on PDA supplemented with 150 μg/mL of the antibiotic G418, and the generated colonies were randomly selected and verified by standard PCR using the two sets of primers *Bd-SCP10*-F/*Bd-SCP10*-R and NEO-F/NEO-R.

2.6 Phenotype analysis

For the growth rate analysis, mycelial plugs (5 mm diameter) excised from colony margins were placed in the center of PDA (at least 3 replicates) and then incubated for 5 d at 25 °C in the dark (Wei et al., 2019). The per day radial growth rate (Oledibe et al., 2023) was calculated with formula [(Colony diameter – Plug diameter ÷ 2) × Number of incubation days] and per day biomass production rate (Novotna et al., 2023) was calculated with formula (Colony weight ÷ Number of incubation days) and final measurements were taken at 5 days post-inoculation (dpi). The hyphal tips of fungal strains were observed under a Ni90 microscope (Nikon, Japan) after 5 dpi incubation, following the previous method (Aboelfotoh Hendy et al., 2019; Zhang et al., 2020b).

2.7 Virulence assay

Virulence assay was performed on pear fruits (*Pyrus bretschneideri* var. huangguan) with the mycelial plugs (5 mm diameter) derived from actively growing colonies (at least 6 replicates), and uncolonized PDA plugs were involved in parallel as a control (CK). Mechanically produced wounds with a sterile needle on the fruits were used for inoculation by reversely placing mycelial plugs. After inoculation, the fruits were incubated at 25 °C with 100% relative humidity. The resulting lesions were measured at 5 days post-infection (dpi), and photos were taken to document lesion development.

2.8 Stress response assays

For a stress response assays, mycelia of Bd-wt, complementary strains, and mutants were quantitatively analyzed after cultured on unamended PDA or amended PDA [supplemented with different stress agents (at least 6 replicates), including 0.04% sodium dodecyl sulfate (SDS), 0.5 M calcium chloride ($CaCl_2$), 1 M glucose ($C_6H_{12}O_6$), 1.5 M sodium chloride (NaCl), 1 M potassium chloride (KCl), and 0.05% hydrogen peroxide (H_2O_2)] for 5 d, respectively. The percentage growth inhibition rates were calculated with the formula [(Do – Dt ÷ Do) × 100], where Do represents the mean colony diameter on PDA, and Dt represents the mean colony diameter on amended PDA (Khanh et al., 2024).

2.9 Statistical analysis

The quantitative data were statistically analyzed using Statistix v. 8.1 (Analytical Software, Florida, USA) with ANOVA and the least significant difference (LSD) test at $P \leq 0.05$. The bar graphs were drawn on GraphPad Prism v. 8.0 (GraphPad Software, California, USA).

3 Results

3.1 Phenotypic and virulence assay of the *B. dothidea* wildtype strain

For phenotypic analysis, the CK and Bd-wt were cultured on PDA for 5 d at 25 °C. CK culture showed a plain dish of PDA without fungal growth, while Bd-wt culture showed the whitish color of the colony with a fluffy cotton-like white margin and a relatively thick mycelium mat, as shown in Supplementary Figure S1A. For virulence assays, CK does not induce disease on pear fruits (var. huangguan, 6 replicates). However, lesions induced by Bd- wt can be seen in Supplementary Figure S1B after 5 dpi. Therefore, these results suggested that Bd-wt is a virulent strain.

3.2 Identification and characterization of the *Bd-SCP10* gene

The MEROPS database analysis of amino acid sequences similar to *SCPs* belonging to the peptidase S10 family revealed its homolog in *B. dothidea*, which was tentatively named as *Bd-SCP10*. *Bd-SCP10* shared the highest identity (40.9%, *E-value* = $8.9E^{-133}$) with the homolog in *Microsporum canis* (EEQ30006.1), a member of the family Arthrodermataceae. A phylogenetic tree was constructed based on the amino acid sequences of *Bd-SCP10* together with other homologs of *SCPs* chosen from 12 fungal species based on percentage amino acid sequence identity and *E-value* (32% to 40.9%, and $8.9E^{-133}$ to $7.9E^{-57}$, respectively). The neighbor-joining phylogenetic tree showed that all the fungal *SCPs* were grouped into 3 clusters (a to c), and *Bd-SCP10* was located in a separate clade far from other members in cluster A and that has been shown in Figure 1A. The multiple sequence alignment results depicted that *Bd-SCP10* belongs to the peptidase S10 family (PF00450) and this family have 43 conserved amino acids among in all of the selected phytopathogenic fungi shown in Figure 1B.

3.3 Knockout of the *Bd-SCP10* gene from a wildtype strain

To verify the gene function of *Bd-SCP10*, Bd-wt induced long lesions (approximately 35.8 mm) as inoculated on pear fruits (*Pyrus bretschneideri* var. huangguan) as shown in Supplementary Figures S1A, B, was subjected to knockout for the target gene through split marker strategy, i.e., *Bd-SCP10* gene was replaced with a HYG resistance cassette through homologous recombination (Dong and Guo, 2020) of the flanking parts around the targeted gene and schematic representation has been shown in Figure 2A. The first-round PCR was conducted to amplify 887 bp UPS and 789 bp DNS fragments, as well as the HY (767 bp) and YG (931 bp) fragments of the HYG resistance cassette as shown in Figure 2B and Supplementary Figure S2A. The UPS fragment was further fused with the HY fragment using fusion PCR, generating the fragment termed as 5′HY (1654 bp). Similarly, fragment DNS was fused with YG to generate a fragment termed as 3′YG (1720 bp), which is shown in Figure 2C and Supplementary Figure S2B. The resulting DNA fragments 5′HY and 3′YG were purified and used to transfect the protoplasts of Bd-wt through PEG-mediated transformation. Upon transfection, a UPS-HYG-DNS combination replaced the *Bd-SCP10* gene through homologous recombination. After transfection, 12 colonies were grown in media containing the antibiotic HYG, and 3 colonies named *ΔBd-SCP10*a, *ΔBd-SCP10*b, and *ΔBd-SCP10*c were selected for identification by a strict PCR strategy with *Bd-SCP10*-F/*Bd-SCP10*-R and HYG-F/HYG-R primers mentioned in Supplementary Table S1, targeting *Bd-SCP10* and HYG fragments, respectively. The results showed that the *Bd-SCP10* amplified fragment of 1200 bp was detected in Bd-wt except in mutants, while the HYG amplified fragment of 1383 bp was present in mutants except for Bd-wt, as depicted in Figure 2D, suggesting that *Bd-SCP10* was successfully knocked out.

3.4 Complementation of the *Bd-SCP10* gene

The mutant *ΔBd-SCP10*a was subjected for complementation of the targeted gene through split marker strategy, i.e., the HYG resistance cassette was replaced with gene *Bd-SCP10* and NEO resistance cassette through homologous recombination (Dong and Guo, 2020) of the flanking parts around the HYG resistance cassette and schematic representation can been seen in Figure 3A. The first-round PCR was conducted to amplify the 2800 bp UPS and 832 bp DNS fragments, along with the NE (975 bp) and EO (543 bp) fragments of the NEO resistance cassette, as shown in Figure 3B and Supplementary Figure S3A. The UPS fragment was further fused

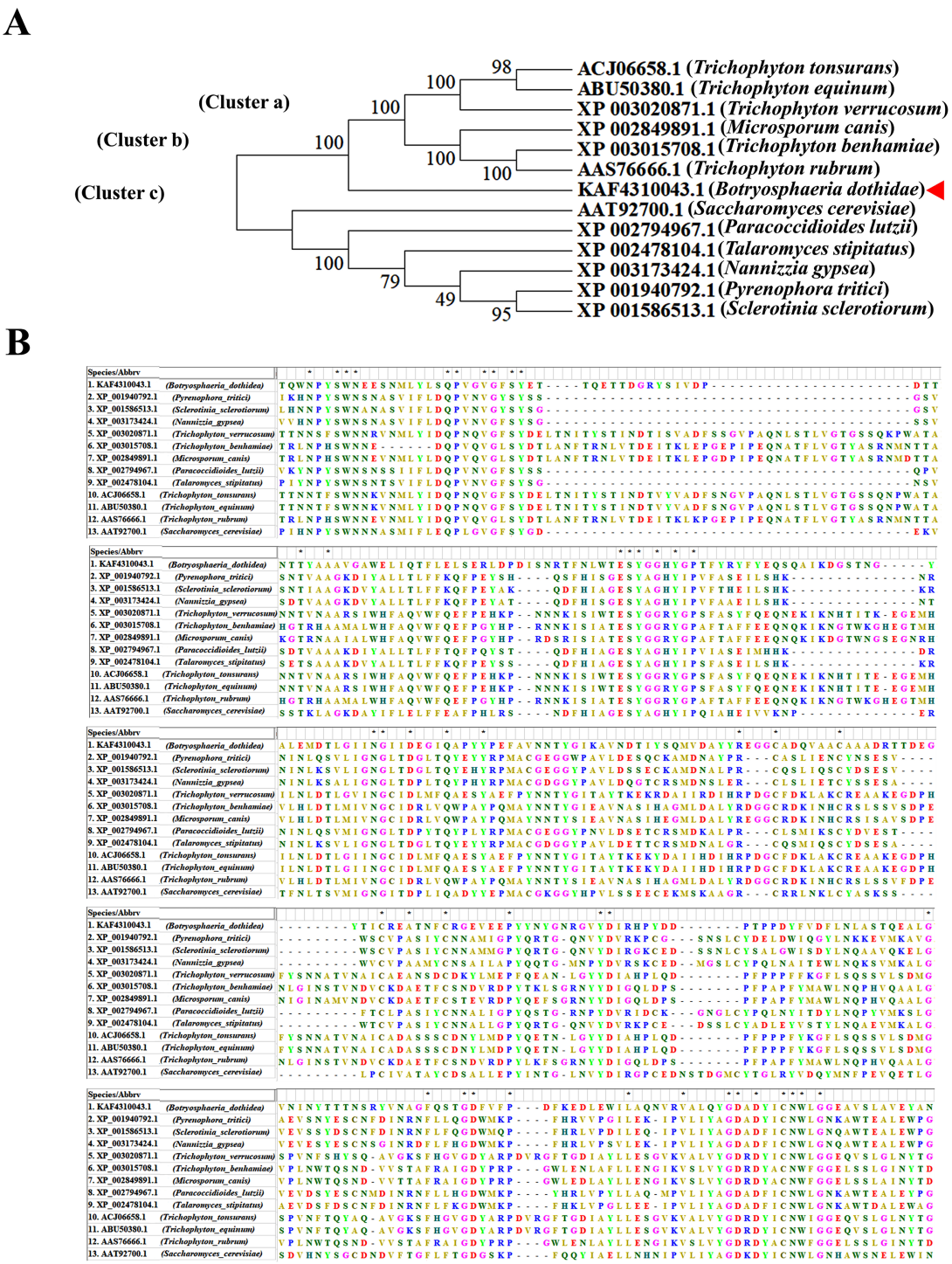

FIGURE 1
Phylogenetic analysis and multiple sequence alignment of *Bd-SCP10* together with other fungal homologs of *SCPs*. **(A)** The phylogenetic tree was generated using MEGA v. 7.0 with the neighbor-joining method, and fungal *SCPs* were grouped into 3 clusters (a to c) as indicated by the arrow. The number beside the branch nodes refers to the bootstrap value, and the host's fungal name is presented in brackets, followed by the homolog accession number. *B. dothidea* is indicated with a triangle ahead of its accession number. **(B)** The sequences of amino acids are aligned using Clustal Omega, and conserved amino acids among the selected pathogenic fungi are denoted by an asterisk (*).

with the NE fragment using fusion PCR, resulting in the 5′NE (3775 bp) fragment. At the same time, the DNS with EO generated the 3′EO (1375 bp) fragment, as depicted in Figure 3C and Supplementary Figure S3B. The resulting DNA fragments 5′NE and 3′EO were purified and used to transfect the protoplasts of the mutant *ΔBd-SCP10*a through PEG-mediated transformation. Upon transfection, a UPS-NEO-DNS combination replaced the HYG resistance cassette through homologous recombination. After

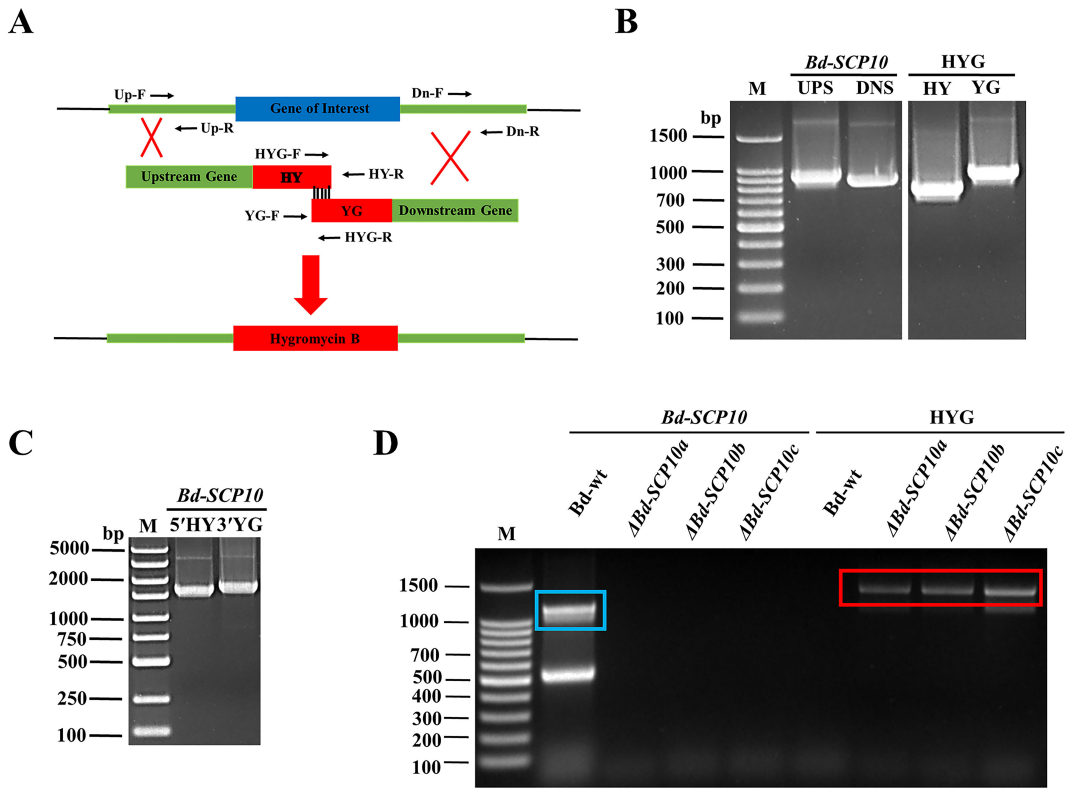

FIGURE 2
Targeted knockout of *Bd-SCP10* from *B. dothidea* through split marker strategy and PCR identification of the mutants. **(A)** Schematic representation of the split marker strategy for deleting *Bd-SCP10* from Bd-wt. **(B)** First-round PCR amplified fragments (UPS: 887 bp, DNS: 789 bp, HY: 767 bp, and YG: 931 bp). **(C)** Fusion PCR products showing the synthesis of the two recombinant fragments 5′HY (1654 bp) and 3′YG (1720 bp) used for transformation. **(D)** PCR identification for the *Bd-SCP10* gene and HYG resistance cassette in Bd-wt and mutants. Amplification of *Bd-SCP10* (blue box, amplified band of 1200 bp) was detected only in Bd-wt, while amplification of the HYG cassette (red box, amplified band of 1383 bp) was detected only in mutants (*ΔBd-SCP10a*, *ΔBd-SCP10b*, and *ΔBd-SCP10c*), confirming successful gene knockout. Here, M is denoted for DNA markers (Note: The original gel documentation figures for **(B, C)** can be seen in Supplementary Figure S2).

transfection, 8 colonies were grown in the media containing G418 antibiotic, and colonies *CΔBd-SCP10*a, *CΔBd-SCP10*b, and *CΔBd-SCP10*c were picked for identification by PCR strategy with *Bd-SCP10*-F/*Bd-SCP10*-R and NEO-F/NEO-R primers described in Supplementary Table S1, targeting *Bd-SCP10* and NEO fragments, respectively. The results showed that the amplified fragment of 1200 bp *Bd-SCP10* was detected in Bd-wt together with complementary strains, while the NEO amplified fragment of 1200 bp was present in complementary strains except for Bd-wt, as shown in Figure 3D, suggesting that complementation of *Bd-SCP10* was successful and complementary strains were generated from mutant *ΔBd-SCP10*a.

3.5 *Bd-SCP10* gene is required for vegetative growth and virulence

To test whether *Bd-SCP10* is related to the fungal vegetative growth, the mutants and complementary strains, along with Bd-wt, were cultured on PDA in triplicate for 5 d and subjected to assessment of their phenotype, growth, and biomass. These mutants exhibited snowy white and compact aerial mycelium throughout the entire colonies, characterized by random radial grooves. In contrast, both complementary strains and Bd-wt showed a collapsed and cleared mycelial growth in the colony center. At the same time, upward fluffy and cottony mycelia in the margins can be seen in Figure 4A. Additionally, the mutants exhibited growth rates ranging from 2.1 mm/d (*ΔBd-SCP10*b) to 2.4 mm/d (*ΔBd-SCP10*c), which were substantially reduced compared to Bd-wt (15.9 mm/d). However, the growth rates for *Bd-SCP10* complementary strains ranged from 15.4 mm/d (*CΔBd-SCP10*a) to 15.5 mm/d (*CΔBd-SCP10*c), which are nearly identical to Bd-wt, and are shown in Figure 4B and Supplementary Table S2. The biomass production for the mutants was observed, ranging from 0.018 g/d (*ΔBd-SCP10*b) to 0.019 g/d (*ΔBd-SCP10*c), which were significantly lower than Bd-wt (0.2 g/d), while complementary strains produced biomass approximately 0.2 g/d (*CΔBd-SCP10*b to *CΔBd-SCP10*c), similar to Bd-wt, as shown in Figure 4C and Supplementary Table S2. Moreover, the hyphal tips of Bd-wt and complementary strains have fewer septa at hyphal tips and more dense mycelial growth than mutants, as observed in Supplementary Figures S4A, B. The results showed that *Bd-SCP10* is involved in the phenotypic development and vegetative growth of *B. dothidea*. To test whether *Bd-SCP10* is associated with fungal pathogenicity,

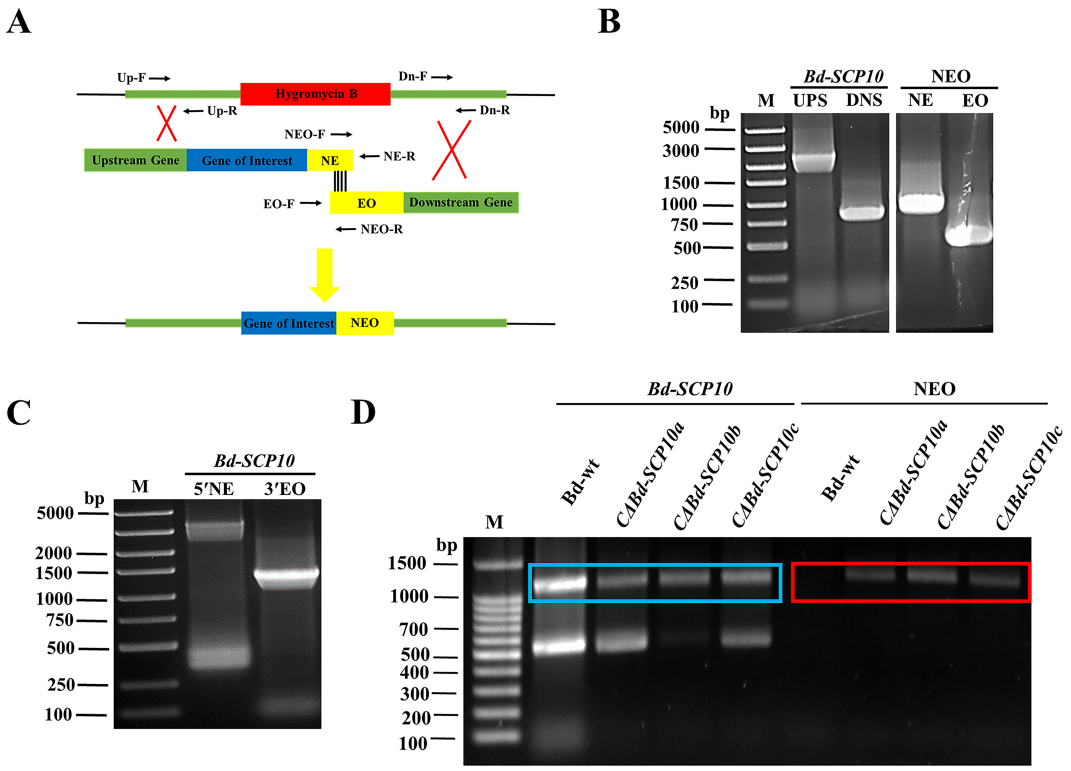

FIGURE 3
Complementation of the *Bd-SCP10* mutant through the split marker strategy and PCR identification of the complementary strains. **(A)** Schematic representation of the complementation through the split marker strategy, in which *Bd-SCP10* was reintroduced into mutant *ΔBd-SCP10a* with the NEO resistance cassette. **(B)** First-round PCR fragments (UPS: 2800 bp, DNS: 832 bp, NE: 975 bp, and EO: 543 bp). **(C)** Fusion PCR products, which showed recombinant fragments (5′NE, 3775 bp; 3′EO, 1375 bp), were used for transformation. **(D)** PCR identification for the *Bd-SCP10* gene and NEO resistance cassette in Bd-wt and complementary strains. *Bd-SCP10* (blue box, amplified band of 1200 bp) was detected in Bd-wt and complementary strains (*CΔBd-SCP10a*, *CΔBd-SCP10b*, and *CΔBd-SCP10c*), while the NEO cassette (red box, amplified band of 1200 bp) was detected only in complementary strains, confirming restoration of *Bd-SCP10* expression in *ΔBd-SCP10a*. Here, M is denoted for DNA markers (Note: The original gel documentation figures for **(B, C)** are shown in Supplementary Figure S3).

the mutants and complementary strains together with Bd-wt were assessed on the pear fruits (var. huangguan, 6 replicates). At 5 dpi, the *Bd-SCP10* complementary strains induced lesions ranging from 28.4 mm (*CΔBd-SCP10*c) to 29.1 mm (*CΔBd-SCP10*b). It is almost similar to the lesion lengths (31.1 mm) induced by Bd-wt. In contrast, the mutants did not induce lesions, as shown in Figures 4A, D, and Supplementary Table S3. These results suggested that *Bd-SCP10* is responsible for the pathogenicity of *B. dothidea*.

3.6 *Bd-SCP10* gene plays a role in stress tolerance and cell wall integrity

Mutants and complementary strains, along with Bd-wt, were cultured on PDA amended with 0.04% SDS to analyze the level of tolerance to cell wall disruption. The results showed significantly higher growth inhibition rates ranging from 45.0% to 49.9% in mutants compared to Bd-wt (27.6%) and complementary strains (29.3% to 33.9%). Similarly, on PDA amended with chemicals used to response against hyperosmotic stresses (0.5 M $CaCl_2$, 1 M $C_6H_{12}O_6$, 1.5 M NaCl, and 1 M KCl) all mutants showed significantly reduced growth rates on PDA amended with 0.5 M $CaCl_2$, 1 M $C_6H_{12}O_6$, and 1 M KCl (42.8 to 49.3%, 15.9 to 25.2%, and 42.2 to 48%, respectively) as compared to Bd-wt (7.5%, 5%, and 15.2%) and the complementary strains (8.6 to 14.2%, 15.9 to 25.2%, and 22.8 to 30%). In contrast, the mutants did not show a significant difference in the growth inhibition rates on PDA amended with 1.5 M NaCl (72.4 to 74.7%) as compared with Bd-wt (75.31%) or the complementary strains (76 to 77.2%). Moreover, on PDA amended with 0.05% H_2O_2, the response of strains against oxidative stress was observed. The results highlighted that mutant had a significantly higher growth inhibition rate from 46% to 59% than Bd-wt (1.6%) and complementary strains (0.8 to 2.5%), as shown in Figures 5 and 6, along with Supplementary Tables S4 and S5. These results suggested that the *Bd-SCP10* gene is involved in cell wall integrity and contributes to the resistance against hyperosmotic and oxidative stresses in *B. dothidea*.

4 Discussion

SCPs were functionally reported to be involved in protein processing and degradation, as well as the production of secondary

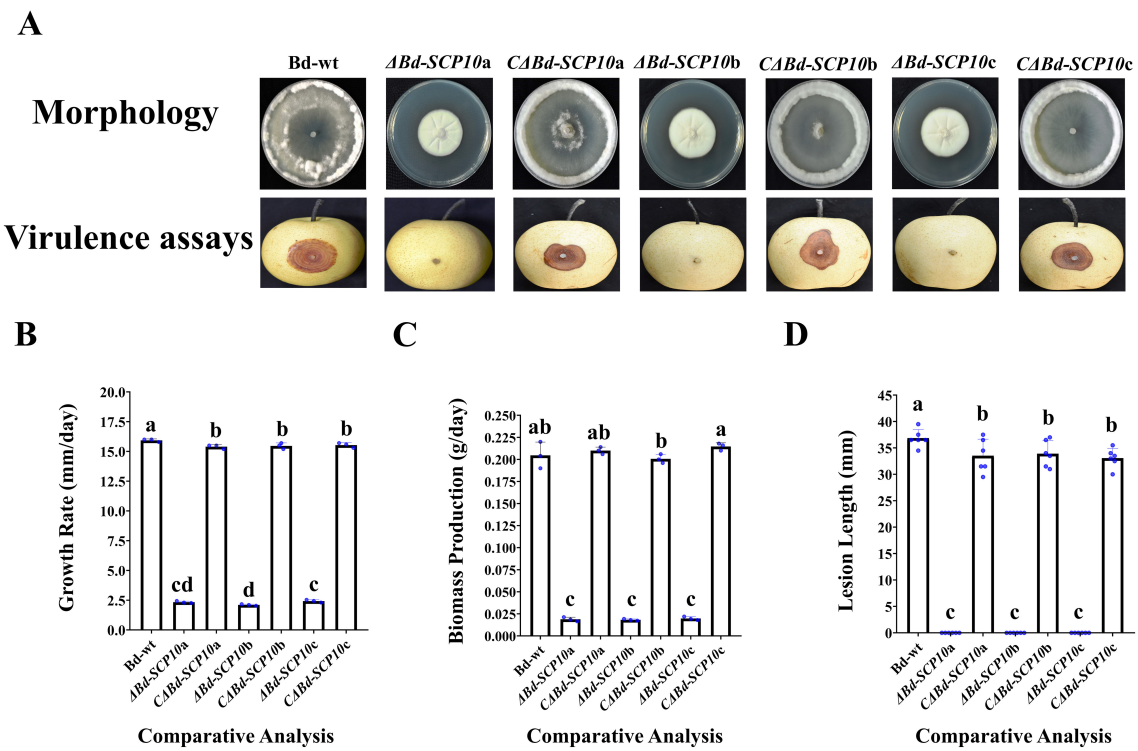

FIGURE 4
Comparative analysis of Bd-wt, mutants, and complementary strains for vegetative growth, biomass production, and virulence. **(A)** Phenotype and induced symptoms on the inoculated pear fruits (*Pyrus bretschneideri* var. huangguan) for Bd-wt, mutants, and complementary strains. **(B-D)** Bar graphs for the growth rates, biomass, and lesion lengths on the inoculated pear fruits for Bd-wt, mutants, and complementary strains, respectively. The alphabet on a column represented analysis of variance (ANOVA) with the least significant difference (LSD) at $P \leq 0.05$. During this experimental process, 3 replicates were used for vegetative growth and biomass production, and 6 replicates were used for the virulence assay.

metabolites (Chen et al., 2022). This study aligns with emerging evidence that secreted peptidases, particularly *SCPs* belonging to the S10 family, are key virulence factors (Iqbal et al., 2018; Zhang et al., 2019) in phytopathogenic fungi (Semenova et al., 2020). *SCPs* were also identified as potential regulators of phenotypes, habitat adaptation, and growth (Iqbal et al., 2018). However, the functions of *SCPs* in the phytopathogenic fungus *B. dothidea* are still unknown. In this study, we performed functional characterization of the *Bd-SCP10* gene, a homolog of the *SCPs* in *B. dothidea*. Our experimental data confirmed that *Bd-SCP10* plays a key role in vegetative growth, pathogenicity, and stress response, as demonstrated by generating mutants and complementary strains using a split marker strategy. *FgSCP* was previously reported for its role in the virulence of *F. graminearum*, and affects fungal growth, stress tolerance, and pathogenicity. It also suppresses cell death triggered by the *INF1* elicitor, indicating its role in modulating plant immune responses (Liu et al., 2024). The substantial reduction in radial growth of Bd-wt (2.1–2.4 mm/d vs. 15.9 mm/d) and biomass production (0.018–0.019 g/d vs. 0.2 g/d) in mutants underscores the importance of the *Bd-SCP10* in fungal physiology. Similar observations were found in *Botrytis cinerea* and *Sclerotinia sclerotiorum*, highlighting that peptidases often facilitate nutrient acquisition by hydrolyzing host proteins into assimilable amino acids (Urbanek and Kaczmarek, 1985; Clark et al., 1997). Moreover, it was reported that *Magnaporthe oryzae* wildtype and complementary strains have denser mycelial development than mutants, as the hyphal tips of the wildtype strain have longer cell lengths and less septation as compared to the mutant, which has more septation and shorter cell lengths (Aboelfotoh Hendy et al., 2019; Zhang et al., 2020b). Our microscopic studies revealed that the thin and compact mycelia of mutants suggested that *Bd-SCP10* regulates hyphal expansion or septation, processes that require precise proteolytic activity to remodel cell walls or recycle proteins (Zhang et al., 2020b). Furthermore, we did not find any differences in colony pigmentation among the mutants, suggesting that the production of secondary metabolites (e.g., melanin or polyketide-derived pigments) was not noticeably affected under PDA culture conditions. Even so, *SCPs* have been reported for the regulation of fungal secondary metabolism in other fungal species (Madhu et al., 2020). It suggested that the *Bd-SCP10* gene is involved in the fungal growth and the phenotypic development of *B. dothidea*. *SCPs* regulate virulence in *Phellinus sulphurascens* (Williams et al., 2014) and *Clonostachys rosea* (Iqbal et al., 2018). A secreted peptidase, BEC1019, regulating a virulence factor, was identified in *Blumeria graminis*, which is required for haustorium development. Silencing of *BEC1019* induced hypovirulence in the fungus (Zhang et al., 2019). An ortholog *Rs-SCP1* was identified in the plant-parasitic nematode *Radopholus similis* and was involved in reducing pathogenicity (Huang et al., 2017b). Mutations in the *FgSCP* gene compromise nutritional growth and stress tolerance, and deletion leads to reduced

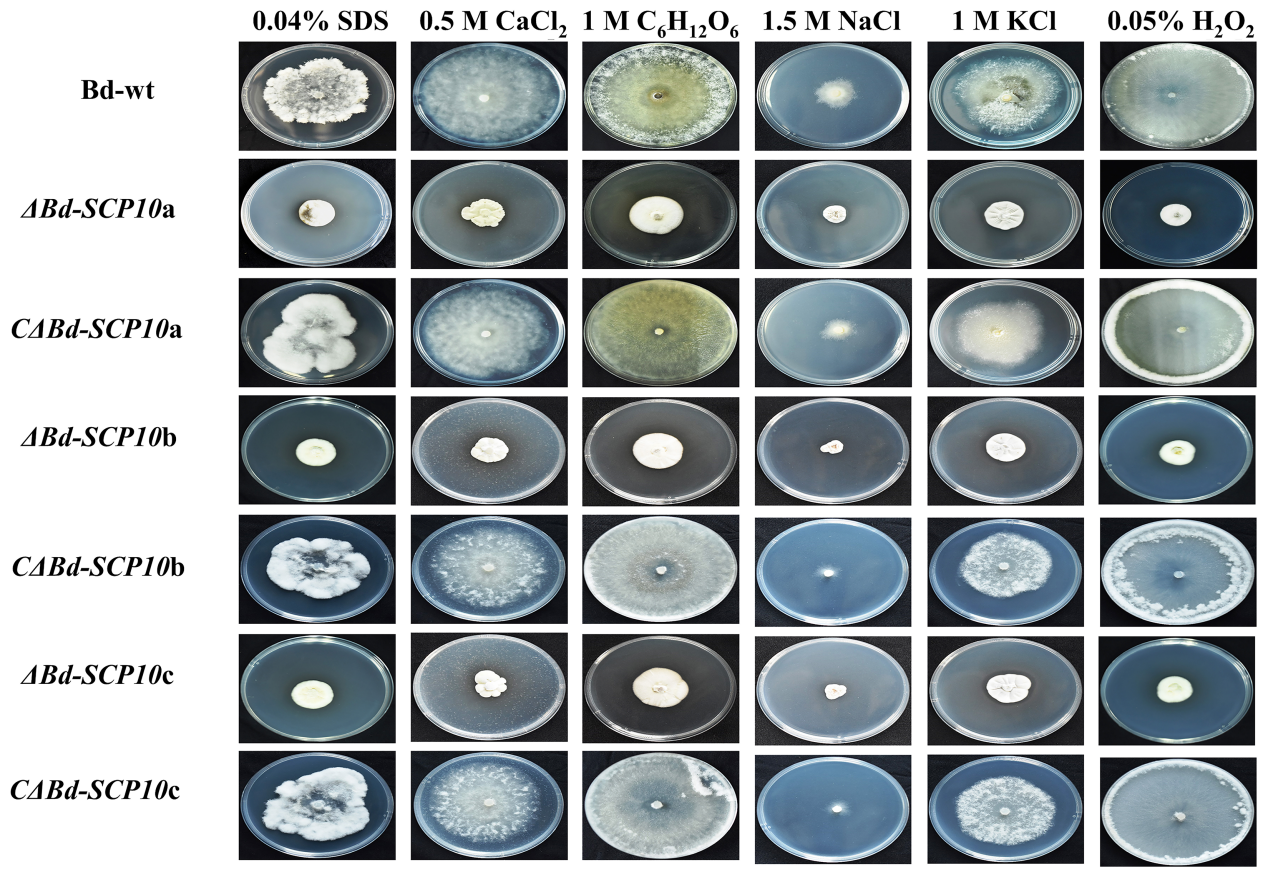

FIGURE 5
Phenotypic comparison of Bd-wt, mutant, and complementary strains on PDA amended with 0.04% SDS, 0.5 M $CaCl_2$, 1 M $C_6H_{12}O_6$, 1.5 M NaCl, 1 M KCl, and 0.05% H_2O_2 after 5 d at 25 °C. Mutants exhibited reduced growth relative to Bd-wt and complementary strains, particularly under SDS, $CaCl_2$, $C_6H_{12}O_6$, KCl, and H_2O_2 stress.

pathogenicity in *F. graminearum*. Expression is upregulated during infection, suggesting involvement in invasion and potentially by suppressing host defense genes (Liu et al., 2024). The full loss of pathogenicity in mutants on pear fruits and the restoration of pathogenicity in complementary strains represented the essential role of *Bd-SCP10* in infection. Mirror findings in *Fusarium culmorum* revealed that secreted peptidases degrade host defense proteins, enabling tissue colonization by *Fusarium culmorum* (Urbanek and Yirdaw, 1984). Notably, *B. dothidea* inoculation relied on wounded fruit surfaces, implying that *Bd-SCP10* acts post penetration by degrading plant cell wall components or suppressing host immune responses. For instance, fungal proteases in *Glomerella cingulata* cleave pathogenesis-related (PR) proteins, neutralizing plant defenses (Clark et al., 1997). The hypersensitivity of *ΔBd-SCP10* mutants to cell wall disrupting agents (0.04% SDS) and hyperosmotic stressors (0.5 M $CaCl_2$, 1 M $C_6H_{12}O_6$, and 1 M KCl) emphasized the role of *Bd-SCP10* in maintaining cell wall integrity and osmotic homeostasis. These results align with studies related to *Aspergillus fumigatus*, in which *SCPs* were reported to stabilize the cell wall under stress by processing structural proteins (Gravelat et al., 2012). Mannoproteins present in the cell wall of *Candida albicans* play important roles in cell wall remodeling under stress. These proteins interact with cell wall integrity and stress-activated signaling pathways, such as the high-osmolarity glycerol (HOG) and mitogen-activated protein kinase (MAPK) pathways (e.g., Cek1 and Mkc1), which explain how cell wall protein processing ties into stress tolerance (Ibe and Munro, 2021). Although direct evidence connecting *SCPs* to the processing of fungal wall proteins is lacking, the moonlighting capacity of extracellular fungal proteases (Satala et al., 2023) supports the hypothesis that *Bd-SCP10* may serve a functional role in vegetative growth, pathogenicity, and stress tolerance. However, the unaltered sensitivity to 1.5 M NaCl in mutants suggested that *Bd-SCP10* selectively regulates osmotic stress pathways, possibly via interactions with calcium or potassium signaling cascades rather than sodium-specific transporters. In plants, the rapid production and accumulation of reactive oxygen species (ROS) are considered the initial response to invading pathogens (Shetty et al., 2007; Imam et al., 2016). The H_2O_2 is a critical ROS that host plants can produce in response to fungal infection and initiate lipid peroxidation, DNA damage, formation of hydroxyl radicals, and protein oxidation (Rolke et al., 2004). Therefore, proper cell wall integrity and stress tolerance are essential for successful fungal infection and thus required for pathogenicity in numerous phytopathogenic fungi (Kim et al., 2009). Similarly, oxidative stress

10.3389/fpls.2025.1678786

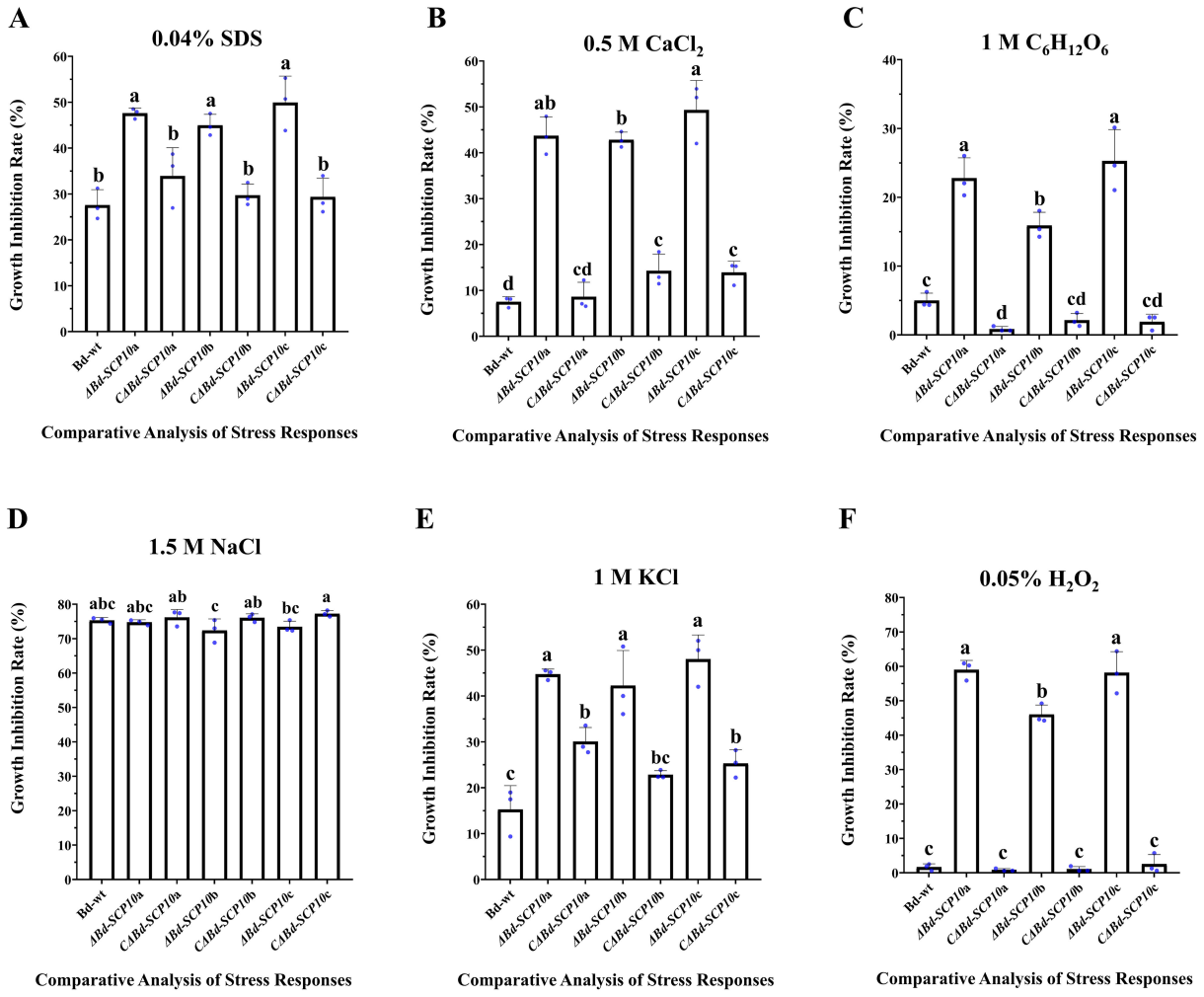

FIGURE 6
Comparative analysis of stress responses of Bd-wt, mutant, and complementary strains. Growth inhibition rates were measured on PDA amended with 0.04% SDS **(A)**, 0.5 M $CaCl_2$ **(B)**, 1 M $C_6H_{12}O_6$ **(C)**, 1.5 M NaCl **(D)**, 1 M KCl **(E)**, and 0.05% H_2O_2 **(F)**. Alphabet on a columns depicted ANOVA with the LSD at $P \leq 0.05$, mutants exhibiting pronounced sensitivity to cell wall disrupting, osmotic, and oxidative stresses, underscoring the importance of *Bd-SCP10* in fungal stress tolerance.

hypersensitivity (0.05% H_2O_2) suggests that *Bd-SCP10* may mitigate ROS generated during host invasion, a strategy employed by *Magnaporthe oryzae* to counteract plant oxidative bursts (Zhang et al., 2020b). The partial restoration of stress tolerance in complementary strains indicated the potential epistatic interactions or incomplete genetic rescue, warranting further transcriptomic analyses to map regulatory networks involving *Bd-SCP10*. In addition, the HOG pathway is associated with hyperosmotic stresses and the osmoregulation ability of fungal pathogens, primarily due to its involvement in an environment characterized by hyperosmotic stresses (Yaakoub et al., 2022). However, our studies found that mutants showed hypersensitivity in response to hyperosmotic stresses (0.5 M $CaCl_2$, 1 M $C_6H_{12}O_6$, and 1 M KCl, except for 1.5 M NaCl). Deletion of *Bd-SCP10* from Bd-wt has no link with the osmoregulation of 1.5 M NaCl, and we found the same results as mutant *Bdo-05381* from *B. dothidea* strains HTLW03 and ZY7 (Dong and Guo, 2020). These results indicate that *Bd-SCP10* is a positive modulator of the HOG pathway for the hyperosmotic stress response against 0.5 M $CaCl_2$, 1 M $C_6H_{12}O_6$, and 1 M KCl but a negative modulator for the hyperosmotic stress response against 1.5 M NaCl. Phylogenetically, *SCPs* are conserved in phytopathogenic fungi (Lv et al., 2023). However, *Bd-SCP10* clusters separately from *SCPs* homologs found in other fungi. These results suggest evolutionary divergence personalized to the host range or environmental niche of *B. dothidea*. This divergence may explain its unique regulatory roles, such as its apparent lack of relevance to NaCl tolerance. Comparative genomics could elucidate whether homologs of *Bd-SCP10* in related pathogens share similar functional specializations. While this study provides compelling evidence for multifunctionality, limitations exist for *Bd-SCP10*. The split marker knockout strategy although is reliable method however it does not rule out off-target effects. CRISPR-Cas9 validation could strengthen conclusions. Additionally, *in vitro*, fruit assays may not fully replicate field conditions, where host-pathogen interactions

involve complex environmental and immunological variables. Future studies should aim to identify the direct substrates of *Bd-SCP10* through proteomic approaches to clarify its mechanistic role in host invasion. Host response profiling using transcriptomics or metabolomics could reveal how *Bd-SCP10* modulates plant defense pathways, particularly ROS detoxification and PR protein activity. In planta, validation under natural conditions will be essential to assess its role in systemic colonization and disease spread. Moreover, exploring *Bd-SCP10* associated stress regulatory networks and evolutionary comparisons with homologs of *SCPs* in related fungi may uncover unique adaptations. Finally, screening for specific inhibitors of *Bd-SCP10* could provide novel, eco-friendly strategies for controlling *B. dothidea* infections.

5 Conclusion

This study provides the first functional characterization of *Bd-SCP10*, a homolog of serine carboxypeptidase belonging to the S10 family in *B. dothidea*. Our results demonstrate that *Bd-SCP10* is essential for pathogenicity and stress tolerance, also revealing its role in maintaining growth and cell wall integrity. The complete loss of pathogenicity in mutants suggested that *Bd-SCP10* is an essential determinant of pathogenicity. However, identifying *Bd-SCP10* as a functional regulator of vegetative growth, pathogenicity, and stress tolerance, this work provides a foundation for developing eco-friendly control strategies against *B. dothidea* and related pathogens.

Data availability statement

The raw data supporting the conclusions of this article will be made available by the authors, without undue reservation.

Author contributions

MU: Data curation, Methodology, Writing – review & editing. NA: Validation, Writing – review & editing. MM: Conceptualization, Investigation, Methodology, Software, Writing – original draft, Writing – review & editing. YL: Project administration, Writing – review & editing. KA: Formal analysis, Writing – review & editing. AA: Formal analysis, Writing – review & editing. PL: Funding acquisition, Resources, Supervision, Writing – review & editing.

Funding

The author(s) declare financial support was received for the research and/or publication of this article. This work was supported by grants from the China NSFC Research Fund for International Young Scientists (grant number: 32250410291) and a Special Project for the Academician Team Innovation Centre of Hainan Province (grant number: YSPTZX202206).

Acknowledgments

The authors extend their appreciation to the Deanship of Research and Graduate Studies at King Khalid University for funding work through the Large Research Project under grant number RGP2/316/45.

Conflict of interest

Th authors declare that the research was conducted in the absence of any commercial or financial relationships that could be construed as a potential conflict of interest.

The author(s) declared that they were an editorial board member of Frontiers, at the time of submission. This had no impact on the peer review process and the final decision.

Generative AI statement

The author(s) declare that no Generative AI was used in the creation of this manuscript.

Any alternative text (alt text) provided alongside figures in this article has been generated by Frontiers with the support of artificial intelligence and reasonable efforts have been made to ensure accuracy, including review by the authors wherever possible. If you identify any issues, please contact us.

Publisher's note

Supplementary material

The Supplementary Material for this article can be found online at: https://www.frontiersin.org/articles/10.3389/fpls.2025.1678786/full#supplementary-material

References

Aboelfotoh Hendy, A., Xing, J., Chen, X., and Chen, X. L. (2019). The farnesyltransferase B-subunit *ram1* regulates localization of RAS proteins and appressorium-mediated infection in *Magnaporthe oryzae*. *Mol. Plant Pathol.* 20, 1264–1278. doi: 10.1111/mpp.12838

Ahmad, S. U., Khan, M. S., Jan, Z., Khan, N., Ali, A., Rehman, N., et al. (2021). Genome wide association study and phylogenetic analysis of novel SARS-COV-2 virus among different countries. *Pakistan J. Pharm. Sci.* 34, 1305-1313.

Chen, Y., Liao, X., Zhang, C., Kong, X., and Hua, Y. (2022). Hydrolyzing behaviors of endogenous proteases on proteins in sesame milk and application for producing low-phytate sesame protein hydrolysate. *Food Chem.* 385, 132617. doi: 10.1016/j.foodchem.2022.132617

Chethana, K. W. T., Jayawardena, R. S., Chen, Y. J., Konta, S., Tibpromma, S., Abeywickrama, P. D., et al. (2021). Diversity and function of appressoria. *Pathogens* 10, 746. doi: 10.3390/pathogens10060746

Clark, S. J., Templeton, M. D., and Sullivan, P. A. (1997). A Secreted Aspartic Proteinase from *Glomerella cingulata*: Purification of the Enzyme and Molecular Cloning of the cDNA. *Microbiol-SGM* 143, 1395–1403. doi: 10.1099/00221287-143-4-1395

Da Silva, B. A., Dos Santos, A. L., Barreto-Bergter, E., and Pinto, M. R. (2006). Extracellular peptidase in the fungal pathogen Pseudallescheria boydii. *Curr. Microbiol.* 53, 18–22. doi: 10.1007/s00284-005-0156-1

Da Silva, R. R. (2018). Commentary: Fungal lifestyle reflected in serine protease repertoire. *Front. Microbiol.* 9. doi: 10.3389/fmicb.2018.00467

Dong, B.-Z., and Guo, L.-Y. (2020). An efficient gene disruption method for the woody plant pathogen *Botryosphaeria dothidea*. *BMC Biotechnol.* 20, 14. doi: 10.1186/s12896-020-00608-z

Dong, Z., Yang, S., and Lee, B. H. (2021). Bioinformatic mapping of a more precise Aspergillus Niger degradome. *Sci. Rep.* 11, 693. doi: 10.1038/s41598-020-80028-3

Gravelat, F. N., Askew, D. S., and Sheppard, D. C. (2012). Targeted Gene Deletion in *Aspergillus fumigatus* using the Hygromycin-Resistance Split-Marker Approach. *Methods Mol. Biol.* 845, 119–130. doi: 10.1007/978-1-61779-539-8_8

Huang, C., Cun, Y., Yu, H., Tong, Z., Xiao, B., Song, Z., et al. (2017a). Transcriptomic profile of tobacco in response to tomato zonate spot orthotospovirus infection. *Virol. J.* 14, 153. doi: 10.1186/s12985-017-0821-6

Huang, X., Xu, C. L., Chen, W. Z., Chen, C., and Xie, H. (2017b). Cloning and characterization of the first serine carboxypeptidase from a plant parasitic nematode, *Radopholus similis*. *Sci. Rep.* 7, 4815. doi: 10.1038/s41598-017-05093-7

Ibe, C., and Munro, C. A. (2021). Fungal cell wall proteins and signaling pathways form a cytoprotective network to combat stresses. *J. Fungi (Basel)* 7, 739. doi: 10.3390/jof7090739

Imam, J., Mandal, N. P., Variar, M., and Shukla, P. (2016). "Advances in molecular mechanism toward understanding plant-microbe interaction: A study of M. oryzae versus rice," in *Frontier discoveries and innovations in interdisciplinary microbiology* (India: Springer), 79–96. doi: 10.1007/978-81-322-2610-9_6

Iqbal, M., Dubey, M., Gudmundsson, M., Viketoft, M., Jensen, D. F., and Karlsson, M. (2018). Comparative evolutionary histories of fungal proteases reveal gene gains in the mycoparasitic and nematode-parasitic fungus Clonostachys rosea. *BMC Evol. Biol.* 18, 171. doi: 10.1186/s12862-018-1291-1

Jash, S., Sarkar, A., Moinuddin, G., and Kundu, R. (2025). "Botryosphaeria," in *Compendium of Phytopathogenic Microbes in Agro-Ecology*. Eds. N. Amaresan and K. Kumar (Springer Nature Switzerland, Cham), 43–74. doi: 10.1007/978-3-031-81770-0_3

Jasim, J. H. M., Othman, A. S., Nordin, F. A., and Talkah, N. S. M. (2024). High-quality genomic DNA extraction methods of Yellow Spathoglottis Blume complex for next-generation sequencing. *Biodiversitas J. Biol. Diversity* 25, 654-663. doi: 10.13057/biodiv/d250224

Khanh, N. V., Dutta, S., Kim, C. S., and Lee, Y. H. (2024). Features of bacterial and fungal communities in the rhizosphere of *Gastrodia elata* cultivated in greenhouse for early harvest. *Front. Microbiol.* 15. doi: 10.3389/fmicb.2024.1389907

Kim, K. W., Kim, K. R., and Park, E. W. (2016). Effects of interrupted wetness periods on conidial germination, germ tube elongation and infection periods of *Botryosphaeria dothidea* causing apple white rot. *Plant Pathol.* 32, 1–7. doi: 10.5423/ppj.Oa.07.2015.0131

Kim, J. E., Lee, H. J., Lee, J., Kim, K. W., Yun, S. H., Shim, W. B., et al. (2009). Gibberella zeae chitin synthase genes, GzCHS5 and GzCHS7, are required for hyphal growth, perithecia formation, and pathogenicity. *Curr. Genet.* 55, 449–459. doi: 10.1007/s00294-009-0258-6

Krishnan, P., Ma, X., Mcdonald, B. A., and Brunner, P. C. (2018). Widespread signatures of selection for secreted peptidases in a fungal plant pathogen. *BMC Evol. Biol.* 18, 7. doi: 10.1186/s12862-018-1123-3

Kumar, S., Stecher, G., and Tamura, K. (2016). MEGA7: molecular evolutionary genetics analysis version 7.0 for bigger datasets. *Mol. Biol. Evol.* 33, 1870–1874. doi: 10.1093/molbev/msw054

Lin, L., Wu, Q., Wang, S., Gong, Q., Huang, X., Abubakar, Y. S., et al. (2025a). Recycling of trans-golgi SNAREs promotes apoplastic effector secretion for effective host invasion in magnaporthe oryzae. *Plant Cell Environ.* 48, 6047–6065. doi: 10.1111/pce.15582

Lin, X., Yang, Y., Huang, C., Xiong, D., Qiu, X., and Tian, C. (2025b). Transcriptome analysis reveals that a Gti1/Pac2 family gene, CpSge1, regulates fungal growth, stress response, and virulence in *Cryphonectria parasitica*. *Phytopathology* 115, 521–534. doi: 10.1094/PHYTO-11-24-0354-R

Liu, K., Wang, X., Qi, Y., Li, Y., Shi, Y., Ren, Y., et al. (2024). Effector protein serine carboxypeptidase fgSCP is essential for full virulence in Fusarium graminearum and is involved in modulating plant immune responses. *Phytopathology* 114, 2131–2142. doi: 10.1094/PHYTO-02-24-0068-R

Looi, H. K., Toh, Y. F., Yew, S. M., Na, S. L., Tan, Y. C., Chong, P. S., et al. (2017). Genomic insight into pathogenicity of dematiaceous fungus Corynespora cassiicola. *PeerJ* 5, e2841. doi: 10.7717/peerj.2841

Lv, B., Zhao, X., Guo, Y., Li, S., and Sun, M. (2023). Serine protease CrKP43 interacts with MAPK and regulates fungal development and mycoparasitism in Clonostachys chloroleuca. *Microbiol. Spectr.* 11, e0244823. doi: 10.1128/spectrum.02448-23

Madhu, S. N., Sharma, S., and Gajjar, D. U. (2020). Identification of proteases: carboxypeptidase and aminopeptidase as putative virulence factors of Fusarium solani species complex. *Open Microbiol. J.* 14, 266–277. doi: 10.2174/1874434602014010266

Munzert, K. S., and Engelsdorf, T. (2025). Plant cell wall structure and dynamics in plant-pathogen interactions and pathogen defence. *J. Exp. Bot.* 76, 228–242. doi: 10.1093/jxb/erae442

Muszewska, A., Stepniewska-Dziubinska, M. M., Steczkiewicz, K., Pawlowska, J., Dziedzic, A., and Ginalski, K. (2017). Fungal lifestyle reflected in serine protease repertoire. *Sci. Rep.* 7, 9147. doi: 10.1038/s41598-017-09644-w

Ning, Y., Hu, B., Yu, H., Liu, X., Jiao, B., and Lu, X. (2022). Optimization of protoplast preparation and establishment of genetic transformation system of an arctic-derived fungus *Eutypella* sp. *Front. Microbiol.* 13. doi: 10.3389/fmicb.2022.769008

Novotna, A., Mennicken, S., De Paula, C. C. P., Vogt-Schilb, H., Kotilinek, M., Tesitelova, T., et al. (2023). Variability in nutrient use by orchid mycorrhizal fungi in two medium types. *J. Fungi (Basel)* 9, 88. doi: 10.3390/jof9010088

Oda, K., Dunn, B. M., and Wlodawer, A. (2022). Serine-carboxyl peptidases, sedolisins: from discovery to evolution. *Biochemistry* 61, 1643–1664. doi: 10.1021/acs.biochem.2c00239

Oledibe, O. J., Enweani-Nwokelo, I. B., Okigbo, R. N., and Achugbu, A. N. (2023). Formulation of fungal media from local plant materials. *Advanced Gut Microbiome Res.* 2023, 1711026. doi: 10.1155/2023/1711026

Rauwane, M. E., Ogugua, U. V., Kalu, C. M., Ledwaba, L. K., Woldesemayat, A. A., and Ntushelo, K. (2020). Pathogenicity and virulence factors of Fusarium graminearum including factors discovered using next generation sequencing technologies and proteomics. *Microorganisms* 8, 305. doi: 10.3390/microorganisms8020305

Rawlings, N. D. (2020). Twenty-five years of nomenclature and classification of proteolytic enzymes. *Biochim. Biophys. Acta Proteins Proteom.* 1868, 140345. doi: 10.1016/j.bbapap.2019.140345

Rolke, Y., Liu, S., Quidde, T., Williamson, B., Schouten, A., Weltring, K. M., et al. (2004). Functional Analysis of H_2O_2-Generating Systems in *Botrytis cinerea*: the Major Cu-Zn-superoxide dismutase (BCSOD1) Contributes to Virulence on French bean, Whereas a Glucose Oxidase (BCGOD1) is Dispensable. *Mol. Plant Pathol.* 5, 17–27. doi: 10.1111/j.1364-3703.2004.00201.x

Satala, D., Bras, G., Kozik, A., Rapala-Kozik, M., and Karkowska-Kuleta, J. (2023). More than just protein degradation: the regulatory roles and moonlighting functions of extracellular proteases produced by fungi pathogenic for humans. *J. Fungi (Basel)* 9, 121. doi: 10.3390/jof9010121

Savojardo, C., Babbi, G., Martelli, P. L., and Casadio, R. (2021). Mapping OMIM disease–related variations on protein domains reveals an association among variation type, Pfam models, and disease classes. *Front. Mol. Biosci.* 8. doi: 10.3389/fmolb.2021.617016

Semenova, T. A., Dunaevsky, Y. E., Beljakova, G. A., and Belozersky, M. A. (2020). Extracellular peptidases of insect-associated fungi and their possible use in biological control programs and as pathogenicity markers. *Fungal Biol.* 124, 65–72. doi: 10.1016/j.funbio.2019.11.005

Shetty, N. P., Mehrabi, R., Lütken, H., Haldrup, A., Kema, G. H. J., Collinge, D. B., et al. (2007). Role of Hydrogen Peroxide during the Interaction Between the Hemibiotrophic Fungal Pathogen *Septoria tritici* and Wheat. *New Phytol.* 174, 637–647. doi: 10.1111/j.1469-8137.2007.02026.x

Shi, Y., Yang, B., Linghu, Y., Liu, Y., Li, H., Xing, Y., et al. (2025). Piezo1 senses hyphae and initiates host defense against pathogenic fungi. *Cell Rep.* 44, 115839. doi: 10.1016/j.celrep.2025.115839

Urbanek, H., and Kaczmarek, A. (1985). Extracellular proteinases of the isolate of *Botrytis cinerea* virulent to apple tissues. *Acta Biochim. Pol.* 32, 101–109.

Urbanek, H., and Yirdaw, G. (1984). Hydrolytic Ability of Acid Protease of *Fusarium culmorum* and its Possible Role in Phytopathogenesis. *Acta Microbiol. Pol.* 33, 131–136.

Varabyou, A., Erdogdu, B., Salzberg, S. L., and Pertea, M. (2023). Investigating open reading frames in known and novel transcripts using ORFanage. *Nat. Comput. Sci.* 3, 700–708. doi: 10.1038/s43588-023-00496-1

Wang, B., Liang, X., Gleason, M. L., Zhang, R., and Sun, G. (2018). Comparative genomics of *Botryosphaeria dothidea* and *B. kuwatsukai*, causal agents of apple ring rot, reveals both species expansion of pathogenicity-related genes and variations in virulence gene content during speciation. *IMA Fungus* 9, 243–257. doi: 10.5598/imafungus.2018.09.02.02

Wang, F., Shen, T., Cao, C., Shan, S., Sun, J., and Zhu, R. (2025). Virtual screening of inhibitor against Penicillium expansum and its application for controlling blue mold decay in apples. *Food Biosci.* 68, 106741. doi: 10.1016/j.fbio.2025.106741

Wei, S., Bian, R., Andika, I. B., Niu, E., Liu, Q., Kondo, H., et al. (2019). Symptomatic plant viroid infections in phytopathogenic fungi. *Proc. Natl. Acad. Sci.* 116, 13042–13050. doi: 10.1073/pnas.1900762116

Williams, H. L., Sturrock, R. N., Islam, M. A., Hammett, C., Ekramoddoullah, A. K., and Leal, I. (2014). Gene expression profiling of candidate virulence factors in the laminated root rot pathogen *Phellinus sulphurascens*. *BMC Genom.* 15, 603. doi: 10.1186/1471-2164-15-603

Xia, Y. (2004). Proteases in pathogenesis and plant defence. *Cell Microbiol.* 6, 905–913. doi: 10.1111/j.1462-5822.2004.00438.x

Yaakoub, H., Sanchez, N. S., Ongay-Larios, L., Courdavault, V., Calenda, A., Bouchara, J. P., et al. (2022). The high osmolarity glycerol (HOG) pathway in fungi (dagger). *Crit. Rev. Microbiol.* 48, 657–695. doi: 10.1080/1040841X.2021.2011834

Yang, C., Li, W., Huang, X., Tang, X., Qin, L., Liu, Y., et al. (2022). SsNEP2 contributes to the virulence of sclerotinia sclerotiorum. *Pathogens* 11, 446. doi: 10.3390/pathogens11040446

Yang, S., Zhuo, Y., Lin, Y., Huang, M., Tang, W., Zheng, W., et al. (2023). The signal peptidase FoSpc2 is required for normal growth, conidiation, virulence, stress response, and regulation of light sensitivity in Fusarium odoratissimum. *Microbiol. Spectr.* 11, e0440322. doi: 10.1128/spectrum.04403-22

Yuan, G., Lu, H., De, K., Hassan, M. M., Liu, Y., Islam, M. T., et al. (2023). Split selectable marker systems utilizing inteins facilitate gene stacking in plants. *Commun. Biol.* 6, 567. doi: 10.1038/s42003-023-04950-8

Zhang, S., Lin, C., Zhou, T., Zhang, L. H., and Deng, Y. Z. (2020b). Karyopherin MoKap119-mediated Nuclear Import of Cyclin-dependent kinase Regulator *MoCks1* is Essential for *Magnaporthe oryzae* Pathogenicity. *Cell Microbiol.* 22, e13114. doi: 10.1111/cmi.13114

Zhang, M. Z., Sun, C. H., Liu, Y., Feng, H. Q., Chang, H. W., Cao, S. N., et al. (2020a). Transcriptome analysis and functional validation reveal a novel gene, BcCGF1, that enhances fungal virulence by promoting infection-related development and host penetration. *Mol. Plant Pathol.* 21, 834–853. doi: 10.1111/mpp.12934

Zhang, Y., Xu, K., Yu, D., Liu, Z., Peng, C., Li, X., et al. (2019). The highly conserved barley powdery mildew effector BEC1019 confers susceptibility to biotrophic and necrotrophic pathogens in wheat. *Int. J. Mol. Sci.* 20, 4376. doi: 10.3390/ijms20184376

Zhang, Q., Zhao, L., Shen, M., Liu, J., Li, Y., Xu, S., et al. (2022). Establishment of an Efficient Polyethylene Glycol (PEG)-Mediated Transformation System in Pleurotus eryngii var. ferulae Using Comprehensive Optimization and Multiple Endogenous Promoters. *J. Fungi (Basel)* 8, 186. doi: 10.3390/jof8020186

Zhao, Z., Liu, H., Wang, C., and Xu, J.-R. (2013). Comparative analysis of fungal genomes reveals different plant cell wall degrading capacity in fungi. *BMC Genom.* 14, 274. doi: 10.1186/1471-2164-14-274

frontiers | Frontiers in Plant Science

TYPE Original Research
PUBLISHED 20 January 2026
DOI 10.3389/fpls.2025.1709648

OPEN ACCESS

EDITED BY
Manoj Kumar Solanki,
University of Silesia in Katowice, Poland

REVIEWED BY
Becky Nancy Aloo,
University of Eldoret, Kenya
Weiqi Kuang,
Chinese Academy of Sciences (CAS), China
Vivek Pattani,
Atmiya University, India

*CORRESPONDENCE
Haiyan Li
lhyxrn@163.com
Tao Li
litao@ynu.edu.cn

†These authors have contributed equally to this work

RECEIVED 20 September 2025
REVISED 23 November 2025
ACCEPTED 22 December 2025
PUBLISHED 20 January 2026

CITATION
Lao R, Fang S, Fang W, Zhao Z, Li H and Li T (2026) Nature's pre-installed helpers: diverse seed endophytes enhance rice nitrogen use efficiency.
Front. Plant Sci. 16:1709648.
doi: 10.3389/fpls.2025.1709648

Nature's pre-installed helpers: diverse seed endophytes enhance rice nitrogen use efficiency

Ruimin Lao[1,2†], Shaoxing Fang[2†], Wenjun Fang[2], Zhiwei Zhao[2], Haiyan Li[1*] and Tao Li[2*]

[1]Medical School, Kunming University of Science and Technology, Kunming, China, [2]State Key Laboratory for Conservation and Utilization of Bio-Resources in Yunnan, Yunnan University, Kunming, China

Nitrogen is a key limiting factor for crop growth, and improving nitrogen use efficiency (NUE) is critical for achieving high crop yields. In this study, both culture-independent and culture-dependent approaches were employed to systematically analyze the community composition and functional traits of seed endophytic bacteria in rice varieties with contrasting NUE. The results revealed diverse endophytic bacterial communities across the four rice varieties, with Shannon indices ranging from 2.95 to 3.23. However, significant compositional differences were observed among varieties. Rare taxa accounted for over 51% of operational taxonomic units (OTUs) in each variety and were the primary drivers of community diversity and differentiation. In contrast, core taxa (shared OTUs) were highly conserved across varieties, largely composed of abundant taxa (OTUs > 39%, total relative abundance > 93%), and occupied central positions in co-occurrence networks, thereby contributing to community stability. Five representative strains exhibited diverse plant growth-promoting (PGP) traits *in vitro*, including siderophore production, phosphate solubilization, and indole - 3 - acetic acid (IAA) synthesis. These functions were partially redundant, but individual strains exhibited distinct strengths, indicating functional complementarity. Inoculation experiments demonstrated that all strains improved rice growth, nitrogen accumulation, and NUE, with their effectiveness modulated by both strain identity and nitrogen availability. This study reveals rice seed endophytic bacteria as "natural microbial allies" that support host growth and adaptation under low-nitrogen conditions. These endophytes represent valuable microbial resources for the development of next-generation biofertilizers in sustainable agriculture.

KEYWORDS

rice seed endophytes, microbial communities, rata taxa, core taxa, plant growth promotion (PGP), nitrogen use efficiency (NUE)

1 Introduction

Nitrogen, as an essential macronutrient for plant growth and development, plays a critical role in determining crop performance and yield. In agricultural ecosystems, nitrogen use efficiency (NUE) varies significantly both between and within crop species (Fan et al., 2020). For instance, at the subspecies level, indica and japonica rice exhibit marked divergence in the regulatory pathways of nitrate uptake and assimilation, such as the transcription factor OsWRKY23 (Zhang et al., 2025a). Even at the variety level, the maize variety "Denghai605" shows significantly higher NUE than "Ludan981" under both nitrogen-rich and nitrogen-deficient conditions (Shao et al., 2022). Consequently, integrated strategies that combine traditional phenotypic selection, molecular breeding, and artificial intelligence-based prediction have become effective approaches for developing high-NUE crop varieties and mitigating nitrogen fertilizer pollution (Anas et al., 2020; Zhang et al., 2025b). Notably, plant-associated microbiomes, often referred to as the plant's "second genome," have demonstrated great potential in enhancing crop NUE. Harnessing the functional capabilities of these microbiomes has emerged as a promising frontier in breeding high-NUE varieties of economically important crops (Xu et al., 2025).

Plant-associated microbiomes, especially functional microbes in the rhizosphere, have been shown to improve host NUE through diverse interaction mechanisms. On the one hand, both free-living and symbiotic nitrogen-fixing bacteria contribute directly to nitrogen availability via biological nitrogen fixation (Guo et al., 2023). On the other hand, plant-associated microbes can also modulate the expression of host genes involved in nitrogen uptake and assimilation, thereby enhancing nitrogen metabolism. For instance, the arbuscular mycorrhizal (AM) fungus Rhizophagus irregularis promotes the uptake and assimilation of ammonium (NH_4^+) in Medicago sativa by upregulating key mycorrhizal nitrogen transporter genes, RicPSI and RicARI (Wang et al., 2024). Similarly, the plant growth-promoting bacterium Azospirillum brasilense can significantly enhance nitrogen assimilation efficiency in rice (Oryza sativa cv. Nipponbare) by upregulating the expression of multiple genes, including nitrate transporter and nodulin gene MtN3 (Thomas et al., 2019). Moreover, rhizosphere microbial colonization can influence root system architecture, thereby indirectly facilitating nitrogen uptake. For example, Wu et al. (2025) found that Pseudomonas spp. stimulate lateral root development in Leuce poplar through the secretion of indole - 3 - acetic acid (IAA), expanding root surface area and enhancing nitrogen acquisition. In addition, high-NUE varieties have the capacity to selectively enrich specific functional microbial taxa in the rhizosphere, thereby reshaping microbial community composition and accelerating nitrogen transformation rates in soil, ultimately improving plant NUE. ^{15}N isotope tracing studies have shown that high-NUE rice varieties can restructure their rhizosphere microbiomes compared to bulk soil, leading to faster nitrogen turnover and improved nitrogen use efficiency (Chen et al., 2025). Collectively, these findings provide important theoretical foundations for microbial strategies to improve plant NUE.

Although rhizosphere microbial communities play a significant role in enhancing crop NUE, their functional performance is often constrained by multiple factors, including environmental conditions (e.g., soil moisture and nutrient availability) and host plant genotypes (Rodriguez et al., 2009). In particular, the colonization compatibility between microbes and host tissues is critical for the expression of microbial functions. For example, Wu and Chang (2024) demonstrated that the differential colonization ability of the crown rot–antagonistic strain Bacillus altitudinis in various soybean varieties significantly affected the level of disease resistance. In contrast, seed-associated microbes—an integral part of the plant microbiome—possess distinctive and inherently stable advantages. First, the vertical transmission of seed endophytes ensures the stable fidelity of the microbiome during intergenerational transfer (Johnston-Monje et al., 2016). Second, as a primary inoculum, the seed microbiome can colonize the root system early during seedling establishment, preemptively occupying ecological niches and forming dominant rhizosphere communities (Shade et al., 2017). Third, seed-borne microbes serve as natural microbial allies, playing key roles in host development and in mediating adaptive responses to environmental stresses (Truyens et al., 2015).

As a globally important crop with a high dependency on nitrogen, rice presents significant research value for exploring the composition of its seed microbiome and its functional role in enhancing host NUE. In this study, we conducted a comparative analysis of high- and low- NUE rice varieties and proposed the following hypotheses: (1) seeds act as reservoirs of diverse endophytic bacteria, and the seed microbiome composition varies across rice varieties; (2) seed-borne endophytes possess functional traits that contribute to improving host NUE; and (3) the functional characteristics of seed endophytes are consistent with, and may extend, the physiological traits of their host plants. Therefore, investigating the diversity and functional roles of seed-borne 'primary inoculum' in rice varieties with contrasting NUE can uncover microbial candidates for improving host NUE and offer new insights into the biological strategies for enhancing nitrogen use in rice.

2 Materials and methods

2.1 Rice cultivars and nitrogen use efficiency characteristics

In this study, a systematic review of 20 publications from 2010 to 2022 was conducted to identify four widely cultivated rice varieties in China that exhibit significant differences in NUE as candidate materials. These cultivars were grown under greenhouse conditions for 30 days with either normal nitrogen (42.23 mg kg^{-1}, N42) or low nitrogen (7.39 mg kg^{-1}, N7) treatments. Based on key physiological traits—including biomass, nitrogen accumulation,

and NUE—two high-NUE varieties, Tianyouhuazhan (H_{TY}) (Feng et al., 2014; Hu et al., 2019) and Y Liangyou 1# (H_{Y1}) (Cui et al., 2010); and two low-NUE varieties, Xiushui 134# (L_{XS}) (Feng et al., 2014) and Fuyuan 4# (L_{FY}) (An et al., 2014) (Supplementary Table S1). For downstream analyses, 10 g of seeds from each of the four representative varieties were surface-sterilized by sequential immersion in 75% ethanol for 1 minute, followed by 5 minutes in 10% sodium hypochlorite, and then rinsed 3–5 times with sterile distilled water, according to the protocol of Zhang et al. (2021). The sterilized seeds were then transferred into 5 mL EP tubes and homogenized using a tissue grinder (Jingxin, Shanghai, China) at 50 Hz for 200 s to prepare seed suspensions for further experiments.

2.2 DNA extraction and sequencing of seed endophytic bacteria

Total environmental DNA for bacterial community analysis was extracted from the 2 g seed suspensions prepared as described above, using the MolPure® Plant DNA kit (Guangzhou Feiyang Bioengineering Co., Ltd., China), according to the manufacturer's instructions. DNA was eluted in 50 µl of purified water and quantified using a Nanodrop spectrophotometer (ThermoFisher, Massachusetts, USA). The V5-V6 region of the bacterial 16S rRNA gene was amplified using universal primers 799F (5′-AAC MGG ATT AGA TAC CCK G-3′) and V6R (3′-GGG TTG CGC TCG TTG CG-5′) (Yang et al., 2024). PCR reactions were performed in 20 µL volumes containing 4 µL 5× FastPfu Buffer, 2 µL 2.5 mM dNTPs, 0.8 µL of each primer (5 µM), 0.4 µL FastPfu DNA polymerase (Beijing TransGen Biotech Co., Ltd., China), 0.2 µL BSA, and 10 ng of template DNA. The thermal cycling protocol consisted of 3 min at 95°C for pre-denaturation, followed by 30 cycles of 95°C for 30 s, 58 °C for 30 s, and 72°C for 45 s, with a final extension at 72°C for 10 min. PCR products were purified using a PCR Clean-Up Kit (Axygen Co. Ltd., USA) and quantified with a Qubit 4.0 Fluorometer (Thermo Fisher Scientific, USA). Library construction was performed using the NEXTFLEX Rapid DNA-Seq Kit (Shanghai Xinrui Biotechnology Co., Ltd., China), and sequencing was carried out on the Illumina Nextseq2000 platform.

2.3 Diversity analysis of seed endophytic bacterial communities

Raw sequencing reads were subjected to quality filtering using Fastp (v0.19.6), followed by paired-end read merging using FLASH (v1.2.11). Sequences with > 97% similarity were clustered into operational taxonomic units (OTUs) using UPARSE (v7.1) (Edgar, 2013). OTU classification and abundance were annotated using the RDP Classifier (v2.11) with a confidence threshold of 97% (Wang et al., 2007). OTUs were categorized as abundant taxa (AT, abundance > 0.1%), intermediate taxa (IT, 0.01% ≤ abundance ≤ 0.1%), and rare taxa (RT, abundance< 0.01%) according to Zhao et al. (2022). Alpha diversity indices were calculated using Mothur (v1.30.2) (Schloss et al., 2009), and Bray-Curtis principal component analysis (PCA) was used to assess community structure similarity (Siebyła et al., 2024). The top 50 most abundant bacterial OTUs were selected for microbial co-occurrence network analysis, and network topological parameters such as modularity and clustering coefficient were calculated using Gephi (version 0.10.1) (Barberán et al., 2012). Bacterial functional prediction was performed with the FAPROTAX database (Louca et al., 2016). Indicator species analysis was conducted on the Majorbio Cloud Bioinformatics Platform (https://www.majorbio.com), and OTUs with IndVal > 0.7 and $p < 0.05$ were considered cultivar-specific indicators. Based on Yuan et al. (2021), network robustness was assessed using the Top 50 most abundant OTUs per cultivar in R (v4.4.3). Robustness was defined as the proportion of remaining nodes after randomly removing 50% of network nodes. The raw sequence data are deposited in NCBI SRA under BioProject PRJNA1303560.

2.4 Isolation and identification of seed endophytes from high NUE varieties

For bacterial isolation, 2 g of seeds from the H_{TY} and H_{Y1} cultivars were surface-sterilized, homogenized, and serially diluted following the procedure described above. Aliquots (100 µL) from 5^{-4} to 5^{-4-6} dilutions were spread onto Luria Bertani (LB), Nutrient Agar (NA), and Reasoner's 2A (R_2A) agar plates, and incubated at 37°C overnight, respectively (Ahn et al., 2014; Ezraty et al., 2014; Zhang et al., 2022). Single colonies were selected and identified using 16S rRNA gene amplification with primers 27F (5′-AGA GTT TGA TCC TGG CTC AG-3′) and 1492R (5′-TAC GGC TAC CTT GTT ACG ACT T-3′), and M5 Hiper Mix DNA polymerase (Xi'an Zhuangzhi Biotechnology Co., Ltd., China) (Hou et al., 2018). PCR reactions (20 µL) contained 2 µL DNA template, 0.5 µL primers, and 10 µL enzyme mix. Cycling conditions were: 95°C for 3 min; 35 cycles of 94°C for 25 s, 55°C for 25 s, 72°C for 90 s; final extension at 72°C for 5 min. Sequences were trimmed and clustered at ≥ 99% similarity using SeqMan and Mothur. Representative sequences were taxonomically identified via BLAST searches against the NCBI database. Closely related reference sequences were retrieved from GenBank and aligned with the target sequences in MEGA (v11.0.13). A Neighbor-Joining phylogenetic tree was subsequently constructed, and node reliability was assessed with 1,000 bootstrap replicates (Koester et al., 2019; Tamura et al., 2013).

2.5 Plant growth-promoting traits of representative seed endophytic strains

(1) Phosphate solubilization: Each strain (OD_{600} = 0.3) was spot-inoculated (2 µL) onto solid National Botanical Research Institute Phosphate (NBRIP) medium supplemented with 5 g/L of either phytate calcium or tricalcium phosphate as the only phosphorus source. Plates were incubated at 37°C for 2 days. The

phosphate solubilization ability was assessed by the formation of clear halos around colonies using the cross-line method, in which two perpendicular lines were drawn through the center of the colony and the distance from the colony edge to the halo edge along each line was recorded. For quantitative analysis, 1 mL of each strain was inoculated into 100 mL sterile NBRIP liquid medium and incubated at 37°C, 180 rpm for 3 days with five replicates. A sterile, uninoculated medium served as the control. After centrifugation at 10,000 rpm for 3 min, the pH of the supernatant was measured using a pH meter (FiveEasy Plus, FE28, Shanghai, China). Soluble phosphorus concentrations were determined using the molybdenum blue colorimetric method, following the Chinese national standard NY/T 2017-2011 (Watanabe and Olsen, 1965). OD_{700} was measured with a microplate reader (Molecular Devices, FlexStation 3, Shanghai, China).

(2) Siderophore production: Each bacterial strain (OD_{600} = 0.3) was spot-inoculated (2 μL) onto chrome azurol S (CAS)-based double-layer agar plates prepared with LB medium and incubated at 37°C for 48 hours. The presence of orange halos around colonies indicated siderophore production (Pérez-Miranda et al., 2007). For quantitative assessment, 1 mL of bacterial culture was added to 100 mL sterile iron-limited Modified King's B (MKB) liquid medium and incubated at 37 °C, 180 rpm for 3 days (5 replicates). After centrifugation at 4,500 rpm for 5 min, 1 mL of supernatant was mixed with 1 mL CAS assay solution and incubated at room temperature for 1 hour. Distilled water was used as a blank control. OD_{630} was measured for each sample, and siderophore units (SU) were calculated as follows (Schwyn and Neilands, 1987):

$$\mathrm{SU}\ (\%) = \frac{100 \times (Ar - As)}{Ar}$$

Where *As* is the OD_{630} value of the treatment group, and *Ar* is the OD_{630} value of the control group. Siderophore production capacity was standardized by dividing SU of the bacterial culture.

(3) Quantification of IAA Production: IAA production was quantified according to the method described by Carvajal et al. (2024), with minor modifications. 1 mL of bacterial suspension was inoculated into 50 mL of sterilized modified LB liquid medium supplemented with 100 mg·L^{-1} L-tryptophan. Cultures were incubated at 37 °C with shaking at 180 rpm for 3 days. Each treatment was conducted with five replicates, and an uninoculated medium served as the control. After incubation, cultures were centrifuged at 8000 rpm for 10 min. Then, 50 μL of the supernatant was mixed with an equal volume of Salkowski reagent. In parallel, IAA standards were prepared at concentrations of 0, 10, 20, 30, 40, and 50 mg mL^{-1}, each with three replicates, and processed identically. All samples were incubated in the dark at room temperature for 30 min. Absorbance was measured at 530 nm for each sample. A linear regression of standard concentration (x) against absorbance (y) was used to generate the calibration equation (R^2 = 0.9953). The IAA concentration of each sample was subsequently calculated from the standard curve. Double-distilled water (ddH_2O) served as a blank control.

2.6 Effects of seed endophyte on rice growth and NUE

Well-filled seeds of the low-NUE rice variety L_{XS} (with husks removed) were selected, soaked in sterile water for 8 hours, and then surface-sterilized following the procedure described above. The disinfected seeds were sown onto 1/2 Murashige Skoog (MS) medium supplemented with 1% Plant Preservative Mixture (PPM™, Beijing Coolibor Technology Co., Ltd., Beijing, China) and 0.25% agar. After 2 days of incubation in darkness, the germinated seeds were transferred to a light chamber and cultivated for 2 weeks. Embryo-derived sterile seedlings were obtained by carefully excising the endosperm and removing any adhering MS medium. Uniformly grown sterile seedlings were used as hosts for inoculation with each of five representative endophytic bacterial strains. Autoclaved bacterial inocula (121°C, 20 min) served as negative controls. For the inoculation treatments, a root-dipping method was employed: sterile rice seedling roots were immersed in 10 mL of a bacterial suspension (OD_{600} = 0.3) for pre-inoculation. The pre-inoculated seedlings were then transplanted into pots (9 × 23.5 × 5 cm; top diameter × height × bottom diameter) containing 350 g of growth substrate, after which the remaining bacterial suspension was applied and watered around the root zone to promote effective colonization (Wang and Gottwald, 2017). The growth substrate was composed of commercial vermiculite, farmland soil, and commercial humus soil mixed at a ratio of 50:1:1 (w/w) (organic matter = 12.93 g kg^{-1}, total N = 0.216 mg kg^{-1}, total P = 4.182 mg kg^{-1}, total K = 34.25 mg kg^{-1}, available N = 0.0481 mg kg^{-1}, available P = 7.544 mg kg^{-1}, available K = 75.41 mg kg^{-1}, and pH = 6.89). The substrate was sterilized at 121 °C for 120 minutes, with 3 consecutive treatments (24 hours apart each time). Two nitrogen treatments were established by supplementing the substrate with nutrient solution containing urea (Tianjin Fengchuan Chemical Reagent Co., Ltd., Tianjin, China) as the N source: low N (N7, 7.39 mg kg^{-1}) and normal N (N42, 42.23 mg kg^{-1}). Each pot contained one seedling, with five replicates per treatment. In total, the experiment comprised 2 nitrogen levels × 6 inoculants (5 bacteria + ck) × 6 replicates = 72 pots. Plants were grown for 60 days in a greenhouse under natural light at 15–30 °C and irrigated with 60 mL sterile water every two days. Prior to harvest, plant height, tiller number, fresh leaf number, and number of senescent leaves were recorded. Leaf chlorophyll content was measured using a SPAD-502 Plus chlorophyll meter (Konica Minolta, Japan). After 60 days, both shoot and root tissues were separately harvested for further analysis.

2.7 Sample digestion and quantification of nitrogen-related parameters

Following the Chinese national standard "Determination of nitrogen, phosphorus and potassium in plants" (NY/T 2419-2013), plant tissues were digested using the concentrated sulfuric

acid–hydrogen peroxide method. Total nitrogen content was then determined using a Kjeldahl nitrogen analyzer (SKD-800, Shanghai Peiou Analytical Instrument Co., Ltd., Shanghai, China), according to the manufacturer's instructions.

Nitrogen Transport efficiency (NTE), Nitrogen Uptake efficiency (NUpE), Nitrogen Utilization efficiency (NUtE) and Nitrogen Use efficiency (NUE) was calculated using the following formula (Cheng et al., 2011; Liu et al., 2025):

$$\text{Nitrogen Transport Efficiency (NTE, \%)} = \frac{\text{Total shoot N accumulation}}{\text{total plant N accumulation}} \times 100\,\%$$

$$\text{Nitrogen Uptake Efficiency (NUpE, \%)} = \frac{\text{total plant N accumulation}}{\text{total N investment}} \times 100\,\%$$

$$\text{Nitrogen Utilization Efficiency (NUtE, g/g)} = \frac{\text{plant dry matter}}{\text{total plant N accumulation}}$$

$$\text{Nitrogen Use Efficiency (NUE, g/g)} = \text{NUpE} \times \text{NUtE}$$

2.8 Statistical analysis

Statistical analyses were conducted using SPSS software (version 24.0; IBM, Armonk, NY, USA), and data visualization was performed with Origin 2018 (OriginLab, Northampton, MA, USA). Two-way ANOVA was used to evaluate the main and interaction effects of endophyte inoculation and nitrogen level, assuming homogeneity of variance and normality. When significant effects were detected, one-way ANOVA, followed by post-hoc Tukey's HSD test, was used to detect significant difference in rice biomass, plant height, chlorophyll content, nitrogen concentration, and NUE among the bacterial inoculation treatments and the control (CK) under the same nitrogen level ($p < 0.05$). Independent-samples t-tests were applied to compare the effects of nitrogen treatments on these parameters in the CK group. Data are expressed as means ± standard error (SE).

3 Results

3.1 Diversity of seed endophytic bacteria between High- and Low-NUE rice cultivars

3.1.1 Characteristics of seed endophytic bacterial communities

A total of 500 OTUs of seed endophytic bacteria were annotated across the four rice cultivars, with individual cultivars containing 214 (L_{XS}) to 311 (H_{Y1}) OTUs. Among these, 92 OTUs (18.4%) were shared across all cultivars, yet accounting for over 94.5% of total abundance, reaching up to 98.4% in L_{FY} variety. Rare taxa (RT) dominated OTU richness, representing over 51% of OTUs in all cultivars, although their total abundance was below 0.6%. In contrast, abundant taxa (AT) comprised only 15.1% (H_{Y1}, 47 OTUs) to 23.4% (L_{XS}, 50 OTUs) of OTUs but contributed more than 96.8% of total abundance. Cultivar-specific OTUs ranged from 36 (7.2%, L_{XS}) to 75 (15%, H_{Y1}), primarily consisting of RT, with total abundances below 0.35% in all cultivars (Figure 1a). Shannon diversity indices indicated high microbial diversity among cultivars, ranging from 2.95 ± 0.03 (L_{FY}) to 3.23 ± 0.04 (H_{Y1}), with significant differences ($p < 0.05$, one-way ANOVA, Figure 1b). All cultivars showed significantly higher Shannon diversity of rare taxa than intermediate and abundant taxa, while AT exhibited the lowest diversity (Figure 1b). Twelve bacterial phyla and 172 genera were identified, including 50 dominant genera with abundance > 0.1%. The number of dominant genera per cultivar ranged from 26 (L_{FY}) to 35 (H_{Y1}). Seventeen dominant genera were shared across all cultivars, including Methylobacterium, Xanthomonas, Buttiauxella, and Sphingomonas (Figure 1c).

3.1.2 Community composition differences

PCA revealed significant differences in seed endophytic bacterial communities among cultivars ($p < 0.05$, ANOSIM, Figure 2a). Hierarchical clustering showed that cultivars with the same NUE type clustered more closely, with H_{TY} and H_{Y1} (high-NUE) forming a distinct group (Figure 2b). Among the 172 identified genera, 60 (34.9%) showed significant abundance differences across cultivars ($p < 0.05$, Kruskal-Wallis H test). For example, Sphingomonas, which was dominant across all cultivars, was enriched in low-NUE cultivars (> 7.7% in L_{XS}, 15.5% in L_{FY}) but accounted for< 3.8% in both high-NUE cultivars (Figure 2c). Salmonella was dominant in H_{TY} (1.19%) and H_{Y1} (1.24%), but significantly reduced in L_{FY} (0.26%) and L_{XS} (0.76%). Conversely, Rhodanobacter was dominant in H_{Y1} (3.73%) but low (< 0.84%) in the other three cultivars. Additionally, some genera showed NUE-specific distributions, where Midichloria (0.002% in H_{TY}, 0.016% in H_{Y1}), Weissella (0.11% in H_{TY}, 0.07% in H_{Y1}), and Lichenibacterium (0.013% in H_{TY}, 0.007% in H_{Y1}) were found exclusively in high-NUE cultivars, whereas Sanguibacter (0.02% in L_{FY}, 0.01% in L_{XS}) was specific to low-NUE cultivars. (Figure 2c).

3.1.3 Characteristics of microbial co-occurrence networks and indicator species

Co-occurrence network analysis revealed similar topologies across four cultivars, with comparable numbers of edges and modularity indices, and predominantly positive correlations (Figure 3a; Supplementary Table S2). Several core OTUs, including Kineococcus (OTU286) and Pseudomonas (OTU310), served as shared network hubs across all cultivars, indicating structural similarity among networks. Network robustness indices ranged from 0.23 to 0.26 with no significant differences ($p > 0.05$, one-way ANOVA, Figure 3b). Indicator species analysis identified 76 cultivar-specific indicator OTUs (IndVal > 0.7, $p < 0.05$), none of which were shared among cultivars. The number of indicator OTUs

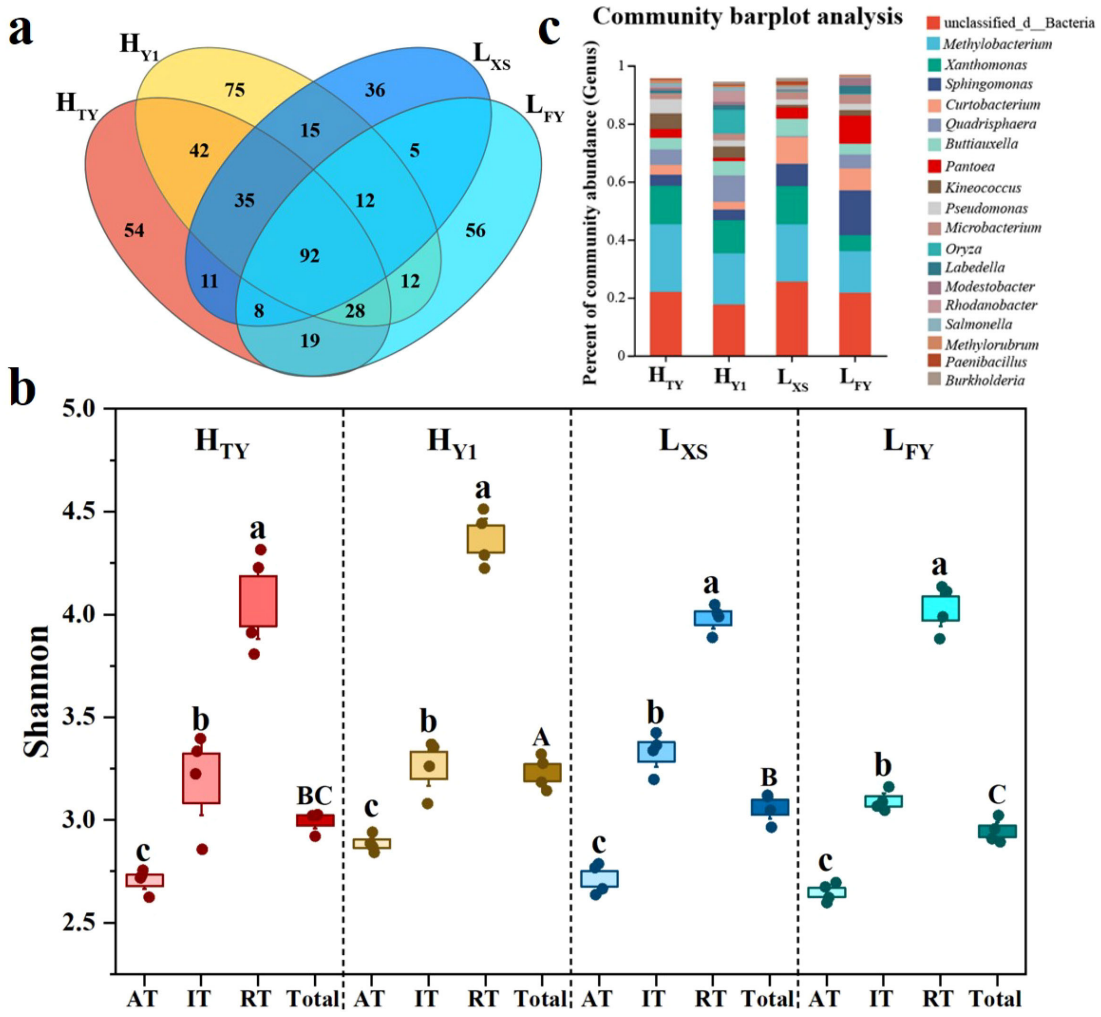

FIGURE 1
Diversity of seed endophytic bacterial communities in rice cultivars with high (H_{TY}, H_{Y1}) and low (L_{FY}, L_{XS}) nitrogen use efficiency. **(a)** Venn diagram, **(b)** Shannon indices, and **(c)** Community composition. AT, IT and RT represent abundant, intermediate and rare bacterial taxa, respectively, while 'Total' refers to all taxa in the seed endophytic bacterial communities. Different letters indicate significant differences between groups ($p < 0.05$, one-way ANOVA, $n = 4$).

ranged from 6 (H_{TY}) to 27 (L_{XS}). Specific indicators included Priestia (OTU207) for H_{TY}, Actinomycetospora (OTU356) for H_{Y1}, Aureimonas (OTU250) for L_{XS}, and Clavibacter (OTU70) for L_{FY}. Indicator OTUs for H_{Y1}, L_{FY}, and L_{XS} were primarily from Actinobacteria and Proteobacteria, while H_{TY}'s indicators belonged mostly to Firmicutes (Supplementary Table S3).

3.1.4 Functional prediction of bacterial communities

A total of 41 functional groups were annotated using the FAPROTAX database. Of these, 33 functions (80.5%) showed significant differences among cultivars ($p < 0.05$). Among the differential functions, 27.3% (9/33) were nitrogen-related (e.g., nitrogen fixation, nitrate reduction, urea decomposition), 21.2% were carbon cycling-related, and others involved sulfur cycling (9.09%) and pathogenicity (18.18%) (Supplementary Figure S2).

3.2 Isolation and growth-promoting potential of cultivable endophytes in high-NUE varieties

3.2.1 Isolation and identification of cultivable endophytes

A total of 369 cultivable endophytes were isolated from seeds of H_{TY} and H_{Y1} cultivars. 16S rRNA gene sequencing revealed affiliation to 15 genera, with the most frequently isolated being Enterobacter (66.04%), Pantoea (21.03%), and Acinetobacter (4.04%). Based on frequency, diversity, and functional prediction, five representative strains were selected for the following experiments, including Bacillus thuringiensis T328, Xanthomonas sacchari Y003, Pantoea agglomerans Y013, Curtobacterium citreum Y089, and Pantoea dispersa Y163 (Figure 4; Supplementary Table S5).

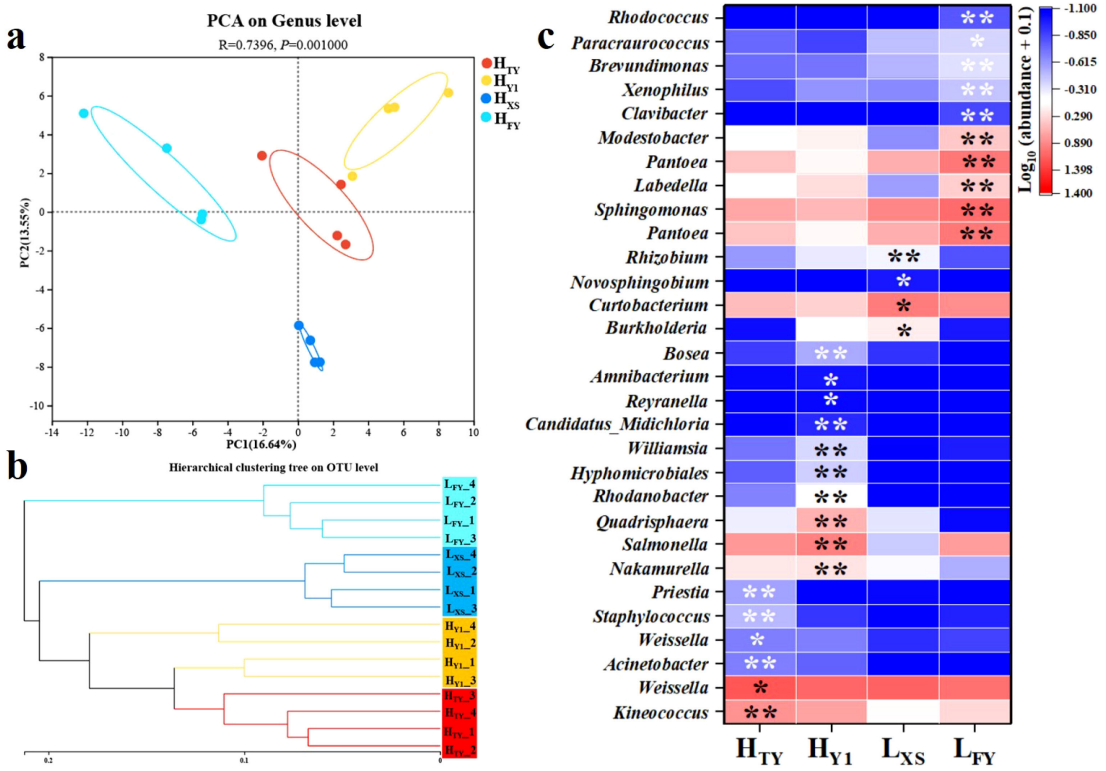

FIGURE 2
Principal component analysis (PCA) **(a)**, Hierarchical clustering **(b)**, and differential abundance analysis **(c)** of seed endophytic bacterial communities in High- (H_{TY}, H_{Y1}) and Low-NUE (L_{FY}, L_{XS}) rice varieties. Significance determined by Kruskal-Wallis H test: * $p < 0.05$, ** $p < 0.01$ ($n = 4$).

3.2.2 Growth-promoting traits of cultivable endophytes from high-NUE rice

Five representative endophytes exhibited diverse plant growth-promoting traits, including phosphate solubilization, siderophore production, and IAA synthesis. Soluble phosphorus concentrations in fermentation broths ranged from 2.18 mg L^{-1} to 763.98 mg L^{-1}. The siderophore units (SU) ranged from 0.139 to 0.733, and IAA concentrations varied between 2.67 mg L^{-1} and 289.38 mg L^{-1}. Significant differences were observed in the dominant functions among strains. For example, P. dispersa Y163 exhibited the strongest phosphate solubilization ability, significantly higher than the other five strains, but its IAA production was lower than that of P. agglomerans Y013. Furthermore, the siderophore production index of P. dispersa Y163 was significantly lower than those of the other four strains, at only 0.139 ($p < 0.05$, one-way ANOVA, Figure 5).

3.3 Functional role of seed endophytes in enhancing rice growth and NUE

3.3.1 Effects of seed endophytes on rice growth under different N levels

Compared with the uninoculated control, inoculation with five representative endophytes enhanced rice growth, including biomass, plant height, chlorophyll content, tiller number, number of fresh leaves, and root length, while reducing the number of withered leaves across treatments (Figure 6; Supplementary Figure S3). However, the inoculation effect was influenced by the combined factors of bacterial strain type and nitrogen level. Under normal nitrogen conditions (N42), most strains inoculation—particularly C. citreum Y089, P. dispersa Y163 and X. sacchari Y003—significantly increased shoot dry biomass ($p < 0.05$, one-way ANOVA). In contrast, B. thuringiensis T328 and P. agglomerans Y013 showed no significant effect ($p > 0.05$, one-way ANOVA). Interestingly, under low nitrogen conditions (N7), all strains promoted rice growth significantly ($p < 0.05$, one-way ANOVA, Figure 6a). Among the five representative endophytes, C. citreum Y089 consistently exhibited superior growth-promoting effects under both normal and low nitrogen conditions, indicating its potential as the most effective plant growth-promoting strain (Figure 6a).

3.3.2 Seed endophytes enhance nitrogen accumulation and NUE in rice

Compared to the uninoculated control, inoculation with the five representative endophytes did not significantly increase the average N concentration in rice under either nitrogen regime and even showed a general decreasing trend (Figure 6d). In contrast, total N accumulation per plant was significantly improved by bacterial inoculation in all treatments. Notably, inoculation with C. citreum Y089 increased total N accumulation by 20.5% under N42 and 55.7% under N7 conditions, respectively (Figure 6e).

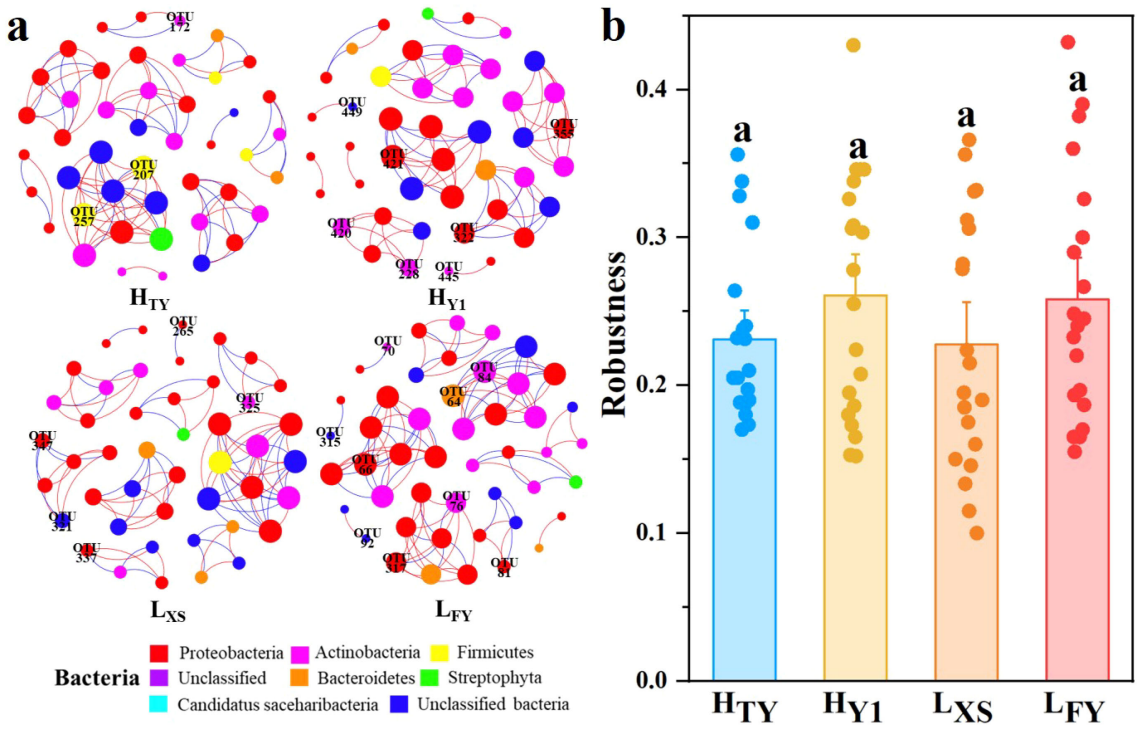

FIGURE 3
Co-occurrence network analysis **(a)** and microbial network robustness analysis **(b)** of seed endophytic bacteria in High- (H_{TY}, H_{Y1}) and Low- (L_{FY}, L_{XS}) NUE rice varieties. In the network, nodes are colored by phylum and node size reflects the degree. Red and blue edges indicate positive and negative correlations, respectively; OTU numbers correspond to indicator species identified in each cultivar.

Correspondingly, inoculation with representative endophytes also enhanced N uptake efficiency (NUpE), nitrogen utilization efficiency (NUtE), and nitrogen use efficiency (NUE) of rice, but did not affect N transport efficiency (NTE). C. citreum Y089 showing the most pronounced effect: its NUtE increased significantly by 53.1% under N42 and 33.6% under N7. Meanwhile, its NUE was markedly enhanced by 0.84-fold under N42 and 1.1-fold under N7 compared with the CK group ($p < 0.05$, one-way ANOVA) (Figure 6). It is worth noting that the effect of bacterial inoculation on NUE was influenced by both bacterial strain and nitrogen availability (Figure 6i). For example, B. thuringiensis T328 and P. agglomerans Y013 did not significantly improve NUE under normal nitrogen conditions, but under N7 they increased NUE by 21.17% and 20.22%, respectively ($p < 0.05$, one-way ANOVA, Figure 6h).

4 Discussion

Using both culture-dependent and culture-independent approaches, we detected a rich and diverse array of endophytic bacterial taxa in the seeds of all four rice cultivars examined, with Shannon diversity indices ranging from 2.99 to 3.23. These findings are consistent with those of Deckert et al. (2019), who identified highly diverse seed endophytic communities in two representative gymnosperms, Pinus edulis and P. ponderosa, including four mycorrhizal fungal genera (e.g., Gymnopilus). A meta-analysis by Simonin et al. (2022) encompassing seed microbiota from 50 plant species further confirmed the widespread high diversity of microbial communities residing within plant seeds. Together, these findings support the view that plant seeds represent a rich reservoir of endophytic microbes and form an integral part of the plant microbiome (Nelson, 2018).

We found that the composition of seed endophytic bacterial communities varied significantly among different rice cultivars. Such variation is commonly observed not only across different plant species but also among genotypes within the same species. Simonin et al. (2022) reported substantial diversity in seed endophytic communities across 50 plant species, with taxonomic richness ranging from a single taxon to several thousand, averaging 95 taxa per seed (34 prokaryotic and 61 fungal taxa). Similarly, Wang et al. (2023a) observed pronounced differences in seed endophytic bacterial composition among 11 genetically correlated hybrid rice seeds with different rice blast resistance levels, even among hybrids with similar genetic constitutions, such as those sharing the same female parent but different male parents, and vice versa. It is widely accepted that the composition of seed-associated endophytes results from the interplay of multiple factors, with host genotype being one of the most critical drivers (da Silva et al., 2014). In a more recent study, Lobato et al. (2024) compared the impact of plant genotype, domestication, and breeding on endophytic bacterial communities in the seeds of 46 Cannabis genotypes, including early domestication genotypes obtained through natural

FIGURE 4
Neighbor-joining (NJ) phylogenetic tree based on the 16S rRNA sequences of 369 cultivable seed endophytic bacterial strains. The numbers above the nodes indicate bootstrap support values from 1,000 replicates. Colors in the inner circle distinguish bacterial genera, while the percentages in the outer ring show the isolation frequency. Arabic numerals in parentheses denote the number of isolates.

and artificial selection, as well as modern genotypes obtained through artificial selection. The study found that the heterogeneous genetic background of Cannabis influences its seed microbiome. In addition to genetic factors, abiotic environmental variables such as soil type, climate, moisture, and nutrient availability also contribute to shaping the seed microbiome (Durán et al., 2022), suggesting the combined influence of host genotype, environmental factors, and microbial ecological interactions (Franić et al., 2020).

Among the four rice cultivars analyzed, flexible rare taxa (RT) played a dominant role in shaping both the diversity and composition of the seed endophytic microbiome. RT exhibited the highest OTU richness and Shannon diversity despite their low relative abundance. This pattern aligns with observations from diverse soil ecosystems, where rare taxa frequently contribute disproportionately to overall diversity and serve as key regulators of microbial compositional variation (Yang et al., 2025). In contrast to the high variability of RT, a subset of abundant taxa (AT, > 93% of total relative abundance) was consistently detected in the seeds of all four rice cultivars, indicating broad host adaptability. For example, genera such as Sphingomonas, Methylobacterium, and Pantoea are not only prevalent in major crops like rice, maize, and wheat but also widely distributed in woody or leguminous hosts (Suman et al., 2020; Simonin et al., 2022). Notably, these taxa can also persist under extreme environmental stresses, including drought, salinity, and heavy metal contamination (Asaf et al., 2017; Li et al., 2023; Tai et al., 2024). Importantly, these abundant and shared core taxa also showed strong genetic conservation across various rice cultivars and were similarly conserved across multiple hybrid generations and geographical regions (Walitang et al., 2019). Collectively, these findings suggest that vertical transmission and genetic conservation of core seed endophytes contribute to their long-term association with host plants and play a critical role in plant–microbiome co-evolution.

We also observed that these core taxa frequently occupied central positions within the microbial co-occurrence networks, suggesting their critical role in maintaining community stability (Jiao et al., 2019; Li et al., 2021). In particular, core microbes

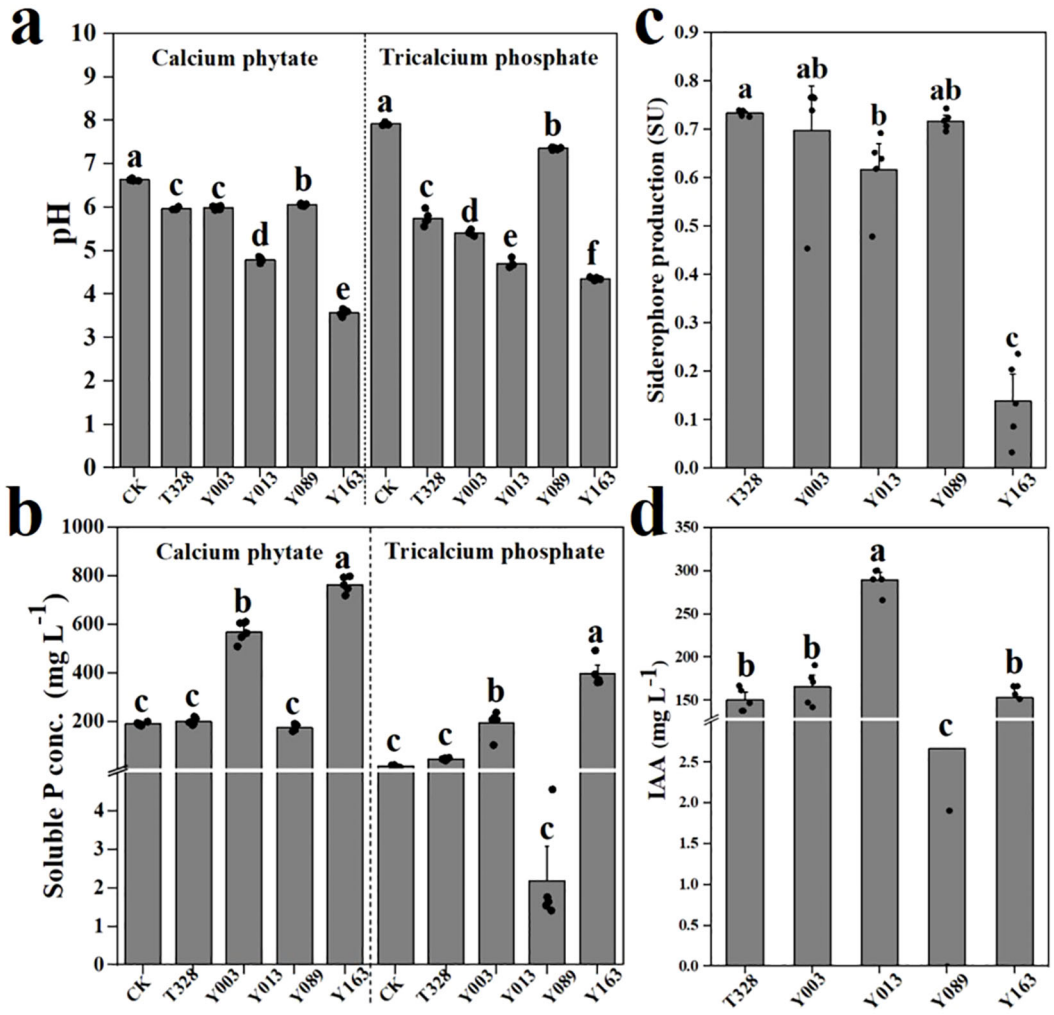

FIGURE 5
Plant growth-promoting (PGP) traits of five representative endophytes under *in vitro* conditions. **(a)** pH of the culture medium, **(b)** soluble phosphorus concentration in Pikovskaya (PVK) medium supplemented with calcium phytate and tricalcium phosphate as the sole phosphorus sources after 3 days of inoculation; **(c)** Siderophore production; and **(d)** IAA production. Data are means ± SE (n = 5); significance by one-way ANOVA ($p < 0.05$).

contributing to essential host functions—such as nitrogen fixation or disease resistance—may be selectively retained by the host to ensure the stability and integrity of microbiome function (Walitang et al., 2019). In parallel, rare taxa also contribute significantly to ecosystem functioning. On one hand, they harbor a highly diverse repertoire of functional genes, serving as a vast gene reservoir within the microbial community (Chen et al., 2020; Zhou et al., 2022). The functional diversity among RT increases microbial functional redundancy, providing "backup" capacities that buffer the community against external disturbances and thereby enhance ecological stability and resilience (Kang et al., 2015; Louca et al., 2018). On the other hand, rare taxa serve as a "microbial seed bank" within the community. Conditionally rare taxa can dynamically shift between rare and abundant states depending on environmental conditions, thereby influencing both the structure and function of the microbial community (Lynch and Neufeld, 2015; Hu et al., 2023). Although low in abundance, rare taxa exert disproportionate influence on microbial community diversity and functional capacity. They are now recognized as essential contributors to the stability and resilience of microbial ecosystems (Lynch and Neufeld, 2015; Jousset et al., 2017). Taken together, the conserved core taxa and the highly variable rare taxa confer a "dual-stability" to the seed microbiome, characterized by a stable core microbiome and a flexible rare biosphere. This duality may reflect an evolutionary strategy for microbial adaptation to host selection.

We found that representative endophytes in rice exhibited diverse and functionally redundant PGP traits. However, these strains displayed differentiated strengths in their functional profiles, indicating a degree of functional complementarity. Such functional diversity and redundancy are common features among seed-associated endophytes in various plant species. For instance, numerous endophytic bacteria isolated from rice and tomato seeds have been shown to produce IAA, siderophores, and solubilize essential minerals such as phosphorus and potassium (Jana et al., 2023; Roy et al., 2024). Functional redundancy and complementarity among microbial PGP traits are key mechanisms

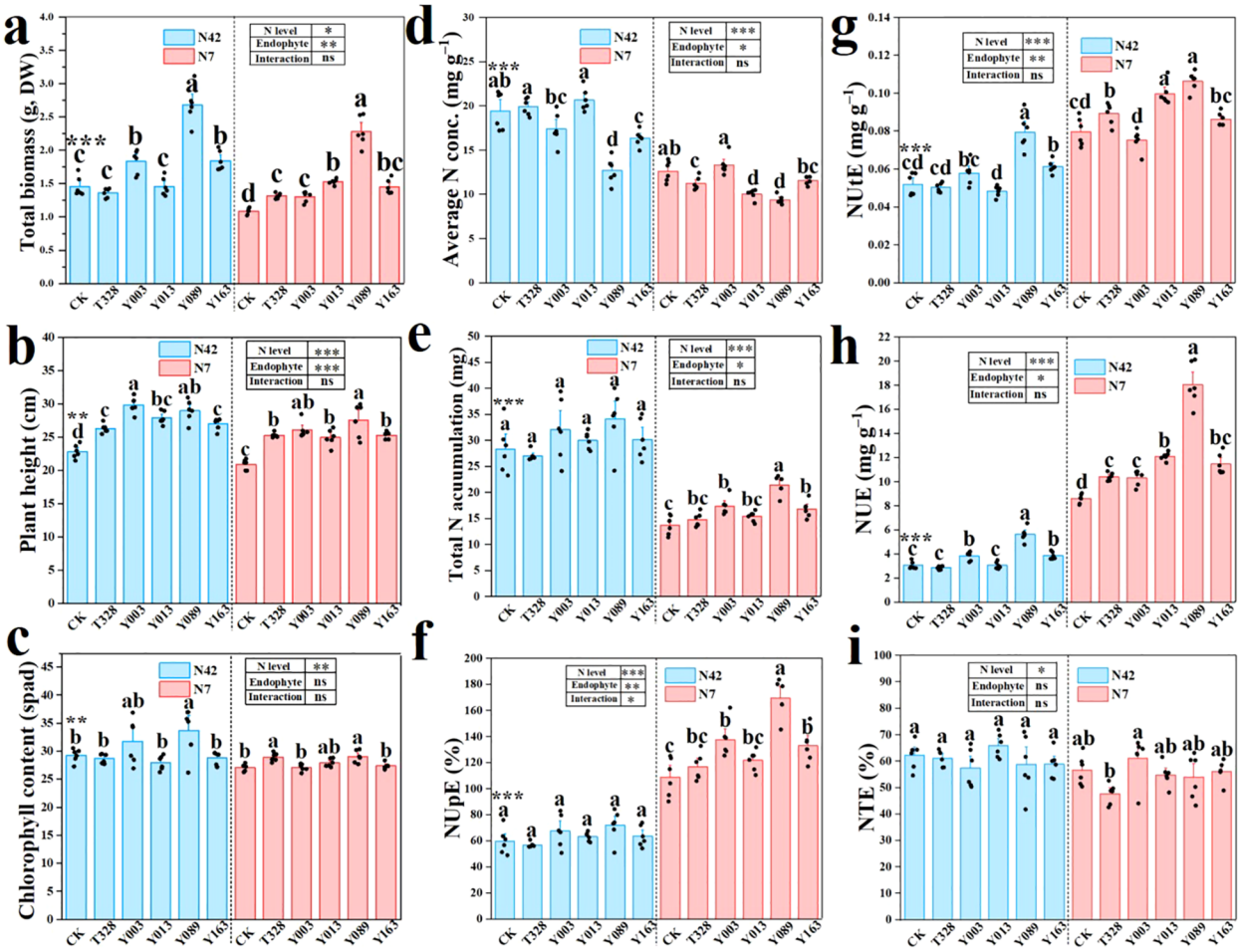

FIGURE 6
Effects of inoculation with five representative endophytes on rice total biomass **(a)**, plant height **(b)**, chlorophyll content **(c)**, average N concentration **(d)**, total N accumulation **(e)**, N uptake efficiency (NUpE) **(f)**, N utilization efficiency (NUtE) **(g)**, N use efficiency **(h)**, and N transport efficiency (NTE) **(i)**, under normal nitrogen (N42) and low nitrogen (N7) treatments. Mean ± SE (n = 6). Different lowercase letters indicate significant differences at the same N level ($p < 0.05$, one-way ANOVA).

supporting host growth and adaptive capacity. On one hand, functional redundancy ensures the stability of host-associated benefits under variable environmental conditions by mitigating the loss of any single strain (Vandenkoornhuyse et al., 2015; Wang et al., 2023b). On the other hand, complementary interactions among functionally distinct strains can enhance the host's functional diversity, thereby promoting greater ecological adaptability (Singh et al., 2015; Finkel et al., 2017). For example, compared to single-strain inoculation, Paenibacillus sp. B1 acidified the rhizosphere pH through organic acid secretion, thereby enhancing the high-level expression of the nifH gene in the co-inoculated strain Paenibacillus beijingensis and activating soil nitrogenase activity. This co-inoculation significantly promoted wheat growth, particularly increasing root nitrogen and phosphorus accumulation in wheat roots by 27% and 63%, respectively (Li et al., 2020). Therefore, when assessing the functional roles of seed microbiota, it is important to consider both functional redundancy and complementarity among strains. By following these principles, the rational design of effective functional microbial communities can be achieved, laying the theoretical groundwork for the practical use of seed endophytes in agriculture (Northen et al., 2024; Zhu et al., 2025).

The five representative endophytes significantly enhanced rice growth, nitrogen accumulation, and NUE, likely through multiple synergistic mechanisms. Firstly, nitrogen-fixing seed endophytes can effectively convert atmospheric nitrogen (N_2) into plant-available forms, such as ammonium (NH_4^+), thereby increasing the nitrogen supply to the host (Huang et al., 2023). Secondly, numerous endophytic bacteria can modulate host nitrogen metabolism and contribute to nitrogen cycling in the rhizosphere (Liang and Bowatte, 2022). For example, Epichloë gansuensis significantly enhances the activities of nitrate reductase, nitrite reductase, and glutamine synthetase in Achnatherum inebrians, thereby accelerating the conversion of NO_3^{-4} to organic nitrogen and improving NUE (Wang et al., 2018). Thirdly, endophytic fungi can modify and improve the rhizosphere microenvironments, creating favorable niches for beneficial microbes, including nitrogen fixers (Li et al., 2020; Kour et al., 2021). For example,

seed endophytes such as Fictibacillus rigui and Priestia aryabhattai accelerate the reduction of Fe^{3+} to Fe^{2+} increasing electron availability for the DNRA pathway. This, in turn, selectively recruits DNRA-performing Clostridium spp., strengthening nitrogen-conserving processes and ultimately enhancing rice NUE (Liu et al., 2025). Moreover,many seed endophytes, such as Burkholderia vietnamiensis RS1, can produce plant hormones like IAA, which stimulate root cell division and elongation. This promotes the formation of lateral roots and root hairs, ultimately enhancing nitrogen uptake (Shinjo et al., 2022). Collectively, these findings underscore the critical role of seed endophytes in facilitating nitrogen acquisition and translocation in host plants.

However, we also observed that the growth-promoting effects of seed endophytes are co-determined by bacterial strain and nitrogen conditions. Firstly, different bacterial strains can trigger distinct host response mechanisms, leading to variable growth outcomes. For instance, multiple strains of Paenibacillus inoculated into wheat, cucumber, and tomato exhibited markedly different PGP effects by suppressing ethylene levels and promoting root development (Liu et al., 2019). Interestingly, even the same bacterial strain may exhibit different PGP effects under varying environmental stress conditions. For example, under low-nitrogen conditions, inoculation with Bradyrhizobium japonicum enhanced soybean nitrogen accumulation by approximately 40% through symbiotic nitrogen fixation. However, under high-nitrogen conditions, soybean plants favored the energy-efficient strategy of direct nitrogen uptake over the energetically costly process of symbiosis. As a result, B. japonicum inoculation had no significant effect on nitrogen accumulation in high-nitrogen environments (Perkowski et al., 2024). These findings highlight the importance of considering both microbial and environmental factors in the practical application of seed endophytes. Optimal outcomes depend not only on selecting the appropriate bacterial strains but also on understanding their functional traits in relation to specific environmental conditions.

5 Conclusion

This study compared the composition of seed endophytic bacterial communities between high- and low-NUE rice cultivars. The results revealed that rice seeds harbor highly diverse endophytic bacterial communities, with significant differences in community structure among cultivars. Despite these differences, all four cultivars exhibited a common dual pattern: rare taxa serve as key drivers of community diversity and compositional variation, while core taxa display strong genetic conservation across cultivars. The representative seed endophytic bacteria possessed diverse, functionally redundant, and complementary PGP traits, which significantly enhanced rice growth and NUE. However, the magnitude and consistency of their beneficial effects were modulated by both the bacterial strain and environmental nitrogen availability. Overall, this study offers important theoretical insights into the diversity and functional potential of the rice seed microbiome, providing a solid foundation for developing and applying seed endophytes as microbial resources to enhance nitrogen use efficiency in rice cultivation.

Data availability statement

The original contributions presented in the study are included in the article/Supplementary Material. Further inquiries can be directed to the corresponding authors.

Author contributions

RL: Methodology, Data curation, Formal analysis, Software, Visualization, Writing – original draft. SF: Data curation, Methodology, Software, Visualization, Writing – original draft, Investigation. WF: Investigation, Methodology, Software, Writing – original draft. ZZ: Methodology, Funding acquisition, Supervision, Writing – review & editing. HL: Funding acquisition, Methodology, Writing – review & editing, Conceptualization, Investigation, Project administration. TL: Conceptualization, Funding acquisition, Investigation, Methodology, Project administration, Supervision, Validation, Writing – review & editing.

Funding

The author(s) declared that financial support was received for this work and/or its publication. This research was financially co-supported by Yunnan International Joint Laboratory of Research and Development of Crop Safety Production on Heavy Metal Pollution Areas (202403AP140035), the National Natural Science Foundation of China (No. 32271708, No. 42367003) and the "Double First-Class" University Project of Yunnan University; the Science and Technology Innovation Base Construction Project (No. 202307AB110011).

Conflict of interest

The author(s) declared that this work was conducted in the absence of any commercial or financial relationships that could be construed as a potential conflict of interest.

Generative AI statement

The author(s) declared that generative AI was not used in the creation of this manuscript.

Any alternative text (alt text) provided alongside figures in this article has been generated by Frontiers with the support of artificial

intelligence and reasonable efforts have been made to ensure accuracy, including review by the authors wherever possible. If you identify any issues, please contact us.

Publisher's note

All claims expressed in this article are solely those of the authors and do not necessarily represent those of their affiliated organizations, or those of the publisher, the editors and the reviewers. Any product that may be evaluated in this article, or claim that may be made by its manufacturer, is not guaranteed or endorsed by the publisher.

Supplementary material

The Supplementary Material for this article can be found online at: https://www.frontiersin.org/articles/10.3389/fpls.2025.1709648/full#supplementary-material

References

Ahn, Y., Kim, J. M., Ahn, H., Lee, Y. J., LiPuma, J. J., Hussong, D., et al. (2014). Evaluation of liquid and solid culture media for the recovery and enrichment of Burkholderia cenocepacia from distilled water. *J. Ind. Microbiol. Biotechnol.* 41, 1109–1118. doi: 10.1007/s10295-014-1442-3

An, J., Liu, X., Xu, C., Cui, J., Xu, K., Ling, F., et al. (2014). Photosynthetic physiological characteristics of rice varieties with high nitrogen use efficiencies. *J. Northwest A&F Univ.* 42, 29–38 + 45. doi: 10.13207/j.cnki.jnwafu.2014.12.003

Anas, M., Liao, F., Verma, K. K., Sarwar, M. A., Mahmood, A., Chen, Z. L., et al. (2020). Fate of nitrogen in agriculture and environment: agronomic, eco-physiological and molecular approaches to improve nitrogen use efficiency. *Biol. Res.* 53, 47. doi: 10.1186/s40659-020-00312-4

Asaf, S., Khan, M. A., Khan, A. L., Waqas, M., Shahzad, R., Kim, A. Y., et al. (2017). Bacterial endophytes from arid land plants regulate endogenous hormone content and promote growth in crop plants: an example of Sphingomonas sp. and Serratia marcescens. . *J. Plant Interact.* 12, 31–38. doi: 10.1080/17429145.2016.1274060

Barberán, A., Bates, S., Casamayor, E., and Fierer, N. (2012). Using network analysis to explore co-occurrence patterns in soil microbial communities. *ISME J.* 6, 343–351. doi: 10.1038/ismej.2011.119

Carvajal, M., Godoy, L., Gebauer, M., Catrileo, D., and Albornoz, F. (2024). Screening for indole-3-acetic acid synthesis and 1-aminocyclopropane-carboxylate deaminase activity in soil yeasts from Chile uncovers Solicoccozyma terrea as an effective plant growth promoter. *Plant Soil.* 496, 83–93. doi: 10.1007/s11104-023-05906-x

Chen, Q. L., Ding, J., Zhu, D., Hu, H. W., Delgado-Baquerizo, M., Ma, Y. B., et al. (2020). Rare microbial taxa as the major drivers of ecosystem multifunctionality in long-term fertilized soils. *Soil Biol. Biochem.* 141, 107686. doi: 10.1016/j.soilbio.2019.107686

Chen, S., Zhao, C., Yang, W., Wang, W., Zhu, Q., He, M., et al. (2025). Enhancing rice nitrogen use efficiency via plant-microbe-soil interactions: Insights from ^{15}N tracing. *Appl. Soil Ecol.* 207, 105931. doi: 10.1016/j.apsoil.2025.105931

Cheng, J. F., Jiang, H. Y., Liu, Y. B., Dai, T. B., and Cao, W. X. (2011). Methods on identification and screening of rice genotypes with high nitrogen efficiency. *Rice Sci.* 18, 127–135. doi: 10.1016/S1672-6308(11)60018-8

Cui, X., Zhu, X., Long, S., Hui, J., Hong, S., Hong, Z., et al. (2010). Response of super hybrid rice "Y Liangyou No. 1" to N-fertilizer dose and its N use efficiency. *Chin. J. Eco-Agric.* 18, 9457–9949. doi: 10.3724/SP.J.1011.2010.00945

da Silva, D. A. F., Cotta, S. R., Vollú, R. E., Jurelevicius, D., de, A., Marques, J. M., et al. (2014). Endophytic microbial community in two transgenic maize genotypes and in their near-isogenic non-transgenic maize genotype. *BMC Microbiol.* 14, 332. doi: 10.1186/s12866-014-0332-1

Deckert, R. J., Gehring, C. A., and Patterson, A. (2019). "Pine seeds carry symbionts: Endophyte transmission re-examined," in *Seed endophytes: biology and biotechnology*. Eds. S. K. Verma and J. F. White (Cham: Springer), 335–361. doi: 10.1007/978-3-030-10504-4_16

Durán, P., Ellis, T. J., Thiergart, T., Ågren, J., and Hacquard, S. (2022). Climate drives rhizosphere microbiome variation and divergent selection between geographically distant Arabidopsis populations. *New Phytol.* 236, 608–621. doi: 10.1111/nph.18357

Edgar, R. (2013). UPARSE: highly accurate OTU sequences from microbial amplicon reads. *Nat. Methods.* 10, 996–998. doi: 10.1038/nmeth.2604

Ezraty, B., Henry, C., Hérisse, M., Denamur, E., and Barras, F. (2014). Commercial Lysogeny Broth culture media and oxidative stress: a cautious tale. *Free Radical Riol Med.* 74, 245–251. doi: 10.1016/j.freeradbiomed.2014.07.010

Fan, Y., Wang, Z., Liao, D., Raza, M., Wang, B., Zhang, J., et al. (2020). Uptake and utilization of nitrogen, phosphorus and potassium as related to yield advantage in maize - soybean intercropping under different row configurations. *Sci. Rep.* 10, 9504. doi: 10.1038/s41598-020-66459-y

Feng, Y., Chen, H., Hu, X., Zhou, W., Xu, F., and Cai, H. (2014). Nitrogen efficiency screening of rice cultivars popularized in South China. *J. Plant Nutr. Fert.* 20, 1051–1062. doi: 10.11674/zwyf.2014.0501

Finkel, O. M., Castrillo, G., Herrera Paredes, S., Salas González, I., and Dangl, J. L. (2017). Understanding and exploiting plant beneficial microbes. *Curr. Opin. Plant Biol.* 38, 155–163. doi: 10.1016/j.pbi.2017.04.018

Franić, I., Eschen, R., Allan, E., Hartmann, M., Schneider, S., and Prospero, S. (2020). Drivers of richness and community composition of fungal endophytes of tree seeds. *FEMS Microbiol. Ecol.* 96, fiaa166. doi: 10.1093/femsec/fiaa166

Guo, K., Yang, J., Yu, N., Luo, L., and Wang, E. (2023). Biological nitrogen fixation in cereal crops: Progress, strategies, and perspectives. *Plant Commun.* 4, 100499. doi: 10.1016/j.xplc.2022.100499

Hou, Q., Bai, X., Li, W., Gao, X., Zhang, F., Sun, Z., et al. (2018). Design of primers for evaluation of lactic acid bacteria populations in complex biological samples. *Front. Microbiol.* 9. doi: 10.3389/fmicb.2018.02045

Hu, Y., Ganjurjav, H., Hu, G., Ji, G., Han, L., Sha, Y., et al. (2023). Responses of bacterial community composition and diversity to multi-level nitrogen addition at different periods of growing season driven by conditional rare taxa in an alpine meadow. *Biol. Fertil Soils.* 59, 939–952. doi: 10.1007/s00374-023-01764-y

Hu, X., Zhong, X., Peng, B., Huang, N., Pan, J., Liang, K., et al. (2019). Yield formation and characteristics of nitrogen utilization in high-yielding rice varieties under reduced nitrogen input. *J. Nucl. Agric. Sci.* 33, 2460–2471. doi: 10.11869/j.issn.100-8551.2019.12.2460

Huang, D., Ren, J., Chen, X., Akhtar, K., Liang, Q., Ye, C., et al. (2023). Whole-genome assembly of A02 bacteria involved in nitrogen fixation within cassava leaves. *Plant Physiol.* 193, 1479–1490. doi: 10.1093/plphys/kiad331

Jana, S. K., Islam, M. M., Hore, S., and Mandal, S. (2023). Rice seed endophytes transmit into the plant seedling, promote plant growth and inhibit fungal phytopathogens. *Plant Growth Regul.* 99, 373–388. doi: 10.1007/s10725-022-00914-w

Jiao, S., Wang, J., Wei, G., Chen, W., and Lu, Y. (2019). Dominant role of abundant rather than rare bacterial taxa in maintaining agro-soil microbiomes under environmental disturbances. *Chemosphere.* 235, 248–259. doi: 10.1016/j.chemosphere.2019.06.174

Johnston-Monje, D., Lundberg, D. S., Lazarovits, G., Reis, V. M., and Raizada, M. N. (2016). Bacterial populations in juvenile maize rhizospheres originate from both seed and soil. *Plant Soil.* 405, 337–355. doi: 10.1007/s11104-016-2826-0

Jousset, A., Bienhold, C., Chatzinotas, A., Gallien, L., Gobet, A., Kurm, V., et al. (2017). Where less may be more: how the rare biosphere pulls ecosystems strings. *ISME J.* 11, 853–862. doi: 10.1038/ismej.2016.174

Kang, S., Ma, W., Li, F. Y., Zhang, Q., Niu, J., Ding, Y., et al. (2015). Functional redundancy instead of species redundancy determines community stability in a typical steppe of inner Mongolia. *PloS One.* 10, e0145605. doi: 10.1371/journal.pone.0145605

Koester, L., Lyte, M., Schmitz-Esser, S., and Allen, H. (2019). PSII-16 Evidence for stratification of rumen wall microbial communities revealed by 16S rRNA based amplicon sequencing. *J. Anim Sci.* 97, 226–227. doi: 10.1093/jas/skz122.398

Kour, D., Rana, K. L., Kaur, T., Yadav, N., Yadav, A. N., Kumar, M., et al. (2021). Biodiversity, current developments and potential biotechnological applications of phosphorus-solubilizing and -mobilizing microbes: A review. *Pedosphere.* 31, 43–75. doi: 10.1016/s1002-0160(20)60057-1

Li, Y., Li, Q., Guan, G., and Chen, S. (2020). Phosphate solubilizing bacteria stimulate wheat rhizosphere and endosphere biological nitrogen fixation by improving phosphorus content. *PeerJ.* 8, e9062. doi: 10.7717/peerj.9062

Li, G., Wu, M., Li, P., Wei, S., Liu, J., Jiang, C., et al. (2021). Assembly and co-occurrence patterns of rare and abundant bacterial sub-communities in rice rhizosphere soil under short-term nitrogen deep placement. *J. Integr. Agr* 20, 3299–3311. doi: 10.1016/S2095-3119(20)63462-1

Li, J., Wu, H., Pu, Q., Zhang, C., Chen, Y., Lin, Z., et al. (2023). Complete genome of Sphingomonas paucimobilis ZJSH1, an endophytic bacterium from Dendrobium officinale with stress resistance and growth promotion potential. *Arch. Microbiol.* 205, 132. doi: 10.1007/s00203-023-03459-2

Liang, D., and Bowatte, S. (2022). Seed endophytic ammonia oxidizing bacteria in Elymus nutans transmit to offspring plants and contribute to nitrification in the root zone. *Front. Microbiol.* 13. doi: 10.3389/fmicb.2022.1036897

Liu, X., Li, Q., Li, Y., Guan, G., and Chen, S. (2019). Paenibacillus strains with nitrogen fixation and multiple beneficial properties for promoting plant growth. *PeerJ.* 7, e7445. doi: 10.7717/peerj.7445

Liu, M., Liu, T., Zhang, Z., Xiao, X., An, H., Wei, P., et al. (2025). Endophytes enhance rice inorganic nitrogen use efficiency and mitigate nitrogen loss via dissimilatory nitrate reduction to ammonium in paddy soils. *Rice.* 18, 66. doi: 10.1186/s12284-025-00814-3

Lobato, C., de Freitas, J. M., Habich, D., Kögl, I., Berg, G., and Cernava, T. (2024). Wild again: recovery of a beneficial Cannabis seed endophyte from low domestication genotypes. *Microbiome* 12, 239. doi: 10.1186/s40168-024-01951-5

Louca, S., Parfrey, L. W., and Doebeli, M. (2016). Decoupling function and taxonomy in the global ocean microbiome. *Science* 353, 1272–1277. doi: 10.1126/science.aaf4507

Louca, S., Polz, M. F., Mazel, F., Albright, M. B. N., Huber, J. A., O'Connor, M. I., et al. (2018). Function and functional redundancy in microbial systems. *Nat. Ecol. Evol.* 2, 936–943. doi: 10.1038/s41559-018-0519-1

Lynch, M., and Neufeld, J. (2015). Ecology and exploration of the rare biosphere. *Nat. Rev. Microbiol.* 13, 217–229. doi: 10.1038/nrmicro3400

Nelson, E. B. (2018). The seed microbiome: Origins, interactions, and impacts. *Plant Soil.* 422, 7–34. doi: 10.1007/s11104-017-3289-7

Northen, T. R., Kleiner, M., Torres, M., Kovács, Á.T., Nicolaisen, M. H., Krzyżanowska, D. M., et al. (2024). Community standards and future opportunities for synthetic communities in plant-microbiota research. *Nat. Microbiol.* 9, 2774–2784. doi: 10.1038/s41564-024-01833-4

Pérez-Miranda, S., Cabirol, N., George-Téllez, R., Zamudio-Rivera, L. S., and Fernández, F. J. (2007). O-CAS, a fast and universal method for siderophore detection. *J. Microbiol. Methods.* 70, 127–131. doi: 10.1016/J.MIMET.2007.03.023

Perkowski, E. A., Terrones, J., German, H. L., and Smith, N. G. (2024). Symbiotic nitrogen fixation reduces belowground biomass carbon costs of nitrogen acquisition under low, but not high, nitrogen availability. *AoB Plants.* 16, plae051. doi: 10.1093/aobpla/plae051

Rodriguez, R. J., White, J. F., Arnold, A. E., and Redman, R. S. (2009). Fungal endophytes: diversity and functional roles. *New Phytol.* 182, 314–330. doi: 10.1111/j.1469-8137.2009.02773.x

Roy, M., Kang, B., Yang, S., Choi, H., and Choi, K. (2024). Characterization of tomato seed endophytic bacteria as growth promoters and potential biocontrol agents. *Plant Pathol. J.* 40, 578–592. doi: 10.5423/PPJ.OA.09.2024.0142

Schloss, P. D., Westcott, S. L., Ryabin, T., Hall, J. R., Hartmann, M., Hollister, E. B., et al. (2009). Introducing mothur: open-source, platform-independent, community-supported software for describing and comparing microbial communities. *Appl. Environ. Microb.* 75, 7537–7541. doi: 10.1128/AEM.01541-09

Schwyn, B., and Neilands, J. B. (1987). Universal chemical assay for the detection and determination of siderophores. *Anal. Biochem.* 160, 47–56. doi: 10.1016/0003-2697(87)90612-9

Shade, A., Jacques, M. A., and Barret, M. (2017). Ecological patterns of seed microbiome diversity, transmission, and assembly. *Curr. Opin. Microbiol.* 37, 15–22. doi: 10.1016/j.mib.2017.03.010

Shao, G., Cheng, H., Dai, H., Zhang, H., Ai, J., Liu, K., et al. (2022). Nitrogen uptake and utilization of two maize hybrids with contrasting nitrogen use efficiencies depending on fertilization amount. *Arch. Agron. Soil Sci.* 69, 2202–2217. doi: 10.1080/03650340.2022.2142573

Shinjo, R., Tanaka, A., Sugiura, D., Suzuki, T., Uesaka, K., Takebayashi, Y., et al. (2022). Comprehensive analysis of the mechanisms underlying enhanced growth and root N acquisition in rice by the endophytic diazotroph, Burkholderia Vietnamiensis RS1. *Plant Soil.* 450, 537–555. doi: 10.1007/s11104-020-04506-3

Siebyła, M., Szyp-Borowska, I., and Młodzińska, A. (2024). Bacterial communities inhabiting the ascomata of the ectomycorrhizal summer truffle (Tuber aestivum). *Appl. Soil Ecol.* 199, 105428. doi: 10.1016/j.apsoil.2024.105428

Simonin, M., Briand, M., Chesneau, G., Rochefort, A., Marais, C., Sarniguet, A., et al. (2022). Seed microbiota revealed by a large-scale meta-analysis including 50 plant species. *New Phytol.* 234, 1448–1463. doi: 10.1111/nph.18037

Singh, M., Awasthi, A., Soni, S., Singh, R., Verma, R. K., and Kalra, A. (2015). Complementarity among plant growth promoting traits in rhizospheric bacterial communities promotes plant growth. *Sci. Rep.* 5, 15500. doi: 10.1038/srep15500

Suman, A., Shukla, L., Marag, P. S., Verma, P., Gond, S., and Sai Prasad, J. (2020). Potential use of plant colonizing Pantoea as generic plant growth promoting bacteria for cereal crops. *J. Environ. Biol.* 41, 987–994. doi: 10.22438/JEB/41/5/MRN-1250

Tai, X., Yang, R., Li, J., Li, A., Chen, W., and Ding, J. (2024). Endophytic bacteria in Halogeton glomeratus from mining areas are mainly Sphingomonas pseudosanguinis, with a Cyanobacteria moving from roots to leaves to avoid heavy metals. *Rhizosphere.* 23, 100993. doi: 10.1016/j.rhisph.2024.100993

Tamura, K., Stecher, G., Peterson, D., Filipski, A., and Kumar, S. (2013). MEGA6: molecular evolutionary genetics analysis version 6.0. *Mol. Biol. Evol.* 30, 2725–2729. doi: 10.1093/molbev/mst197

Thomas, J., Kim, H. R., Rahmatallah, Y., Wiggins, G., Yang, Q., Singh, R., et al. (2019). RNA-seq reveals differentially expressed genes in rice (Oryza sativa) roots during interactions with plant-growth promoting bacteria, Azospirillum, brasilense. *PloS One.* 14, e0217309. doi: 10.1371/journal.pone.0217309

Truyens, S., Weyens, N., Cuypers, A., and Vangronsveld, J. (2015). Bacterial seed endophytes: genera, vertical transmission and interaction with plants. *Env Microbiol. Rep.* 7, 40–50. doi: 10.1111/1758-2229.12181

Vandenkoornhuyse, P., Quaiser, A., Duhamel, M., Van, A. L., and Dufresne, A. (2015). The importance of the microbiome of the plant holobiont. *New Phytol.* 206, 1196–1206. doi: 10.1111/nph.13312

Walitang, D. I., Kim, C. G., Jeon, S., Kang, Y., and Sa, T. (2019). Conservation and transmission of seed bacterial endophytes across generations following crossbreeding and repeated inbreeding of rice at different geographic locations. *MicrobiologyOpen.* 8, e00662. doi: 10.1002/mbo3.662

Wang, Q., Garrity, G. M., Tiedje, J. M., and Cole, J. R. (2007). Naive Bayesian classifier for rapid assignment of rRNA sequences into the new bacterial taxonomy. *Appl. Environ. Microb.* 73, 5261–5267. doi: 10.1128/AEM.00062-07

Wang, Q., and Gottwald, S. (2017). Wheat root-dip inoculation with Fusarium graminearum and assessment of root rot disease severity. *Bio-protocol.* 7, e2189. doi: 10.21769/BioProtoc.2189

Wang, Z., Li, N., Wang, W., and Liu, Y. (2023a). Endophytic bacterial community diversity in genetically related hybrid rice seeds. *Appl. Microbiol. Biotechnol.* 107, 6911–6922. doi: 10.1007/s00253-023-12782-z

Wang, J. F., Nan, Z. B., Christensen, M. J., Zhang, X. X., Tian, P., Zhang, Z. X., et al. (2018). Effect of Epichloë gansuensis endophyte on the nitrogen metabolism, nitrogen use efficiency, and stoichiometry of Achnatherum inebrians under nitrogen limitation. *J. Agric. Food Chem.* 66, 4022–4031. doi: 10.1021/acs.jafc.7b06158

Wang, M., Osborn, L. J., Jain, S., Meng, X., Weakley, A., Yan, J., et al. (2023b). Strain dropouts reveal interactions that govern the metabolic output of the gut microbiome. *Cell.* 186, 2839–2852.e21. doi: 10.1016/j.cell.2023.05.037

Wang, Z., Zhang, S., Liang, J., Chen, H., Jiang, Z., Hu, W., et al. (2024). Rhizophagus irregularis regulates RiCPSI and RiCARI expression to influence plant drought tolerance. *Plant Physiol.* 197, kiae645. doi: 10.1093/plphys/kiae645

Watanabe, F. S., and Olsen, S. R. (1965). Test of an ascorbic acid method for determining phosphorus in water and $NaHCO_3$ extracts from soil. *Soil Sci. Soc Am. J.* 29, 677–678. doi: 10.2136/sssaj1965.03615995002900060025x

Wu, P. H., and Chang, H. X. (2024). Colonization compatibility with Bacillus altitudinis confers soybean seed rot resistance. *ISME J.* 18, wrae142. doi: 10.1093/ismejo/wrae142

Wu, J., Liu, S., Zhang, H., Chen, S., Si, J., Liu, L., et al. (2025). Flavones enrich rhizosphere Pseudomonas to enhance nitrogen utilization and secondary root growth in Populus. *Nat. Commun.* 16, 1461. doi: 10.1038/s41467-025-56226-w

Xu, H., Liu, W., He, Y., Zou, D., Zhou, J., Zhang, J., et al. (2025). Plant-root microbiota interactions in nutrient utilization. *Front. Agric. Sci. Enc* 12, 16–26. doi: 10.15302/J-FASE-2024595

Yang, Q., Liu, H., Tang, B., Yu, C., Dong, S., Li, Y., et al. (2025). Rare taxa as key drivers of soil multi-nutrient cycling under different crop types. *Microorganisms.* 13, 513. doi: 10.3390/microorganisms13030513

Yang, Z., Zhu, Q., Zhang, Y., Jiang, P., Wang, Y., Fei, J., et al. (2024). Soil carbon storage and accessibility drive microbial carbon use efficiency by regulating microbial diversity and key taxa in intercropping ecosystems. *Biol. Fertile Soils.* 60, 437–453. doi: 10.1007/s00374-024-01804-1

Yuan, M. M., Guo, X., Wu, L., Wu, L., Zhang, Y., Xiao, N., et al. (2021). Climate warming enhances microbial network complexity and stability. *Nat. Clim. Change.* 11, 343–348. doi: 10.1038/s41558-021-00989-9

Zhang, S., Ji, Z., Jiao, W., Shen, C., Qin, Y., Huang, Y., et al. (2025a). Natural variation of OsWRKY23 drives difference in nitrate use efficiency between indica and japonica rice. *Nat. Commun.* 16, 1420. doi: 10.1038/s41467-025-56752-7

Zhang, Z., Liu, T., Zhang, X., Xie, J., Wang, Y., Yan, R., et al. (2021). Cultivable endophytic bacteria in seeds of Dongxiang wild rice and their role in plant-growth promotion. *Diversity.* 13, 665. doi: 10.3390/d13120665

Zhang, X., Wu, N., Geng, K., Yang, P., Chu, C., and He, J. (2022). Lysobacter sedimenti sp. nov., isolated from the sediment, and reclassification of Luteimonas lumbrici as Lysobacter lumbrici comb. nov. *Curr. Microbiol.* 79, 381. doi: 10.1007/s00284-022-03084-0

Zhang, D., Xu, F., Wang, F., Le, L., and Pu, L. (2025b). Synthetic biology and artificial intelligence in crop improvement. *Plant Commun.* 6, 101220. doi: 10.1016/j.xplc.2024.101220

Zhao, Z., Ma, Y., Feng, T., Kong, X., Wang, Z., Zheng, W., et al. (2022). Assembly processes of abundant and rare microbial communities in orchard soil under a cover crop at different periods. *Geoderma.* 406, 115543. doi: 10.1016/j.geoderma.2021.115543

Zhou, Z., Zhang, Y., and Zhang, Y. (2022). Abundant and rare bacteria possess different diversity and function in crop monoculture and rotation systems across regional farmland. *Soil Biol. Biochem.* 171, 108742. doi: 10.1016/j.soilbio.2022.108742

Zhu, J., Jia, Q., Tang, Q. Y., Osman, G., Gu, M. Y., Wang, N., et al. (2025). Application of synthetic microbial communities of Kalidium schrenkianum in enhancing wheat salt stress tolerance. *Int. J. Mol. Sci.* 26, 860. doi: 10.3390/ijms26020860

Frontiers in Plant Science

Cultivates the science of plant biology and its applications

The most cited plant science journal, which advances our understanding of plant biology for sustainable food security, functional ecosystems and human health.

Discover the latest Research Topics

See more →

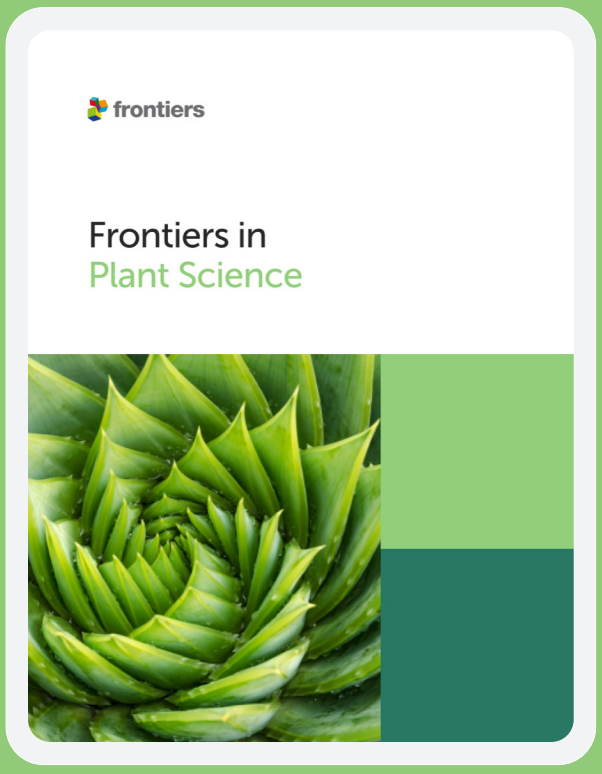

Frontiers

Avenue du Tribunal-Fédéral 34
1005 Lausanne, Switzerland
frontiersin.org

Contact us

+41 (0)21 510 17 00
frontiersin.org/about/contact